

UNIVERSITY OF VALENCIA
FACULTY OF CHEMISTRY
DEPARTMENT OF ANALYTICAL CHEMISTRY



VNIVERSITAT
E VALÈNCIA
[Ò*] Facultat de Química



Thesis presented to obtain the PhD degree in Chemistry under the
“Programa de Doctorado en Química con Mención de Excelencia (R.D.
99/2011)”

**DEVELOPMENT OF NEW STRATEGIES FOR THE DESIGN OF IN
SITU ANALYSIS DEVICES: NANO AND BIOMATERIALS**

Sara Bocanegra Rodríguez

Supervisors:

Prof. Dr. Pilar Campins Falcó

Prof. Dr. Carmen Molins Legua

Prof. Dr. Neus Jornet Martínez

Valencia, October 2021

Departament de Química Analítica

Dña. Pilar Campins Falcó, Profesora Catedrática, Dña. Carmen Molins Falcó, Profesora Catedrática, y Dña. Neus Jornet Martínez, Profesora Ayudante Doctor, pertenecientes al Departamento de Química Analítica de la Universidad de Valencia,

CERTIFICAN

Que la presente memoria, titulada “*Development of new strategies for the design of in situ analysis devices: nano and biomaterials*”, constituye la Tesis Doctoral de Sara Bocanegra Rodríguez para optar al grado de Doctora en Química, y que ha sido realizada en los laboratorios del Departamento de Química Analítica de la Universidad de Valencia, bajo su dirección y supervisión.

Y para que así conste a los efectos oportunos, firman el presente certificado en Valencia, a 28 de Octubre de 2021.

Fdo. Dra. Pilar Campins Falcó

Directora de Tesis

Fdo. Dra. Carmen Molins Legua

Codirectora de Tesis

Fdo. Dra. Neus Jornet Martínez

Codirectora de Tesis

This thesis has been completed thanks to a PhD research grant (PROMETEO program 2016/109 and 2020/078) funded by Generalitat Valenciana in the Analytical Chemistry Department of the University of Valencia. A research stay of three months in Molecular Chemistry Department of the University of Grenoble Alpes was carried out supported by the GV-Union Social Fund (BEFPI19).



VNIVERSITAT [Q*] DE VALÈNCIA Facultat de Química



*“Si he visto más lejos es porque estoy
sentado sobre los hombros de gigantes”*

(Isaac Newton)

Agradecimientos

Esta Tesis es fruto de muchos años de trabajo, dedicación, sacrificio y esfuerzo. Este trabajo no hubiera sido posible sin la participación y el apoyo de mucha gente que me ha acompañado a lo largo del camino y a la que ahora tengo la oportunidad de agradecer.

En primer lugar, quiero dar las gracias a mis directoras, Pilar, Carmen y Neus, las cuales han confiado en mí y han estado a mi lado durante cada una de las etapas. Gracias por vuestra dedicación y transferencia de conocimientos, sois un ejemplo a seguir.

Gracias a Rosa, Jorge y Yolanda por haberme ofrecido vuestra ayuda en cada momento que la he necesitado. Ha sido un placer compartir estos años con vosotros.

También quiero agradecer a todos mis compañeros con los que he compartido la mayor parte del tiempo, Adriá, Lusine, Ana, Lorenzo, Anabel, Pascu, María, Rodrigo, Sergio, Henry, Héctor, Juanlu, Lori, Victor, Cristian y Pepe. Gracias a vosotros he disfrutado mucho de este viaje llamado Tesis, entre otras cosas hemos compartido almuerzos, comidas, celebraciones y congresos. Gracias por vuestra amistad y el tiempo compartido.

Gracias a Serge, Andrew y Fabien por haberme acogido durante tres meses en vuestro grupo de investigación, ha sido una experiencia muy enriquecedora. Gracias a Deborah, Anastasia, Ilaria y Paulo por esos momentos compartidos en varios idiomas a la vez, me hicisteis sentir como en casa.

A mis padres, María Jesús y Pedro, por ayudarme a cumplir mis objetivos como estudiante y persona, gracias a vosotros he llegado hasta aquí. Gracias

por vuestros sabios consejos y por vuestro apoyo, sois mis guías. Gracias hermanita por nuestras largas conversaciones de teléfono, siempre me llamabas en el mejor momento. Gracias por ayudarme a ver la vida desde otro punto de vista. Gracias enano por compartir 20 años conmigo, me has dado una gran lección de vida, siempre juntos.

Gracias a Carmen, Alina, Vera y Guillermo, compañeros de carrera y amigos, con quienes empecé mi aventura de estudiante de universidad. Sé que siempre puedo contar con vosotros.

También quiero agradecer a Néstor, mi compañero de vida, por estar siempre a mi lado. Gracias por ayudarme a levantarme y darme ánimos en cada obstáculo que encuentro. Me haces la vida más fácil y siempre me sacas una sonrisa.

A todos y todas, también a las personas que no he mencionado pero forman parte de mi vida.

RESUMEN

Resumen

La literatura actual muestra una gran necesidad, en general, de desarrollar metodologías analíticas sostenibles basadas en la miniaturización, simplificación y automatización de procesos analíticos con el objetivo de reducir el impacto ambiental sin comprometer la selectividad y sensibilidad del método analítico. Concretamente, los (bio)sensores están surgiendo como método rápido y simple para la detección in situ de compuestos en varios campos como por ejemplo, el sanitario, la industria alimentaria y de bebidas, incluyendo el monitoreo medioambiental y de seguridad entre otros. Las ventajas del análisis in situ son (1) en la mayoría de los casos la determinación se lleva a cabo sin aislar el analito de su entorno, por lo que la muestra no se altera de sus condiciones originales y (2) el proceso analítico incluido en el muestreo se lleva a cabo físicamente en el espacio y en el tiempo reduciendo el tiempo de análisis químico en comparación con los métodos tradicionales, que en ocasiones, implican largos procesos de análisis que pueden impedir una actuación rápida en caso de que los resultados obtenidos así lo requieran. Además, el análisis in situ generalmente no requiere un tratamiento de muestra que, de acuerdo con los principios de la Química Verde, minimiza la generación de residuos. Concretamente, “la Química Verde se define como la química que se centra en el diseño, obtención, fabricación y uso de productos químicos que tengan un potencial de contaminación reducido o nulo”. Nació en Estados Unidos a principios de la década de 1990 a través de la Agencia de Protección Ambiental como para lograr un aumento de la protección del medio ambiente y fue expresada en 12 principios establecidos por Paul Anastas y John Warner en 1998. Entre los 12 principios se encuentran prevenir la producción de residuos, seleccionar métodos que incorporen al máximo en el producto final todos los materiales utilizados durante su

proceso, seleccionar la síntesis que genere menos o ninguna toxicidad para la salud humana y medio ambiente, utilizar reactivos químicos y disolventes seguros, pensar en aumentar la eficiencia energética de las reacciones, utilizar materias primas renovables, reducir derivatizantes, utilizar productos químicos que se descompongan en productos de degradación inocuos, realizar análisis en tiempo real para prevenir la contaminación y establecer una química segura para la prevención de accidentes. Los principios antes mencionados están relacionados con la optimización de procesos a escala industrial, por lo que Galuzka et al. decidieron llevar a cabo una adaptación de estos principios a las características y necesidades de la química analítica, incluyendo además principios socio-económicos, dando lugar a la creación de los 12 principios de la Química Analítica Verde. Tanto los principios de la Química Verde como los principios de la Química Analítica Verde incluyen el uso de materiales y métodos seguros y limpios para disminuir o evitar los efectos adversos que produce la contaminación en el medio ambiente. El uso de (bio)materiales a base de polímeros como polisacáridos y proteínas aparece como una opción responsable con el medio ambiente ya que permite a los microorganismos degradar estos materiales y reducir directamente la generación de residuos. Además, los (bio)materiales han generado un gran interés por su biocompatibilidad en el sector alimentario y médico.

La Tesis describe el concepto de análisis in situ y (bio)materiales que han dado lugar al desarrollo de varios dispositivos de análisis in situ para el análisis de una gran variedad de analitos en diferentes matrices: ambientales, biológicas, alimentarias, entre otros. Estos dispositivos se basan principalmente en la inmovilización de reactivos en soportes sólidos. Se han empleado nano y (bio) materiales en el desarrollo de varios (bio) sensores o kits. Para el desarrollo de los dispositivos se consideraron los siguientes dos

puntos críticos: i) la selección de los materiales de soporte donde tiene lugar la inmovilización de los reactivos, ii) la reacción involucrada en el procedimiento. Es importante estudiar la reacción entre el material y los reactivos para comprender la liberación del reactivo a la disolución o la entrada de los analitos al soporte sólido. El material de soporte no debe reaccionar con el reactivo ni interferir con la medida. Es de destacar que los dispositivos sólidos evitan problemas de manipulación y pueden aumentar la estabilidad de reactivos derivatizantes. Algunos de los materiales propuestos en esta Tesis como soportes sólidos para el diseño de dispositivos in situ han sido zeína, nailon, PDMS y nanocelulosa. Asimismo, se ha realizado la caracterización de los dispositivos desarrollados.

Como se ha comentado anteriormente, otro de los retos que aborda la Tesis es realizar determinaciones in situ, es decir, la posibilidad de realizar el análisis en el lugar donde se encuentra el compuesto de interés. Esto presenta grandes ventajas como por ejemplo que se evita el transporte de la muestra al laboratorio lo que conlleva una reducción de tiempo, costes y recursos, y paralelamente se minimiza también el riesgo de alteración indeseada de la muestra, como por ejemplo contaminación o degradación. Para desarrollar un método de análisis in situ se deben considerar varios aspectos incluyendo las características del analito a determinar, la matriz de analito y el soporte entre otras. Es de destacar que los sistemas complejos que ofrecen un alto rendimiento analítico pueden no ser adecuados debido a la necesidad de recursos de alto costo, como equipos de análisis costosos y personal cualificado. Durante la última década, el número de publicaciones sobre métodos analíticos in situ ha aumentado debido al enorme interés por utilizar métodos portátiles, baratos, selectivos, sensibles y robustos.

Los dispositivos de análisis se basan en tres componentes esenciales: la muestra o analito de interés, el elemento de reconocimiento y el transductor. En la zona de reconocimiento del dispositivo, la información química se convierte en una señal analítica medible por el transductor. En esta Tesis se han desarrollado dispositivos eléctricos y colorimétricos. Ambos tipos de dispositivo permiten la detección in situ del analitos. La determinación a través de dispositivos eléctricos se basa en cambios de la señal eléctrica y los colorimétricos se basan en cambios de color. Los dispositivos colorimétricos exhiben un potencial prometedor gracias al hecho de que un cambio de color en presencia del analito puede detectarse fácilmente a simple vista, para ello suelen ir acompañados de una carta de colores donde se indica la concentración del analito dependiendo del color final del dispositivo después del contacto con la muestra. Asimismo, la lectura in situ de los dispositivos colorimétricos puede ser realizada con instrumentos ópticos portátiles y mediante el análisis de imágenes digitalizadas. Para la imagen digital, es necesario un dispositivo electrónico como un escáner o un teléfono inteligente. Posteriormente, se utiliza una herramienta de procesamiento de imágenes digitales como por ejemplo GIMP, Adobe Photoshop, GNU, entre otros, para convertir una señal de colores en valores numéricos. Se pueden usar diferentes códigos de color, los más comunes son rojo-verde-azul (RGB), cian-magenta-amarillo-negro (CMYK), valor de saturación de tono (HSV) y cambio de color de luminancia desde rojo a verde y amarillo a azul (CIELAB). Como se puede observar, la etapa de adquisición de imagen es muy importante para obtener resultados de calidad ya que estos modelos pueden estar sujetos a interferencias debidas a las condiciones de iluminación. Recientemente, los grandes avances en el área de las telecomunicaciones han permitido el desarrollo de aplicaciones para la cuantificación de analitos a

través de dispositivos, como teléfonos móviles o tabletas. Estas aplicaciones permiten el análisis en tiempo real sin tratamiento previo de imágenes. En esta Tesis se emplearon el software GIMP y el modelo CMYK para la descomposición de color de las imágenes de los sensores realizadas con un teléfono móvil. Las interferencias debidas a la iluminación se corrigieron insertando puntos de referencia en la imagen.

El objetivo general de esta Tesis ha sido demostrar cómo los nuevos nano y (bio)materiales pueden mejorar significativamente los métodos analíticos establecidos, así como crear nuevas herramientas de análisis que contribuyan al desarrollo de metodologías más eficientes en cuanto a funcionalidad y sostenibilidad. Estas metodologías se han centrado en el análisis in situ. Para lograr con éxito este objetivo se han realizado diferentes etapas:

- Estudio del estado del arte de diferentes materiales y sus propiedades fisicoquímicas con el fin de tener información sobre su aplicabilidad en Química Analítica.
- Selección de materiales sostenibles para su aplicación en el desarrollo de dispositivos de análisis in situ para la determinación de compuestos determinados. En esta tesis se han seleccionado materiales que no interfieran en la medida y que posean una alta sensibilidad y reproducibilidad. Se han seleccionado como materiales de soporte inertes para los reactivos diferentes polímeros como PDMS, TEOS-MTEOS, zeína y nylon. También se han seleccionado nanomateriales como CNT y nanocelulosa.
- Complementar el procedimiento con una respuesta óptica o eléctrica sensible y selectiva para obtener un dispositivo in situ sostenible. Se han utilizado técnicas ópticas y eléctricas dependiendo del analito y la sensibilidad requerida.

Importancia de la elección del material en el desarrollo de dispositivos sólidos como encapsuladores y dispensadores de reactivos

El estudio de las propiedades de los diferentes materiales ha sido fundamental para seleccionar los materiales adecuados para las aplicaciones de detección deseadas. La selección ha dependido principalmente del analito y la reacción analítica empleada. Los reactivos o enzimas pueden permanecer atrapados o adheridos en los soportes y se pueden observar dos comportamientos diferentes, i) los reactivos difunden hacia la solución ii) los analitos entran en el soporte sólido. Por lo tanto, la reacción química puede llevarse a cabo en disolución o en el soporte. Por consiguiente, la determinación del analito de interés se realizará en la disolución o en el dispositivo utilizando las técnicas analíticas adecuadas para cada situación. En esta Tesis se han estudiado los siguientes materiales:

La zeína es un material biodegradable procedente del maíz, concretamente es una proteína. Es un material de bajo costo, biocompatible y sostenible. La zeína se puede utilizar para realizar películas que pueden atrapar o adsorber reactivos y enzimas. Esta película puede ser modificada con diferentes compuestos como el glicerol o sorbitol para obtener films con la flexibilidad y permeabilidad deseada, además permite la estabilización de los reactivos. En esta Tesis se ha utilizado la zeína como soporte para atrapar diferentes especies químicas, reactivos orgánicos como 3-O-metilfluoresceína-6-fosfato (OMFP), sustancias inorgánicas como cloruro de hidroxilamonio y cloruro de hierro (III) hexahidrato, y se han adsorbido biomoléculas como la alcalina fosfatasa (ALP). El soporte actúa como dispositivo de dispensación de reactivos. La zeína se ha utilizado para desarrollar dos sensores:

Sensor para la determinación de fosfato inorgánico: la fabricación del sensor tiene lugar en una placa de 96 multipozos y se realiza añadiendo una solución hidroalcohólica que contiene zeína y OMFP, se deja a temperatura ambiente y solidifica. Posteriormente se añade una delgada capa compuesta por zeína y glicerol y luego se adsorbe la ALP. La reacción se lleva a cabo añadiendo la muestra al pocillo que tiene el sensor y se produce una señal quimioluminiscente inversamente proporcional a la concentración de fosfato inorgánico.

Sensor para la determinación de grupos éster: se fabrican dos sensores de zeína con glicerol; uno contiene encapsulado cloruro de hierro y el otro hidroxilamonio. Para llevar a cabo la reacción se añade el sensor de hidroxilamonio a una disolución acuosa básica junto con la muestra y se calientan hasta ebullición. Cuando la disolución se encuentra a temperatura ambiente, la disolución se acidifica y se añade el sensor de hierro. Se centrifuga y se mide la absorbancia de la disolución.

El nailon es un polímero sintético que tiene la capacidad de teñirse fácilmente, por lo que se puede utilizar para desarrollar sensores colorimétricos y realizar determinaciones semicuantitativas a simple vista o cuantitativas con el uso de dispositivos de captura de imágenes. Además, el nailon es blanco, por lo que su propio color no interfiere con el color final desarrollado tras la reacción. Posee excelentes propiedades mecánicas y es flexible. En esta Tesis se ha demostrado su aplicación en el desarrollo de sensores para la determinación de plata en biocidas. Los reactivos rojo de pirogalol (PGR) y 1,10-fenantrolina se retuvieron juntos en este soporte. La fabricación del sensor se lleva a cabo haciendo pasar una disolución de PGR y 1,10-fenantrolina a través de una membrana de nailon situada en un portafiltros acoplado a una jeringa de modo que quedan atrapados. Este sensor

se pone en contacto con la muestra y se añade persulfato potásico y ácido sulfúrico. Se deja reaccionar durante 30 o 50 minutos (dependiendo de la sensibilidad requerida) y el sensor se extrae para proceder a la medida de la señal analítica. Como la oxidación del reactivo PGR por parte del persulfato potásico tiene lugar en el soporte, el cambio de color se produce en el mismo. El análisis cuantitativo se lleva a cabo mediante medida de absorbancia por reflectancia difusa y/o medida del valor cian, magenta, amarillo y negro a través de una imagen digital obtenida mediante dispositivos de captura de imágenes como un teléfono móvil.

El polidimetilsiloxano (PDMS) es un material hidrófobo y es el polímero más usado como soporte encapsulante de reactivos, asimismo les proporciona gran estabilidad. Ópticamente es transparente y puede actuar como dispensador de reactivos desde el soporte a la solución o como soporte sólido donde tiene lugar la reacción de derivatización en su interior. Es biocompatible y de bajo coste ofreciendo múltiples posibilidades en el ámbito de la química analítica. En esta Tesis se ha demostrado la inmovilización covalente de la enzima peroxidasa de rábano (HRP) en el dispositivo PDMS que permite la determinación de peróxido de hidrógeno (H_2O_2). Para realizar el sensor, el agente gelificante se adiciona en una proporción 1:10 respecto de la base polimérica. Después de homogeneizar la dispersión, la mezcla se vierte en tubos de poliestireno y se deja gelificar en la estufa a 30°C. A continuación, la superficie del PDMS se activa y se funcionaliza. El último paso consiste en la unión covalente de la HRP. El análisis de H_2O_2 se lleva a cabo añadiendo una disolución de luminol y la muestra. La señal quimioluminescente se captura a los 10 s.

Los reactivos tetraetilortosilicato (TEOS) y metiltrietoxisilano (MTEOS) en medio básico pueden formar un sol-gel y actuar como material

encapsulante de diferentes compuestos. El sol-gel puede ser combinado con plastificantes como polimetilmetacrilato (PMMA) o polietilenglicol (PEG) para modificar su flexibilidad. El sol-gel es transparente en el rango espectral UV y visible, por lo que, en esta Tesis, se ha aplicado para el desarrollo de un sensor de amonio y nitrógeno orgánico mediante el uso de técnicas ópticas. Para realizar el sensor se mezclan TEOS, MTEOS, agua y una disolución básica de luminol. Cuando se obtiene una dispersión homogénea, se deposita en el fondo de un tubo de poliestireno. Posteriormente los tubos son calentados a 40°C durante 4 horas. Para llevar a cabo la reacción primero se mezcla la muestra con hipoclorito sódico durante 1 min y luego la mezcla se introduce en el tubo que contiene el sensor. La señal quimioluminescente se captura a los 10 s.

La nanocelulosa bacteriana (BCN) es un biomaterial producido por bacterias. Es hidrofílico y presenta alta capacidad de hidratación, además, su superficie contiene varios grupos hidroxilo que pueden ser funcionalizados. Es un material poroso y permeable. En esta Tesis, se ha utilizado la BCN como material de soporte para desarrollar un sensor electroquímico de H₂O₂. Primero se realiza una dispersión de nanotubos de múltiples paredes de carbono en N-metilpirrolidone. Se depositan en un electrodo de carbono vítreo y se secan a vacío durante 2 horas. A continuación, se modifican los electrodos con diferentes derivados del pireno (ácido butírico, N-hidroxisuccinimida ester, ácido acético entre otros) para estudiar la respuesta del sensor. Finalmente se realiza de la inmovilización de la enzima HRP en el electrodo junto con la BCN. Se ha demostrado que la película de BCN aumenta la estabilidad de la enzima.

Los nanotubos de carbono (CNT) tienen una gran superficie y una gran estabilidad. Tienen una buena capacidad de interactuar con varios compuestos

a través de mecanismos no covalentes, por lo que se pueden funcionalizar. En esta Tesis, se han estudiado cinco derivados del pireno adsorbidos en los CNT para desarrollar un sensor electroquímico de H₂O₂. Asimismo, se ha estudiado el efecto de la BCN en estos sensores.

La importancia de las mediciones in situ

La detección y el control de biomarcadores in situ representa un gran avance en el *campo de la medicina*. La medicina preventiva se centra en la ausencia de enfermedades mediante su control y detección precoz. Las tecnologías emergentes ayudan en el desarrollo de dispositivos de medicina preventiva y personalizados no invasivos al incluir métodos de detección de biomarcadores. Los dispositivos in situ aparecen como una opción eficaz para conseguir retos en el campo de la medicina. El dispositivo tiene que ser selectivo, sensible, barato y portátil, por lo que no debe necesitar energía externa. Además, la posibilidad de miniaturización hace que el análisis sea más rentable gracias a la reducción de reactivos, tiempo de análisis y residuos generados.

En esta Tesis, se ha desarrollado un sensor para la determinación de fosfato inorgánico en suero y orina que permite realizar multianálisis, lo que resulta en una notable disminución del tiempo de análisis. De esta forma se puede obtener un resultado rápido que conduce a reducir el tiempo de diagnóstico de enfermedades. El fosfato inorgánico desempeña un papel fundamental en numerosas funciones fisiológicas normales, incluidas las relacionadas con el metabolismo energético, la mineralización ósea y la señalización intracelular, por lo que la concentración de fosfato inorgánico en suero y orina es importante para la salud humana. Los niveles de fósforo en suero se encuentran normalmente entre 3,4 y 4,5 mg dL⁻¹ según la

Organización Mundial de la Salud (OMS). Algunas condiciones patológicas pueden modificar la concentración de fosfato inorgánico fisiológico en suero y orina.

Asimismo, se ha desarrollado un dispositivo para realizar análisis cuantitativo de H_2O_2 en medios de cultivo celular que previamente han estado en contacto con células. Este método proporciona mediciones in situ de alta precisión y sensibilidad. Además, las mediciones se pueden obtener en solo 10 s. Cabe destacar que el dispositivo es reutilizable, permitiendo su uso más de sesenta veces. Su determinación es importante ya que el H_2O_2 se considera una de las especies reactivas del oxígeno y se puede encontrar en los fluidos humanos. Aunque es poco reactivo, es capaz de formar otros intermedios altamente reactivos como el radical hidroxilo ($OH \bullet$). Por otro lado, se sabe que el H_2O_2 es una molécula de señalización inter e intracelular que regula los procesos celulares. La concentración de H_2O_2 en biofluidos puede verse alterada en muchas patologías como cáncer, diabetes mellitus, Alzheimer, aterosclerosis y enfermedad de Parkinson entre otras, considerando que es un biomarcador de estrés oxidativo.

Por otro lado, las tecnologías de monitoreo in situ en el *área de control de calidad* han aparecido como un avance para complementar los métodos clásicos de análisis químico en el laboratorio, concretamente en el análisis medioambiental, farmacéutico, de alimentos y bebidas. Además, el obtener resultados en cortos periodos de tiempo permiten decidir si desea recolectar más muestras para realizar nuevos ensayos. En algunos casos, los sensores se utilizan para el análisis complementario con el fin de proporcionar más información para mejorar la toma de decisiones. A lo largo de la Tesis, se han desarrollado cinco dispositivos que permiten la medición in situ.

Se han desarrollado dos dispositivos sólidos de zeína en los cuales se han inmovilizado dos reactivos, cloruro de hidroxilamonio y cloruro de hierro. Estos dispositivos se han utilizado para realizar análisis de control de calidad de rutina de medicamentos y productos farmacéuticos que contienen grupos éster. El método permite el análisis semicuantitativo que se realiza a simple vista y el análisis cuantitativo a través de espectrofotometría VIS. La reacción produce un cambio de color de amarillo a marrón debido a la formación del complejo hidroxámico férrico. Cabe destacar que, el análisis de medicamentos requiere un control muy estricto ya que el nivel de dosificación es la clave para obtener resultados deseados y evitar efectos adversos. El método se ha aplicado para cuantificar atropine and ramipril en la industria farmacéutica.

Como se ha comentado anteriormente, se ha desarrollado un dispositivo para la determinación de H_2O_2 . Este dispositivo también se ha aplicado para la determinación de H_2O_2 en comprimidos de parafarmacia. Gracias a su gran poder oxidante, estos comprimidos se usan como agente antibacteriano, antifúngico, antimoho y antiviral. Este dispositivo se ha utilizado para evaluar la liberación de H_2O_2 por parte de los comprimidos a una disolución acuosa y para evaluar el consumo progresivo de H_2O_2 tras la adición de una dentadura usada.

Se ha desarrollado un sensor colorimétrico en nailon para la determinación de iones de plata en biocidas. El sensor ayuda a detectar fácilmente desajustes en los niveles de plata en aguas procedentes de sistemas de refrigeración que pueden provocar un aumento del crecimiento de bacterias. El crecimiento bacteriano tiene un gran impacto en la industria ya que puede producir daños estructurales que incluyen la corrosión de materiales y la formación de bioincrustaciones. El sensor está acompañado de

una carta de colores que permite realizar un análisis semicuantitativo a simple vista. Además, se puede realizar un análisis cuantitativo por DR o a través de dispositivos que permiten capturar imágenes. Los proveedores de sistemas de refrigeración generalmente recomiendan concentraciones de iones de plata ($0.02\text{--}0.08\text{ mg}\cdot\text{l}^{-1}$) para controlar la legionella de manera efectiva.

Se ha desarrollado un sensor encapsulando luminol en su interior para llevar a cabo la determinación de nitrógeno orgánico y amonio. El método produce una señal de luminiscencia que se puede medir con un luminómetro portátil. Cabe señalar que el método es de fácil manejo por personal no cualificado y permite obtener los resultados en el lugar donde se tomó la muestra. El método se ha aplicado al análisis de varias muestras de agua reales. La importancia de determinar nitrógeno orgánico y amonio en aguas radica en que ambos compuestos contribuyen a aumentar los niveles de nitrógeno. La concentración de nitrógeno en el agua se considera uno de los principales factores que intervienen en el aumento de la eutrofización del agua. Este fenómeno también puede verse afectado por factores ambientales como temperatura, salinidad, niveles de dióxido de carbono, luz solar, etcétera. Además, puede verse afectado por actividades humanas que contribuyen al aumento de la tasa de aportación de nutrientes debido al crecimiento de la población, la industrialización y la intensificación de las actividades agrícolas. Esto da lugar a la creación de densas floraciones de algas que limitan la penetración de luz y la concentración de oxígeno proporcionando como resultado condiciones ambientales de hipoxia que aumentan la mortalidad de la biota viva.

Para concluir, los dispositivos de medida in-situ propuestos en esta Tesis pueden ser considerados como una alternativa sostenible y eficaz a los métodos instrumentales convencionales. Estos dispositivos han sido

aplicados para la determinación de compuestos relevantes como H₂O₂, fosfato, biocidas o fármacos en matrices reales complejas como muestras de suero, orina o agua ambiental. Las metodologías propuestas han sido validadas y sus propiedades han sido comparadas con otras metodologías existentes. Además, la inmovilización de reactivos o enzimas en un soporte sólido evita la necesidad de preparar disoluciones que resultan ser inestables.

La importancia de los materiales para desarrollar metodologías de análisis in situ ha quedado demostrada:

- 1. La zeína es un biomaterial que permite encapsular y adsorber reactivos y enzimas en su superficie. Asimismo, es un material que se puede utilizar como liberador de especies químicas.*
- 2. El nailon tiene una gran capacidad de tinción por lo que es útil para el desarrollo de sensores colorimétricos.*
- 3. El PDMS es un excelente material encapsulante de reactivos. Además, es ópticamente transparente y permite la activación de su superficie gracias a su estructura.*
- 4. La mezcla de TEOS y MTEOS produce un sol-gel que capaz de encapsular reactivos. Puede ser modificado con diversos materiales para modificar su permeabilidad.*
- 5. La nanocelulosa bacteriana es un material respetuoso con el medio ambiente que forma fácilmente films flexibles y permeables.*
- 6. Los nanotubos de carbono presentan excelentes propiedades eléctrica y poseen una elevada superficie de contacto lo que posibilita su modificación química.*

ABSTRACT

Abstract

There is great need, in general, to develop sustainable analytical methodologies based on the miniaturization, simplification and analytical process automation, with the aim of reducing the environmental impact without compromising the selectivity and sensitivity. Specifically, biosensors, are emerging as a fast and simple method for the in situ detection of compounds in several fields such as healthcare and food and drink industry including environmental and security monitoring among others. The advantages of in situ analysis are (1) in most cases the determination is carried out without isolation of the analyte from its environment, so the sample is not altered from its original conditions and (2) the analytical process including sampling is physically carried out in space and in time reducing the time of the analysis. Traditional chemical analysis, sometimes, involves a long analysis process that prevents rapid action in the event that the results obtained require it. Also, in situ analyses generally do not require sample treatment which, according to Green Analytical Chemistry principles, minimizes waste generation.

On the other hand, Green Chemistry includes the use of safe and clean material and methods to decrease the adverse effects of pollution on the environment. The use of polymer-based biomaterials such as polysaccharides and proteins appears as a responsible option since it allows microorganisms to degrade these materials and directly reduce waste generation. Moreover, biomaterials have generated great interest due to their biocompatibility in food and medical area.

Several aspects should be considered in order to choose an in situ analysis method. In some cases, complex systems that offer high analytical

performance may be unsuitable due to the need for high cost resources such as expensive analysis equipment and qualified personnel. During the last decade, the number of publications about in situ analytical methods has increased given the enormous interest to use portable, cheap, selective, sensitive and robust methods.

The Thesis describes the concept of in situ analysis and biomaterials which have been resulting in the development of several situ devices. These devices are mainly based on the reagent immobilization in solid supports. Nano and (bio) materials have been employed in the development of several (bio)sensors or kits. In order to develop the devices, the two critical points were considered: i) the selection of the support materials where the immobilization of the reagents takes place, ii) the reaction involved in the procedure. It is important to study the reaction between the material and the reagents in order to understand the reagent release to dissolution or the entry of analytes to the solid support. The support material must not react with the reagent or interfere with the measurement. Some of the materials proposed in this Thesis as solid supports for the design of in-situ sensors have been zein, nylon, PDMS and nanocellulose. The characterization of the devices has been performed

New methodologies for analysis in situ based on the employment of (bio)sensors have been proposed for the determination of relevant compounds such as H₂O₂, phosphate or drugs in complex real matrices like serum, urine or environmental water samples. These analyses have employed different analytical responses depending on the sensibility required. These approaches have been validated and its analytical properties have been compared with other already existing.

INDEX

INDEX

Agradecimientos	i
Resumen.....	iii
Abstract.....	xix
CHAPTER 1. INTRODUCTION	1
1.1. IN-SITU DEVICES	3
1.1.1. Optical sensors	10
1.1.2. Electrochemical sensors	17
1.2. MATERIALS.....	24
1.2.1. Zein	28
1.2.2. Nylon.....	32
1.2.3. Siloxane groups materials	35
1.2.3.1. PDMS.....	35
1.2.3.2. TEOS/MTEOS	39
1.2.4. Nanomaterials	42
1.2.4.1. Bacterial nanocellulose	42
1.2.4.2. Carbon nanotube	46
1.3. ANALYTES AND ANALYTICAL TECHNIQUES	50
1.3.1. Inorganic phosphate	50
1.3.2. Ester groups from drugs: atropine, cocaine and ramipril	54
1.3.3. Silver ion.....	57
1.3.4. Hydrogen peroxide.....	60
1.3.5. Ammonium and organic amino nitrogen	66
CHAPTER 2. OBJECTIVES.....	71
CHAPTER 3. EXPERIMENTAL METHODOLOGY	79
3.1 CHEMICALS AND REAGENTS	81
3.2 INSTRUMENTATION	84
3.2.1 Spectroscopic techniques	85
3.2.1.1 UV-Vis spectrophotometry	85

3.2.1.2	Reflectance diffuse spectrophotometry (DR).....	86
3.2.1.3	Infrared spectroscopy (IR)	86
3.2.1.4	Quimioluminescence.....	87
3.2.1.5	Fluorescence	88
3.2.1.6	Mobile phone	89
3.2.2	Electrochemical techniques.....	89
3.2.2.1	Voltammetry	89
3.2.3	Microscopic techniques.....	89
3.2.3.1	Light microscopy	89
3.3	FABRICATION OF SENSORS	90
3.3.1	Zein/glycerol-ALP and Zein/glycerol-OMFP sensors	90
3.3.2	Iron and Hydroxylammonium Sensors	92
3.3.3	Nylon/1,10-phenantroline/PGR sensor	94
3.3.4	PDMS/peroxidase sensor	95
3.3.5	TEOS/MTEOS/luminol sensor	96
3.3.6	Nanocellulose/HRP/ MWCNT sensor	97
3.4	PROCEDURES AND EXPERIMENTAL CONDITIONS	99
3.4.1	Experimental conditions of polymeric sensors	99
3.4.2	Electrochemical conditions	102
3.4.3	Response of zein sensors.....	102
3.4.3.1	Response to inorganic phosphate.....	102
3.4.3.2	Response to ester groups.....	104
3.4.4	Response of nylon sensor.....	106
3.4.5	Response of PDMS sensor.....	108
3.4.6	Response of TEOS/MTEOS sensor	109
3.4.7	Response of nanocellulose sensor.....	111
3.5	SAMPLES.....	112
3.5.1	Biological samples	112
3.5.1.1	Serum	112
3.5.1.2	Urine	113
3.5.1.3	Culture medium DMEM-F12 incubated with neuroblast cells .	113

3.5.2	Drug and parapharmaceutical samples.....	114
3.5.2.1	Atropine sulphate drug.....	114
3.5.2.2	Oxygen Bio-Active tablets.....	114
3.5.3	Environmental samples.....	114
3.5.4	Industrial sample.....	115
CHAPTER 4. RESULTS AND DISCUSSION.....		117
4.1.	ZEIN AS SUPPORTING MATERIAL FOR SENSOR DEVELOPING	119
4.1.1.	Inorganic phosphate determination.....	119
4.1.1.1.	Optimization of both enzyme and substrate immobilization ...	120
4.1.1.2.	Analytical parameters and stability.....	125
4.1.1.3.	Determination of phosphate in real samples.....	127
4.1.1.4.	Conclusions.....	129
4.1.2.	Ester drugs determination.....	130
4.1.2.1.	Optimization of support material and reagents immobilization	130
4.1.2.2.	Analytical parameters and stability.....	131
4.1.2.3.	Determination of atropine in real samples.....	135
4.1.2.4.	Conclusions.....	136
4.2.	NYLON AS SUPPORTING MATERIAL FOR SENSOR DEVELOPING.....	137
4.2.1	Optimization of the Nylon sensor.....	137
4.2.2	Characterization of the nylon sensor.....	142
4.2.3	Interference study.....	144
4.2.4	Analytical parameters.....	144
4.2.5	Analysis of samples.....	148
4.2.6	Conclusions.....	151
4.3.	SILOXANE GROUPS AS SUPPORTING MATERIAL FOR SENSOR DEVELOPING.....	153
4.3.1.	PDMS-based sensor containing HRP for the estimation of hydrogen peroxide.....	153
4.3.1.1.	Optimization of the HRP/PDMS sensor.....	154
4.3.1.2.	Characterization of the HRP/PDMS sensor.....	159

4.3.1.3.	Kinetic Analysis.....	161
4.3.1.4.	Analytical parameters, stability and reusability	163
4.3.1.5.	Analysis of real samples	165
4.3.1.6.	Conclusions.....	167
4.3.2.	Sensor based on TEOS/MTEOS/luminol sol-gel for controlling dissolved ammonium and organic amino nitrogen	168
4.3.2.1.	Optimization of reagent concentration.....	169
4.3.2.2.	Optimization of luminol immobilization	170
4.3.2.3.	Characterization of the TEOS/MTEOS device	173
4.3.2.4.	Analytical parameters, stability and interferences	175
4.3.2.5.	Determination of ammonium and organic ammonium in real water samples.....	177
4.3.2.6.	Conclusions.....	179
4.4.	NANOCELLULOSE AS SUPPORTING MATERIAL FOR SENSOR DEVELOPING	180
4.4.1.	Bioelectrocatalysis of HRP/pyrene-modified MWCNT bioelectrodes	180
4.4.2.	Bioelectrocatalysis of pyrre-NHS modified HRP bioelectrodes with nanocellulose.....	188
4.4.3.	Conclusions.....	194
	CHAPTER 5. GENERAL CONCLUSIONS.....	195
	REFERENCES	203
	ANNEX	257
A.1.	Abbreviations.....	259
A.2.	Figure list	265
A.3.	Table list.....	273
A.4.	PhD contributions to publications.....	277

CHAPTER 1. INTRODUCTION

Since the end of the 20th century, the field of analytical chemistry has been evolving rapidly thanks to the technological developments and the incorporation of new (nano)materials (Jornet-Martínez et al., 2017). Specifically, technological development has been related to the computer science evolution, this allows to automatize processes leading to a reduction of analysis time and an improvement of data processing. Moreover, the evolution has allowed to have a control of the different processes and a quick actuation in the case of not expected outcomes (Addepalli et al., 2017; D. Singh et al., 2021). Other advance has been the miniaturization of methods which has resulted in a process simplification and a reduction in qualified personnel. Moreover, the use of miniaturized methods has allowed reducing costs, solvents used and waste generated, thus, more sustainable analysis methods have been obtained (Pena-Pereira et al., 2021).

In this context, the development of in situ analysis devices together with the use of (nano) material are acquiring importance. The different materials used throughout history have changed as science evolves. Plastics as support material have been widely used due to their favourable properties, however, there is currently an increase in the demand of biodegradable materials as there is an increase in environmental concern (Reshmy et al., 2021; Wang et al., 2021; Xia and Larock, 2010).

1.1. IN-SITU DEVICES

In situ monitoring technologies appeared as an advance for complementing the classical methods in the laboratory. The concept of in situ analysis employed has been described by Jornet et al. (Jornet-Martínez et al., 2017). In the analytical context, in situ analysis can be defined as a function

of the place where the analytical process is carried out, which means at the same place where the phenomenon occurs.

The advantages of in situ analysis are (1) in most cases, the determination is carried out without isolation of the analyte from its environment, so the sample is not altered from its original conditions and (2) the analytical process including sampling is physically carried out in space and in time reducing the time of analysis.

Based on the way in which the analytical process is carried out, the analytical methods for in situ analysis can be classified into two categories: on-line and in-line methods (*Figure 1*). On-line methods, the sample is drawn into the system for being processed and for analyte(s) determination. They involve fixed installations and are generally used for air or water monitoring. These instruments collect a considerable amount of data. In-line monitoring methods generally involve the use of an analytical device, which is placed directly in contact with the sample, for example, portable optical or electrochemical devices and/or portable instrumentation. On the other hand, there are the off-line methods which the sample is collected in situ and transported to an external testing area. Because there is a distance from the sampling site to the analytical device or instrument, so the sample is collected in situ. These methods cannot be classified as in situ methods, the whole analytical process is not carried out on place and in real time. These methods require samplers and a protocol about optimal conditions to transport the samples to the laboratory for their analysis (Bowler et al., 2020; Z. Li et al., 2021; Lourenço et al., 2012; Morin et al., 2021).

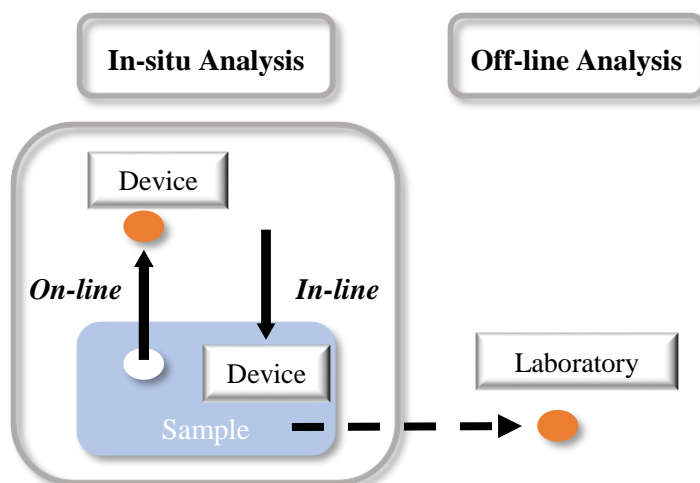


Figure 1. Schematic representation of online, in-line and off-line analytical methods.

Table 1 classifies the in situ devices in monitoring stations, portable instruments, electrochemical devices and optical devices, and the strength and concerns of the method are outlined. This table provides some characteristics of devices such as the need for specialized operators, maintenance, and sampling types: active/passive and continuous and/or noncontinuous monitoring (Campins-Falcó et al., 2013; Jornet-Martínez et al., 2017; Junqueira et al., 2021; Martínez-Aviño et al., 2021b; Wirojsaengthong et al., 2021). Active devices need an energy source for sampling, generally a pump. Whereas the interaction in the analyte-analytical device in the passive modality is carried out usually through a diffusion process and, so, energy consumption is not needed. Other way of classification is according to the monitoring process, the in situ devices can work either continuously or discontinuously. In continuous methods, the samples are taken and analyzed at fixed or variable intervals to obtain the analytical response. In the discontinuous methods, the response is generally achieved after discrete sampling.

Type of in situ methods	Some characteristics	Advantages and disadvantages	
<i>Monitoring stations</i> <i>(fixed or mobile)</i>	<ul style="list-style-type: none"> ▪ Operator: High specialized ▪ Calibration: Regular ▪ Sampling: Active -Routine analysis ▪ Monitoring: Continuous sub-hourly and remote 	<ul style="list-style-type: none"> ✓ High accuracy ✓ High precision ✓ High sensibility ✓ Multiple analysis 	<ul style="list-style-type: none"> × Expensive × Easy environmental access × High power consumption × Radio interference × High EF
<i>Portable instruments</i> Spectrophotometer Fluorimeter Infrared analysed Chromatography Electrochemical	<ul style="list-style-type: none"> ▪ Operator: High specialized ▪ Calibration: Regular and check the power supply ▪ Sampling: Active, routine analytes ▪ Monitoring: Non-continuous 	<ul style="list-style-type: none"> ✓ Portability ✓ Moderate accuracy ✓ Portable ✓ Low/non- power consumption 	<ul style="list-style-type: none"> × Moderate power × Moderate cost

Table 1. Classification and some properties of the in situ devices

Type of in situ methods	Some characteristics	Advantages and disadvantages	
<p><i>Electrochemical devices</i></p> <p>Amperometric</p> <p>Voltamperometric</p> <p>Potentiometric</p> <p>Chemioresistor</p> <p>Conductimetric</p>	<ul style="list-style-type: none"> ▪ Operator: Low/non- specialized ▪ Calibration: Check the power supply ▪ Sampling: Active, routine analytes and specific ▪ Monitoring: Non-continuous, weekly 	<ul style="list-style-type: none"> ✓ Low/non power consumption ✓ Sensibility ✓ May need reconditioning 	<ul style="list-style-type: none"> × Moderate/low stability × Selectivity × Moderate/Low accuracy
<p><i>Optical devices</i></p> <p>Colorimetric</p> <p>Fluorescence</p> <p>Chemiluminescence</p>	<ul style="list-style-type: none"> ▪ Operator: Low/non- specialized ▪ Sampling: Passive or active and specific substances ▪ Monitoring: Non-continuous 	<ul style="list-style-type: none"> ✓ Easy to use ✓ Very low cost ✓ Personal/ portable ✓ Low/non-power consumption ✓ Simple ✓ Reliable 	<ul style="list-style-type: none"> × Moderate/low accuracy × Snap-hot × Moderate sensibility

In this context, sensors appear as a reliable alternative which can be applied to numerous analytical processes in several fields such as healthcare and food and drink industry including environmental and security monitoring (Bocanegra-Rodríguez et al., 2018a; Jornet-Martínez et al., 2019; Jornet-Martínez et al., 2017). The aforementioned literature is according with the following 12 principles of green chemistry described by Paul Anastas and John Warner (Anastas and Warner, 1998) which included, wastes prevention, atom economy, less hazardous chemical syntheses, designing safer chemicals, use safer solvents and auxiliaries, design methods for energy efficiency, use of renewable feedstocks, reduce derivatives, use catalytic reactions, design for degradation, real-time analysis and inherently safer chemistry for accident prevention. At a later stage, Gazluzka et al. (Gałuszka et al., 2013) decided to carry out an adaptation of these principles to the characteristics and needs of analytical chemistry. The green analytical chemistry principles describe the guidelines for the development of sustainable analytical methodologies, reducing negative impacts on health and the environment. As a consequence, current trends are aimed at the development of analytical methods that allow an economical, sustainable and real-time analysis at the same time as high quality results.

During the last years, the number of publications about sensors and in-situ analysis are growing (*Figure 2*). The type of the most in situ devices reported in the literature are electrochemical and optical devices. We observed as a trend to the development of in situ devices that for electrochemical devices, they were miniaturized improving energy consumption, low cost, and portability, while for the optical devices, the digital camera of the mobile phones was used for the measurements (Goud et al., 2021; Martínez-Aviño et al., 2021b; Romanholo et al., 2021). Remote and

continue measurement can be done using these approaches together. The accessibility of the population to mobile phone explains the increasing interest to use them for real-time and in situ measurements. The ideal sensor should be selective, sensitive, cheap, portable and reusable. This approach can be combined with the use of portable instruments for both transductions and in situ analysis, and these instruments are smaller and cheaper than laboratory analytical instruments and easy to handle by nonqualified personnel. Moreover, the possibility of miniaturization makes the analysis more cost-effective because of the reduction of analysis time and needed reagents (Jornet-Martínez et al., 2021; Martínez-Aviño et al., 2021b, 2021a).

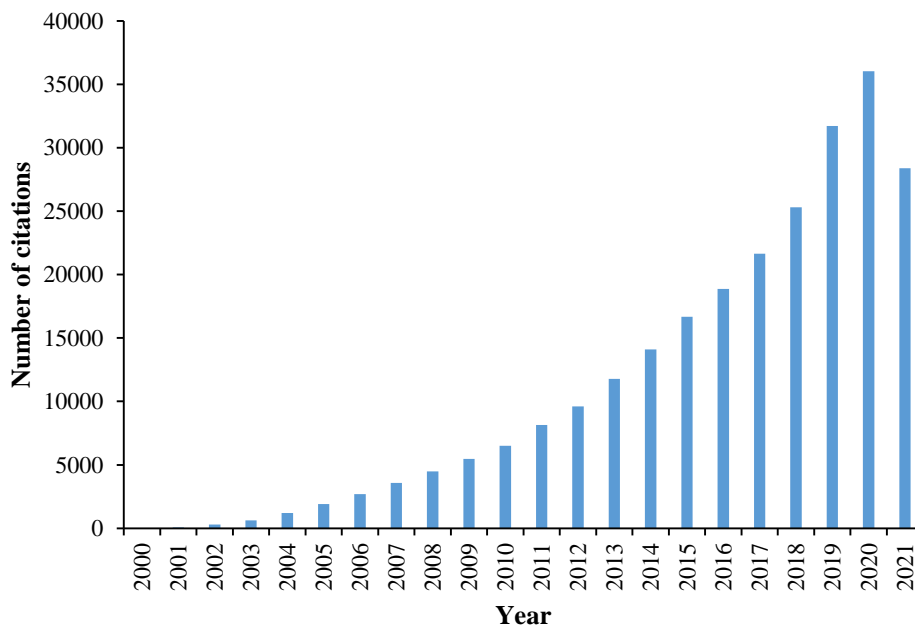


Figure 2. Number of citations on Web of Science for matching the following search term ‘in-situ analysis’ AND ‘sensor’ in the 2000-2021 period (September 2021).

1.1.1. Optical sensors

According to the current challenges to carry out analysis in real time, optical sensors are each day more important in our world becoming smaller, more efficient, cost-effectiveness and interconnected to the internet of the things. Moreover, optical analysis techniques are considered one of the best analysis techniques for sensor development due to their sensitivity, selectivity, and durability (Leonardi et al., 2021). *Table 2* shows the last covered topics of optical sensors in 34 recent review articles published from database web of science ('optical' AND 'sensor' review September 2021). These papers show the need of new knowledge for improving their responses, uses and utilities. During the last 5 years, it has been published more than 3500 reviews concerning to this topic.

Covered Topic	Reference
Graphene-based sensors for food adulterants and toxicants detection	(Raghavan et al., 2021)
Optical glucose biosensor	(Reda et al., 2021)
Nanomaterial bio/sensors for infectious diseases detection	(Sheikhzadeh et al., 2021)
Carbon quantum dots for the development of optical sensors	(Nazri et al., 2021)
Optical fiber sensors for glucose detection	(Gong et al., 2021)
Photoactive metal-organic frameworks for optical applications	(Whelan et al., 2021)
Doped graphene quantum dots for fluorescence applications	(B. Li et al., 2021)

Chapter 1. Introduction

Covered Topic	Reference
Arrays sensor for glycosaminoglycans discrimination	(Jia et al., 2021)
Strategies for enhanced sensitivity of polydiacetylene-based biosensors	(C. Kim et al., 2021)
Determination of water in organic solvents with optical sensors	(Jouyban and Rahimpour, 2021)
Nanomaterials for designing aptasensors	(Kurup et al., 2021)
Silicon nanostructures to develop biosensing platforms	(Leonardi et al., 2021)
Biocompatible and biodegradable light-emitting materials	(Kong et al., 2021)
Organic light-emitting diodes for biomedical applications	(Murawski and Gather, 2021)
Optical lithium sensors	(Villemin and Raccurt, 2021)
Noble metal nanomaterial-based biosensors for respiratory viruses detection	(Choi et al., 2021)
Therapeutic drug monitoring by using optical biosensors	(Ong et al., 2021)
Detection of milk contaminants	(Farag et al., 2021)
Hydrogel-derived luminescent scaffolds for biomedical applications	(Y. Yang et al., 2021)
Integrated Optical Biosensors for Point-of-Care Applications	(Chen et al., 2020)
Plasmon resonance sensors for biosensing applications	(D. M. Kim et al., 2021)

Chapter 1. Introduction

Covered Topic	Reference
Perylene diimide-based sensors	(P. Singh et al., 2021)
Plasmonic biosensors for food control	(Balbinot et al., 2021)
Sensing device for the detection of COVID-19	(Sadighbayan and Ghafar-Zadeh, 2021)
Irreversible bonding techniques for the fabrication of microfluidic platforms	(Ali Hasim et al., 2021)
Sensors for smart food packaging	(Rodrigues et al., 2021)
Nanomaterials sensors for acrylamide detection in processed foods	(Rayappa et al., 2021)
Organic polymers for the development of fluorescence sensors	(Skorjanc et al., 2021)
Detection of emerging contaminants	(Ryu et al., 2021)
Detection of trace metals	(Ekrami et al., 2021)
Smartphone-based optical analysis systems	(Di Nonno and Ulber, 2021)
Non-enzymatic (bio)sensors for detection of pesticide residues	(Majdinasab et al., 2021)
Nanosensing to evaluate liquid foods quality	(Manoj et al., 2021)
Trends in sensor development for the determination of mercury	(Lim et al., 2021)

Table 2. Covered topics of the optical sensor in the 34 review articles. Database web of science (access September 2021).

As we can see in *Table 2*, many authors have written reviews for diverse medical purposes which are widely used in clinics due to the easy monitoring of diseases (Chen et al., 2020; Choi et al., 2021; Gong et al., 2021; Jia et al., 2021; Murawski and Gather, 2021; Ong et al., 2021; Reda et al., 2021; Sadighbayan and Ghafar-Zadeh, 2021; Sheikhzadeh et al., 2021; Y. Yang et al., 2021). Quality control to find impurities (Frag et al., 2021; Jouyban and Rahimpour, 2021) and environmental analysis (Ekrami et al., 2021; Ryu et al., 2021; Villemin and Raccurt, 2021) are also one of the prominent topics. In addition, the literature shows a growing demand on analytical methods for food quality control (Balbinot et al., 2021; Lim et al., 2021; Majdinasab et al., 2021; Manoj et al., 2021; Raghavan et al., 2021; Rayappa et al., 2021), including smart food packaging (Rodrigues et al., 2021). There is a deep concern about improve analytical parameters from optical sensors (Ali Hasim et al., 2021; D. M. Kim et al., 2021; Leonardi et al., 2021; B. Li et al., 2021; Nazri et al., 2021; P. Singh et al., 2021; Whelan et al., 2021), moreover, a wide range of materials have been studied for the development of these sensors (C. Kim et al., 2021; Kong et al., 2021; Kurup et al., 2021; Skorjanc et al., 2021). Several reviews indicated the importance of in situ analysis, however not all of them show the possibility to carry out it (Raghavan et al., 2021, Reda et al., 2021, Villemin and Raccurt, 2021, Chen et al., 2020, Sadighbayan and Ghafar-Zadeh, 2021, Rodrigues et al., 2021, Rayappa et al., 2021, Ekrami et al., 2021, Majdinasab et al., 2021, Manoj et al., 2021, Lim et al., 2021). Recent developments show an increasing interest in the use of smartphones as analytical devices (Di Nonno and Ulber, 2021, Reda et al., 2021).

As we can appreciate in the literature mentioned above, one of the current challenges of analytical chemistry is the detection of analytes through in situ

procedures. Optical sensors have demonstrated to be very simple and cost-effective devices. They consist of a recognition element, which interact with a target molecule and a signal transducer, which produce detectable changes in their optical signal. Specifically, colorimetric devices exhibit promising potential thanks to the fact that a color change in the presence of the analyte can be easily detected by naked eye, the color change can take place in solution or in the device. The color change is proportional to the analyte concentration.

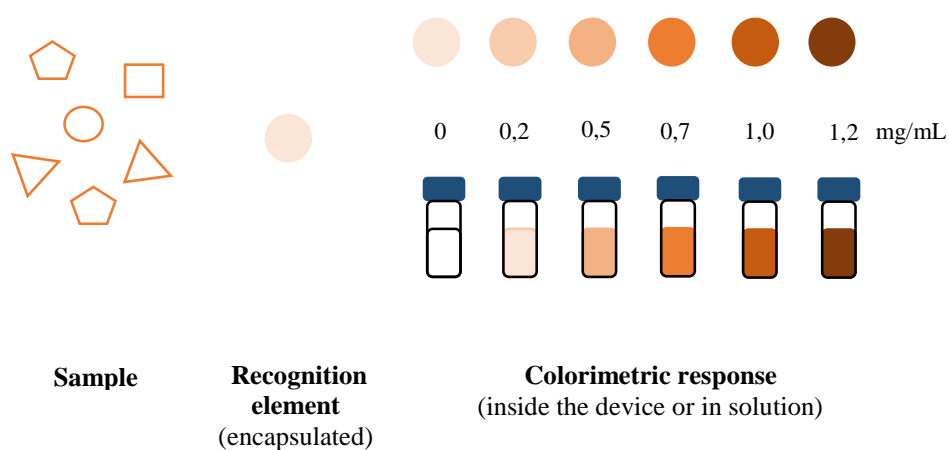


Figure 3. Schematic of a colorimetric device.

Several colorimetric devices have been reported in the literature. *Devices for delivery reagents (Figure 3)* are based on the immobilization of the reagents necessary to carry out a derivatization reaction on a solid support. The methodology consists of immersing the devices in the sample solution. Then, the reagent release from the support to the solution is produced. Finally, the derivatization reaction is carried out in the solution (Jornet-Martínez et al., 2016a; Prieto-Blanco et al., 2015). *Solid sensors* contain a chromophore reactive which is immobilized in a solid support. The reactive is not released,

it is the analyte which diffuses into the sensor. Thus, the derivatization process occurred inside the sensor where a color change is visible. MINTOTA group has developed some (bio)sensor based in this methodology (*Figure 3*) (Argente-García et al., 2016b, 2016a; Argente-García et al., 2017; Jornet-Martínez et al., 2016b; Pla-Tolós et al., 2018). *Test kit* consists in a different reagents solution; when they are in contact with the analyte, a color change can be observed, which is related with the concentration of the analyte. These kits are common to determine pH or chlorine in swimming pools, moreover, they are very useful in forensic analysis and the identification of illicit drugs (Beeharry et al., 2018). Following this line, *test strips* appear as a simple method which have several applications in biomedicine, food and environmental fields (Kriss et al., 2021; Schwenke et al., 2019). These types of devices include chromophores that are immobilized on a solid support, generally paper. The main advantages of test strips are speed, specificity and low cost. In addition, they allow more than one analyte to be measured at the same time. However, test strips only allow to carry out qualitative or semi-quantitative analysis (Chin et al., 2007). *Microfluidic platforms* also allow the analysis of several analytes at the same time. They are miniaturized devices in which the reagents are deposited on a support, generally cellulose. The sample circulates by capillarity, producing a color change when the analyte reaches the area where the reagent is located (Demirkol et al., 2011; Mark et al., 2010). For gas analysis, *colorimetric tubes* appear as the best option. These devices consist of a tube filled with porous material impregnated with a chromophore reagent. Air passes through the tube with a pump producing a color change when the analyte is in contact with the reagent (Coffey and Pearce, 2010; Nash and Leith, 2010). *Colorimetric arrays* are based on multiple colored dyes adsorbed on a support whose color change come from

the interaction with analytes. Pattern recognition is based on the combined response from numerous sensors. Colorimetric arrays allow the analyses and identification of several substances as polysaccharides (Jia et al., 2021), explosives (Fan et al., 2020; Kangas et al., 2017; Zhao et al., 2019), soft drinks (Zhang and Suslick, 2007), environmental analysis (Alberti et al., 2020) and volatile organic compounds (Long et al., 2011). The developed of *plasmonic sensors* are increasing due to the use of metallic NPs such as silver nanoparticles (AgNPs) and gold nanoparticles (AuNPs) as an alternative of reagents. Both substances, AgNPs and AuNPs own a surface plasmon resonance located in the visible region which changes (broad or shift) when they are aggregated due to the contact with the analyte. The analyte can be quantified measuring the optical changes by absorbance or diffuse reflectance (DR). Plasmonic sensors hold high sensitivity and selectivity thanks to the excellent properties of nanoparticles. In the literature, we can find application examples of plasmonic sensors for the analysis in several field such as food (Balbinot et al., 2021; Tseng et al., 2017), medicine (Masson, 2017; S and S, 2016) and environmental analysis (Wei et al., 2015).

Optical colorimetric sensors are usually accompanied by a color chart for one or more analytes, this allows a semiquantitative analysis by visual inspection. A quantitative analysis can be carried out by absorbance, DR measurements and digital image (DI) (Argente-García et al., 2016a; Argente-García et al., 2017a; Jornet-Martínez et al., 2016b; Pla-Tolós et al., 2018; Prieto-Blanco et al., 2015). For the digital image, an electronic device such as scanner or smartphone is necessary (Capitán-Vallvey et al., 2015; Oncescu et al., 2013; Roda et al., 2016). Then, a digital image-processing tool (eg. GIMP or Adobe Photoshop) is used to convert the colors into numeric values. Different color codes can be used according to the method, the most common

are red-green-blue (RGB), cyan-magenta-yellow-black (CMYK), hue-saturation-value (HSV) and luminance-color change from red to green and yellow to blue (CIELAB) (Jornet-Martínez et al., 2021; Martínez-Aviño et al., 2021b). In this Thesis, the model CMYK is employed to perform the quantification of analyte. These models can be subject to interferences such as lighting conditions, which can be corrected by inserting reference points (white and black). Recently, the great advances in the area of telecommunications have allowed the development of applications for the quantification of analytes through devices such as mobile phones or tablets. These applications allow the analysis in real time without prior image treatment (Hosu et al., 2017; Martínez-Aviño et al., 2021b; Vashist et al., 2015).

To sum up, color changes of the colorimetric assays can be carried out in solution or on a solid support. Compared to the solution assays, the use of solid supports is increasing over the years due to several advantages as improve the stability, reduce the amount of reagents their manipulation. Moreover, they enable direct and real-time monitoring of many biological and chemical substances with a high specify, sensitivity and cost-effectiveness.

1.1.2. Electrochemical sensors

According to the trends in exploring sensors for in-situ analysis, electrochemical sensors have received intensive attention. *Table 3* shows covered topics of electrochemical sensors in 33 review articles published from database web of science ('electrochemical' AND 'sensor' review September 2021). During the last 5 years, it has been published more than 2800 reviews concerning to this topic.

Chapter 1. Introduction

Covered Topic	Reference
Graphene-based sensors for food adulterants and toxicants detection	(Raghavan et al., 2021)
Noble metal nanomaterial-based biosensors for respiratory viruses detection	(Choi et al., 2021)
Detection of emerging contaminants	(Ryu et al., 2021)
The use of shaped metal nanoparticles to improve the electrochemical response electrodes	(Torres-rivero et al., 2021)
Detection of trace metals	(Ekrami et al., 2021)
Eco-friendly green synthesis of graphene quantum dots	(Bressi et al., 2021)
Nanocomposites based on graphene and metal materials to determine nitrate/nitrite in food samples	(Akbari et al., 2021)
Non-enzymatic (bio)sensors for detection of pesticide residues	(Majdinasab et al., 2021)
Graphene oxide nanocomposite based for monitoring foodborne pathogenic bacteria	(Yu et al., 2021)
Nanosensing to evaluate liquid foods quality	(Manoj et al., 2021)
Black phosphorus-based electrochemical sensors	(Q. Li et al., 2021)
Electrochemical monitoring of zearaleone in food	(De Rycke et al., 2021)
Biomimetic electrochemical sensors	(Romanholo et al., 2021)
Detection of biomarkers by using potentiometric based biosensors	(Karimi-Maleh et al., 2021)

Chapter 1. Introduction

Covered Topic	Reference
Trends in sensor development for the determination of mercury	(Lim et al., 2021)
Detection of abiotic stress biomarkers in plants	(Z. Li et al., 2021)
Nanoarchitected porous conducting polymers	(Luo et al., 2021)
MXene in electrochemical sensors	(Wu et al., 2021)
Screen-printed electrochemical (bio)sensors to detect estrogens	(Musa et al., 2021)
Pillararene-based self-assemblies to develop electrochemical biosensors	(S. Cao et al., 2021)
Determination of metronidazole in drugs and biological samples	(Meenakshi et al., 2021)
Glucose monitoring systems	(Lee et al., 2021)
Phosphorene and other layered pnictogens as a new source of 2D materials	(Tapia et al., 2021)
Fluorite and perovskite-based dual-ion conducting solid oxide fuel cells	(J. Cao et al., 2021)
Detection of bisphenols in food	(Y. Zhang et al., 2021)
Magnetic nanomaterials for develop electrochemical sensors in food analysis	(Garkani Nejad et al., 2021)
Detection of bromate in water and food samples	(Balogun and Fayemi, 2021)
Electrospun nanofibers to develop electrochemical devices	(Review, 2021)

Covered Topic	Reference
Nanoceria for electrochemical sensing applications	(Hartati et al., 2021)
Conductive 3D-printed electrodes based upon polymers/carbon nanomaterials using a fused deposition modelling	(Omar et al., 2021)
Electrochemical biosensors in food safety	(Curulli, 2021)
Diagnostics of infectious viral diseases	(Goud et al., 2021)
Protein detection by using peptide-based electrochemical biosensors	(Vanova et al., 2021)
Carbon nanomaterial hybrids via laser writing for high-performance non-enzymatic electrochemical sensors	(Simsek and Wongkaew, 2021)

Table 3. Covered topics of the electrochemical sensor in the 33 review articles. Database web of science (access September 2021).

As we can see in the *Table 3*, electrochemical sensors have grown rapidly and have found several applications in biomedical (Choi et al., 2021; Goud et al., 2021; Karimi-Maleh et al., 2021; Lee et al., 2021; Vanova et al., 2021), environmental sensing (Ekrami et al., 2021; Lim et al., 2021; Majdinasab et al., 2021; Musa et al., 2021; Ryu et al., 2021), food (Akbari et al., 2021; Balogun and Fayemi, 2021; Curulli, 2021; De Rycke et al., 2021; Garkani Nejad et al., 2021; Manoj et al., 2021; Raghavan et al., 2021; Y. Zhang et al., 2021), agriculture (Z. Li et al., 2021), pharmaceutical (Meenakshi et al., 2021) among others. In the modern society, specifically in biomedicine, they have been of great value since they allow patients to self-control their medication. This is due to the fact that electrochemical sensors are accurate, selective, easy to use and require small sample volume to determine a clinical

parameter. Moreover, easily they are capable to be portable. Various studies from researchers are focused on increasing the analytical performance, biocompatibility and biodegradability of electrochemical devices by using new conducting materials such as fluorite, pillaranene, nanoceria, black phosphorus among others (J. Cao et al., 2021; S. Cao et al., 2021; Hartati et al., 2021; Q. Li et al., 2021; Luo et al., 2021; Omar et al., 2021; Review, 2021; Romanholo et al., 2021; Simsek and Wongkaew, 2021; Tapia et al., 2021; Torres-Rivero et al., 2021; Wu et al., 2021). Moreover, the continuous increase in environmental impact due to the use of fossil resources has led researchers to study innovative strategies and green routes to carry out eco-friendly analysis (Bressi et al., 2021). Most reviews include sensor developed for in situ analysis (Raghavan et al., 2021, Ekrami et al., 2021, Romanholo et al., 2021, Z. Li et al., 2021, Wu et al., 2021, Musa et al., 2021, S. Cao et al., 2021, Lee et al., 2021, Zhang et al., 2021, Balogun and Fayemi, 2021, Simsek and Wongkaew, 2021).

Electrochemical sensors works are based on the changes of electrical signal due to chemical reactions whose are applicable to quantify analytes. The electrochemical sensors are mainly divided into three types: potentiometric, conductometric, and amperometric or voltammetric. In this Thesis, voltammetric technique has been used to developed an electrochemical sensor (Bocanegra-Rodríguez et al., 2021). Voltammetric sensor monitors the change in current due to redox reaction of an electroactive species with the surface at a certain potential.

The structure of an electrochemical sensor is based on three essential components (see *Figure 4*): the sample or analyte, the recognition element and a transducer to convert the reaction into a measurable electrical signal.

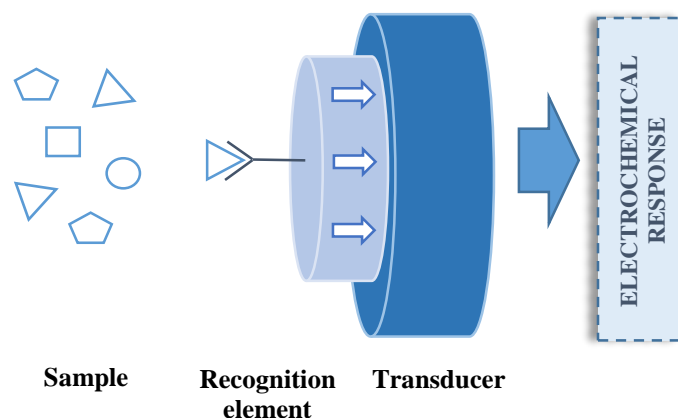


Figure 4. Schematic of an electrochemical biosensor.

The selectivity of the sensor is attributed to the recognition element and the sensitivity is the responsibility of the transducer and the electrochemical technique used. Thus, the good selection of the recognition element is essential to develop analyte-specific electrochemical sensors. Recognition elements usually are enzymes such as glucose oxidase (GOx), glucose dehydrogenase (GDH), uricase, bilirubin oxidase (BOx), laccase among others. The use of enzymes has several limitations; the selection of enzymes has to be deeply studied. Louchis and Driscoll use GOx as enzyme to determine glucose, they were found that the GOx available decreases over time (Louchis and Driscoll, 2011). Laccases generally demonstrate good activity at acidic pH but low activity and/or stability at neutral pH (Le Goff et al., 2015). Both enzymes, laccases and BOx are degraded or inhibited by ubiquitous hydrogen peroxide (H_2O_2) and halogens such as chloride (Antiochia et al., 2019; Valles et al., 2020). The emergence of advanced nanomaterials has shown a remarkable research interest into the development of non-enzymatic sensors. Many researchers have paid attention to these materials due to the several advantages that they offered such as similar sizes to enzymes and easy functionalization, high surface area and attractive

electrical conductivities (Ali A. Ensafi et al., 2016). Despite the tremendous effort made by various authors to develop medical electrochemical dispositives based in enzyme-free sensors, they have found many limitations. Nanomaterials such as Co, Ni and Cu, which electrocatalyze the glucose oxidation reaction, works under alkaline pH conditions. Pt nanomaterial has special interest since it operates under physiological pH. In addition, the synergic effect in electrochemical sensor produces by bimetallic nanostructures has also studied. It is described in the literature that Pt-based alloy catalysts exhibited better catalytic activity, biocompatibility and long-term stability than pure Pt. Cu or other metals is often added to Pt (Cao et al., 2013; Zhang and Yang, 2017).

Moreover, the selection of the transducer is also important in order to design electrochemical sensors. The most widely used transducers in electrochemistry are carbon-base material, gold and silver nanoparticles. Carbon-base material include carbon nanotubes (CNTs), graphene, carbon/graphene quantum dots, mesoporous carbon and carbon black. These materials have been used in electrochemical sensing applications due to their great properties such as high chemical stability, high electrical conductivity and high surface/volume ratio. Carbon/graphene quantum dots are considered one of the most promising materials due to the lower toxicity and large number of functional site. In addition, carbon-based nanomaterials can improve their electrochemical properties by functionalizing or combining with metal ions and organic metal skeletons (Hu and Zhang, 2020). Gold and silver nanoparticles have a special interest since they have high porosity, provide excellent electron transfer rates and are biocompatible (Juska and Pemble, 2020; Nantaphol et al., 2015).

In addition, the use of polymers for the development of electrochemical sensors has attracted considerable attention. Polymers have free amine and alcohol groups which can improve the biomolecules immobilization such as enzymes, DNAs and antibodies/antigens. Moreover, polymers can ensure the high electron transfer rate, stability and biocompatibility of electrochemical (bio)sensors. The most used polymers included chitosan (Karrat and Amine, 2020; Zhang et al., 2014), dextran (Aziz et al., 2020; Heurich et al., 2011), zein (Rouf et al., 2020) and nanocellulose (Golmohammadi et al., 2017) among others. Incluir algo más sobre la modificación con pirenos. Tienes una introducción bastante extensa en el artículo de eléctricos.

Hence, the general aim of this Thesis is the investigation of (nano)and (bio) materials for their application in the development of in situ analysis devices to achieve the new challenges of the analytical chemistry.

1.2. MATERIALS

Over time a wide variety of materials have been used, however, due to socio-political reasons, the use of new materials is being investigated. There is an increasing interest in using (bio)polymers to replace and reduce the consumption of conventional polymers derived from petroleum, such as polyethylene, acrylics, and polycarbonate (Xia and Larock, 2010).

Investigation of new materials is a trend in Analytical Chemistry. Over the last decade nanomaterials have been considered very important in the development of (bio)sensors. The large specific surface area is very useful for

immobilization of (bio) molecules. These materials have unique physicochemical properties which are difficult to find in small molecules.

In this Thesis, materials with different properties have been studied in order to use them as solid supports for developing in situ devices. *Table 4* shows features of different solid supports described in the literature in order to obtain a broad vision of materials. Zein and paper are both the most available materials, due to their cost is very low. However, paper is the most known. In the literature, there are several developed paper-colorimetric sensors for its application in different areas such as medical (Ali et al., 2019; G. Dai et al., 2017), environmental analysis (Wang et al., 2018; Li et al., 2019; Bordbar et al., 2019), food control (Kim et al., 2018; Popa et al. 2020) and beverage industry among others (Wang et al., 2016). Jornet-Martínez et al. have proposed a biokit based on zein film to delivery alkaline phosphatase and substrates (Jornet-Martínez et al., 2016), moreover, Alqahtani et al have been used zein in the pharmaceutical industry to oral drug delivery (Alqahtani et al., 2017). On the other hand, polydimethylsiloxane (PDMS) is widely employed as support material for embedding chromogenic reagents, quantum dots and nanoparticles (Jornet-Martínez et al., 2021, 2018a; N. Jornet-Martínez et al., 2019b; Pla-Tolós et al., 2018). Pla-Tolós et al. have been proposed a PDMS glucose biosensor integrated in a multi-well microplate to analyse human serum samples (Pla-Tolós et al., 2018). As PDMS is transparent, the colorimetric response can be determined without interferences in the measurement. The high surface/volume ratio and homogeneity among others properties of nylon it has been selected as a support material for the development of a plasmonic assay based on the aggregation of silver nanoparticles (Jornet-Martínez et al., 2019). Yuan et al. have proposed a nylon support to develop a flexible and breathable strain

sensor (Yuan et al., 2020). Sol-gel support composed by tetraethylortosilicate/methyltriethoxysilane (TEOS/MTEOS) are highly porous, thus a large diffusion can be carried out (Serra-Mora et al., 2018a). Glass is also used as support material, a humidity sensor using microfiber-ZnO nanorods coated glass structure is reported in the literature (Jali et al., 2021). Carbon nanotubes (CNTs) also provide high surface/volume ratio, moreover, CNTs are a conducting material very useful to develop electrochemical sensors due to their unique electronic, chemical and mechanical properties (Amin et al., 2020; Deep et al. 2018; Argente-García et al., 2016). On the other hand, the humidity has a huge impact on the electrical conductivity (Shooshtari et al., 2021). Ahamed et al. have compared different materials such as glass, CNT, paper among others to study the environmental footprint of voltammetric sensors (Ahamed et al., 2021).

From all these materials, zein, nylon, PDMS, TEOS/MTEOS, nanocellulose and CNTs have been selected in this Thesis as supporting materials for developing in-situ sensors due to their advantages that will be exhaustively assessed below.

Properties	Zein	Nylon	PDMS	TEOS/ MTEOS	Silica	Glass	Paper	CNTs
Surface/volume ratio	High	High	Low	High	Low	Low	High	High
Flexibility	Medium	Yes	Yes	No	No	No	Yes	Yes
Fluid flow	Diffusion	Capillarity	Diffusion	Diffusion	Forced	Forced	Capillarity	-
Humidity effect	Yes	No	No	Yes	No	No	Yes	Yes
Easy availability	Yes	No	No	No	No	No	Yes	No
Easy handling	Medium	Yes	Medium	Yes	No	No	Yes	No
Homogeneity	Yes	Yes	Yes	Yes	Yes	Yes	No	Yes
Cost	Low	Low	Low	Low	High	Medium	Low	Medium

Table 4. Features of different solid supports. See text for more explanation.

1.2.1. Zein

Zein is a biodegradable material being a protein from corn. It is mainly obtained as a waste of bioethanol manufacturing. Bioethanol production from corn utilizes drygrind processing, leaving behind protein-rich distiller's dried grains with solubles (DDGS) as a byproduct, which later on is used as low cost feedstock. The zein is extracted from DDGS (Shukla and Cheryan, 2001). The production of bioethanol from corn has increased over the years, and therefore, as a byproduct, zein can be obtained in large amounts at low cost. The study of the extraction and processing processes of zein, as well as its discoloration, is increasing due to its characteristics have a high value in the industry (Ali et al., 2021; Du et al., 2020). This fact is reflected in *Figure 5*, which shows the number of citations on the zein since 2010. As can be seen, the number of citations since 2010 has increased exponentially. This is due to social awareness about the use of biodegradable materials. The use of plastic is being seriously affected since it produces wastes which are not degraded, posing serious problems for the environment.

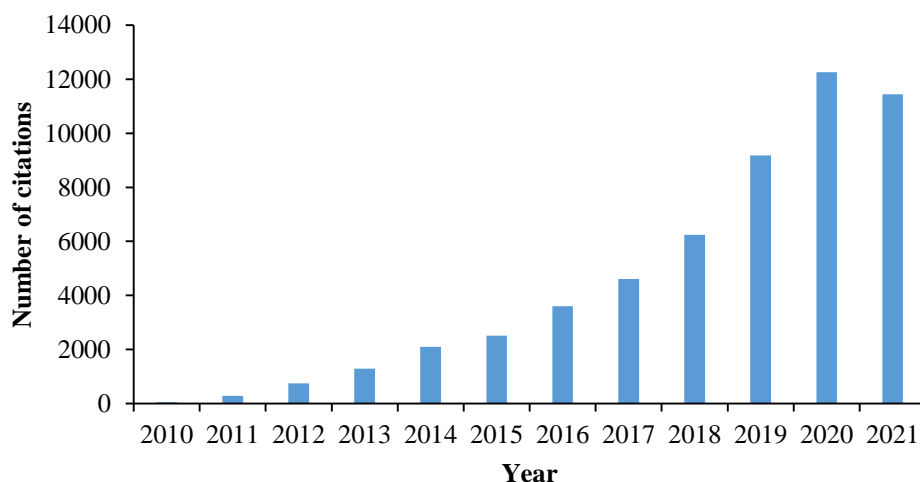


Figure 5. Number of citations on Web of Science for matching the following search term 'zein' in the 2010-2021 period (September 2021).

Figure 6 shows record count versus the investigation area since 2010. Zein is a widely used material in different areas such as chemistry, material and food science technology, molecular biochemistry, nutrition dietetics cell biology, agriculture and pharmacology among others.

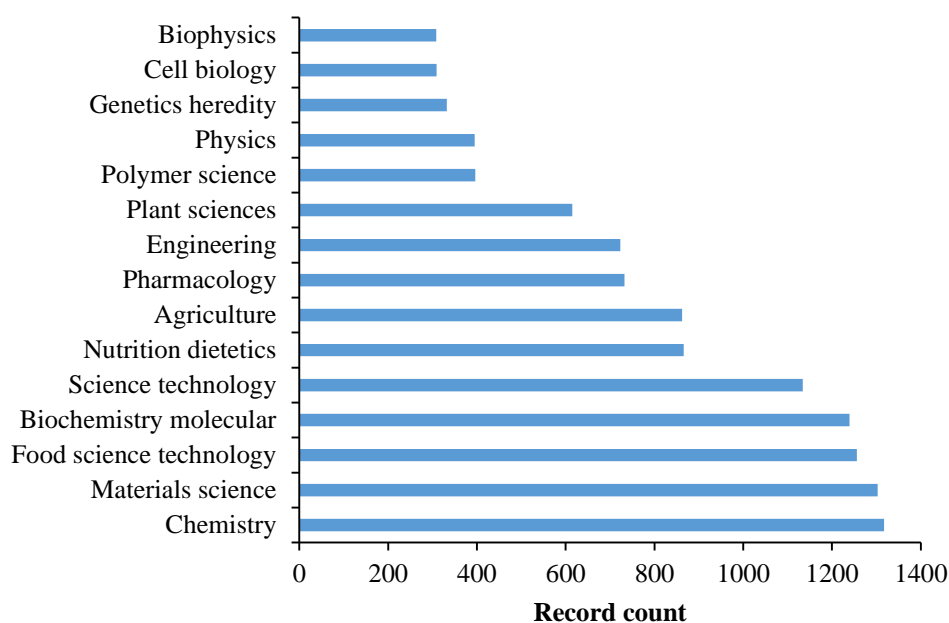


Figure 6. Number of record account on Web of Science for matching the following search term 'Zein' in the 2010-2021 period (September 2021).

Zein is comprising by a mixture of different peptides that have several molecular sizes, solubilities, and charges see Table 5 (Ali et al., 2021; Postu et al., 2019; Shukla and Cheryan, 2001). It is a heterogeneous protein that can be divided into α -Zein, β -zein and δ -zein. Specifically, α -Zein (22 and 24 kDa) is the most abundant prolamin in corn, achieving more than 35% of the total zein content (Jouber et al., 2001; Torres-Giner et al., 2008). Zein is rich in hydrophobic amminoacids as leucine (20%), proline (10%) and alanine (10%), although it also has an important content in glutamic acid (21–26%) which is a hydrophilic amminoacid. Thus, zein cannot be dissolved in water,

but it is soluble in 95% aqueous alcohol, 85% aqueous isopropanol, highly concentrated aqueous urea solutions, aqueous alkaline solutions (pH 11) and in anionic detergent-containing solutions (Lawton, 2002; Momany et al., 2006; Postu et al., 2019). This strong hydrophobicity makes zein a unique natural biopolymer, and its manipulation has resulted in the development of films, gels, coatings, and micro- and nano-particles. Although, proteins have been used in some fields, like alimentary and pharmaceutical industries (Alqahtani et al., 2017; Liang et al., 2017; Lu et al., 2017; Zou et al., 2017), not many applications have been performed in the analytical field or in sensor fabrication (Farhadi et al., 2014; Gezer et al., 2016; Jangju et al., 2017; Jornet-Martínez et al., 2016a). Zein has excellent properties to form films thanks to its chemical structure. The films obtained are permeable to gas and organic solvents with low polarity, moreover are resistant, hard but breakable. Experimentally it has been shown that zein can be used together with other materials to modify their own properties. Components such as glycerol, sorbitol, oleic acid, diethyl tartrate and sucrose allow modifying its plasticity and achieving a more flexible film. In addition, it is demonstrated that zein allows the immobilization and stabilization of different compounds, such as enzymes, metallic salts, and aromatic and small organic compounds (Jornet-Martínez et al., 2016a; Luo and Wang, 2014; Paliwal and Palakurthi, 2014; Subramanian and Sampath, 2007). These studies show that zein is a versatile material that allows its use in different fields, at the same time, it presents low cost, biocompatible and sustainable, thus, zein is an attractive alternative to conventional materials such as petroleum derivatives.

In this thesis, based on the properties previously described, it is intended to evaluate the Zein as support material for reagents delivering (section 4.1).

	Characteristics	Observations	Studies and applications	Reference
Composition	Rich in glutamic acid, leucine, proline and alanine	Poor in basic and acidic amino acids	Physico-chemical and biological characterization	(Ali et al., 2021)
Molecular weight	About 40 kDa	α -Zein (22 and 24 kDa), β -zein (24, 22, and 14 kDa), δ -zein (18 and 27 kDa)	Zein as drug delivery	(Torres-Giner et al., 2008)
Extraction	1) Filtration protocol 2) Solubility method	1) using NaOH/H ₂ SO ₄ 2) Using NaOH/Urea	-	(Ali et al., 2021)
Solubility	Hydrophobic	Soluble in alcohol, aqueous alcohol, aqueous isopropanol, highly concentrated aqueous urea and in anionic detergent-containing solutions. Soluble pH 11	Mass spectrometric characterization of zein	(Postu et al., 2019)
Optical	Yellow	Zein decolorization via low-temperature precipitation and via activated carbon	Zein recovery and pigment clearance rates	(Du et al., 2020)
Mechanical	Permeability	Permeable to gas and organic solvents with low polarity. No permeable to water. Low water vapour permeable. Plasticizers as glycerol increase the water permeability	Material for effective delivery of reagents	(Jornet-Martínez et al., 2016a)
	Flexibility	Elastic		
Toxicity	No toxic	Biocompatible and biodegradable	Synthesis of zein-coated Au nanoparticles	(Suganya et al., 2017)
Manufacturer	Sigma Aldrich	174€/kg	-	Zein Product Information (Sigma Aldrich)
Fabrication sensor	Easy	Zein, ethanol, glycerine and water. Mix and repose 8h at room temperature	Delivering reagents and enzymes.	(Jornet-Martínez et al., 2016a)

Table 5. Zein.

1.2.2. Nylon

Nylon is a synthetic polymer composed of an amidic group in the main chain. The general formula is $[C_6H_{11}NO]_n$ (Thongsai et al., 2020). Different types of nylon are denoted by the number of monomers such as nylon 6, nylon 66, nylon 12 among others. Nylon is available as an homopolymer, co-polymer or reinforced. Nylon might also be blended with other engineering plastics to improve determined aspects of performance. *Figure 7* shows record count versus the investigation area since 2010. Nylon is a widely used material in different areas such as materials science, engineering, chemistry, science technology, physics and polymer science among others.

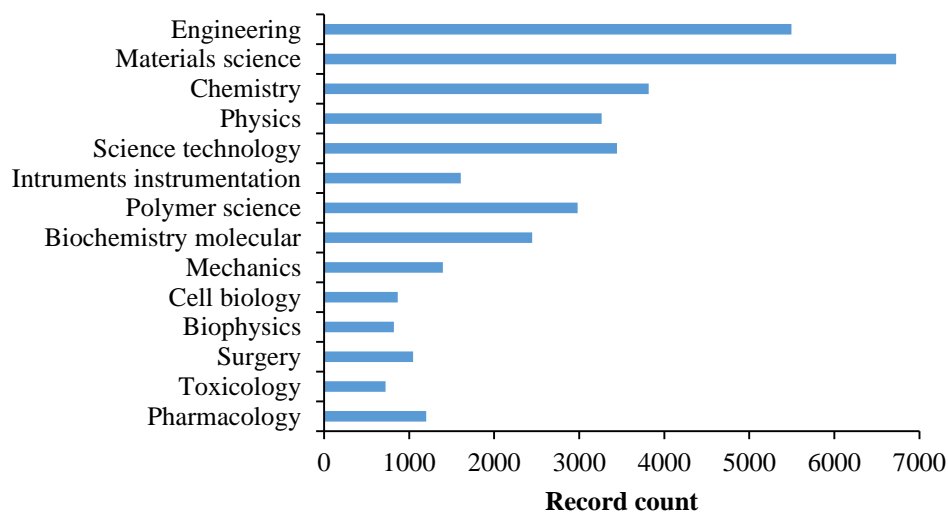


Figure 7. Number of record count on Web of Science for matching the following search term 'Nylon' in the 2010-2021 period (September 2021).

Nylon can be synthesised by two methods (see *Table 6*). The first via involves a polycondensation reaction between a diacid chloride and a diamine (Pandey et al., 2018) and the second method includes a polymerization reaction of an amino acid or opening up a monomer containing a lactam ring (Mukhopadhyay, 2009). Nylon is hydrophilic and as membrane is widely used for particle removing filtration in both aqueous and organic solvent for

analytical determination. Nylon membranes are chemically resistant to organic solvents and alkaline solutions. Moreover, nylon membranes are materials with highly porous structures that can provide a large specific surface area for biomolecular immobilization (Farahmand et al., 2015; Kenji Onodera, Jean d'Offay, 2002). They can be sterilized in an autoclave at 121°C or 134°C and, ethylene oxide and gamma irradiation. Nylon has high thermal stability although is thermoformable. It has great tensile and low mechanical strength (Mukhopadhyay, 2009; Yuan et al., 2020). As nylon is chemically inert, no toxic and no induces inflammatory reaction, it has relevance in clinical use (Dart and Dart, 2011). No form of nylon is biodegradable although it is being studied the biodegradability of nylon 4 in the natural environment (Tachibana et al., 2013).

In the literature, different applications of nylon are described due to the excellent mechanical, thermal properties and high chemical resistance. Moreover, nylon can be combined with other polymers or plastics such as chitosan, polypropylene, polyvinyl alcohol among others to design materials with specific properties (Nunes and Magalhães, 2016; Wei et al., 2021; C. Zhang et al., 2021). Nylon has also the capacity to easy to dye, thus, colorimetric sensors can be developed for semiquantitative analysis by visual inspection or quantitative analysis (Bocanegra-Rodríguez et al., 2020a; Fu et al., 2021). Nylon have been widely used in the textile industry during year, however, in the last decade, nylon is being replaced by polyester due to low price production and similar proprieties (Mukhopadhyay, 2009).

In this Thesis, a colorimetric sensor based on pyrogallol red (PGR) and 1,10-phenanthroline (1,10-phen) immobilization on nylon membrane has been developed to detect silver ions from refrigerate water which are responsible of Legionella control (section 4.2).

	Characteristics	Observations	Studies and applications	Ref
Chemical formula	$[C_6H_{11}NO]_n$	-	Nylon 6 derived CDs	(Thongsai et al., 2020)
Pore size	0.22 and 0.45 μm	-	-	Nylon membrane product information Sartorius
Synthesis	Polycondensation	Diacid chloride and a diamine	Use of polymers	(Pandey et al., 2018)
Solubility	Hydrophilic	Non soluble. Particle-removing filtration of water, aqueous solutions and solvents	Nylon 6 films spin coated onto different substrates	(Zhou et al., 2013)
Optical	White	Change to color after filtration the dye	Development of a colorimetric assay for H_2O_2	(Tong et al., 2016)
Mechanical	Permeability Flexibility	Good gas permeability. Great tensile and low mechanical strength	MXene/nylon fabric network sensor	(Yuan et al., 2020)
Thermic	Insulate	High thermal stability	Treatment of Nylon 6,6 for water filtration	(Syakinah et al., 2019)
Reactivity	Inert	No induce inflammatory reaction	Properties of suture materials	(Dart and Dart, 2011)
Toxicity	No toxic	No biodegradable	Study of nylon 4 biodegradability	(Tachibana et al., 2013)
Manufacturer	Vidrafoc	46€/100uds.	Membrane 13mm and 0.22 μm pore	Nylon membrane product information Sartorius
Fabrication sensor	Easy	Introduce de solution with a syringe	Silver Nanoparticles on Nylon	(Neus Jornet-Martínez et al., 2019)

Table 6. Nylon properties

1.2.3. Siloxane groups materials

Siloxane materials include –Si-O repeat units. Traditional silicones have insufficient mechanical toughness, poor interfacial adhesion, and lacking recyclability, however, the implementation of dynamic design into siloxane-based materials have solve several limitations. These materials have exceptional physicochemical and mechanical properties; therefore, they pose a wide range of applications in daily life and industry.

1.2.3.1. PDMS

PDMS is a widely used material in different areas such as engineering, materials science, chemistry, physics, science technology among others. This fact is reflected in *Figure 8*, which shows the record count versus the investigation area since 2010.

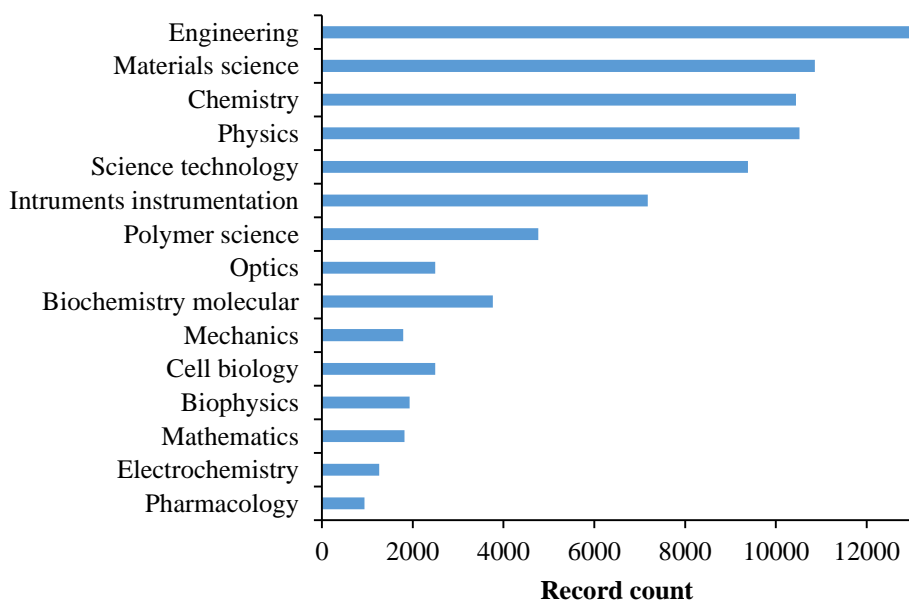


Figure 8. Number of record count on Web of Science for matching the following search term 'PDMS' in the 2010-2021 period (September 2021).

PDMS is a silicon-based homopolymer characterized for the covalent bonds of several units of $[-\text{Si}(\text{CH}_3)_2\text{O}-]_n$ groups (see *Table 7*). PDMS usually forms long chains where the molecules can rotate around the covalent bonds which provides flexibility (Kahveci et al., 2017; Mata et al., 2005). Its molecular weight is variable and depends on the length of the chains (Mojsiewicz-Pieńkowska, 2012). The synthesis of PDMS usually is carried out through a hydrosilylation catalytic reaction (Lukin et al., 2020). PDMS is a hydrophobic material which swells in contact with nonpolar solvents. The degree of swelling depends on the solubility of the solvent in PDMS. Several studies have evaluated the compatibility of solvents through the solubility parameter (Lee et al., 2003; Vinothkumar et al., 2011). As PDMS is permeable to gas and organic solvents with low polarity, PDMS devices can be used to extract analytes from aqueous media. Moreover, PDMS is optically transparent and it is possible the covalent immobilization of reagents inside the device (Ali Hasim et al., 2021). Thus, PDMS composites can be used to the analysis and quantification of analytes which penetrates inside the device without color interferences from PDMS (Argente-García et al., 2017b; Jornet-Martínez et al., 2016d; N. Jornet-Martínez et al., 2019b). The PDMS hydrophobicity can sometimes be a limitation, however, several studies propose its modification with physical treatments such as plasma oxidized and chemical treatments such as polyvinyl alcohol (PVA) (Trantidou et al., 2017), polyethylene glycol (PEG) (Long et al., 2017; Zhu et al., 2018), ionic liquid (1-methyl-3-octylimidazolium hexafluorophosphate) (Ballester-Caudet et al., 2021) among others. In addition, PDMS can also be used as support material for the covalent immobilization of molecules onto its surface. In order to perform it, a combination of different procedures which first step consist in an activation process is necessary to carry out the covalent

binding (Ibarlucea et al., 2011; Kreider et al., 2013; Sassolas et al., 2012). One of the main applications of PDMS is their use as embedding or encapsulation agent of electronic components in the circuit chips (Chang and You, 2020). It is noteworthy that PDMS shows low chemical reactivity, good thermal stability, biocompatibility (Jornet-Martínez et al. 2016b) and has a non-toxic nature, thus, it is a versatile material and it can be used in several fields such as biomedicine (catheters, dialysis membranes, micro valves, adaptive lenses) (Victor et al., 2019), cosmetic (Kuah and Loh, 2016) or engineer (microchips) (Gale et al., 2016) among others. In addition, PDMS is a material easy to use and cheap (Martínez-Aviño et al., 2021b).

In this thesis, based on the properties previously described, it is intended to evaluate the PDMS as a support material for the development of portable sensors (section 4.3.1).

	Characteristics	Observations	Studies and applications	Ref
Chemical formula	$[-\text{Si}(\text{CH}_3)_2\text{O}-]_n$	-	Stabilization of formaldehyde into PDMS	(Jornet-Martínez et al., 2019a)
Molecular weight	0.237-139 KDa	-	Quantification of dimeticone and simeticone	(Mojsiewicz-Pieńkowska, 2012)
Synthesis	Hydrosilation reaction catalyzed with platinum	Homogeneous catalysis High reproducibility and selectivity	Hydrosilation reactions used in the organosilicon industry	(Lukin et al., 2020)
Solubility	Swell	Solvents between 7.3–9.5 cal $\frac{1}{2}$ cm-3/2 are soluble Solvents ≥ 9.5 cal $\frac{1}{2}$ cm-3/2 are no soluble	Organic solvents as chloroform, ether and xylene	(Vinothkumar et al., 2011)
Optical	Transparent	Transparent down to 240 nm	PDMS for microfluidic platforms	(Ali Hasim et al., 2021)
Mechanical	Permeability Flexibility	Permeable to gas and organic solvents with low polarity. No permeable to water. Flexible and elastic	PDMS for biomedical micro and nanosystems	(Mata et al., 2005)
Thermic	Aislant	Stable between -45 and 200 °C	-	Sylgard Elastomer 184 Kit Product Information
Reactivity	Inert	No react with several chemicals	Analyse microelectromechanical systems	(Gale et al., 2016)
Toxicity	No toxic	Biocompatible and no biodegradable	Delivery of reagents to determine ammonium	(Prieto-Blanco et al., 2015)
Manufacturer	Dow Corning Sylgard 184	165 €/Kg	-	Sylgard Elastomer 184 Kit Product Information
Sensor fabrication	Kit	Mix elastomer base and curing (10:1)	Quantification of ammonium and proline	(Prieto-Blanco et al., 2019)

Table 7. PDMS

1.2.3.2. TEOS/MTEOS

TEOS and MTEOS are the most common reagents used in the fabrication of silica sol-gel materials. These reagents have innumerable applications in different areas such as material science and engineering. This fact is reflected in *Figure 9* where is shown the record count versus the investigation area since 2010.

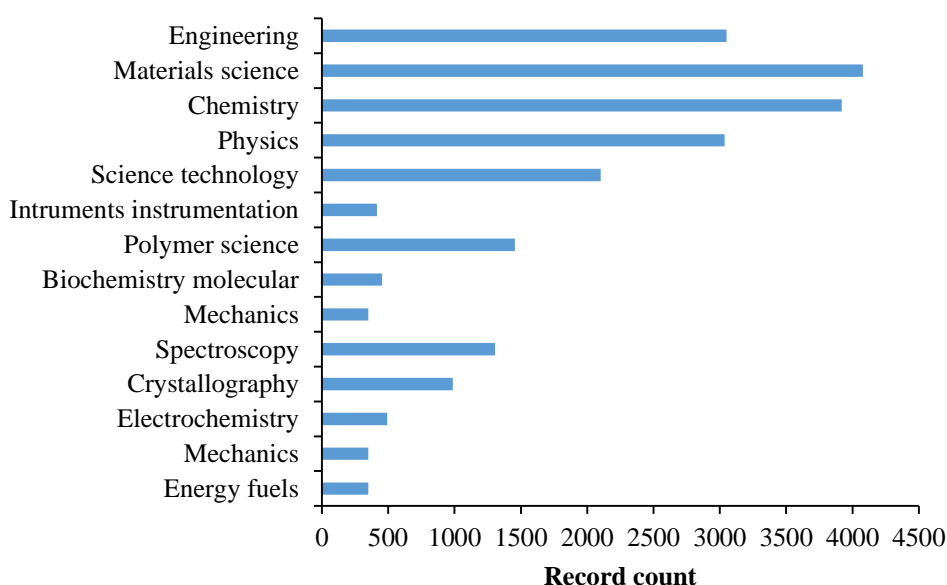


Figure 9. Number of record count on Web of Science for matching the following search term 'TEOS' or 'MTEOS' in the 2010-2021 period (September 2021).

TEOS is characterize for the covalent bonds of several units of $\text{SiCH}_3(\text{OCH}_2\text{CH}_3)_3$ and MTEOS is composed of several units of $\text{Si}(\text{OCH}_2\text{CH}_3)_4$ (Ciriminna et al., 2013). *Table 8* shows several characteristics of TEOS, MTEOS and sol-gel material. Both reagents are hydrophobic. The sol gel formation process starts with a basic or acid hydrolysis with the posterior condensation. Through condensation reactions between colloids, the evolution of the sol gives rise to the formation of a porous solid network. Parameters such as sol pH, solvent content, processing temperature and

drying conditions affect to the porosity of the sol gel. Basic catalysis produces a slow hydrolysis and fast condensation giving to highly branched particulate structures with large average pore sizes and high surface area. It is permeable to gas, organic solvents and water (McDonagh et al., 2002). Sol gel can be combined with plasticizers such as polymethylmethacrylate (PMMA) or PEG to increase the flexibility of the material and produce uncracked films. Sol gel supports usually present good chemical and thermal stability (Kunst et al., 2017). They are transparent in the UV and visible spectral range, thus, they are widely applied in analytical chemistry by using optical techniques such as chemiluminescence, fluorescence and spectroscopy (Owens et al., 2016). Moreover, TEOS-MTEOS sol-gel have the capacity of act as sorbent material, Serra et al have proved TEOS-MTEOS for the on-line enrichment of many organic pollutants from aqueous matrices prior to their analysis by liquid chromatography (LC) material for in-tube-solid-phase microextraction (IT-SPME) (Serra-Mora et al., 2018b). Moreover, TEOS-MTEOS can be reinforced with several particles such as silica nanoparticles (SiO₂ NPs) (Serra-Mora et al., 2018b), TiO₂ nanoparticles (Lin et al., 2008) and Fe₃O₄ NPs (Moliner-Martínez et al., 2012) among others in order to modify the interaction with the analyte.

As can be observed in the literature, sol gel materials are found in applications of cutting-edge scientific fields such as the preparation of nanostructured materials, encapsulation of biological materials or preparation of membranes, coatings and sensors (Ashraf et al., 2015; Ciriminna et al., 2013; Owens et al., 2016; Wang and Bierwagen, 2009).

In this thesis, based on the properties previously described, it is intended to assess the TEOS/MTEOS sol-gel as support material to develop chemiluminescent sensors (section 4.3.2).

	Characteristics	Observations	Studies and applications	Ref
Chemical formula	MTEOS: SiCH ₃ (OCH ₂ CH ₃) ₃ TEOS: Si(OCH ₂ CH ₃) ₄	Low viscosity of TEOS allows it to penetrate in the stone	Applications of silica-based materials	(Ciriminna et al., 2013)
Solubility	Hydrophobic	Large number of Si OH groups	Properties of silica aerogels	(Rao et al., 2003)
Optical	Colorless	Transparent in the UV and visible spectral range	Applications of silica-Based Materials	(Owens et al., 2016)
Mechanical	Permeability Flexibility	High porosity. Permeable to gas, organic solvents and water. Flexible with plasticizers	Porosity for oxygen sensor	(McDonagh et al., 2002)
Thermic	Stable	Resistant to thermal degradation	Effect of plasticizers	(Kunst et al., 2017)
Manufacturer	Sigma Aldrich	TEOS: 61.30€/L MTEOS: 58.90€/250g	-	TEOS and MTEOS Product Information (Sigma Aldrich)
Fabrication sensor	Easy	TEOS, MTEOS, water and NH ₄ OH 0.1 M. Heat at 40°C for 4h.	Comparison of IT-SPME coupled to nano LC and capillary LC	(Serra-Mora et al., 2017)

Table 8. TEOS and MTEOS

1.2.4. Nanomaterials

Nanotechnologies involve designing and producing structures at a very small scale, 100 nanometres or less. Nanotechnology has a high potential in the material field which include nanoparticles, nanopolymers, organic nanomaterials and carbon-based among others. Thus, nanomaterials are one of the main products of nanotechnologies. Specifically, nanomaterials have gained great attention from many researchers in the area of sensor technology. They have high surface area for the functionalization and display unique properties such as high physical and chemical stability (Akgöl et al., 2021; Kurup et al., 2021).

1.2.4.1. Bacterial nanocellulose

Nanocellulose is a linear rigid chain homopolymer composed of β -1,4-linked anhydro-D-glucose units. Specifically, bacterial nanocellulose is produced by bacterial strain such as *Gluconacetobacter xylinus*, *Axylinum* and *Lactobacillus mali* among others (Jozala et al., 2016; Stanisławska, 2016). The production is carried out in a solution with several nutrients, glucose as carbon source, $\text{pH} < 5$ and optimal temperature (25-290°C). These parameters can be varied depend of the bacterial strain, moreover, each bacterial strain have its own efficiency (Stanisławska, 2016).

In the last years, bacterial nanocellulose (BNC) has been drawing enormous attention because of its remarkable physical and chemical properties. BCN is a widely used material in different areas such as materials science, chemistry, science technology, engineering, polymer science and molecular biochemistry among others. This fact is reflected in *Figure 10*,

which shows the number of record count versus the investigation area since 2010.

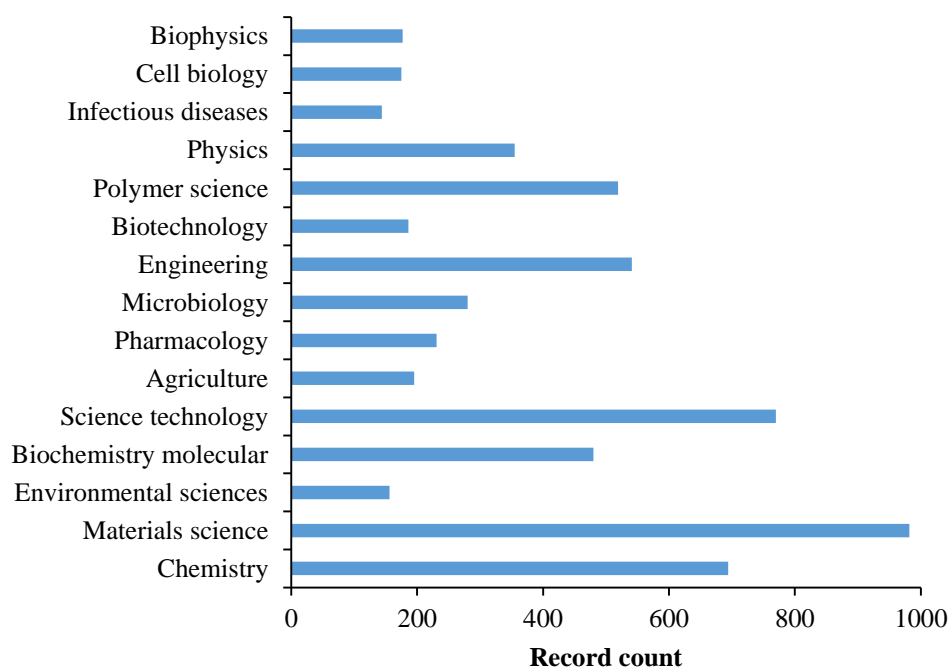


Figure 10. Number of record count on Web of Science for matching the following search term 'Bacterial nanocellulose' in the 2010-2021 period (September 2021).

BNC is hydrophilic and present high capacity of hydration, in contact with water swells (Abol-Fotouh et al., 2020) (see *Table 9*). Optically, BNC is transparent or white (Stanisławska, 2016). BCN is a porous material which is permeable and it can act as adsorbent material. Moreover, its surface contains a plentiful of hydroxyl groups which can easily be modified, thus it can be functionalized (Dai et al., 2019; Phanthong et al., 2018). BCN has high chemical purity, it is biocompatible, hypoallergenic and no toxic, thus, it is widely used in medicine and cosmetic. In addition, it is biodegradable (Stanisławska, 2016).

As it can be seen, BCN offers several advantages compared with other biomaterials due to its good mechanical strength, high flexibility, high absorbency, the possibility of forming any shape and size, eco-friendly processing, and low production costs among others. It is described in the literature the use of bacterial nanocellulose membranes to remove heavy metals, dyes, dissolved organic pollutants, oil and other undesired chemicals from waste water (Dai et al., 2019; Voisin et al., 2017). BCN can be used in electrochemical sensor in order to improve electrode flexibility however, it is not exploited as part of the catalytic matrix to enhance bioelectrocatalysis (Tominaga et al., 2020; Yuen et al., 2019). BCN is nonconductive material, nevertheless, it can be introduced into their matrix electroactive (nano)materials (Golmohammadi et al., 2017). Wang and coworkers developed a second-generation horseradish peroxidase (HRP) biosensor based on gold nanoparticles with a quinone mediator and bacterial cellulose that offered high performance. The absence of comparative data limits makes it difficult to define the enhancement effects specifically related to the nanocellulose (Wang et al., 2011). BCN is getting attentions due to its versatile properties, it is widely used in medicine (Cherian et al., 2013), pharmaceutical industry (Cabral, 2018), cosmetology (Almeida et al., 2021), textile fabric (Felgueiras et al., 2021), paper industry (Skočaj, 2019), environmental protection (Shufang et al., 2013) and food industry (Azeredo et al., 2019), among others.

In the present thesis, the addition of nanocellulose was studied in an electrochemical H_2O_2 sensor (see section 4.4) in order to improve the catalytic current and stability.

	Characteristics	Observations	Studies and applications	Ref
Chemical formula	[D-glucose] _n	β-1,4-linked	Extraction and application of nanocellulose	(Phanthong et al., 2018)
Synthesis	Bacterial strain	Gluconacetobacter xylinus among other	Different efficiency	(Jozala et al., 2016)
Solubility	Hydrophilic	High capacity of hydration	Low cost bacterial nanocellulose production	(Abol-Fotouh et al., 2020)
Optical	White and transparent	Applications is medicine: Artificial leather, vascular implants, dental implants	Bacterial nanocellulose applications	(Stanisławska, 2016)
Mechanical	Permeability Flexibility	Porous material. Highly permeable. Flexible	Absorb pollutants, heavy metals, dyes	(Dai et al., 2019)
Electrical	Nonconductive	Introduce conducting electroactive (nano)materials into their matrix	(Bio)sensing applications	(Golmohammadi et al., 2017)
Reactivity	Several compounds	Can be modified chemically due to the numerous hydroxyl groups	Nanocellulose as advanced materials	(Zhu and Lin, 2019)
Toxicity	No toxic	Biocompatible and biodegradable	Bacterial nanocellulose in medicine	(Stanisławska, 2016)
Manufacturer	Nano Novin Polymer Co.	85 €/kg	Bacterial nanocellulose gel (1%)	(Jozala et al., 2016)
Fabrication sensor	Easy	Mix with phosphate buffer and leave to dry at room temperature	Crocin bacterial nanocellulose membrane	(Abba et al., 2019)

Table 9. Bacterial nanocellulose properties

1.2.4.2. Carbon nanotube

CNT is one form of allotropes of carbon as the diamond and graphite. They were discovered by a Japanese scientist Sumio Iijima in 1991 (Iijima, 1991). The structure of CNT consists of graphene sheet rolled up into a cylindrical shape with diameter of the order of a nanometer. There are two main types of CNT, single-walled carbon nanotubes (SWCNTs) which consist of a single layer of graphite rolled into a seamless cylinder and multi-walled carbon nanotubes (MWCNTs) which are formed by the rolling of multiple layers of graphite on themselves by van der Waals forces to form a tube shape (Eatemadi et al., 2014; Ganesh, 2013). The size, shape, and properties make CNTs a potentially revolutionary material for diverse applications in electronic devices, drug carriers, electrochemical and biological sensors, among many others (Tian et al., 2013). This fact is reflected in *Figure 11*, which shows the number of registers versus the investigation area since 2010.

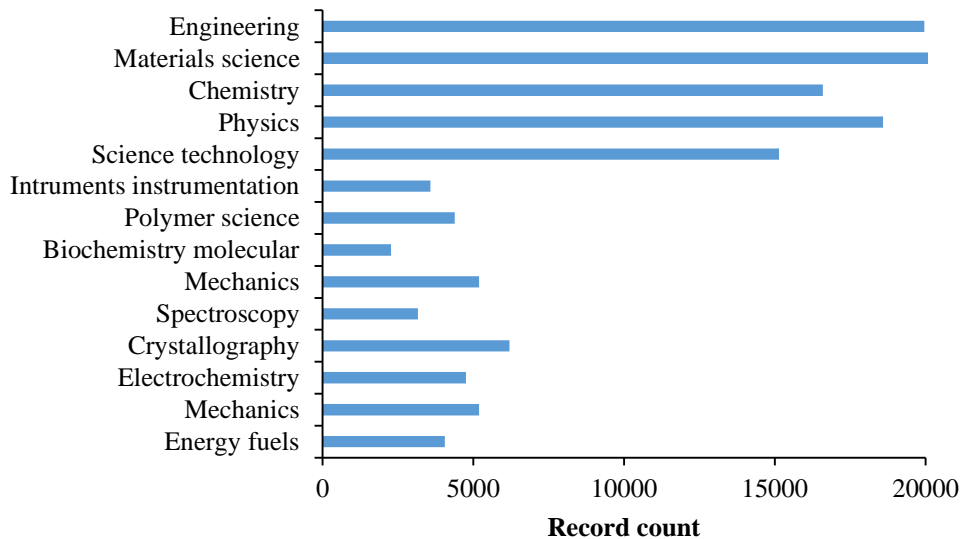


Figure 11. Number of record count on Web of Science for matching the following search term 'CNT' in the 2010-2021 period (September 2021).

CNT structures can be synthesized by several techniques which include gas phase processes. Laser-ablation and carbon arc-discharge techniques have been substituted by chemical vapour deposition technique due to the low temperature processes (<800°C), moreover it can be with precision controlled the nanotube length, diameter, purity, density and CNT orientation (Eatemadi et al., 2014). CNTs are hydrophobic (see *Table 10*), they can be dispersed in aqueous and organic media. Typical solvents include dimethylformamide (DMF), dimethylacetamide (DMAc) and dimethyl sulfoxide (DMSO). The addition of different polymers such as a PMMA and polyacrylonitrile (PAN) and surfactants have been extensively studied in order to obtain a homogeneously dispersed mixtures of CNTs (Deep and Mishra, 2018; Fatemi and Foroutan, 2016; Pramanik et al., 2017). Moreover, the dispersion can be helped by a mechanical approach which consists of ultra-sonication and high shear mixing (Fatemi and Foroutan, 2016).

CNTs show excellent mechanical, electrical and thermic properties, which make them widely used for the detection of chemical and biological compounds, as well as catalytic supports. CNTs are flexible and can create resilient and high electrically conductive films. SWCNTs are longer, stronger and more conductive than MWCNTs (Ganesh, 2013; Lu et al., 2018). They are very good thermal conductors, in addition, they can resist high temperatures (>750°C) due to the strength of the atomic bonds (Eatemadi et al., 2014). CNTs have a good capacity of interact with several compounds through non-covalent mechanisms such as π - π stacking interactions, hydrogen bonding, electrostatic and van der Waals forces, thus CNTs can act as a sorbent material and can be functionalized to change its polarity and to enhance the electrical wiring of enzymes for biosensors and biofuel cells (A Argente-García et al., 2016; Blanchard et al., 2019). Nevertheless, it is

reported in the literature that CNTs have harmful effect on the human body. Compared with micron-sized carbon-based particles, CNTs are considered to have carcinogenicity and following long-term inhalation can induce inflammation, fibrosis and lung tumours (Kobayashi et al., 2017).

Outstanding mechanical, electrical, thermal and reactivity properties of CNTs makes them a promising candidate for design sensors with a wide variety of applications, such as food safety (Malhotra et al., 2015; Nguyen et al., 2013; Pan et al., 2019; Sun et al., 2007), automotive industry (Camilli and Passacantando, 2018; Saxena and Srivastava, 2020), diagnostic and monitor diseases (Ghica and Brett, 2014; Pang et al., 2007; Pauliukaite et al., 2010), detecting and tracking pollutants in the environment (Liu et al., 2012; Sekhar et al., 2010) among others. Thus, CNT sensors can offer advantages due to its several possibilities, they can be used to achieve greater safety, security, product monitoring and individualized health care.

In this Thesis, five pyrene derivatives adsorbed at multi-walled carbon nanotubes electrodes were tested to shed light on their ability to promote direct electron transfer in a H₂O₂ sensor (section 4.4).

	Characteristics	Observations	Studies and applications	Ref
Chemical formula	Carbon atoms organized in a hexagonal pattern	Graphene sheet rolled into a cylindrical shape	-	(Ganesh, 2013)
Synthesis	1) Chemical vapour deposition 2) Laser-ablation 3) Carbon arc-discharge	CVD is more common due to the low temperature	Comparison between SWNT and MWNT	(Eatemadi et al., 2014)
Solubility	Hydrophobic	Dispersed in aqueous and organic media	Study of PMMA and PAN polymers	(Pramanik et al., 2017)
Mechanical	Flexibility	Flexible and resilient	Development of CNT composite films	(Lu et al., 2018)
Electrical	Conductor or semi-conductor	Electronic behaviour of atom in chiral CNT	Structure of CNTs	(Ganesh, 2013)
Thermal	Conductor	Resist up to 750°C at normal and 2800°C in vacuum atmospheric pressures	Medical applications of CNTs	(Eatemadi et al., 2014)
Reactivity	React	Can be functionalized and sorbs several compounds	CNT modified coatings for amphetamines determination	(A Argente-García et al., 2016; Blanchard et al., 2019)
Toxicity	Toxic	Pulmonary toxicity and carcinogenic	Toxicity studies of CNT	(Kobayashi et al., 2017)
Manufacturer	Nanocyl	MWCNTs, Ø = 9.5 nm, 90% purity	-	NC7000 Product Information
Fabrication sensor	Easy	MWCNT dispersion in NMP	Diazonium Electrografting vs. Physical Adsorption of Azure A	(Gross et al., 2020)

Table 10. CNTs

1.3. ANALYTES AND ANALYTICAL TECHNIQUES

1.3.1. Inorganic phosphate

Inorganic phosphate is one of the key indicators of eutrophication level in water environment. Phosphorous and nitrogen are both essential nutrients for living organisms in order to perform most of the metabolic processes by including the photosynthesis, respiration and energy release. High levels of inorganic phosphate in water disrupts aquatic life by leading to an increase plant growth and algae bloom that can cause a reduction of oxygen in water with the consequent death of aquatic animals. Phosphorous in water comes from both natural and human sources (Duffy and Regan, 2017). Moreover, inorganic phosphate plays a critical role in numerous normal physiologic functions, including those related to energy metabolism, bone mineralization and intracellular signalling, thus inorganic phosphate concentration in serum and urine is important for human health. The levels of phosphorus in serum are normally between 3.4 and 4.5 mg dL⁻¹ according to the World Health Organization (WHO). Some pathological conditions can modify physiological inorganic-phosphate concentration in serum (Glassmaker and Rahimi, 2019; Moe, 2008).

Several methods which included a sensor for the determination of inorganic phosphate have been reported in the literature, a comparison of detection performance is shown in *Table 11*. Both analytical parameters such as detection limits and linear range, and different characteristics as ability to perform multianalysis and respect the principles of green chemistry have been compared. Multianalysis is considered to perform various analysis at the same time. A wide variety of methodologies can be used to determine inorganic phosphate by including chromatographic, optical and electrochemical techniques. Chromatographic methods provide accurate and selective data but

they need large equipment and furnish long detection time, moreover, there are no described sensors in the literature. Spectrophotometric methods (Duffy et al., 2017; Mesquita et al., 2011) are based on the phosphate complexation with molybdenum, this complex can be detected using a spectrometer. These approaches have shown high levels of sensitivity and selectivity, however, these methods require costly instruments and well-trained operator for the measurement in laboratory. Moreover, they use as reagents molybdenum and acids which are not good considered in green chemistry. Kahveci et al (Kahveci et al., 2017) have developed a fluorimetric sensor avoiding high toxic reagents, however the achieved sensitivity is low. Fadhel et al (Fadhel et al., 2017) have proposed a fluorescent sensor to determine inorganic phosphate in urine samples which no need of sample pre-concentration steps, therefore the analysis time is reduced. Nevertheless, the sensor is not portable. The method developed by Bocanegra-Rodríguez et al (Bocanegra-Rodríguez et al., 2018a) is based on the fluorescent signal of 3-O-methylfluorescein (OMF) produced by dephosphorylation of OMFP carried out by ALP. The ALP is inhibited in the presence of phosphate. Electrochemical methods such amperometry (Bai et al., 2013; Kulkarni et al., 2015; Talarico et al., 2015), potentiometry (Glassmaker and Rahimi, 2019; Pourbeyram et al., 2019) and voltamperometry (Cinti et al., 2016; Song et al., 2015) also have been compared. These methods provide low detection limit and fast and accurate response; specifically, potentiometric sensors present the advantage that not require for an external power supply, thus it provides great potential for future applications in portable real-time monitoring. Most of electrochemical methods (Bai et al., 2013; Cinti et al., 2016; Song et al., 2015; Talarico et al., 2015) are based on the molybdate complex reaction, this includes the use of several toxic reagents. As *Table 11* shows, not many methodologies are

focused to carry out the analysis by using green methods and there is no sensor which included multianalysis.

In this Thesis, we propose a device (Bocanegra-Rodríguez et al., 2018a) which contains the substrate entrapped and the enzyme adsorbed to a biodegradable support. The developed biosensor allows determine inorganic phosphate respecting the principles of green chemistry, in this case, reagents like ammonium heptamolybdate tetrahydrate, potassium ferrocyanide, glutaraldehyde were avoided. Moreover, the biosensor has improved the time process compared with the other methods as long as our device allows to perform multianalysis. Our experiments show that this device display good selectivity and sensitivity toward inorganic phosphate with low detection limits and also demonstrated is successfully used to detect this analyte in real serum and urine samples.

Reaction	Methodology	LODs (μM)	Linear range (μM)	Multianalysis/ Green method	Ref.
Molybdate complex	Amperometric	0.1	0.5 - 100	-/+	(Talarico et al., 2015)
L-ascorbic acid-2-phosphate	Amperometric	0.5	1 - 40	-/++	(Kulkarni et al., 2015)
Molybdate complex	Amperometric	0.66	1 - 5000	-/+	(Bai et al., 2013)
[Tb-EDTA] ⁻¹ , Au NPs-CTAB	Chemiluminescence	3.8	11.7 - 750	-/++	(Fadhel et al., 2016)
NiO/NiOOH-PrC	Potentiometric	1	10 - 1000000	-/+	(Glassmaker and Rahimi, 2019)
P/Zr/rGO-PGE	Potentiometric	0.011	1 - 250	-/++	(Pourbeyram et al., 2019)
Molybdate complex	Spectrophotometric	0.05	0.14 - 8.4	-/+	(Duffy et al., 2017)
Molybdate complex	Voltammetry	4	10 - 300	-/+	(Cinti et al., 2016)
Molybdate complex	Voltammetry	0.06	0.1 - 10.52	-/+	(Song et al., 2015)
HTMA-PFP	Fluorimetric	370	1000 - 5000	-/++	(Kahveci et al., 2017)
ALP-OMFP	Fluorimetric	2	5 - 51.5	+ /+++	(Bocanegra-Rodríguez et al., 2018a)

Table II. Determination of inorganic phosphate on solid supports through different methods

1.3.2. Ester groups from drugs: atropine, cocaine and ramipril

According to the World Health Organization (WHO) a drug is any substance with the potential to prevent or cure disease or increase physical or mental health. Modifies the physiological and biochemical processes of tissues or organisms. Therefore, we all take drugs daily without any kind of control. On the one hand we can talk about illegal drugs and on the other hand about legal drugs. Specifically, the consumption, production and commercialization of illegal drugs must be detected to avoid misuse since these substances are stimulants of the central nervous system (CNS). In addition, the consumption of these substances causes tolerance, which makes people need to consume more and more to obtain the same effect. It is important to add that the use of these drugs to modify the behaviour of third parties against their willingness has also to be detected. As mentioned above, drugs are also used to treat different pathologies. These drugs have a strict control in the pharmaceutical industry since dosage level is key to the effective treatment of diseases without producing adverse reactions, thus, their quantification is important to produce safe drugs (Zhang et al., 2016).

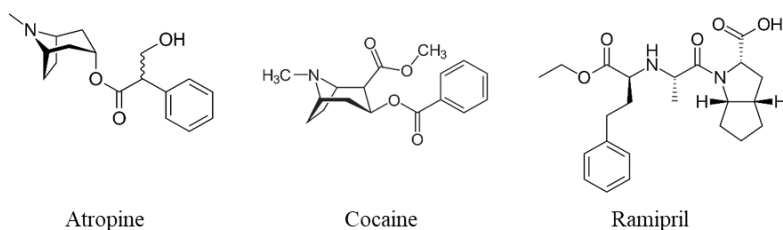


Figure 12. Structure of atropine, cocaine and ramipril.

Since there is a large number of drugs that exist, this Thesis focuses on the quality control pharmaceutical industry of atropine and ramipril which contain in their molecular structure an ester group. As an illicit drug, cocaine was determined (Figure 12).

Many methods are reported in the literature to measure atropine, cocaine and ramipril concentration including liquid chromatography/mass spectrometry (Silveira et al., 2016; F. Yang et al., 2021), electrochemical (Capelari et al., 2021; Rocha et al., 2021), molecular imprinted polymers (Sorribes-Soriano et al., 2020), spectrophotometry (Afiero et al., 2012; Bankey et al., 2009) and fluorescent (Adegoke et al., 2020) methods among others. However, the demand for in situ analysis methods is growing as they do not require expensive instrumentation neither long analysis time. *Table 12* shows several in situ methods that have been developed for atropine and ramipril rapid quantification in the pharmaceutical industry and for cocaine quantification in drug abuse area. Bocanegra-Rodríguez et al (Bocanegra-Rodríguez et al., 2018a) have developed a in situ method based on the ferric hydroxamate colour reaction which result in a reddish-brown color complex (Ramu et al., 2011). Analytical parameters as the achieved detection limit (LOD) and linear range of concentrations, and measured sample are given in *Table 12*. As we can observe, no many recent sensors or assays have been proposed for quantifying atropine and ramipril in the pharmaceutical industry. There are several in situ sensors in the literature to determine cocaine and atropine in human fluids and wastewater.

In this Thesis, a colorimetric sensor for in situ quantifying of ester groups from drugs was developed. Zein was used as biodegradable support material which allows the release of the reagents to the aqueous media where the reaction takes place. A color change can be observed by visual inspection for semiquantitative analysis, thus the proposed method provides rapidity and cost-effectiveness in reference to the usual methods. Moreover, a nonqualified operator could carry out the assay. It was demonstrated its successfully applicability in pharmaceutical samples.

Drug	Interface	LODs	Linear Range	Sample	Reference
Atropine	CO ₃ O ₄ reduced graphene	0.03 μM	0.1-3.2 μM	Drugs	(Bagheri et al., 2015)
Atropine	Ru(bpy) ₃ ²⁺ /carbon nanospheres/Nafion		0.5-250 μM	Injection drugs	(Zhang et al., 2016)
Atropine	bromphenol blue	1.2 μM	1.7-138 μM	Drugs	(Mahmood, 2012)
Cocaine	AuNPs based aptasensor	440 pM	2-100 nM	Human serum	(Abnous et al., 2018)
Cocaine	Magnetic nanoparticles based LFA	16 nM	0.016-1.6 μM	Urine	(Wu et al., 2017)
Cocaine	MoS ₂ -AuNPs	7.49 nM	0-1 μM	Serum	(Gao et al., 2020)
Ramipril	Modified SPEs	-	0.5-10000 μM	Tablets, serum and urine	(Yossri Frag et al., 2020)
Ramipril	Modified SPEs	-	0.5-10000 μM	Drugs and biological fluids	(Mohamed et al., 2019)
Atropine		0.04 mM	0.12-100 mM	solution drugs	
Cocaine	iron-zein and hydroxylammonium-zein	0.01 mM	0.02-80 mM	-	(Bocanegra-Rodríguez et al., 2018a)
Ramipril		0.11 mM	0.36-300 mM	-	

Table 12. *In situ* methods for atropine and ramipril quantification in the pharmaceutical industry and for cocaine quantification in drug abuse area

1.3.3. Silver ion

Silver ions have long been known to have antibacterial properties. It has been proposed that silver ion interacts with the bacterial cell membrane and with molecules inside the cell through thiol groups, which are present in enzymes and proteins, and also contributes to the production of reactive oxygen species, which finally lead to the death of bacteria (Kędziora et al., 2018; Woo et al., 2008). For this reason, silver-based compounds have found a variety of applications in this context (DiRienzo, 2006). It is reported that concentrations higher than 1.6 nM are toxic to fish and microorganisms, and the maximum contaminant level for total silver in drinking water is set to 900 nM (Quality, 1996; “Silver ; CASRN 7440-22-4,” 1987). WHO also states that special situations exist where silver may be used to maintain the bacteriological quality of drinking water and higher levels of up to 100 µg/L could be tolerated in such cases without risk to health (Herschly, 2012). Bacterial growth has a great impact on industry including structural damage like corrosion of materials and formation of biofouling (Firooz et al., 2012; Roger et al., 2008). Biofilm formation is a dynamic process in which extracellular polymeric substances play an important role in the attachment and colonization of surfaces (Czaczyk and Myszka, 2007; Kerr et al., 2003). Therefore, the application of antibacterial agents as preventive and control strategies can be suitably applied for controlling bacterial colonization and to avoid undesirable contaminations. Equipment manufacturers generally recommend silver (0.02–0.08 mg/l) ion concentrations to control legionella effectively (“Health and safety executive. Legionnaires’ disease 2014.,” 2020).

Among the many methods reported for silver quantitation, atomic absorption spectroscopy (Karimi et al., 2011; Zia et al., 2009) and atomic

emission spectroscopy are often used as reference methods as well as various electrochemical methods such as voltammetry and ion-selective electrode potentiometry (Dadkhah et al., 2014; Hassouna et al., 2010; Zejli et al., 2007). No many optical sensors or assays have been proposed for quantifying silver ions in aqueous matrices as it can be seen in the web of science database. Analytical parameters of selected assays or sensors (Chen et al., 2018; González-Fuenzalida et al., 2013; Haghazari et al., 2013; Lee et al., 2015; Omran et al., 2016; Safavi et al., 2017; Sánchez-Pomales et al., 2013; Shahamirifard et al., 2018) can be seen in *Table 13*. Analytical parameters as the achieved LOD and linear range of concentrations, and different characteristics as kind of samples analysed and the time needed to prepare the sensor and to carry out the sample analysis are given in *Table 13*. As it can be seen, the silver ion can be determined by using several instrumental techniques, achieving different levels of concentration. Bocanegra-Rodríguez et al (Bocanegra-Rodríguez et al., 2020a) have proposed a colorimetric sensor based on the silver-catalyzed oxidation reaction of PGR by persulfate in the presence of 1,10-phenantroline as activator. The in situ method uses the colorimetric reagent (PGR) to develop a colorimetric sensor. As it is shown in this table, although some methods can reach limits of detection at μM levels, those ones require analysis time around 24 hours for drinking water analysis.

In this Thesis, a new strategy for developing portable solid optical sensors for *in situ* monitoring of silver ion by passive detection from its catalyst action is presented (Bocanegra-Rodríguez et al., 2020b). In response to the aforementioned demand, the entrapment or adsorption of reagents in polymers can be a good alternative to perform in situ analysis. In this sense, nylon was selected because it has resistance to common organic solvents, good mechanical properties and ultra-high specific surface area.

	Measurement	Reagent	LOD	Linear range	Time*	Samples	Ref.
Assays	Colorimetric	AuNPs	0.41 μM	1 - 9 μM	1 hour	Water (waste, river)	(Safavi et al., 2017)
		Benzo-15-crown-5/AuNPs	12.5 nM	20 - 950 nM	> 24 hours	Water (lake and drinking)	(Haghnazari et al., 2013)
		TMB	5,6 μM	14 - 140 μM	30 minutes	AgNPs dispersions	(González-Fuenzalida et al., 2013)
	X-ray Fluorescence		27.9 μM	0.093 - 93 mM	15 minutes	Dietary Supplements	(Sánchez-Pomales et al., 2013)
Sensors	Colorimetric	Rose-bengal	0.098 μM	0.823 - 3.24 μM	> 24 hours	Water (drinking, river, mineral)	(Shahamirifard et al., 2018)
		Pyrogallol red and 1,10-phenantroline	3 μM	10 - 100 μM	20 minutes	Tap water and refrigerate system waters containing silver (I) as biocide	(Bocanegra-Rodríguez et al., 2020a)
			1.5 μM	5 - 50 μM	30 minutes		
			0.3 μM	1 - 25 μM	40 minutes		
	0.1 μM	0.4 - 10 μM	1 hour				
	Fluorescent	CupR protein	-	0.1 - 10 μM	22 hours	Water (tap, pond)	(Chen et al., 2018)
Potentiometric	p-tert-butylthiacalix[4]arene	3.9 μM	7 μM - 8 mM	> 24 hours	Pharmaceutical (silver nitrate solution 0.5%)	(Omran et al., 2016)	
Quartz Crystal Microbalance	Quartz cristal and Cytosine	100 pM	-	> 24 hours	Water (drinking)	(Lee et al., 2015)	

(*) Assay/sensor time estimated: preparation and analysis. For references see the main paper.

Table 13. Some analytical parameters for selected assays and sensors developed for silver ion estimation.

1.3.4. Hydrogen peroxide

Hydrogen peroxide (H_2O_2) is present in a large variety of products and it has a great importance in pharmaceutical, clinical, chemical, industrial, and environmental analyses (Ali A Ensafi et al., 2016; Ensafi et al., 2014; Habibi and Jahanbakhshi, 2015; Nasirizadeh et al., 2015; Zhai et al., 2017). H_2O_2 is considered one of the reactive oxygen species, and it can be found in human fluids. Although it is poorly reactive, it is able to form other highly reactive intermediates such as hydroxyl radical ($\text{OH}\bullet$). On the other hand, H_2O_2 is known to be an inter- and intracellular signalling molecule which regulates cellular processes. Thus, the H_2O_2 concentration in biofluids can be altered in many disease conditions including cancer, diabetes mellitus, Alzheimer, atherosclerosis, and Parkinson's disease among others, considering that it is a biomarker of oxidative stress (Bai and Jiang, 2013; Valero et al., 2013; Wagner et al., 2013; Zong et al., 2017). Furthermore, H_2O_2 is widely used in industry because of its oxidizing power. It is antibacterial, antifungal, antimold and antiviral (Donnell, G., Denver, 1999).

Different optical and electrochemical methods have been proposed for the quantification of H_2O_2 which including HRP immobilized in a solid support. In *Table 14* some relevant features as the analytical signal, detection limit, linear range, portability, reusability and stability have been compared. It was considered portable method when the measuring instrument can easily be moved to the sampling place (weight < 2 kg) and it does not require to be connected to a supply.

Although luminescence methods present lower LODs (Li et al., 2018; Liu et al., 2015; Luo et al., 2017; Navas A., Ramos M. C., Torrijas M.C., 1998) than spectrophotometric methods (Hosu et al., 2019; Liu et al., 2017; Pla-

Tolós et al., 2016), only one reported article allows the reutilization of the sensor by 7 times; in addition, it is not a portable sensor and it has not been tested in real samples (Luo et al., 2017). The fluorescence methods were not very successful because of the higher LOD of the sensor; however, they were reusable (Burmistrova et al., 2014; Duong and Rhee, 2019). Electrochemical methods (H. Dai et al., 2017; Fazilati, 2012; Jiang et al., 2020; Liu et al., 2017; Murphy et al., 2020; Sardarelli et al., 2021; Shin et al., 2020; Silwana et al., 2017; Vianello et al., 2007) are not usually tested in real samples; therefore, difficulties from the sample analysis are not described (H. Dai et al., 2017; Fazilati, 2012; Liu et al., 2017; Silwana et al., 2017; Vianello et al., 2007). As we know, there is only one article which provides a lower linear range than the biosensor proposed in this Thesis (Bocanegra-Rodríguez et al., 2020b); however it does not allow in situ monitoring because it is not portable and it needs a power supply (Liu et al., 2017). Although some authors proposed a reusable amperometric sensor, the LOD achieved was higher than that achieved by the proposed biosensor, and in addition, it is not portable (H. Dai et al., 2017). Amplex Red has widely been described for quantifying H₂O₂ at very low levels. Qian et al. developed a ratiometric sensor using a combination of Amplex Red and fluorescent scopoletin capable of detecting H₂O₂ concentrations at 150 nM (higher than that provided by the proposed biosensor). However, the ratiometric sensor requires incubation at 25 °C for 5 h (Qian et al., 2019). Similar commercial assays using Amplex Red, in the best cases, require incubation at room temperature for at least 20–30 min. The determination of H₂O₂ by using reactions catalyzed by HRP is a common practice. Electrochemical methods are based on the direct electron transfer between the enzyme and the electrode (Bocanegra-Rodríguez et al., 2021). Moreover, H₂O₂ can be determined by a

chemiluminescent reaction based on the use of luminol as an oxidizable substrate with HRP as catalyst (Bocanegra-Rodríguez et al., 2020b).

The biosensor proposed in this Thesis (Bocanegra-Rodríguez et al., 2020b) shows great results by comparing the abovementioned parameters with those given in *Table 14* for other methods. The developed biosensor allows the determination of H₂O₂ with a good LOD and linear range and to determine it in situ using a portable luminometer as the transducer. Moreover, the covalent binding of the HRP permits the reusability of the sensor, and in this case, the biosensor can be used more than 60 times. Concerning the stability, the biosensor can be used after a long time (more than 3 months) of its fabrication by storing it in a freezer. It should be marked that the developed biosensor allows reducing costs in reagents because of its small size; in addition, it provides reduced toxicity compared with other methods and simplifies the analysis. Moreover, a nonqualified operator could carry out the assay. On the other hand, chemiluminescent probes demonstrated to be very sensitive to H₂O₂ and allow very fast detection (in few seconds). This characteristic is very suitable in order to carry out studies about the H₂O₂ liberation. Our strategy to improve the cost efficiency of the assay has been to study the immobilization of the enzymatic catalyst (HRP) onto a solid PDMS-based support in order to obtain a reusable biosensor, in addition to propose a portable assay for in situ H₂O₂ determination.

Support of HRP	Methodology	LODs (nM) Linear range(μM)	Portable/ Reusable (uses)	Stability (months)	Sample	Reference
PDMS-TEOS-SiO ₂ -TMB	Spectroscopy	400 1.2-72	Yes/ No	3	Cosmetics	(Pla-Tolós et al., 2016)
poly(ANI-co-AA)	Spectroscopy	- 25-500	Yes/ No	1	-	(Hosu et al., 2019)
PEG	Fluorescence	9100 30-300	No/ Yes	1	Cell nutrition medium	(Burmistrova et al., 2014)
Sol-gel	Fluorescence	11000 100-1000	No/ Yes (30)	-	Wastewater	(Duong and Rhee, 2019)
UVNPs@PSIO Am	Chemiluminescence	64 0.1-5	No/ No	-	Serum	(Liu et al., 2015)
Sol-gel	Chemiluminescence	- 100-3000	No/ Yes (5)	2	Contact lenses solutions	(Navas A., Ramos M. C., Torrijas M.C., 1998)
PDMS	Chemiluminescence	20 0.06-10	Yes/ Yes (60)	3	Cell culture medium Cleaning denture tablet	(Bocanegra-Rodríguez et al., 2020b)

Support of HRP	Methodology	LODs (nM) Linear range(μ M)	Portable/ Reusable (uses)	Stability (months)	Sample	Reference
HEPNP/rGO/Au	Amperometry	- 0.01-100	No/ -	-	Serum	(Shin et al., 2020)
NH ₂ -MIL-53/HRP/MWCN Ts/GCE	Amperometry	28 0.1-1	No/ -	0.5	Living cells	(Jiang et al., 2020)
MIP/P(β -CD)/GCE	Amperometry	400 1-15	No/ Yes (50)	0.5	Serum	(Sardaremelli et al., 2021)
HRP/TBA-COOH-IL/MWCNT/GCE	Amperometry	6000 20-4300	No/ Yes (50)	1	Milk and juice	(Murphy et al., 2020)
PGN/GCE-2	Amperometry ^a	0.0267 0.00008-0.664	No/ Yes (50)	-	Living cells	(Liu et al., 2017)
MIL-100(Cr)-B	Amperometry	100 0.5-3000	No Yes (100)	1	Living cells	(H. Dai et al., 2017)

^a Logarithmic calibration

Table 14. Comparison of HRP immobilization methods on solid supports for H₂O₂ sensing.

In addition, a new type of HRP bioelectrode incorporating hydrated nanocellulose as an environmentally friendly and sustainable component to determine H_2O_2 have also been developed in this Thesis (Bocanegra-Rodríguez et al., 2021). Horseradish peroxidase (HRP) is a robust and readily available heme-containing glycoprotein capable of direct electron transfer (DET) bioelectrocatalytic $2 e^-/2 \text{H}^+$ reduction at carbon electrodes such as graphite (Andreu et al., 2007; Ferapontova and Puganova, 2002), single-walled (Shu et al., 2016), double-walled (Agnès et al., 2013), and multi-walled carbon nanotubed (Abreu et al., 2018; Elouarzaki et al., 2015), 3D printed graphene (López Marzo et al., 2020), and nanofiber composites (Jia et al., 2010). HRP is therefore an excellent candidate for the development of reagentless third generation H_2O_2 electrochemical biosensors (Xu et al., 2015). HRP bioelectrodes are also of interest to simplify biocathodes for biofuel cell applications, offering mediator-free bioelectrocatalysis at a high onset potential. The DET H_2O_2 reduction reaction with immobilised HRP has generally been obtained at potentials of *ca.* +100 to -50 mV *vs.* Ag/AgCl, although higher onset potentials up to *ca.* +400-600 mV *vs.* Ag/AgCl have been reported at oxygenated porous carbon electrodes (Jia et al., 2010). Schumann, Stoica and coworkers made important developments on carbon fiber/CNT composites, highlighting the important roles of the hierarchically porous structure and the chemical functionalities, pyrene hexanoic or butyric acid, to achieve H_2O_2 reduction as high as +600 mV *vs.* Ag/AgCl (Jia et al., 2010; Ruff et al., 2018). Several studies highlighted the benefit of introducing oxygenated functionalities to the carbon surface, including specifically carboxylic acid groups, to improve hydrophilicity for DET bioelectrocatalysis (López Marzo et al., 2020; Yamamoto et al., 2003). In this Thesis, a comparative study of five pyrene derivatives adsorbed at multi-walled carbon

nanotube electrodes have been carried out to shed light on their ability to promote direct electron transfer with horseradish peroxidase for H₂O₂ reduction. Specifically, the pyrNHS ester derivative provided access to the highest catalytic current of 1.4 mA cm⁻² at 6 mmol L⁻¹ H₂O₂, high onset potential of 0.61 V vs. Ag/AgCl, insensitivity to parasitic H₂O₂ oxidation, and large linear dynamic range that benefits from insensitivity to HRP “suicide inactivation” at 4 to 6 mmol L⁻¹ H₂O₂. Furthermore, the use of nanocellulose in the development of the biosensor has made possible to reduce its the preparation time and to improve its stability.

1.3.5. Ammonium and organic amino nitrogen

Nitrogen can be found in natural water as dissolved inorganic N (DIN) and dissolved organic N (DON). Ammonium, nitrite and nitrate are the main species of DIN which are from explosives, agricultural activities, domestic sewage discharge, alimentary and cosmetic factory and atmospheric deposition (Jeong et al., 2013; Šraj et al., 2014). DON included complex peptides, free amino acids, amino sugars and nucleic acids. Mainly, DON are from organic bases created by the metabolic activity of plant, animals and microorganisms (Jørgensen, 2009; Zhu et al., 2015a). DON only contributes a relatively small portion of the total dissolved nitrogen (TDN) in surface waters. However, nitrate and ammonium play a more important role in water quality. The TDN is estimated as sum of DIN and DON (Xu et al., 2010).

$$\text{TDN} = \text{DIN} + \text{DON} = (\text{NH}_3/\text{NH}_4^+ + \text{NO}_3^- + \text{NO}_2^-) + \text{DON}$$

Nitrogen concentration in water is considered one of several factors that are involved in the rise of water eutrophication. It is produced by an excessive increase of some nutrients in water, although it also can be affected by environmental factors such as temperature, salinity, carbon dioxide levels,

sunlight, etc., and microbial and biodiversity ecosystem. Moreover, it can be enhanced by human activities that increase the rate of nutrient input in water due to population growth, industrialization and intensifying agricultural activities (Schindler et al., 2006; Udvardi et al., 2015). The consequences including the creation of dense algae blooms which limit the light penetration and the oxygen consumption resulting in hypoxia environmental conditions which increase the mortality of living biota (Kobetičová and Černý, 2019). Surface water quality criteria included the main parameters to evaluate water quality of oceans, seas, lakes, rivers, or wetlands. However, there are no included the criteria for assessing water eutrophication. Generally, nutrient concentration, algae chlorophyll, water transparency and dissolved oxygen are the main parameters which are involved in this phenomenon. Thus, it is necessary to evaluate nitrogen species in water (Karydis, 2009; Paerl and Piehler, 2008; Yang et al., 2008).

There are no simple analytical procedures for quantifying TDN, it is estimated through Kjeldahl method which is the reference method established by the European Directive, it is named total Kjeldahl nitrogen (TKN). This method requires a laborious process which include high waste of energy and measuring time. Moreover, the method can be considered incomplete because it not includes NO_3^- and NO_2^- determination thus, it provides the sum of DON and ammonia contents. TDN can also be determined by measuring each compound separately, however majority methods described in the literature are not in situ. *Table 15* shows different sensors reported in the literature for the quantification of ammonium. Some relevant features as analytical signal, detection limit, linear range, portability and stability have been compared. The most widely used method for the determination of ammonium is optical which includes the Nessler, Indophenol, Indothymol and luminol essays (Li

and Dasgupta, 1999; Meseguer-Lloret et al., 2002; Moliner-Martínez et al., 2005; Molins-Lagua et al., 2006; Prieto-Blanco et al., 2020, 2015; Qin et al., 1999; Bocanegra-Rodríguez et al., 2021). Luminol assays are based on the oxidation reaction of luminol carried out by hypochlorite. First, the ammonium and nitrogen group from organic compounds react with hypochlorite reagent in alkaline media to generate chloramines. Secondly, the remaining hypochlorite reacts with luminol by producing a chemiluminescence signal at 425 nm (Meseguer-Lloret et al., 2002; Bocanegra-Rodríguez et al., 2021). Prieto-Blanco et al. have developed an optical sensors which allows the rapid determination of ammonium, moreover, a semi-quantitative analysis can be carried out by naked eye (Prieto-Blanco et al., 2019, 2015). Some spectrophotometric methods have proposed a device which detect ammonia gas, these methods included a previous conversion of ammonium ion to ammonia (Jaikang et al., 2020; Zhou et al., 2019). On the other hand, the usage the electrochemical methods are increasing due to the great advances in the study in reducing ion interference, mainly potassium and sodium ions, which represents a handicap in terms of the measurement quality (Agir et al., 2020; Capella et al., 2020; Uzunçar et al., 2021; Wang et al., 2020; Zamarayeva et al., 2020). Agir et al. propose an ion selective electrode to determine nitrate and ammonium by combining it with the internet of thing concept which has smart features such as analyte calibration and control (Agir et al., 2020). In addition, Vráblová et al have developed a SPRi sensor for simultaneous detection of nitrate and ammonium with a minimal pretreatment of sample (Vráblová et al., 2021). DON was estimated by Kjeldahl method by using acid reactive and high-temperature catalytic oxidation, in addition, water with elevated DIN concentrations provide low accurate results (Badr et al., 2003; Ii, 1955; Lee

and Westerhoff, 2005; Zhu et al., 2015b). There are no sensors for the determination of DON described in the literature.

In this Thesis, a luminescent biosensor to determine both ammonium and organic amino nitrogen was developed. The biosensor allows the in situ measurements of both analytes with a good linear range. Moreover, the analysis is completed only in 1 min. Concerning the stability, the biosensor can be used after more than 7 days of its fabrication by storing it a room temperature. It was demonstrated its successfully applicability in a variety of real water samples. The proposed method provide security, rapidity and cost-effectiveness in reference to the usual methods. Moreover, a nonqualified operator could carry out the assay.

Methodology	Matrix	LOD/Linear range (mg L ⁻¹)	Analysis time (min)	Portability	Sample	Reference
Spectroscopy	PDMS-thymol/nitroprusside	0.12 ¹ /-	5	Yes	Wine and beer	(Prieto-Blanco et al., 2019)
Spectroscopy	PDMS-thymol/nitroprusside	0.4 ¹ /-	5	Yes	Water	(Prieto-Blanco et al., 2015)
Spectroscopy	Paper-butterfly pea flower extract	4/ 10-100 ²	10	Yes	Farming wastewater Chemical fertilizer	(Jaikang et al., 2020)
Spectroscopy	zinc tetraphenylporphyrin	0.1/ 0.2-50 ²	>10	Yes	Industrial samples	(Zhou et al., 2019)
Conductimetry	nano-PANI:PSS	0.48/ 1.8-207 ¹	-	No	-	(Uzunçar et al., 2021)
Potentiometry	ISE	0.07/ 0.13-1800 ¹	-	Yes	Water	(Agir et al., 2020)
Potentiometry	ISE	-/1.8-1800 ¹	60	No	-	(Zamarayeva et al., 2020)
Potentiometry	S-ISM	-/0.18-1800 ¹	-	No	Wastewater	(Wang et al., 2020)
Luminescence	TEOS-MTEOS	0.012/ 0.036-0.350 ³	1	Yes	Water	(Bocanegra-Rodríguez et al., 2021)

Table 15. Comparison of different sensors to determine ammonium, ammonia and organic amino nitrogen. Surface plasmon resonance imaging

CHAPTER 2. OBJECTIVES

The general objective of the Thesis is to demonstrate how new (nano) and (bio)materials can significantly improve established analytical methods, as well as create new ones and also new tools that contribute to the development of more efficient methodologies in their operation and sustainability. These methodologies have been focused on in situ analysis.

In general the number of publications concerning to new materials have increased in the last year in the different scientific areas and also in the field of Analytical Chemistry. In this Tesis (nano) or (bio) materials have been used in order to develop new methodologies for in situ procedures for determination of compound of social interest. The approaches developed are according to the preservation of the environment and follow the guideline developed by Paul Anastas and John Warner that includes the 12 principles of Green chemistry (Anastas and Warner, 1998). Besides to the characteristics of accuracy and precision, other parameters such as cost, safety or ease handling have been sought.

The **first objective** of the thesis has been to study the state of art of different materials and their physicochemical properties in order to have information about their applicability in Analytical Chemistry.

The **second objective** of the thesis has focused on the selection of sustainable materials for application in the development of in-situ analysis devices for determination a given compound. In this thesis, materials that do not interfere and allow high sensitivity and reproducibility have been selected. Different polymers such as PDMS, TEOS-MTEOS, zein and nylon have been selected as inert supporting materials of reagents. These supports will be used as sensor devices. Nanomaterials such as CNT has been selected

for its properties in the transmission of electrical signals, and nanocellulose for its capacity to form a permeable film.

The **third objective** of the thesis is to complement the procedure with a sensitive and selective optical or electrical response in order to have a sustainable in situ device. Several optical and electrical techniques were developed depending on the analyte and the required sensibility.

The *specific objectives* carried out in the thesis included:

1. To propose a biodegradable multiwell device for the determination of in situ phosphate in urine and serum through optical methods.
2. To design a reagent dispensing biodegradable devices for the determination of ester drugs.
3. To develop a new sensor for the colorimetric detection of silver by providing the appropriate sensitivity for monitoring water from refrigeration systems.
4. To develop a reusable sensor for the detection of hydrogen peroxide at low concentrations by including the assay in neuroblast cells and parapharmaceutical tablets.
5. To design a portable sensor for the detection of ammonium and organic amino nitrogen in water.
6. To develop an electrochemical sensor for hydrogen peroxide concentration and to improve its analytical parameters and stability with the use of nanocellulose as a biodegradable material.

The objectives presented above have become possible thanks to the predoctoral scholarships:

- **PROMETEO 2016/109 project:** granted by Generalitat Valenciana - Programa Prometeo para grupos de investigación de Excelencia. “Desarrollo de nuevas estrategias para el diseño de dispositivos de análisis in situ: nano y biomateriales”. Predoctoral contract to trainee research personal to Sara Bocanegra Rodríguez: “Estudio de nuevos materiales”. Carried out in the analytical chemistry department, Faculty of Chemistry, Universidad de Valencia. 3 years (2016-2019).
- **BEFPI 2019 program:** granted to Sara Bocanegra Rodríguez by the Generalitat Valenciana - Subvenciones para estancias de contratados predoctorales en centros de investigación fuera de la Comunitat Valenciana. Internship in molecular chemistry department, Université Grenoble Alpes. 3 months.

In addition, the results of the present Thesis are part of the following research projects granted to the research group Miniaturización y Métodos Totales de Análisis (MINTOTA) of the Analytical Chemistry Department at Valencia University.

- CTQ2014-53916-P Project, granted by Spanish Ministry of Economy and competitiveness and EU from FEDER - Programa Estatal de Fomento de la Investigación Científica y Técnica de Excelencia Subprograma Estatal de Generación de Conocimiento, “Desarrollo de nuevas estrategias para el diseño de técnicas de cromatografía líquida miniaturizada en línea: nanopartículas, contaminación secundaria”, 2015-2017.
- PROMETEO 2016/109 Project, granted by Generalitat Valenciana - Programa Prometeo para grupos de investigación de Excelencia, “Desarrollo de nuevas estrategias para el diseño de dispositivos de análisis in situ: nano y biomateriales”, 2016-2019.

- CTQ2017-90082-P Project, granted by Spanish Ministry of Science, Innovation and Universityes. “Microextracción en fase sólida en tubo acoplada en línea a nanocromatografía líquida: nuevas oportunidades para/desde la nanoescala y cromatografía líquida”, 2018-2021.

Thanks to scholarship and projects, the obtained results and the knowledge acquired through the development of the Thesis have resulted in five scientific papers and one encyclopedia chapter. The corresponding impact factors from the Journal of Citation Reports are shown in each paper.

- **S. Bocanegra-Rodríguez**, N. Jornet-Martínez, C. Molins-Legua, P. Campíns-Falcó. Delivering Inorganic and Organic Reagents and Enzymes from Zein and Developing Optical Sensors, *Anal. Chem.* 90 (2018) 8501–8508. Impact Factor (JCR 2020): 6.986.
- N. Jornet-Martínez, **S. Bocanegra-Rodríguez**, R.A. González-Fuenzalida, C. Molins-Legua, P. Campíns-Falcó. In Situ Analysis Devices for estimating the environmental footprint in beverages industry. In *Processing and Sustainability of Beverages*, Grumezescu, A.M., Holban, A.M., Eds.; Elsevier: Amsterdam, The Netherlands, 2019; Volume 2, Chapter 9; pp. 275–317.
- **S. Bocanegra-Rodríguez**, N. Jornet-Martínez, C. Molins-Legua, P. Campíns-Falcó. New reusable solid biosensor with covalent immobilization of the Horseradish Peroxidase enzyme: in situ liberation studies of hydrogen peroxide by portable chemiluminescent determination. *ACS Omega* 5 (2020) 2419-2427. I.F. : 3.512.
- **S. Bocanegra-Rodríguez**, N. Jornet-Martínez, C. Molins-Legua, P. Campíns-Falcó. Portable solid sensor supported in nylon for silver ion determination: testing its liberation as biocide. *Anal Bioanal Chem* 412 (2020) 4393-4402. I.F.: 4.142.

- **S. Bocanegra-Rodríguez**, C. Molins-Legua, P. Campíns-Falcó. Luminol doped silica polymer sensor for portable organic amino nitrogen and ammonium determination in water. *Separations* 8 (2021) 149. I.F.: 2.777.
- **S. Bocanegra-Rodríguez**, C. Molins-Legua, P. Campíns-Falcó, F. Giroud, A. J. Gross. Monofunctional pyrenes at carbon nanotube electrodes for direct electron transfer H₂O₂ reduction with HRP and HRP-bacterial nanocellulose. *Biosens. Bioelectron.* 187 (2021) 113304. I.F.: 10.257.

During the Thesis, several works have been carried out which have been presented at International and National Conferences. These works are detailed below:

- Neus Jornet-Martínez, **Sara Bocanegra-Rodríguez**, Pilar Campíns-Falcó, Lisa Hall. Zein as sustainable alternative of petroleum-based materials in biokits and biosensors for in-situ analysis. Early Career Researcher Meeting 2017, Warwick (UK).
- **S. Bocanegra-Rodríguez**, N. Jornet-Martínez, C. Molins-Legua, Y. Moliner-Martinez, P. Campíns-Falcó. Biomembranes as supporting material for immobilization of reagents: application to clinical samples. ExTech 2017, Santiago de Compostela (España).
- **S. Bocanegra-Rodríguez**, N. Jornet-Martínez, C. Molins-Legua, Y. Moliner-Martinez, P. Campíns-Falcó. Phosphate determination in serum samples by using fluorescent solid biosensor. XXI Reunión de la Sociedad Española de Química Analítica 2017, Valencia (España).
- C. Molins-Legua, D.L. Palacios-López, M.C. Prieto-Blanco, N. Jornet-Martinez, L. Hakobyan, **S. Bocanegra-Rodríguez**, P.

- Campíns-Falcó. Solid sensor supported in PDMS for derivatizing carbonyl compounds in several matrices. 32nd International Symposium on Chromatography (ISC) 2018, Cannes (Francia).
- N. Jornet-Martinez, **S. Bocanegra-Rodríguez**, C. Molins-Legua, P. Campíns-Falcó. Portable colorimetric sensor supported in nylon for silver ion determination as catalyst. XXII Reunión de la Sociedad Española de Química Analítica 2019, Valladolid (España).
 - C. Molins-Legua, **S. Bocanegra-Rodríguez**, N. Jornet-Martinez, P. Campíns-Falcó. Reusable solid biosensor for in situ chemiluminescent determination of hydrogen peroxide: application to real samples. XXII Reunión de la Sociedad Española de Química Analítica 2019, Valladolid (España).








CHAPTER 3. EXPERIMENTAL METHODOLOGY

3.1 CHEMICALS AND REAGENTS








The European normative includes a section about the classification, labelling and packing of substances and chemical mixtures. *Figure 13* shows different standardized pictograms in order to classify. *Table 16* shows the different reagents used in this Thesis, the commercial suppliers where they were purchased, its security pictograms and the GHS (Globally Harmonized System of Classification and Labelling of Chemicals).

-  Flammable (GHS02)
-  Oxidizing (GHS03)
-  Corrosive (GHS05)
-  Toxic (GHS06)
-  Harmful (GHS07)
-  Health hazard (GHS08)
-  Environmental hazard (GHS09)

Figure 13. Security pictograms which classify the different substances and chemical mixtures.

Reagent	Supplier							
(3-Aminopropyl)triethoxysilane	Sigma-Aldrich			X		X		
1,10-phenantroline	Sigma-Aldrich				X			X
1-methyl-2-pyrrolidone	Sigma-Aldrich					X	X	

Chapter 3. Experimental methodology

Reagent	Supplier							
1-pyreneacetic acid	Sigma-Aldrich							
1-pyrenebutyric acid	Sigma-Aldrich					X		
1-pyrenebutyric acid N-hydroxysuccinimide ester	Sigma-Aldrich					X		
1-pyrenemethylamine hydrochloride	Sigma-Aldrich					X		
3-O-methylfluorescein phosphate cyclohexammonium salt	Sigma-Aldrich							
Acetic acid	Scharlau	X		X				
Acetonitrile	VWR	X				X		
Alkaline phosphatase	Sigma-Aldrich							
Ammonium chloride	Probus					X		
Anhydrous sodium hydrogen phosphate	Panreac							
Argon	Messer							
Bacterial cellulose nanofibers gel	Nano Novin Polymer Co.							
Calcium chloride	Panreac					X		
Chlorhydric acid	Sigma-Aldrich			X		X		
Ethanol	Sigma-Aldrich	X						
Glutaraldehyde	Sigma-Aldrich			X		X	X	X
Glycerol	Sigma-Aldrich							
Horseradish peroxidase	Sigma-Aldrich							
Hydrogen peroxide	Merck		X	X		X		
Hydroxylammonium choride hexahydrate	Riedel-de Haen			X		X	X	X
1-methyl-3-octylimidazolium hexafluorophosphate	Sigma-Aldrich							
Iron (III) chloride hexahydrate	Probus			X		X		
Isopropanol	Sigma-Aldrich	X				X		
Luminol	Sigma-Aldrich					X		

Chapter 3. Experimental methodology

Reagent	Supplier							
Magnesium chloride hexahydrate	Scharlau							
Multi-walled carbon nanotubes	Nanocyl						X	
N,N-Dimethylformamide	Carlo Erba reagents	X				X	X	
N-hydroxysuccinimide ester	Sigma-Aldrich							
Oxygen	Messer		X					
Poly(ethylene glycol)	Sigma-Aldrich							
Polydimethylsiloxane Sylgard®184 Kit	Dow Corning							
Potassium persulphate	Sigma-Aldrich		X			X	X	
Potassium phosphat dibasic	Merck							
Potassium chloride	Panreac							
Pyrene	Sigma-Aldrich							X
Pyrogallol red	Sigma-Aldrich					X		
Silver nitrate	VWR		X	X				X
sodium carbonate	Merck							
Sodium chloride	Fisher Chemical							
Sodium hydrogenocarbonate	Merck							
Sodium hydroxide	Sigma-Aldrich			X				
Sodium hypochlorite	Scharlab			X				X
Sodium percarbonate	Sigma-Aldrich					X		
Sodium phosphate dibasic	Sigma-Aldrich							
Sodium phosphate monobasic	Merck							
Sodium sulphate anhydrous	Scharlau							
Sulfuric acid	Sigma-Aldrich			X				
Tetraethylorthosilicate	Sigma-Aldrich	X				X		
Trichloroacetic acid	Scharlau			X		X		X














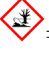
Reagent	Supplier							
Triethoxymethylsilane	Sigma-Aldrich	X						
Tris(hydroxymethyl)aminomethane	Merk							
Zein	Sigma-Aldrich							

Table 16. Reagents list uses in this Thesis with their commercial suppliers and respective security pictogram where  = flammable;  = oxidizing;  = corrosive;  = toxic;  = harmful;  = health hazard;  = environmental hazard.

3.2 INSTRUMENTATION

The following instruments and materials have been used to carry out the different experimental procedures:

- Ultrasonic bath Sonitech (TerraTech, Spain)
- Magnetic stirrer (450 W) (Sstuart Scientific)
- Crison micropH 2000 pH.meter (Crison Instruments, Spain)
- Nanopure II water system (Barnstead, UK)
- Vortex mixer (Labnet International, USA)
- Hettich Zentrifuge EBA 20 (Merck, Germany)
- Nylon membranes (0.2 μm) (Sartorius Stedim, Germany)
- Polystyrene tubes (Labbox, Spain).
- Plastic well-plates (Sigma Aldrich, Germany)

Throughout the development of the Thesis several techniques have been used which can be classified into three groups: spectroscopic, electrochemical and microscopic. The corresponding equipment is described in detail below.

3.2.1 Spectroscopic techniques

3.2.1.1 UV-Vis spectrophotometry

Spectrophotometric measurements were performed on a Cary 60 Fiber Optic UV-Vis spectrophotometer (Agilent Technologies, USA) (*Figure 14A*). The spectral range measured was from 200-900 nm. Data were recorded and processed by using a Cary WinUV software (Agilent Technologies Products, Australia).

In situ spectrophotometric measurements were carried out using the portable spectrophotometer Maya2000 Pro (Ocean Optics, USA) (*Figure 14B*). This spectrophotometer is fitted with an optical fiber accessory (300 μm core size and 2 meters length) (Ocean Optics, USA) (*Figure 14C*). The spectral range measured was from 200-900 nm.

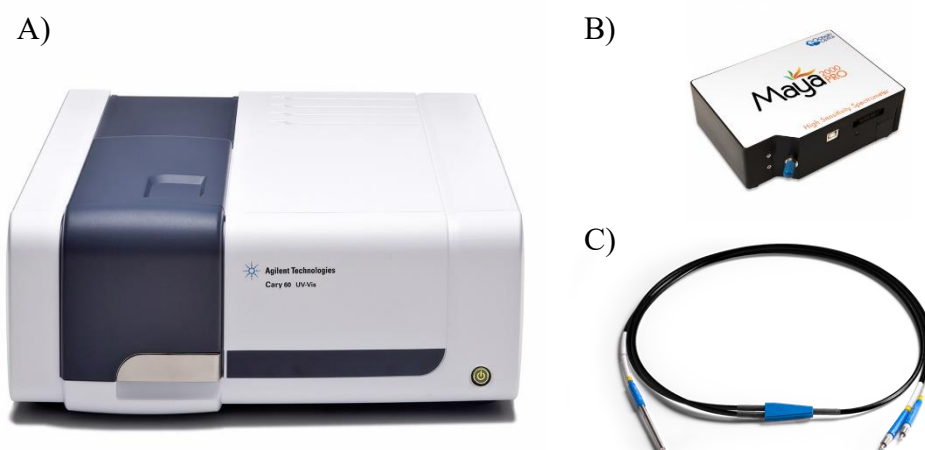


Figure 14. A) Cary 60 Fiber Optic UV-VIS spectrophotometer. B) Portable spectrophotometer Maya2000 Pro. C) Optical fiber accessory.

3.2.1.2 Reflectance diffuse spectrophotometry (DR)

A DR remote fiber optic accessory from Harrick Scientific Products (Pleasantville, NY) was coupled to a Cary 60 Optic UV-Vis spectrophotometer (Agilent Technologies, USA) for DR measurements of solid sensors. This accessory is equipped with a video camera and an integrated light to select the sample point to be measured (*Figure 15*). The spectral range measured was from 200-800 nm. For data collection and processing, Cary WinUV software (Agilent Technologies Products, Australia) was used.



Figure 15. Remote fiber optic DR accessory.

3.2.1.3 Infrared spectroscopy (IR)

An Agilent Cary 630 FTIR spectrophotometer fitted with a diamond ATR accessory (Agilent Technologies, Böblingen, Germany) was used to register the spectra in the frequency range from 4000 to 600 cm^{-1} at a resolution of 4 cm^{-1} . A background scan was made against the air, and 8 scans were averaged for each measurement. Data were recorded and processed by using MicroLab FTIR and ResolutionPro software (Agilent Technologies) (*Figure 16*).



Figure 16. Cary 630 FTIR-ATR spectrophotometer.

3.2.1.4 Quimioluminescence

Quimioluminescence measurements were performed on a spectrofluorometer Jasco FP 750 (Tokyo, Japan) (*Figure 17*). Data were recorded and processed by using a Spectra Manager software (Jasco Corporation).



Figure 17. Spectrofluorometer Jasco FP 750.

In situ quimioluminescent measurements were recorded by a portable tube luminometer from Berthold Technologies (Bad Wildbad, Germany) (*Figure 18*). The data was taken from the equipment screen manually.



Figure 18. Portable tube luminometer from Berthold Technologies.

3.2.1.5 Fluorescence

Fluorescence measurements were carried out using a Cary Eclipse Fluorescence Spectrophotometer (Agilent Technologies, Germany) (*Figure 19A*). An Agilent microplate reader accessory (*Figure 19B*) was used in order to measure inside the white polystyrene 94-well plates from Sigma-Aldrich. Data were recorded and processed by using a Cary WinFLR software (Agilent Technologies, Germany).

A)



B)



Figure 19. A) Cary Eclipse Fluorescence Spectrophotometer. B) Microplate reader accessory.

3.2.1.6 Mobile phone

A mobile phone (iPhone 8) was employed to photograph sensors. The obtained images were analysed by the free image editor software GIMP (version 2.8). The color picker tool on GIMP, with an average of 50 x 50 pixels was used to evaluate the RGB (red, green, blue) and CMYK (cyan, magenta, yellow, key) color intensity.

3.2.2 Electrochemical techniques

3.2.2.1 Voltammetry

Electrochemical measurements were performed at room temperature using a Biologic VMP3 Multi Potentiostat operated with EC-lab software. A three-electrode cell was used comprising a carbon nanotube film-modified glassy carbon (GC) working electrode ($\text{\O} = 3 \text{ mm}$), a silver-silver chloride reference electrode (Ag/AgCl with saturated KCl), and a Pt wire counter electrode.

3.2.3 Microscopic techniques

3.2.3.1 Light microscopy

A Nikon microscope Eclipse E200LED MV Series (Nikon Corporation, Tokyo, Japan) was used to take microscopic images under bright-field illumination with three objective lens (10x, 50x, 100x). A Nis-Elements 4.20.02 Software was used for acquiring and processing the images (*Figure 20*).



Figure 20. Nikon microscope Eclipse E200LED MV Series

3.3 FABRICATION OF SENSORS

3.3.1 Zein/glycerol-ALP and Zein/glycerol-OMFP sensors

Two configurations were tested for developing the multiwell-plate biosensor: (i) the substrate 3-O-methylfluorescein 6-phosphate (OMFP) and the enzyme alkaline phosphatase (ALP) were entrapped inside the zein film, and (ii) the substrate was entrapped and the enzyme was adsorbed on the surface of the film (see *Figure 21*).

First, three solutions were prepared: Solution A was prepared by mixing an aqueous solution of alkaline phosphatase (80 μL of 10 mg mL^{-1}), zein (10 % w/v) in aqueous ethanol (90%, v/v; 1.6 mL), and 90 μL of glycerol. Solution B is composed of 4.8 μM OMFP ethanolic solution (20 μL) and zein (10 % w/v) in aqueous ethanol (90%, v/v; 1.6 mL). Solution C was obtained by mixing glycerol (70% of the zein weight) and zein (10 % w/v) in aqueous ethanol (90%, v/v).

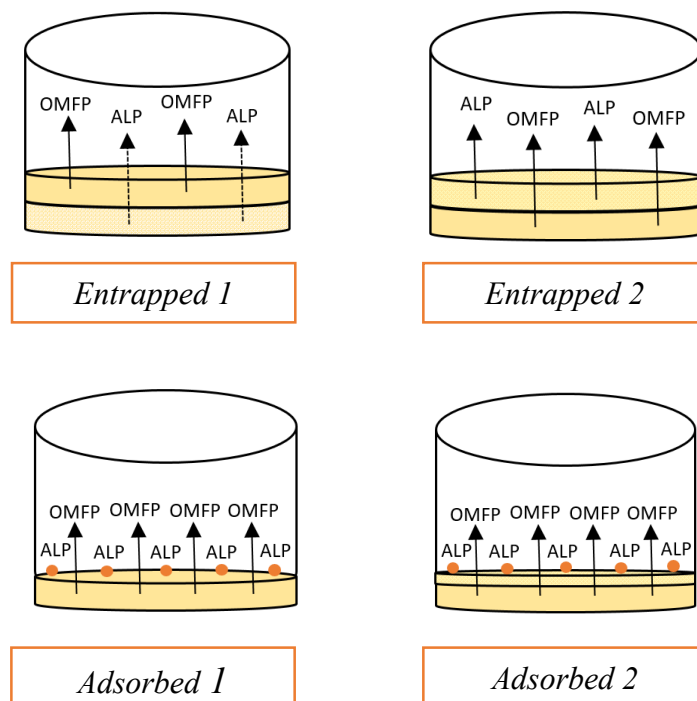


Figure 21. Different configurations tested: (*Entrapped 1*) ALP entrapped at the bottom, (*Entrapped 2*) ALP entrapped at the top, (*Adsorbed 1*) ALP adsorbed on the OMFP sensor, (*Adsorbed 2*) ALP adsorbed on the glycerol layer.

Enzyme entrapment occurred as follows: (1) The biosensor was prepared by the addition of 20 μL of solution A to the bottom of each well. The biosensor was composed of 1 unit of ALP. After 10 h at room temperature, 20 μL of solution B was added (2) The same process was followed, but OMFP was added first and allowed to dry for 8 h; then the ALP was added. Finally, the multiwell-plate biodevice was stored at $-18\text{ }^{\circ}\text{C}$.

Enzyme adsorption occurred as follows: (1) The biosensor was prepared by the addition of 20 μL of solution B into the bottom of each well. After 8 h at room temperature, alkaline phosphatase (10 μL of 0.5 mg mL^{-1} , from commercial ALP, 10 U mg^{-1}) was adsorbed on the surface of the OMFP/zein

membrane (obtained from solution B). (2) The biosensor was designed following the same process, but a second zein membrane was added on the zein layer containing OMFP. This membrane was synthesized by the addition of 15 μL of solution C. After 8 h at room temperature, the ALP was adsorbed on the surface of the glycerol/zein layer. Each well contained 0.05 units of ALP. The multiwell-plate biosensor was stored at $-18\text{ }^{\circ}\text{C}$.

3.3.2 *Iron and Hydroxylammonium Sensors*

Three different supports were essayed in order to develop a good operational sensor to determine ester compounds.

1) Zein support

Two zein-based sensors were obtained (see *Figure 22*). They were prepared by embedding the reagents iron chloride and hydroxylammonium into zein films. The iron/zein and hydroxylammonium/zein sensors were prepared by dissolving 0.16 g of zein (10%, w/v) in aqueous ethanol (90%, v/v, 1.440 mL) to a total volume of 1.6 mL along with glycerol (90 μL) as a plasticizer. Then, the iron(III) chloride hexahydrate (201 mg) or the hydroxylammonium chloride (150 mg), previous ground in a mortar, was added, and the mixture was stirred for 20 min. Finally, 200 μL of the sensor was placed into a well of a multiwell-plate. After 6 h at room temperature, the sensor-reagent packages were obtained. The iron sensors were brown, whereas the hydroxylammonium sensors were yellow.

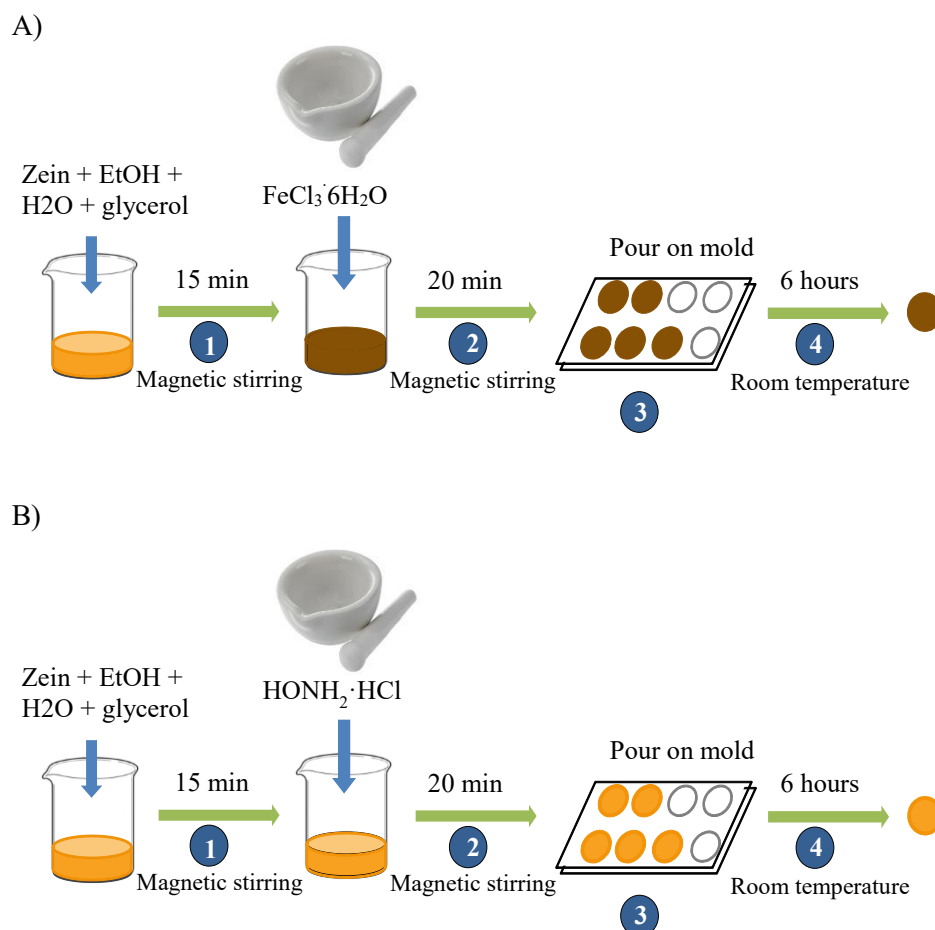


Figure 22. Procedure of (A) iron/zein and (B) hydroxylammonium/zein sensors fabrication.

2) Paper support

Paper sensor (20 mm diameter) was prepared by the addition of the stock solution of iron chloride (3 μ L of 0.186 M).

3) PDMS support

The bulk solid reagent of FeCl₃·6H₂O (76.4 mg) was directly embedded into the polymer. *Figure 23* describes the procedure of sensor fabrication. The

solid reagent (previously ground in a glass mortar in order to obtain suitable homogeneity) was mixed with the elastomer base and curing agent in a ratio of 10:1 (magnetic stirring for 15 min.). This mixture was placed in well polystyrene plates and cured at 35 °C inside an oven for 8 hours. Finally, the mixture did not provide a gel. The incorporation of tetraethylsiloxane, silica nanoparticles (5–15 nm sized spherical particles), or the ionic liquid 1-methyl-3-octylimidazolium hexafluorophosphate did not result in the gelling of the sensor.

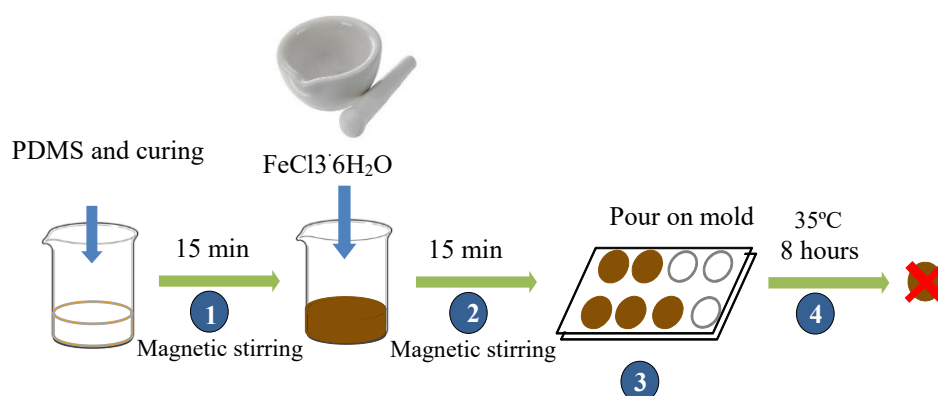


Figure 23. Procedure of iron/PDMS sensors fabrication.

3.3.3 Nylon/1,10-phenantroline/PGR sensor

An ethanolic solution composed of 0.17 M 1,10-phen and 8×10^{-4} M PGR solution was prepared. The nylon sensor was prepared by passing 200 μ L of this solution by using a syringe of 10 mL connected to a 13 mm diameter polypropylene filter holder which contained the nylon membrane (0.2 μ m pore diameter) (see *Figure 24*). Then, the sensor was removed from the holder, and placed on the dark for their storage until its use.

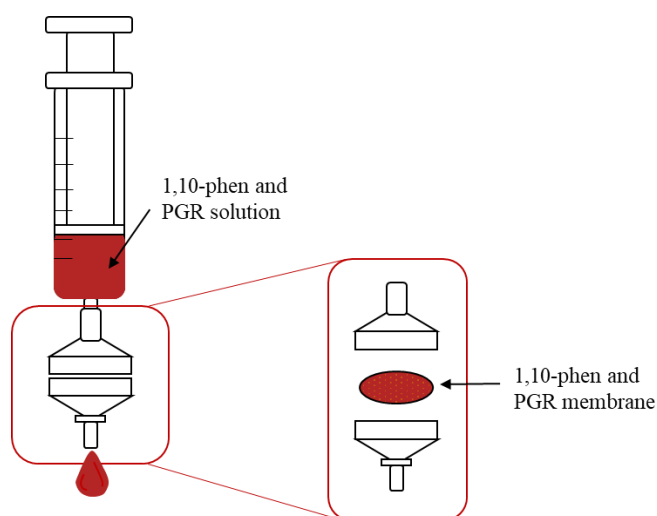


Figure 24. Preparation of the solid sensor containing both reagents, pyrogallol red and 1,10-phenanthroline.

3.3.4 PDMS/peroxidase sensor

The biosensor included the covalent immobilization of HRP on the functionalized PDMS deposited into a polystyrene tube. First, a mixture of PDMS elastomer base and curing reagent in a 10:1 (v/v) proportion was mixed during 10 min with a magnet. 200 μL of the mixture was situated on the bottom of the polystyrene tube at 30 $^{\circ}\text{C}$ for 24 h. Secondly, a solution containing 1 mL amino propyl trimethoxy silane (APTMS), 5 mL of 0.1 M acetic acid and 5 mL of isopropanol was prepared. The mixture was stirred for 2 h at room temperature, then, 89 mL of residual isopropanol were added into. Moreover, a solution of 5% glutaraldehyde was made in 0.1 M sodium phosphate buffer solution (pH = 7.0). Then, the PDMS surface situated on the bottom of the polystyrene tube, prepared the day before, was activated by adding an acidic solution containing H_2O , 37% HCl and 30% H_2O_2 in a 5:1:1 (v/v/v) ratio. After two hours, the tube was washed with distilled water. The amino-silanization process was carried out by incubating the modified PDMS surface with the solution above mentioned, which contains APTMS, and

drying the tube at 70 °C for two hours. The resulting modified PDMS surface was treated with a 5 % w/w glutaraldehyde (GTA) solution in order to form a Schiff base. Then, the tubes were washed two times with phosphate buffer solution pH = 7 and two times with distilled water. Finally, the functionalized PDMS surface was incubated with a HRP enzyme solution ($0.1\text{mg}\cdot\text{mL}^{-1}$) for 1 hour. Thereafter, the tube was washed three times with phosphate buffer solution pH = 7.

3.3.5 TEOS/MTEOS/luminol sensor

The sensor was fabricated by mixing in a glass vial 50 μL of nanopure water, 100 μL of TEOS, 100 μL of MTEOS and 2 mL of luminol 0,04 mM (pH=10.7). To obtain a homogeneous dispersion, the mix was vortexing for 1 minute and after 200 μL of the mixture was deposited on the bottom of the polystyrene tube. Tubes were heated at 40 °C for 4 hours and then they were covered with a polystyrene tube cap and stored at room temperature (*Figure 25*). The same procedure was used to prepare de PEG and glycerol modified sensors. *Table 17* shows the composition of the different studied compositions expressed per unity.

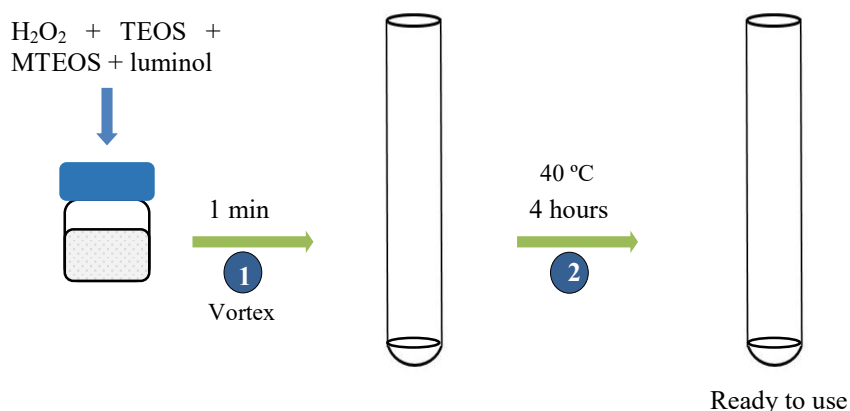


Figure 25. Procedure of TEOS/MTEOS/luminol sensors fabrication.

	Sensor A	Sensor B	Sensor C
TEOS (μL)	8.9	8.9	8.9
MTEOS (μL)	8.9	8.9	8.9
Luminol 0.4 M (pH=10.7) (μL)	177.8	177.8	177.8
PEG (mg)	-	5.8	-
Glycerol (mg)	-	-	1.8

Table 17. Different mixtures tested in order to develop a luminol sensor. For all mixtures 4.4 μL of nanopure water was used.

3.3.6 Nanocellulose/HRP/ MWCNT sensor

Electrochemical sensor composed of HRP between nanocellulose and the modification MWCNT surface was developed. This technique included different steps:

a) MWCNT dispersion

Commercial grade thin multi-walled carbon nanotubes (9.5 nm diameter, purity 90%) were used as received without any purification step. A 2.5 mg mL^{-1} dispersion of MWCNTs in N-methyl pyrrolidone (NMP) was carried out sonicating it 60-120 min to achieve a homogeneous dispersion.

b) Preparation of MWCNT electrodes

MWCNT films were prepared by drop coating 20 μL of a 2.5 mg mL^{-1} dispersion of MWCNTs onto the glassy carbon (GC) electrode surface. The modified electrode was dried under vacuum for two hours.

c) Preparation of pyrene-modified MWCNT electrodes

First, the modified MWCNTs electrodes were obtained by immersion of the electrode in a sealed vial containing 100 μL of 5 mmol L^{-1} modifier solution containing the pyrene derivate in DMF. The solutions tested were

pyrene, pyrene acetic acid, pyrene butyric acid, pyrene methylamine, pyrene N-hydroxysuccinimide ester. After 60 min, the electrode was gently removed from the modifier solution then rinsed with DMF followed by acetonitrile (CAN) to remove weakly adsorbed species. The modified electrodes were rinsed gently with 0.1 mol L^{-1} phosphate buffer (pH 7.0) prior to use.

d) Preparation of HRP-modified MWCNT bioelectrodes

Aliquots of enzyme solution were first prepared at 5 mg mL^{-1} in 0.1 mol L^{-1} phosphate buffer (pH 7.0) and stored at $-20 \text{ }^{\circ}\text{C}$. Prior to use, the aliquot was carefully thawed to room temperature then immediately used for bioelectrode preparation. The pyrene-modified MWCNT electrode was immersed in a sealed vial containing $40 \text{ }\mu\text{L}$ of the enzyme solution then left overnight at $4 \text{ }^{\circ}\text{C}$ in the fridge. Prior to electrochemistry or further modification, the bioelectrode surface was rinsed gently with 0.1 mol L^{-1} phosphate buffer (pH 7.0) to remove weakly adsorbed species.

e) Preparation of nanocellulose-modified HRP MWCNT bioelectrodes

- Layer- by layer method

The HRP modified bioelectrodes were first prepared as described in *Section d*. $10 \text{ }\mu\text{L}$ of the as-received nanocellulose gel (1% nanocellulose) was then mixed with $30 \text{ }\mu\text{L}$ of 0.1 mol L^{-1} phosphate buffer (pH 7.0) in a vial for 60 s by vortexing. $20 \text{ }\mu\text{L}$ of the mixture was then dropcasted onto the bioelectrode. The electrode was left to dry at room temperature for 1 h then gently rinsed with the buffer solution prior to use.

- One-pot method

0.4 mg of HRP, $10 \text{ }\mu\text{L}$ of nanocellulose gel (1% nanocellulose) and $30 \text{ }\mu\text{L}$ of 0.1 mol L^{-1} phosphate buffer (pH 7.0) were mixed together in a vial for 60

s by vortexing. After pre-rinsing of the pyrene-modified MWCNT electrode (*Section c*) with the buffer, either 5 μL or 20 μL of the mixed enzyme/nanocellulose solution was drop-casted on the surface of the electrode. The electrode was left to dry at room temperature for 1 h then gently rinsed with the buffer solution prior to use.

3.4 PROCEDURES AND EXPERIMENTAL CONDITIONS

3.4.1 Experimental conditions of polymeric sensors

Table 18 summarized the experimental conditions for obtaining the response of polymeric sensors developed in this Thesis. The table include the linear range information, sample in which the sensor has been approved its applicability, the support material of the sensor, reagents utilized and analytical technique used to determine de analyte.

Analyte	Linear Range	Matrix	Sensor	Reagents	Sample volume/ Reaction time	Detection	Section
Inorganic phosphate	0.3-5 mg L ⁻¹	Serum Urine	Zein/ALP	Buffer Tris-HCl (100 mM, pH=9) Simulated body fluid	15 µL 0-2 min	Fluorescence λ=(513 nm)	4.1.1
Ester group (Propyl acetate)	0.05-100 mM	Drugs (atropine, cocaine, ramipril)	Zein/H ₃ NO + Zein/FeCl ₃	NaOH (0.5 M) HCl (0.5M)	200 µL 5 min	Absorbance λ=(525 nm)	4.1.2
	0.84-80 mM		Paper/FeCl ₃			Diffuse reflectance λ=(525 nm)	
Silver	0.4-10 µM	Tap and refrigerated systems water	Nylon/PGR/ 1,10-Phen	H ₂ SO ₄ (2 M) K ₂ S ₂ O ₈ (0.1 M)	2000 µL 50 min	Diffuse reflectance λ=(485 nm)	4.2
	0.4-10 µM 1-25 µM				50 min 30 min	GIMP (yellow color)	

Analyte	Linear Range	Matrix	Sensor	Reagents	Sample volume/ Reaction time	Detection	Section
Hydrogen peroxide	0.06-10 μM	Cell culture medium Tablets	PDMS/HRP	Luminol (35 mM)	200 μL 10 s	Chemiluminescence (total emitted light)	4.3.1
Ammonium and organic amino Nitrogen (N)	0.036-0.35 mg L^{-1}	Water	TEOS/MTEOS/luminol	HClO (0.248 μM)	350 μL 10 s	Chemiluminescence (total emitted light)	4.3.2
Hydrogen peroxide	0.25- 4 mmol^{-1}	-	MWCNTs/HRP/	Phosphate buffer pH=7	20 μL 0 s	Voltammetry	4.4

Table 18. Experimental conditions used in several works of this Thesis based on polymeric sensor

3.4.2 Electrochemical conditions

Electrochemical measurements were performed at room temperature using a Biologic VMP3 Multi Potentiostat operated with EC-lab software. A three-electrode cell was used comprising a carbon nanotube film-modified GC working electrode ($\text{\O} = 3 \text{ mm}$), a silver-silver chloride reference electrode (Ag/AgCl with saturated KCl), and a Pt wire counter electrode. GC electrodes were polished using a Presi polishing cloth with $1 \text{ }\mu\text{m}$ alumina or diamond slurry then sonicated for 5 min in distilled water prior to use. Electrochemical experiments were performed in 0.1 mol L^{-1} phosphate buffer (pH 7.0) in the absence of oxygen. Oxygen was removed by purging the solution with argon for 15 min. A gentle argon flow was maintained in the air space above the solution during experiments. Amperometric data was recorded at $E_p = 0 \text{ V}$ vs. Ag/AgCl (sat. KCl). Bioelectrodes were stored in fresh buffer solution between stability experiments performed on different days at $4 \text{ }^\circ\text{C}$ in the fridge. Current densities were estimated based on the geometric surface area of the working electrode (0.071 cm^2).

3.4.3 Response of zein sensors

3.4.3.1 Response to inorganic phosphate

The inorganic phosphate determination was evaluated by fluorescence. The method is based on the reaction between the enzyme ALP and the fluorescent substrate OMFP. The presence of inorganic phosphate inhibits the ALP activity (*Figure 26*); thus it can be appreciating a decrease in the fluorescent specie formation due to the slow velocity reaction. The reaction was carried out in solution and by using the developed multiwell-plate zein biodevice. The method was proved in human urine and serum samples.

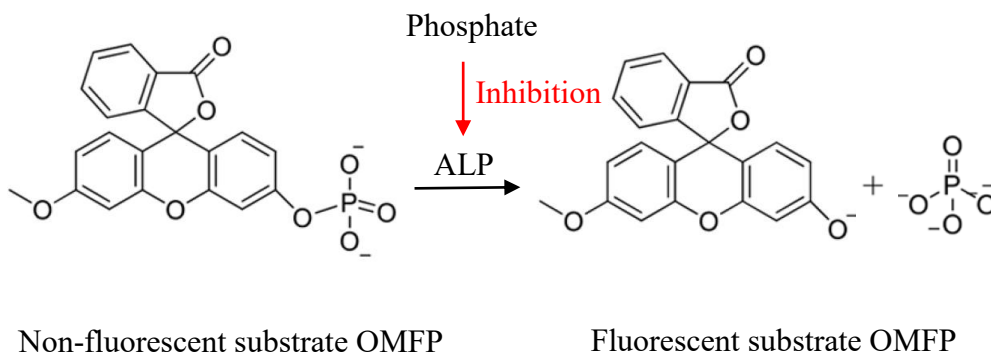


Figure 26. Scheme of the fluorimetric assay based on the inhibition of ALP in the presence of OMFP.

1) Solution

The assay by using the reagents in solution was carried out by the addition of OMFP ($20 \mu\text{L}$ of 0.002 mg mL^{-1}), the inorganic-phosphate standard solution or sample ($15 \mu\text{L}$), and the Tris-HCl buffer solution ($145 \mu\text{L}$, 100 mM , $\text{pH } 9.0$) to the wells. Then, ALP ($20 \mu\text{L}$ of $0.0125 \text{ mg mL}^{-1}$) was added to start the reaction. The fluorescent measurements were read at 485 nm excitation and 513 nm emission every 30 s for up to 2 min . The fluorescence intensity was plotted versus time. The slope obtained was the initial velocity for each concentration. The calibration curve of the inhibition of phosphate was calculated from the initial velocity versus the logarithm of the phosphate concentration from 0.5 to 5 mg L^{-1} .

2) Biosensor

Phosphate standards from 0.5 to 5 mg L^{-1} prepared in a buffer solution (Tris-HCl, 100 mM , $\text{pH } 9$, $200 \mu\text{L}$) were added into each well of the plate containing the biosensor. To carry out the sample analysis, $15 \mu\text{L}$ of each treated sample (*section 3.5.1.1*) was added to $185 \mu\text{L}$ of the Tris-HCl buffer

solution (100 mM, pH 9.0). The signal was registered as mentioned before. All assays were carried out at room temperature by triplicate.

Moreover, phosphate standards were prepared in a simulated-body fluid solution that was made up of different ions, sodium chloride, sodium bicarbonate, potassium chloride, calcium chloride, magnesium chloride hexahydrate, sodium sulphate anhydrous and trys(hydroximethyl) aminomethane according to Marques et al. (Marques et al., 2011), the measurements were carried out as mentioned before.

3.4.3.2 Response to ester groups

The ester group determination was carried out by spectroscopy techniques and diffuse reflectance. The method is based on two reactions, first the ester group react with the hydroxylamine in order to form the hydroxamic acid (high temperature and basics conditions); secondly, hydroxamic acid react with ferric ion with acids conditions to form a colored complex (ferric hydroxamic) (Ramu et al., 2011). Thus, the presence of compounds with ester groups increased the formation of ferric hydroxamic which can be quantify by UV spectrometry due to its reddish-brown color *Figure 27*. The reaction was carried out in solution and by using the three developed sensors (two of them originated in zein and one in paper). The method was proved in drugs samples (atropine, cocaine and ramipril).

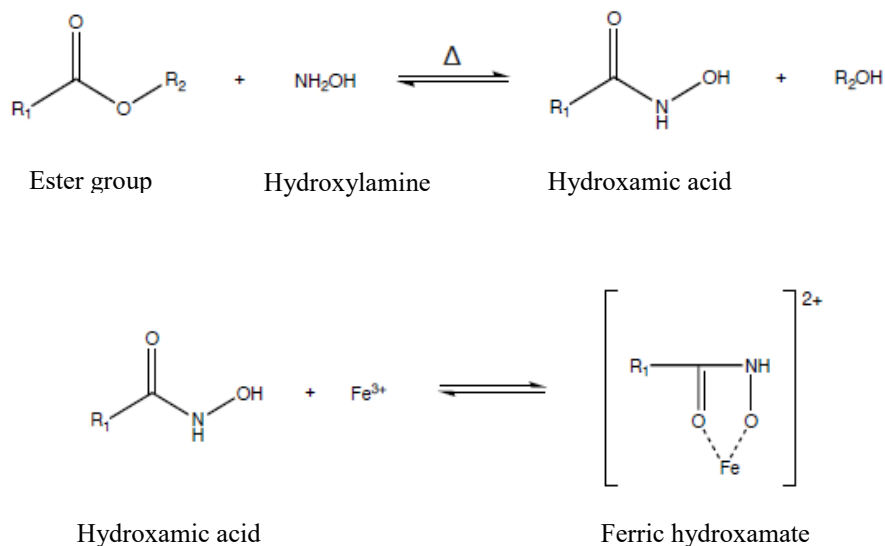


Figure 27. Ester compounds reaction with hydroxylamine.

1) Solution

The assay was carried out by the addition of the stock solution of hydroxylamine (90 μ L of 0.895 M), ester compound (0-50 μ L of 0.1 M) and water (300-250 μ L) into an assay tube that was then heated. Subsequently, the mixture was cooled down to room temperature, and the stock solution of iron chloride (150 μ L of 0.186 M) was added. The solution was measured with a UV spectrophotometer at 525 nm.

2) Zein sensor

The hydroxylammonium sensor was added to basic aqueous solution (250 μ L, 0.5 M NaOH) in an assay tube (Pyrex) for 5 min. Then, the sample or standard was added (20 μ L), and the solution was heated to a boil. After cooling down at room temperature, the solution was acidified (275 μ L, 0.5 M

HCl), and the iron sensor was added. The solution was centrifuged at 5500 rpm for 5 min and then measured with a UV spectrophotometer at 525 nm.

3) Paper sensor

The sample or standard prepared in the stock solution of hydroxylamine (10 μL) was added to the paper sensor which contained iron chloride (3 μL of 0.186 M). After 5 min, the paper-based sensor was measured at 525 nm by diffuse reflectance. A calibration curve was prepared up to 85 mM.

3.4.4 Response of nylon sensor

Nylon support was used to develop a colorimetric sensor for silver ion determination. The method is based on the silver catalytic oxidation of PGR by potassium persulphate in the presence of 1,10-Phen as activator. PGR is the colorimetric reagent (PRG), with which absorbance decreasing at 485 nm is correlated to silver concentration [Sevillano et al., 1986] (see *Figure 28*).

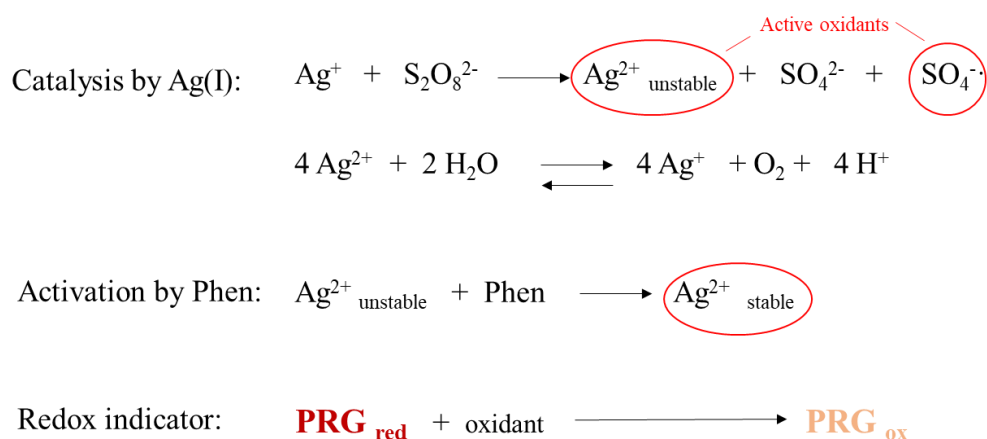


Figure 28. Silver catalytic oxidation of PGR by persulphate ($\text{S}_2\text{O}_8^{2-}$) in the presence of 1,10-phenanthroline (Phen) as activator.

The reaction was carried out in solution and by using the developed nylon sensor. The method was proved in water samples of tap and refrigerate circuits (in which solid biocides leaching Ag^+ were employed).

1) Solution

Standards of silver ion from 0.025 to 0.2 μM prepared in ultrapure water or water samples (2 mL) were acidified with H_2SO_4 2M (40 μL). 1,10-Phen (200 μL of 0.1 M) and potassium persulphate (500 μL of 0.1 M) were added. Then, PGR (200 μL of 8×10^{-4} M) was thrown in to start the reaction. The absorbance signal was captured every 10 s for up to 3 min from 200 to 1000 nm. The calibration curve was calculated by using as analytical signal the difference between the initial absorbance and the absorbance at 3 min (485 nm) versus the silver concentration.

2) Sensor

Water samples or standards (2 mL) were placed in a glass vial containing H_2SO_4 2 M (40 μL) and potassium persulfate (500 μL of 0.1 M). Then, the sensor was put in and after the required time (30 min or 50 min depending on the sensitivity needed), it was taken out of the vial for measurement. Visual inspection of the sensor after exposure was carried out. For quantification purposes, diffuse reflectance measurements at 485 nm and color intensity measurements by GIMP of the images obtained by the smartphone were done (*Figure 29*). The photos were carried out including a non-used sensor on the left of the sample or standard sensor, the first sensor was used for color calibration. Finally, GIMP program was employed to correct the sensor response if necessary, to ensure that the coordinates of the unused sensor with the GIMP were always the same for all measurements; this strategy allows

one to obtain the responses of blank, standards, and samples without variations in light, according to previous studies (Jornet-Martínez et al., 2019; Jornet-Martínez et al., 2017).

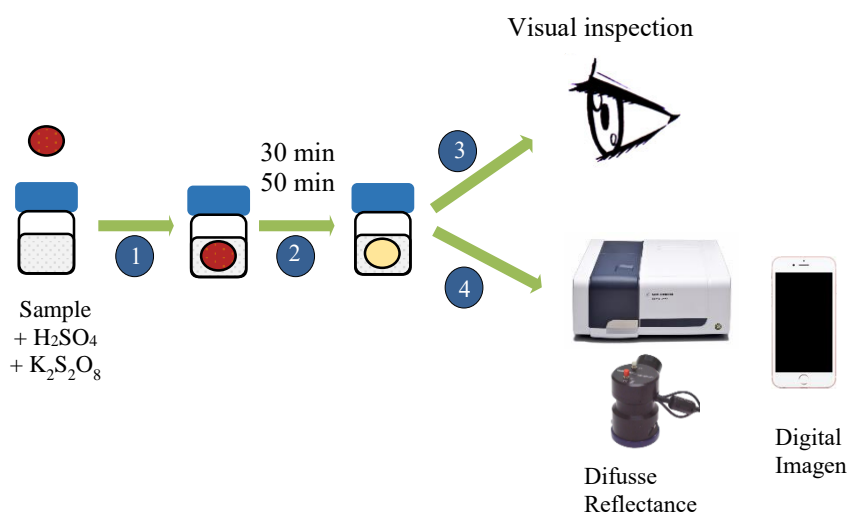


Figure 29. Procedure to obtain the colorimetric response of nylon sensor.

3.4.5 Response of PDMS sensor

PDMS was used as support material to developed a hydrogen peroxide sensor. The method is based on the oxidation reaction of luminol carried out by H_2O_2 and catalysed by HRP which is covalent immobilized on a PDMS surface situated in a polystyrene tube. The oxidation of luminol produces a luminesce signal which is proportional to the H_2O_2 concentration (*Figure 30*). The reaction was carried out in solution and by using the developed PDMS sensor. The method was proved applicability to detect H_2O_2 in culture medium which have been in contact with cells and to measure the H_2O_2 release in denture cleaner tablets.

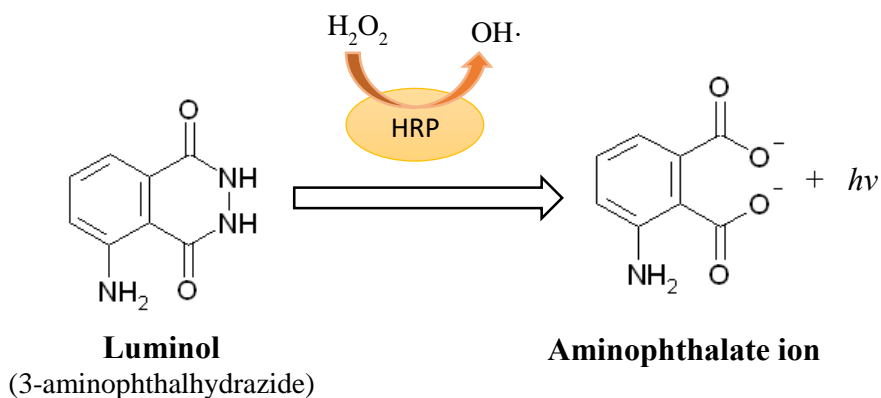


Figure 30. Oxidation of luminol by hydrogen peroxyde.

1) Solution

The assay in solution was performed by adding into the tube 10 μL of 0.01 mg mL^{-1} HRP, 200 μL of 35 mM luminol, and then, 200 μL of H_2O_2 standard solution or sample to start the reaction. At 10 s the luminescence signal was recorded.

2) Sensor

The assay by using the sensor, which contain HRP immobilized, was carried out by adding 200 μL of 35 mM luminol, and then, 200 μL of H_2O_2 standard solution or sample to start the reaction. At 10 s the luminescence signal was recorded. All assays were carried out at room temperature by triplicate.

3.4.6 Response of TEOS/MTEOS sensor

TEOS and MTEOS reagents were used to develop a sol-gel sensor situated in a polystyrene tube which contain luminol immobilized. The sensor allows the analysis of ammonium and organic amino nitrogen. The method is

based on the oxidation reaction of luminol carried out by hypochlorite. First, the ammonium and nitrogen group from organic compounds react with hypochlorite reagent in alkaline media to generate chloramines (Meseguer-Lloret et al., 2006; Pla-Tolós et al., 2015). Secondly, the remaining hypochlorite react with luminol by producing a chemiluminescence signal which is inversely proportional to ammonium and organic amino nitrogen concentration (*Figure 31*). The reaction was carried out in solution and by using the developed TEOS/MTEOS sensor. The method was successfully applicate in a variety of real water samples by including fountain, river, transitional, lagoon and sea water.

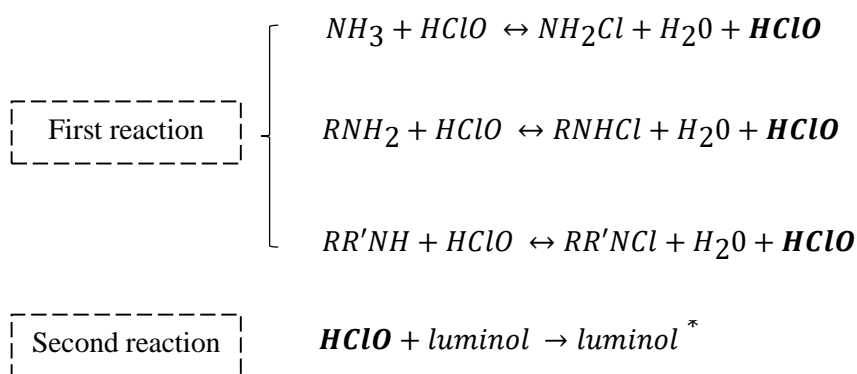


Figure 31. Luminol oxidation reaction carried out by hypochlorite.

1) Solution

First, 20 μL of 0.4 mM luminol were added inside the tube. Then, 400 μL of a solution composed by 50 μL of 0.248 μM sodium hypochlorite and 350 μL of nitrogen standard solution or sample was thrown in to start the reaction. The chemiluminescence (CL) signal was captured at 10 seconds. The same protocol was used for measuring the CL signal by the lab equipment.

2) Sensor

350 μL of the nitrogen standard or sample was mixed with 50 μL of 0.248 μM sodium hypochlorite during 1 minute. Then, the mixture was placed in the tube containing the luminol sensor (this was considered time zero for measuring CL). The CL signal was captured at 10 seconds. All assays were carried out at room temperature by triplicate.

3.4.7 Response of nanocellulose sensor

Nanocellulose polymer was used to develop a stable electrochemical sensor to determine hydrogen peroxide. The method is based on the hydrogen peroxide reduction carried out by enzyme HRP which catalysed this reaction (Xu et al., 2015; Abreu et al., 2018b; Elouarzaki et al., 2015). The reaction was performed with the HRP electrode and with the HRP-nanocellulose electrode.

First, a cyclic voltammetry was performed in 0.01 M phosphate buffer pH=7 to investigate the redox response corresponding to the Fe(III)/Fe(II) redox couple ($v = 5 \text{ mVs}^{-1}$). The solution was put in contact with argon gas for 15 seconds to work in the absence of oxygen. Secondly, the electrocatalytic properties of these modified MWCNT electrodes were investigated towards H_2O_2 reduction. Cyclic voltammetry was performed in 0.01 M phosphate buffer pH=7 by adding different concentrations of H_2O_2 (0.25, 0.5, 1, 2, 4, 6, 8 mM) ($v = 10 \text{ mVs}^{-1}$). Every time that the cell was open to add hydrogen peroxide, argon gas is connected for 15 seconds.

3.5 SAMPLES

In this work, different samples with diverse matrices were analyzed in order to prove the applicability of the developed devices. *Table 19* summarizes the samples and the analytes studied. All samples were analysed in triplicate at room temperature.

Sample	Analyte	Section
Serum	Phosphate	4.1.1.
Urine	Phosphate	4.4.1.
Culture Medium	Hydrogen Peroxide	4.3.1.
Drugs	Ester groups	4.1.2.
Parapharmaceutical tablet	Hydrogen Peroxide	4.3.1.
Waters	Ammonium and organic amino nitrogen	4.3.2.
Refrigeration Systems Water	Silver	4.2.

Table 19. *Samples per analytes studied.*

3.5.1 Biological samples

In this Thesis, biological samples have been analysed to determine inorganic phosphate in serum blood and urine.

3.5.1.1 Serum

Serum samples were collected from different volunteers, both men and women aged between 20-70 years. Serum samples were stored at $-18\text{ }^{\circ}\text{C}$ in

the freezer until use. After defrosting the samples, they were treated with trichloroacetic acid in order to remove the proteins; 100 μL of 10% trichloroacetic acid (TCA) was added to 300 μL of serum samples. Then, the samples were centrifuged for 15 min at 3500 rpm. The clear supernatant was transferred to an Eppendorf tube. To carry out the analysis, 15 μL of each treated sample was added to 185 μL of the Tris-HCl buffer solution (100 mM, pH 9.0). These volumes were placed in the multiwell-plate biosensor. Ninety-six experiments could be performed. The fluorescence signal was measured at 485 nm excitation and 513 nm emission every 30 s for up to 2 min. Recovery studies were carried out by spiking the samples with phosphate concentration 0.5 and 2.5 mg L^{-1} . Each sample was analysed in triplicate.

3.5.1.2 Urine

Urine samples were collected from different volunteers, both men and women aged between 20-70 years. Urine samples were collected using a glass bottle and stores in the freezer at -18°C until use. After defrosting the samples, they were diluted 1000 times in nanopure water, and the same experimental process described for the serum samples was followed. For recovery studies, samples were spiked with a phosphate concentration of 0.5 and 2.5 mg L^{-1} . Each sample was analysed in triplicate.

3.5.1.3 Culture medium DMEM-F12 incubated with neuroblast cells

Samples of culture medium Dulbecco's modified eagle medium F12 (DMEM-F12) GlutaMAX Supplement incubated with neuroblast cells were analysed in order to quantify the produced H_2O_2 . The medium also contains 10 % fetal bovine serum, L-glutamine and Penicillin-Streptomycin. The samples were stored at -70°C in the freezer. After defrosting the samples, they were diluted with water 9:1 (sample:water). To carry out the analysis the

experimental process was followed. Recovery studies were carried out by fortifying with 2 μM H_2O_2 . Each sample was analysed in triplicate.

3.5.2 Drug and parapharmaceutical samples

3.5.2.1 *Atropine sulphate drug*

Two samples were tested: atropine sulphate drug (1 mg mL^{-1}) and Colircusi[®] Atropine 0.5% (which contained 5 mg mL^{-1} atropine sulphate). The experimental process of atropine determination was carried out by adding the sample of the atropine sulphate drug (200 μL) directly without any pretreatment to an assay tube (Pyrex), following the experimental procedure explained in section 3.4.3.2.

3.5.2.2 *Oxygen Bio-Active tablets*

One tablet of Corega[®] Oxígeno Bio-Activo was dissolved in 100 mL of water with and without a denture. The H_2O_2 released from tablets was measured for up to 3 min (time recommended to clean the denture by Corega[®]). At different times (20, 60, 100, 140 and 180 seconds), 200 μL of the sample was taken from the sample and diluted in water (final volume 10 mL). The analysis was carried out following the experimental procedure.

3.5.3 Environmental samples

Water samples from fountain, seawater, transition, lagoon and river were taken from different points of the Valencian Community (Spain). Samples were filtered through 0.45 μm nylon membrane, acidified to pH 2 with HCl and stored in brown glass flasks in the dark at 4 $^\circ\text{C}$, avoiding contact with plastic material. Before using them, we proceeded to alkalize the samples with NaOH to pH 10.5. Samples were analysed in order to quantify

ammonium and organic amino nitrogen. The samples were diluted in nanopure water until it was required in the determination of each analyte present in these waters. For recovery studies, samples were spiked with a nitrogen concentrations of 0.07 mg L^{-1} and 0.105 mg L^{-1} . Each sample was analysed in triplicate.

3.5.4 Industrial sample

Water samples from refrigeration circuits (*Figure 32*), which had been treated with two commercial solid biocides (which contained Ag^+), and tap water were analysed. Moreover, the silver liberation from the solid biocides was studied over time in the laboratory to verify the leaching process; aliquots were taken at 30 s, 1, 3, 5, and 7 h. The samples were filtered or decanted to avoid the presence of solid biocide and stored at room temperature in the dark until analysis if necessary. For recovery studies, samples were spiked with a silver concentration of $0.5 \text{ }\mu\text{M}$ or $1 \text{ }\mu\text{M}$ when the incubation time was 50 min or 30 min, respectively. Each sample was analysed in triplicate.

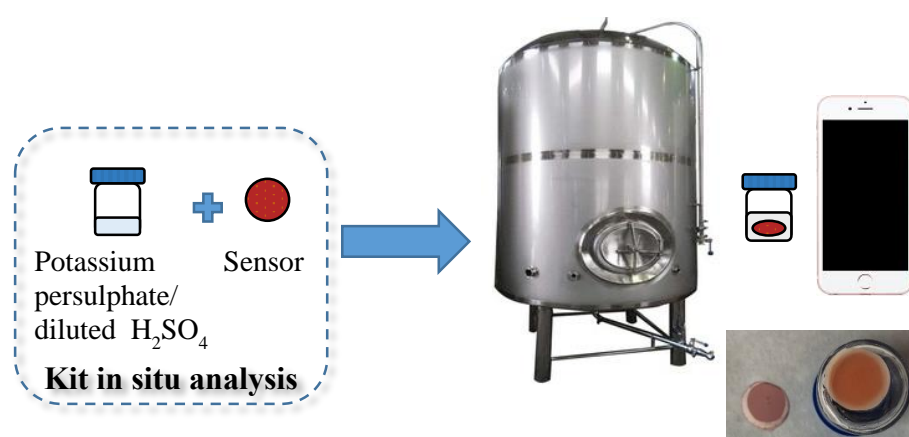


Figure 32. Processing in situ samples by the sensor.

CHAPTER 4. RESULTS AND DISCUSSION

4.1. ZEIN AS SUPPORTING MATERIAL FOR SENSOR DEVELOPING

In this Thesis, Zein is proposed as a biodegradable material for the immobilization of both reagents, substrate and enzyme. As it was described before, Zein is a protein which has excellent chemical properties due to it is composed by a mixture of different peptides which own several molecular size, solubility and charge. Zein is a good alternative to the petroleum derivate materials attributable to its low toxicity and cost.

Based on the interesting features of these material and low cost, we study its potential for the development of biodegradable sensors.

This section has divided in the follow two subsections:

1. Zein-based sensor inorganic for phosphate determination.
2. Zein-based sensor for determination of ester compounds.

4.1.1. Inorganic phosphate determination

In this section, an enzymatic multi-well biosensor fabricated by the immobilization of more than one reagent; the enzyme ALP and the fluorescent substrate OMFP in a zein support was developed. Different immobilization techniques were evaluated in order to achieve a suitable linear range and sensitivity. In addition, parameters as initial velocities, rate constant, linear range, sensibility, precision and stability were estimated. The multi-well plate biodevice was tested to determine inorganic phosphate in human serum and urine samples. Specifically, inorganic phosphate concentration in serum has importance in human health because it has a

critical role in numerous normal physiologic functions including energy metabolism, bone mineralization and intracellular signal. The levels of phosphorus in serum are between 3.4 and 4.5 mg dL⁻¹ according to World Health Organization (WHO). Some pathological conditions could modify the physiological inorganic phosphate concentration in serum and urine (Moe, 2008).

4.1.1.1. Optimization of both enzyme and substrate immobilization

The immobilization of more than one reagent, layer by layer, in one zein sensor through the immobilization techniques of entrapment and adsorption were studied. The reagent was embedded into the film during its formation (entrapment), or the reagent was deposited on the surface of the film (adsorption). As it is known, the activity of an enzyme is intimately related to its structural conformation, which is often highly affected after its immobilization. We demonstrated in a previous paper that the ALP enzyme remained stable and active in the zein film and in contact with the aqueous solutions released from the film into the solution (Jornet-Martínez et al., 2016a). Here, we took a step toward greener methodologies by immobilizing both reagents, the enzyme (ALP) and the substrate (OMFP), in one zein sensor and also by miniaturizing and adapting the fluorimetric assay in a multiwell-plate for multiple analyses. The volume was scaled from 2 mL to 200 μ L (the maximum volume of each well of the plate), and the multiwell device was tested for phosphate determination mainly in human serum, but its application in urine was also tested. In order to develop the multiwell-plate zein-based sensor, several layer configurations (film disposition in the multiwell plate) and reagent immobilization techniques (adsorption and entrapment) were used in the wells of the plate to obtain reliable results. These designs were based on two overlapping layers of zein with the substrate of

the reaction, OMFP, and the enzyme ALP deposited one over the other. In all configurations studied, OMFP was entrapped in the zein film, and ALP was either entrapped (E) or adsorbed (A) (*Figure 33*).

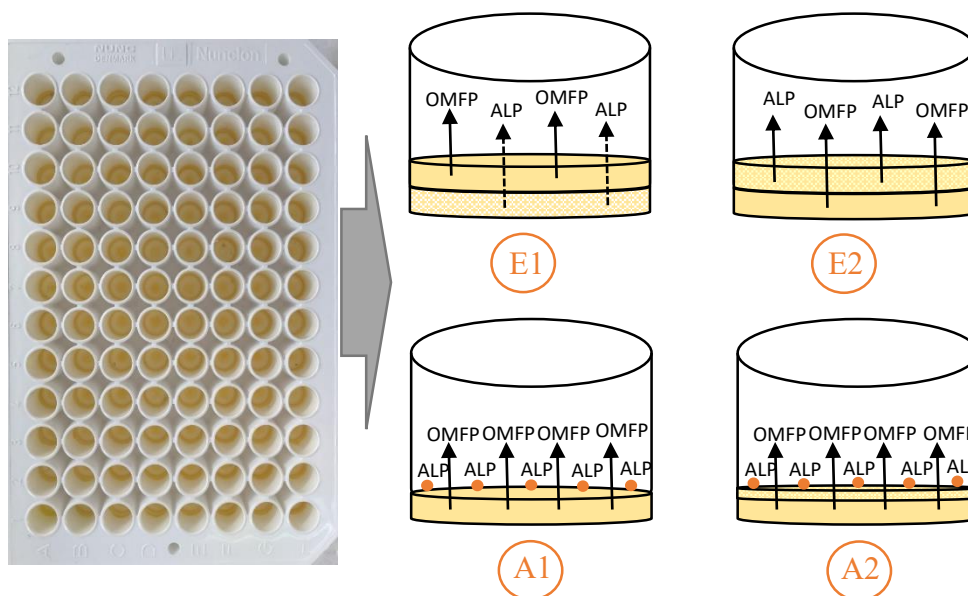


Figure 33. Different configurations tested: (E1) ALP entrapped at the bottom, (E2) ALP entrapped at the top, (A1) ALP adsorbed on the OMFP sensor, and (A2) ALP adsorbed on the glycerol layer.

The fluorimetric assay for phosphate determination using the zein-based sensor is divided into two steps that can take place simultaneously: (1) the reagent release from the zein films to the solution and (2) the inhibition of ALP by phosphate present in solution. In the absence of phosphate, there is an increase of the signal because OMFP is hydrolyzed by ALP to form OMF, which is a fluorescent product. Phosphate inhibits ALP; therefore, the formation of the fluorescent product, OMF, is slowed down. In other words, the initial velocity of the reaction in the presence of phosphate is lower compared with the initial velocity of the reaction without phosphate; compare

the red line in *Figure 34* (no phosphate) with the grey and black lines (0.5 and 2.5 mg L⁻¹ phosphate, respectively).

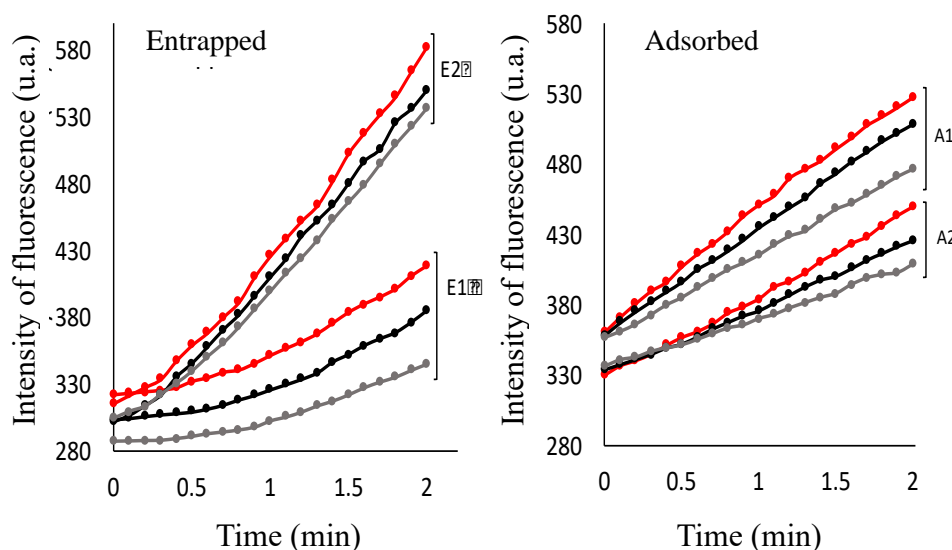


Figure 34. Optimization of the multi-well biosensor. Study of the release (in red) and inhibition by phosphate at 0.5 and 2.5 mg/L (in black and grey respectively) for different configuration of the sensor.

Table 20 compares the initial velocities both in the absence and presence of phosphate. The initial velocity, $V_0(0)$, was the velocity of the formation of OMF between 0 and 2 min based on the available OMFP in solution and active ALP (in the absence of phosphate). In the presence of phosphate, the initial velocity decreased as the concentration of phosphate increased (see *Table 20*, $V_0(0.5)$ and $V_0(2.5)$). In order to obtain the calibration curve for phosphate determination, the initial velocity was represented over the logarithm of the concentration of phosphate up to 5 mg L⁻¹. The slopes obtained for the different configurations (entrapped, E1 and E2, and adsorbed, A1 and A2) were reported in *Table 20* as velocity or rate constants (K).

ALP	Configuration	$V_0(0)^a$ (min ⁻¹)	$V_0(0.5)^a$ (min ⁻¹)	$V_0(2.5)^a$ (min ⁻¹)	K^b (L mg ⁻¹ min ⁻¹)
Solution		109.6 ± 0.9	76.6 ± 0.4	34.6 ± 0.8	-54.3 ± 1.6
Entrapped	Free membranes ^c	94 ± 5	85 ± 5	63 ± 5	-31 ± 2
	E1	49 ± 5	40 ± 5	30 ± 2	-13.4 ± 1.1
	E2	129 ± 9	107 ± 20	102 ± 17	-10 ± 2
	E2 ^d	64.6 ± 1.7	42 ± 2	27.8 ± 1.0	-26.8 ± 1.0
Adsorbed	A1	87 ± 3	74 ± 4	61 ± 2	-17.9 ± 1.6
	A2	58.6 ± 1.1	47 ± 4	35.5 ± 1.5	-18.6 ± 1.2
	A2 ^e	66.5 ± 1.4	56.0 ± 0.6	39.6 ± 0.9	-23.6 ± 0.8

^aInitial velocities obtained for 0, 0.5, and 2.5 mg L⁻¹ phosphate. K is the rate constant in L mg⁻¹·min⁻¹ units, the slope of the calibration curve obtained by representation of the initial velocity against the logarithm of the concentration of phosphate. Only for free membranes 2 mL was employed. ^bRate constant or the slope of the calibration curve obtained by plotting the initial velocity vs the logarithm of the concentration of phosphate. ^cFor free membranes, 2 mL was employed. ^dThe E2 sensor was incubated for 30 s, and the solution was placed in an empty well and measured in the absence and presence of phosphate. ^eWith body fluid.

Table 20. Study of layer configurations for the development of a multiwell biosensor for phosphate determination.

We first studied the release of the reagent immobilized by entrapment in the zein film for two configurations, E1 and E2, by measuring the increment of the intensity over time in the absence of phosphate (*Figure 34*, E1 and E2 in red). As it can be seen in the graphic, E2 showed higher release compared with E1. Also, the linearity was better with E2; for E1, the intensity of fluorescence started to increase after 1 min. This response was probably due to the ALP in E1 was not able to go easily through OMFP sensor because of its high molecular weight. We reduced the distance between ALP and the solution by placing the ALP membrane onto the OMFP membrane in E2 (see *Figure 34*, E2). However, when we tried to inhibit ALP in order to quantify the inorganic phosphate, the E2 configuration presented problems for quantifying different concentrations of phosphate. The inhibition effect was not observed. This was because both processes, the release (which increased the available active ALP and OMFP in solution, which then reacted to form fluorescent OMF) and then the inhibition by phosphate, almost overlap. (In *Table 20* the initial velocities for E2 were almost equivalent). To confirm this hypothesis, the sensor was incubated for 30 s in a buffer solution. The resulting solution was placed in an empty well and phosphate solution was added. The velocity constant obtained in this case was $26.0 \text{ mg L}^{-1} \text{ min}^{-1}$, which was caused by the initial concentrations of ALP and OMFP remaining constant during the measurement (see *Table 20*, E2^d).

As can be seen, for the configuration in which ALP was adsorbed on the surface of the OMFP membrane (A1), the measured initial velocity ($V_0(0)$) was higher than that achieved when the enzyme was entrapped in E1. On the basis of these results, the best configuration so far was A1: the adsorption of ALP onto the OMFP membrane. However, it was observed that during the storage of the sensor (during the thawing process) there was an ALP-OMFP

reaction; thus, the initial velocity was higher. This problem was solved by adsorbing ALP on a zein layer with 70% glycerol (w/w of zein) situated on the top of the OMFP sensor (see configuration A2). Glycerol is a natural plasticizer that has been demonstrated to increase the porosity of zein films (Jornet-Martínez et al., 2016a) to facilitate ALP release.

For the A2 configuration, the sensitivity for phosphate determination using the multiwell device was good enough that a volume 10 times less (200 μL) than that used for free membranes (2 mL) was needed. We showed that the sensitivity of the A2 configuration was better for body medium, probably because of the presence of ions that activate the enzymes (Dean, 2002; Xie et al., 2010). Therefore, the biodevice with the A2 configuration was used for the determination of phosphate in human serum.

4.1.1.2. Analytical parameters and stability

The analytical performance of the developed enzymatic biosensor for determination of inorganic phosphate are summarized in *Table 21*. The measured concentrations of inorganic phosphate were linear in the range from 0.3 to 5 mg L^{-1} . Standard solutions were analysed in triplicate (three wells were employed for each concentration), and the average value was used to construct the standard curve using linear regression. The LOD, defined as the lowest inorganic-phosphate concentration that could be detected, was 0.1 mg L^{-1} . In addition, phosphate concentrations in a simulated-body-fluid solution (*see Section 3.4.3*) that was made up of different ions and spiked with phosphate standards were measured. Although neither Na^+ nor K^+ show any effect on ALP activity, ALP activity is reported to increase in the presence of Mg^{2+} , which is found in the serum (Dean, 2002; Xie et al., 2010). The results

given in *Table 21* show an absolute value for the slope obtained from the body fluid was slightly higher than that achieved with the aqueous standards.

Calibration equation $y = a + b \log x$					
ALP-OMFP	Linear range (mg L^{-1})	$a \pm S_a$	$b \pm S_b$	R^2	LOD (mg L^{-1})
Solution	0.3-5	57.5 ± 0.6	-55.5 ± 1.0	0.998	0.1
A2Biosensor					
Standard in buffer	0.3-5	42.2 ± 0.5	-18.6 ± 1.2	0.992	0.1
A2 Biosensor					
Standard in body fluid	0.3-5	49.1 ± 0.3	-23.6 ± 0.8	0.997	0.1

Table 21. Comparison of the figures of merits obtained for phosphate determination in solution and from the A2 biodevice.

The precision of the method was evaluated by using biosensors synthesized in the same batch and performing the assays on the same day (intraday) and by using biosensors synthesized in different batches and performing the assays on different days (interday). The relative standard deviations (RSD %) obtained were less than 10% for all (i.e., the enzyme free in solution, the A2 biosensor with standards in buffer solution, and the A2 biosensor with standards in body fluid).

The biosensor was demonstrated to be more selective to phosphate compared with the ammonium-molybdate sensor (Campins-Falcó et al., n.d.; Martínez-Soroa et al., 2016), which suffers from interference from arsenates, silicates, sulphides, and oxidizing agents. The biosensor was not affected by other ions such as sodium and potassium.

The operational stability of the biosensor was investigated by consecutive measurements over time (*Figure 35*). The biosensor was preserved by freezing at $-18\text{ }^{\circ}\text{C}$. The reaction rate was measured on different days after 1 h of thawing. The fluorescence response of the biosensor decreased by only 10% after 60 days. About 80% initial activity had been retained after 3 months. The lifetime of the biosensor is markedly longer than that achieved with the solution assay.

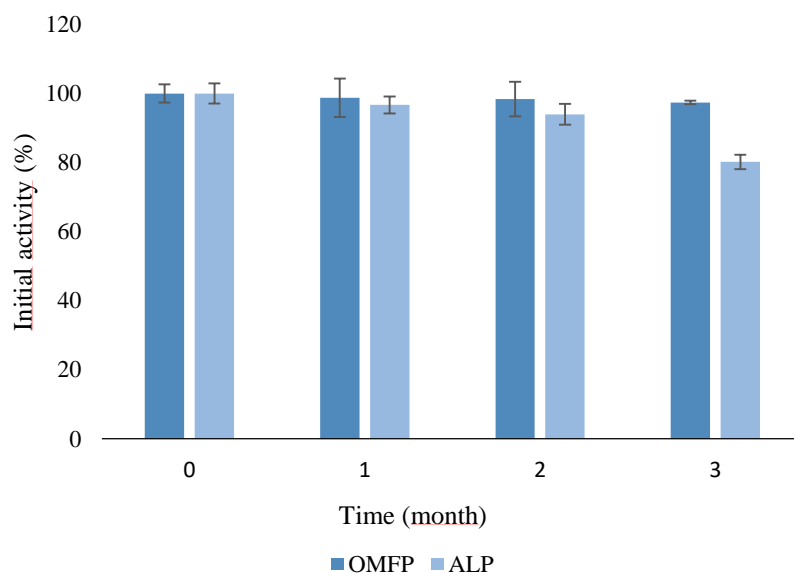


Figure 35. Study of operational stability for the developed sensor by measuring the initial activity over time.

4.1.1.3. Determination of phosphate in real samples

Serum proteins can be precipitated by using several organic solvents (Hušek et al., 2012). Ethanol and trichloroacetic acid were tested in different concentrations and proportions. Finally, 100 μL of 10% trichloroacetic acid was used to precipitate proteins in 300 μL of serum. In order to evaluate the accuracy of the procedure, serum samples were fortified with different

phosphate concentrations between 0.5 and 2.5 mg L⁻¹ (calibration curve obtained: $V_0 = -23.4 \log[\text{phosphate (mg L}^{-1})] + 49$, $R^2 = 0.997$). The recoveries obtained using the body fluid calibration graph were higher than 90% in all cases, and then matrix effect was absent. A confirmation study was carried out by applying the ammoniummolybdate method (Campins-Falcó et al., 2013; Martínez-Soroa et al., 2016). The molybdate method has been commonly used for phosphate determination in water, but the reagent is carcinogenic (Gilbert et al., 2011). Here, we proposed an alternative method that does not use toxic reagents. *Table 22* summarizes the concentrations of inorganic phosphate estimated in serum with our method and the ammonium-molybdate method. The concentrations obtained were statistically similar (paired t test, $p > 0.05$) to those obtained by the proposed method; thus, the A2 biosensor was able to quantify accurately the inorganic phosphate in serum. For all samples except M1, the phosphorus concentration in serum was between 3.4 and 4.5 mg d⁻¹ (0.81 to 1.45 mM), within normal blood-phosphorus levels according to the World Health Organization. The proposed biosensor is a versatile device that allows multiple analyses of phosphorus in serum with accuracy. The achieved figures of merit are similar to those reported for other biosensors proposed recently (Cinti et al., 2016; Upadhyay and Verma, 2015) with the advantage of being a safe and green multianalysis biodevice. In addition, the biosensor was tested with the urine of some healthy volunteers to prove its practicality in other matrices. The urine was diluted (1000×) to be in the linear range of phosphate concentrations, and no matrix effect was found. Recovery experiments were performed by spiking the urine samples with phosphate at 1.5 and 2.5 mg L⁻¹; the recovery values obtained were 100 ± 9 and $98 \pm 13\%$ ($n = 3$), respectively. The concentration found

was $570 \pm 50 \text{ mg L}^{-1}$, in agreement with those reported from the analysis of the urine of healthy individuals (Fadhel et al., 2016; Kratz et al., 2004) .

Samples	Biosensor A2 amount (mg L^{-1})	Ammonium-molybdate amount (mg L^{-1})
M1	51 ± 5	50 ± 1
M2	37.5 ± 0.3	36 ± 6
M3	40 ± 2	41 ± 5
M4	34 ± 4	30 ± 5
M5	36 ± 2	39.3 ± 0.4

Table 22. Confirmatory study of the multiwell plate A2 biosensor vs the ammonium-molibdate method: estimated concentrations of phosphorus in serum samples.

4.1.1.4. Conclusions

Zein is a material extracted from renewable sources it can be degraded naturally, thus the generated wastes do not need to be treated. This work demonstrated that zein can be used as biodegradable material for immobilization of both, enzyme and substrate in the same device without loss of their properties. The focus has also been to develop a multianalysis biodevice, which allows to reduce the time analysis.

Furthermore, the proposed multiwell plate biosensor was successfully utilized to determine inorganic phosphate in serum and urine samples. The resulting device is stable at least 3 months in the freezer and it improves markedly the stability of the ALP in reference to its preparation in solution. The use of the biosensor does not require the addition of external reagents due to the reagents needed for the detection are immobilized in the device. Moreover, the sample volume needed for carrying out the analysis of inorganic phosphate is small and its pre-treatment is simple and quick. Additionally, the developed multiwell plate biodevice had a good

reproducibility and operational stability and improved the greenness, security, rapidity and cost effectiveness in reference to the usual methods.

4.1.2. Ester drugs determination

In this section, two zein-based sensors were developed to obtain a colorimetric device. They were prepared by embedding the reagents iron chloride and hydroxylammonium into zein films. The sensors were used to develop a ferric hydroxamate colorimetric assay, (Feldman and Robb, 1970; Ramu et al., 2011) for routine quality-control analysis of drugs and pharmaceutical products containing ester groups. The characteristics of this assay were compared with those corresponding to the same assay in paper, a natural polymer, and in PDMS, as a petroleum-derived polymer; both of these are widely used for sensor design, and improved results were obtained by zein.

4.1.2.1. Optimization of support material and reagents immobilization

Basic medium was needed for the formation of the hydroxylamine from its salt, hydroxylammonium chloride, and the formation of the ferric hydroxamic complex (second step) requires acid medium. In order to adjust the pH in each step, we tested different concentrations of NaOH (0.75, 0.5, and 1 M) and HCl (0.29, 0.42, 0.5, 0.67, 0.78, 0.89, and 1 M). NaOH and HCl 0.5 M were chosen in further experiments.

Secondly, we study several materials to develop some sensors which contained the reagents involved in the reaction. Following the procedures given in Section 3.3.2, Zein formed stable and functional films. PDMS and paper were assessed, in addition to zein, as supports for carrying out the assay for the determination of ester drugs. We tested PDMS as an example of a petroleum-based material. PDMS-based sensors are easy to manipulate,

highly stable, and biocompatible (A. Argente-García et al., 2016a; Campins-Falcó et al., 2013; Jornet-Martínez et al., 2016d; Prieto-Blanco et al., 2015), but they are not biodegradable. In the case of the PDMS film, the solidification (or gelling) of the PDMS was not produced, as can be seen in *Figure 36A*, and thus it was unsuitable for the above-mentioned application. The functionality of the iron–zein sensor (*Figure 36B*) and the hydroxylammonium–zein sensor (*Figure 36C*) was tested for the determination of ester compounds by ferric hydroxamate formation and spectrophotometry.

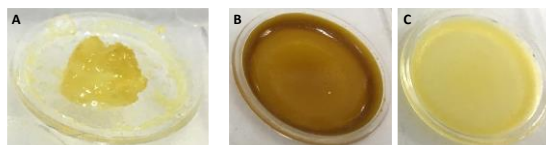


Figure 36. Photography of the sensors after being cured for 1 day. A) iron-PDMS sensor, B) iron-zein sensor and C) hydroxylammonium-zein sensor.

We optimized the amounts of the reagents embedded into the zein films for the Fe(III) sensor and the hydroxylamine sensor. Different amounts of $\text{FeCl}_3 \cdot 6\text{H}_2\text{O}$ (25.15 and 9.38 mg/sensor) and $\text{NH}_2\text{OH} \cdot \text{HCl}$ (18.75 and 3.75 mg/sensor) were tested. Finally, the sensor contains 25.15 mg $\text{FeCl}_3 \cdot 6\text{H}_2\text{O}$ and 18.75 mg $\text{NH}_2\text{OH} \cdot \text{HCl}$.

4.1.2.2. Analytical parameters and stability

The analytical parameters of the colorimetric ferric hydroxamate assay for compounds containing ester groups are reported in *Table 23*. Standard solutions for each compound were analysed in triplicate and the average value was used to construct the standard curve calibration which were determined using sensors synthesized in different batches that showed equivalent results. The calibration curves were calculated from the absorbance at 525 nm measured against the concentration of the analyte (in millimolar).

Analyte	Support material	Calibration equation $y = a + b \cdot \log x^1$			R^2	LOD (mM)
		Linear range (mM)	$b \pm S_b$ (mM)	$a \pm S_a$ (mM)		
Propyl acetate	Zein-based sensors	0.05-100	0.47±0.01	0.36±0.03	0.99	0.01
		0.05-100	0.42±0.02	0.23±0.05	0.99	0.01
	Paper-based sensors	0.84-80	0.31±0.02	34.2±1.1	0.98	0.25
	Solution	7-33	0.037±0.003	-0.01±0.04	0.96	2.36
Atropine	Zein-based sensors ^a	0.12-100	0.15±0.02	0.31±0.03	0.97	0.04
			0.16±0.02	0.23±0.04	0.97	0.04
			0.17±0.01	0.22±0.02	0.99	0.04
			0.17±0.01	0.14±0.02	0.99	0.04
			0.158±0.0009	0.17±0.02	0.99	0.04
Cocaine	Zein-based sensors ^a	0.02-80	1.01±0.01	0.196±0.009	0.99	0.01
			1.02±0.01	0.202±0.007	0.99	0.01
Ramipril	Zein-based sensors	0.36-300	0.053±0.002	0.19±0.01	0.99	0.11

^aSensor obtained from different batches

Table 23. Comparison of the figures of merit obtained the determination of an ester compound (propyl acetate) by the zein and paper-based sensor and by the reagents in solution and analytical parameters using the zein-based sensor for propyl acetate, atropine, cocaine and ramipril.

Figure 37A shows the spectra registered for different ester compounds, namely, propyl acetate, cocaine, ramipril, and atropine, at the given concentrations. The color of the solutions after the assay by increasing concentrations of the mentioned analytes are shown in *Figure 37B*. Higher responses of the sensor (higher absorbances and more intense colors) for propyl acetate and cocaine, compared with those for ramipril and atropine, were obtained.

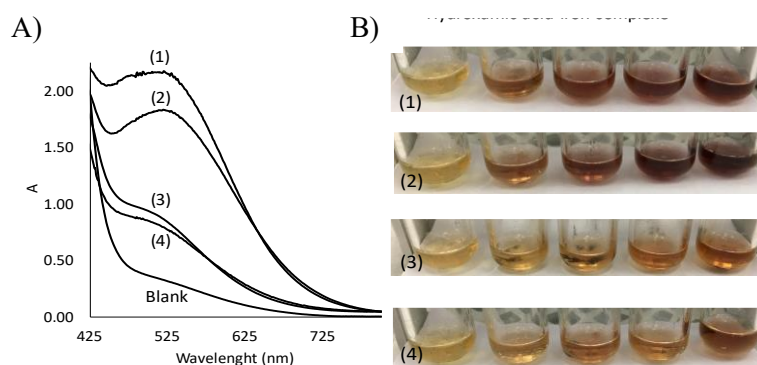


Figure 37. (A) Spectra obtained for (1) 0.1 M propyl acetate, (2) 0.1 M cocaine, (3) 0.3 M ramipril, and (4) 0.1 M atropine. (B) Photographs of the colors of the solution after the assay for the calibration curve: (1) propylacetate from 0 to 3.74 mM, (2) cocaine from 0 to 1.81 mM (3), ramipril from 0 to 11.19 mM, (4) and atropine from 0 to 3.67 mM. The heating temperature was 100 °C.

Furthermore, the same assay was carried out on paper. *Figure 38* shows the color of the reactants (yellow) and product of the reaction (violet-brown) were not homogeneous, and it was more difficult to discriminate between them compared with in the zein-based sensors. The sensitivity achieved for propyl acetate determination on the paper support was lower than that obtained with the zein sensors. In addition, the color in the paper was not stable over time.

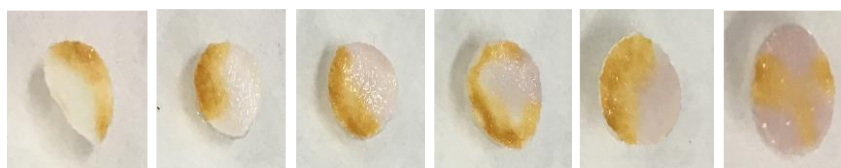


Figure 38. Ferric hydroxamate assay using paper for propyl acetate determination from 0 to 80 mM.

To sum up, the sensitivity was higher for propyl acetate and cocaine (0.1 mM) compared with that for atropine (0.4 mM) or ramipril (0.11 mM). The results for propyl acetate from the zein sensors were compared with those from the paper-based sensor and from the reagent in solution. The results of the zein sensor showed a smaller limit of detection (LOD) and a wider linear range than those obtained from the paper-based sensor and or by using the reagents in solution (see *Table 23*). Moreover, the precision of the method was evaluated with propyl acetate as the target analyte by using sensors synthesized in the same batch and performing the assays on the same day (intraday) and by using sensors synthesized in different batches and performing the assays on different days (interday). The relative standard deviation was calculated for $n = 3$ blanks and $n = 3$ standards of propyl acetate, and the values obtained are reported in *Table 24*.

Batch (n=3)		Relative Standard Deviation (RSD, %)		
		Intraday		Interday
		Day 1	Day 2	Day 1
Batch 1	Blank	1.2	0.6	4.8
	Standard	1.6	10.6	8.5
Batch 2	Blank	0.2	2.4	2.0
	Standard	5.2	3.4	6.9
Batches	Blank	1.9	2.3	3.5
	Standard	5.1	8.5	8.5

Table 24. Inter- and intraday relative-standard-deviation values of the zein sensors. Responses to a blank and a propyl acetate standard obtained in two experiments with the same batch or with different batches.

The assay was carried out with possible interferents, such as paracetamol, glucose, lactose, starch, and caffeine. Only caffeine showed a response, although the solution changed to redbrownish color at the concentration of 250 mM.

The stability was assessed by comparing the atropine determination results obtained from zein sensors after storage at room temperature, at 4 °C, and at -20 °C for 30 days and those obtained from sensors prepared the same day. We showed that the hydroxylammonium sensors stored at 4 and -20 °C did not produce the colored product. On the other hand, the sensors stored at room temperature were structurally and functionally stable and showed ester-determination results similar to those of sensors prepared before the assay. Therefore, the sensors were stored at room temperature.

4.1.2.3. Determination of atropine in real samples

The atropine sulphate drug (1 mg mL⁻¹) was used without pretreatment and was added to the basic solution containing the hydroxylammonium sensor, following the experimental procedure. The concentration obtained was 0.942 ± 0.002 mg mL⁻¹ for $n = 3$ replicates. Also, Colircusi[®] Atropina (which contain 5 mg mL⁻¹ atropine) was analysed. However, the drug contained other ester compounds, such as methyl parahydroxybenzoate and propyl parahydroxybenzoate, in concentrations that were not reported by the manufacturer. The results obtained were 2–3 times higher than the concentration of atropine (5 mg L⁻¹): 11.805, 10.115, and 15.555 mg mL⁻¹; therefore, here, we calculated the total amount of ester compounds contained in the sample, 12 ± 3 mg mL⁻¹, and expressed that as atropine.

4.1.2.4. Conclusions

Zein is a biodegradable polymer obtained as a byproduct of bioethanol production; thus, it is doubly sustainable. Here, we demonstrated that zein is a good support for reagent immobilization and stabilization, moreover, different kind of compounds can be embedded and did not interfere in the formation of the film.

The sensors were successfully applied to the measurement of ester groups in drugs. The LOD achieved, employing the two zein devices for atropine, is 0.12 mM, which is useful for rapid sample screening analysis. In addition, the methodology reported present reliable and green alternative to the conventional method due to its simplicity and low cost. Moreover, the proposed devices minimized the generated waste for the determination procedure.

4.2. NYLON AS SUPPORTING MATERIAL FOR SENSOR DEVELOPING

Nylon membrane as support material for the development of colorimetric sensors has been studied in this Thesis. This material is a suitable support for developing solid sensors to be used in aqueous media.

In this section, a PGR/1,10-phen/Nylon sensor was developed. The stabilization of the reagents (PGR and 1,10-phen) in the nylon support as well as the diffusion of analytes from aqueous samples were studied. Many conditions as reaction medium, reagents concentration and analysis time were studied in order to achieve a suitable linear range and sensitivity. It is noteworthy that by varying the time analysis we can obtain different limit detection values. A quantitative analysis and semi-quantitative was proved as operational applicability to in-situ monitoring of silver ion in water samples and refrigeration systems.

4.2.1 Optimization of the Nylon sensor

Several conditions were studied and optimized in order to carry out the fabrication of a silver ion solid sensor.

Firstly, the influence of pH in the range 1.0 - 8.0 on the catalysed reaction was studied. By using H₂SO₄ 2M and NaOH 0.1 M solutions, the pH solution was adjusted at 1, 2, 6 and 8. The absorbance (400 – 600 nm) as function on time (t=0 and t=3) was registered for the different solutions. *Figure 39* shows that at pH 1 the decrease in the absorbance values was higher, specifically at 485 nm. Moreover, the hydrogen ion concentration will not produce a large oscillation in the absorbance values at low pHs. Therefore, pH 1 was chosen in further experiments.

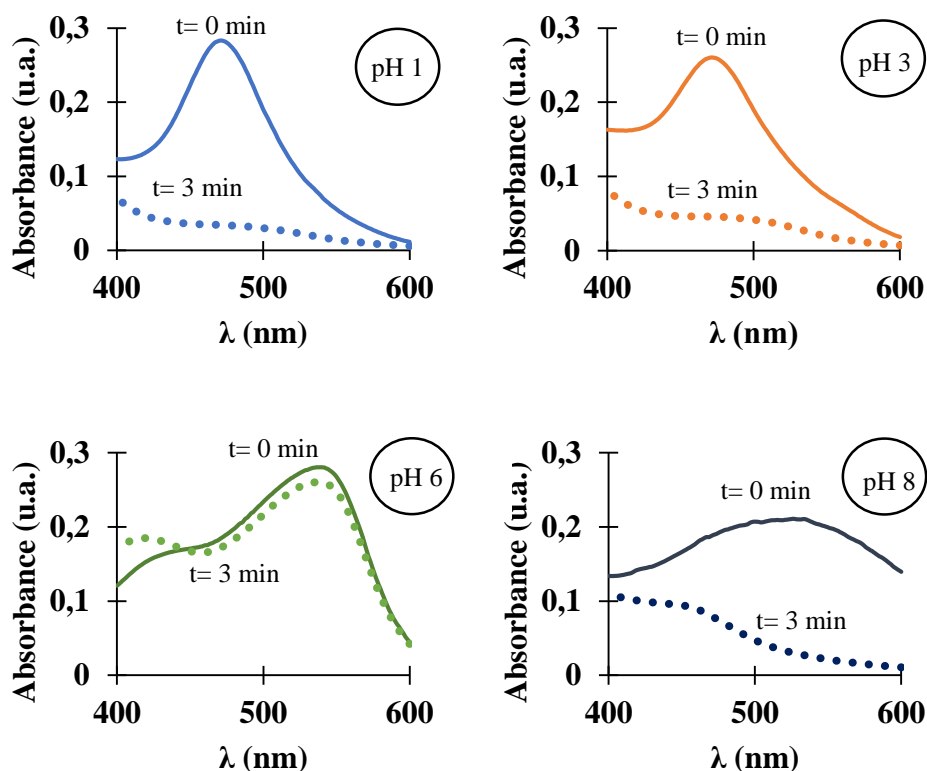


Figure 39. Influence of pH on the catalyzed reaction in solution. Conditions: PGR $5.4 \times 10^{-5} M$, Ag(I) $2 \times 10^{-6} M$, $K_2S_2O_8$ $17 \times 10^{-3} M$, Phén $6.8 \times 10^{-3} M$

PGR reagent, which are involved in the reaction process, were entrapped in several solid supports. Based on our previous experience (Argente-García et al., 2017b; Jornet-Martínez et al., 2018, 2016b, 2016d; Molins-legua, 2018; Pla-Tolós et al., 2016), zein, PDMS and nylon materials could be used to immobilize reagents (Figure 40A). PGR as solid or in solution was entrapped in PDMS and PDMS-TEOS composites, however no response was observed for either. Figure 40B-a shows the PGR-PDMS sensor in a solution containing persulphate and Ag^+ at pH=1 and Figure 40C-a shows the sensor after 50 min. PGR-PDMS sensor and the aqueous medium remained unchanged, this behaviour could be explained to the no diffusion of the PGR

to the solution. Moreover, the persulphate and ion silver could not entry into the PDMS composite due to their ionic character. These phenomena did not allow to perform the reaction neither solution neither nor the solid support. No differences in behaviour were observed between the support of PDMS or PDMS doped with TEOS. On the other hand, PGR was immobilized in zein membrane (*Figure 40A-b*). Zein support releases part of the PGR to the solution (*Figure 40B-b*), therefore no control of the reaction could be taken due to the reaction was carried out in the support and in the solution (*Figure 40C-b*). Finally, nylon was tested as support material (*Figure 40A-c*). The sensor was carried out by passing a PGR solution through the membrane (*Figure 40A-c*). After being in contact with a solution of persulphate and ion silver, no color had the solution (*Figure 40B-c*) and the sensor changed its color due to the PGR oxidation (*Figure 40C-c*). Therefore, nylon membrane was chosen as support material.

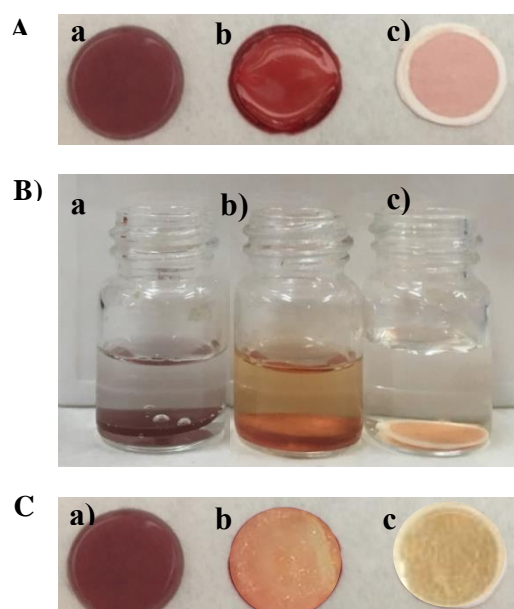


Figure 40. A) Reagents (PGR and Phen) retained in a solid support a) PDMS, b) zein, c) nylon. B) Reagent supports in solution in presence of Ag^+ and persulfate in acid medium. C) Membrane after PGR oxidation reaction a) PDMS, b) zein, c) nylon.

Phenanthroline and potassium persulphate concentrations were studied to evaluate the sensor response for both, silver ion catalysed and non-catalysed reaction. First, 1,10-Phen concentration were varied (0.095 M, 0.12 M, 0.15 M and 0.17 M); PGR and potassium persulphate concentrations were fixed, 8×10^{-4} M and 19.7 mM respectively. *Figure 41A* shows the sensor color response to different silver ion concentration at 50 minutes, the results were obtained selecting yellow color intensity by the GIMP tool. For a given concentration of Phen, the color intensity decreased as function of silver ion concentration due to the oxidation of PGR. Based on the results, 0.17 M of 1,10-Phen was selected. It can be also appreciated in *Figure 41A* the velocity of the catalysed and non-catalysed reaction increased with the phenanthroline concentration. Secondly, potassium persulphate concentration were varied (16.4, 19.7 and 22.7 mM); PGR and 1,10-Phen concentrations were fixed, 8×10^{-4} M and 0.17 M respectively. *Figure 41B* shows the yellow color intensity as function of silver concentration. The velocity of the catalysed and non-catalysed reaction increased with the potassium persulphate concentration. High concentration of potassium persulphate (22.7 mM) produces an undesirable brown color in the sensor and altered its silver ion concentration response (from 1 μ M). The selected concentration of potassium persulphate was 19.7 M.

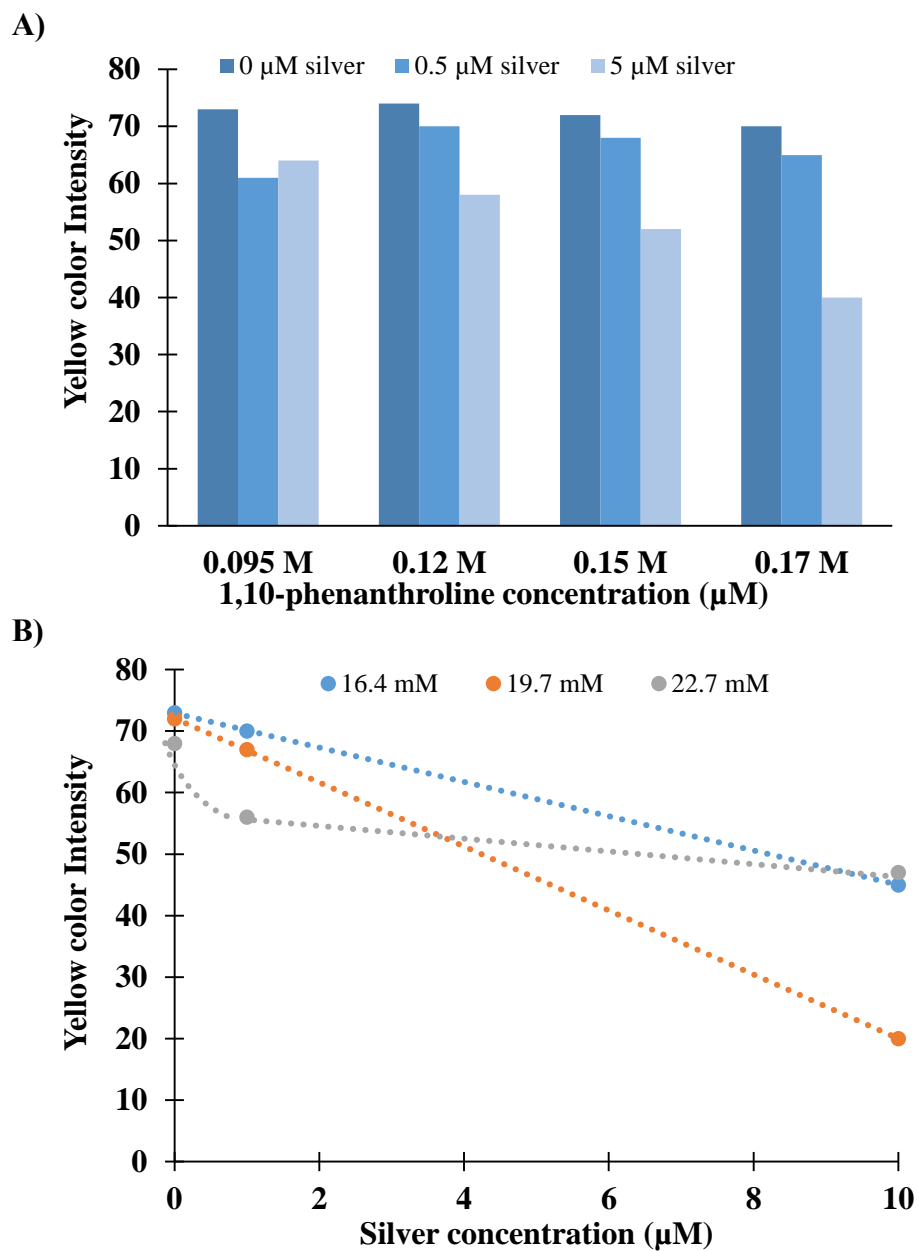


Figure 41. A) Optimization of the sensor development for 1,10-Phen concentration (0.095, 0.12, 0.15, 0.17 M) at 50 min. B) $K_2S_2O_8$ concentration (16.4, 19.7, 22.7 mM) at 50 min.

Incubation time to carried out a qualitative and/or quantitative analysis was studied each 10 min over 1 hour (Figure 42). Silver ion assayed concentrations can be noticeable seen at 30 minutes, however, we can achieve

higher sensitivity at 50 minutes. Since non-catalysed reaction advanced too, longer times did not provide improved analytical parameters. According with the results, it is possible to select incubation time as function of the needed sensitivity due to this parameter is dependent on silver ion concentration (*see section 4.2.4*).

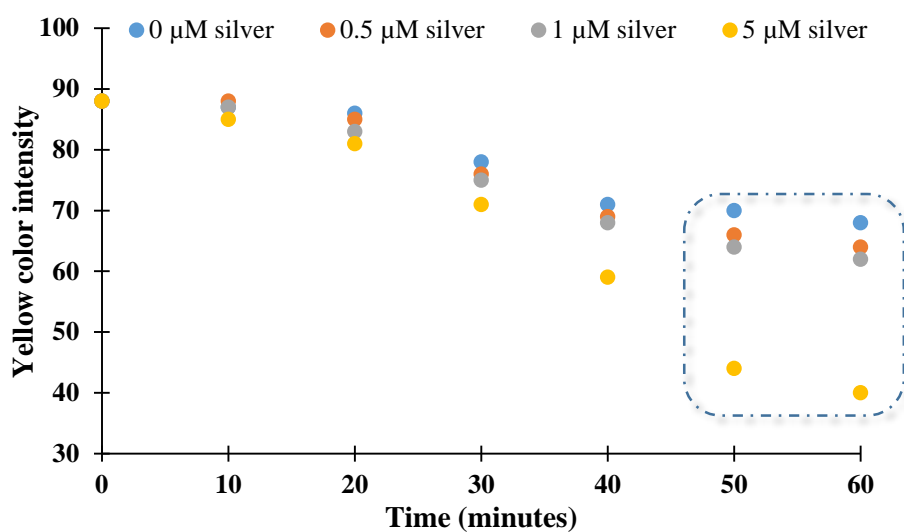


Figure 42. Optimization the reaction time (different Ag^+ standard concentrations 0.5, 1, and 5 μM).

4.2.2 Characterization of the nylon sensor

Nylon sensor was characterized by microscopic and IR technics. *Figure 43A* shows the microscopic images of free nylon support, nylon with reagents (1,10-Phen, PGR) and nylon with reagents in the presence of different Ag^+ concentrations. The color sensor change with the silver ion concentration. IR spectra of nylon membrane, Phen, PGR and nylon membrane with the retained reagents were recorded in *Figure 43B*. Some of the IR bands corresponding to the reagents are present in the nylon containing the reagents.

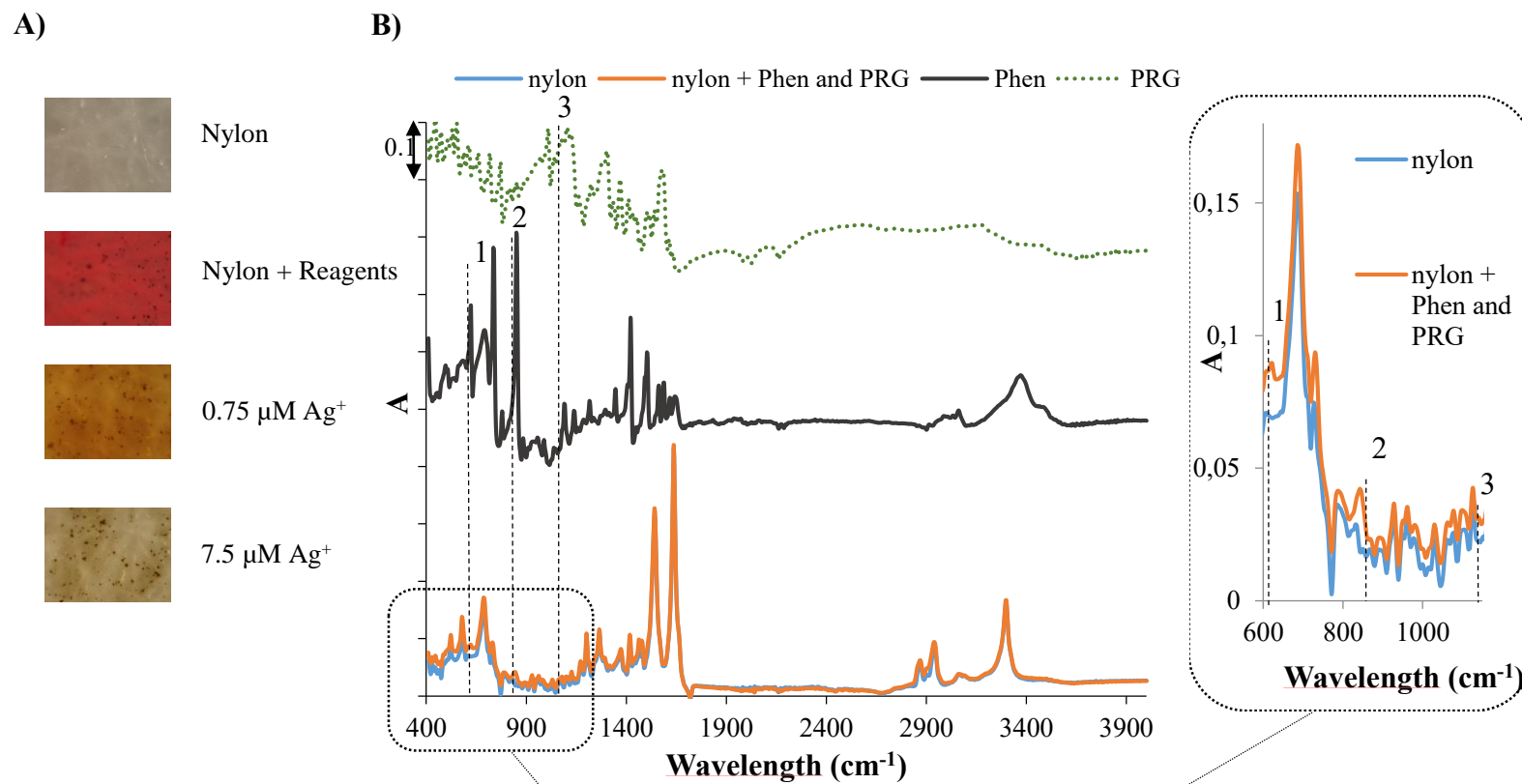


Figure 43. A) Optical microscopic images $\times 10$ of nylon, nylon with the reagents (PGR, 1,10-Phen), and in presence of different Ag(I) concentrations. B) IR spectra

4.2.3 Interference study

The effect of interference by other ions was studied in the samples. The selectivity was according to Sevillano-Cabeza et al (“Study of the Silver-catalysed Pyrogallol Red - Peroxodisulphate Reaction with 1,10-Phenanthroline as Activator,” 1986). The interfering processes may be classified as follows, the values in parentheses being the maximum tolerable concentration ratios of foreign ion to silver: species that accelerate the catalytic activity of silver on the oxidation of PGR, such as Fe^{III} (< 10), Mn^{VII} (≤ 10), Ce^{IV} (≤ 20), Cr^{VI} (≤ 20), Al^{III} (≤ 3000) and Zn^{II} (≤ 3000); species that inhibit the catalytic oxidation of PGR, such as Ni^{II} (≤ 5000), Cu^{II} (≤ 5000); and species that do not interfere (> 10.000), ClO^3- , ClO^4- , Cr^{III} and Mn^{II} . Thus, we can conclude that the method was appropriate for estimating silver ion in water samples.

4.2.4 Analytical parameters

The nylon sensor proposed in this work, changes its color from red to white as function of silver ion concentration. *Figure 44* shows the spectra and the sensor images corresponding to different silver ion concentration after 50 min as incubation time. It should be noted that the difference in the color of the sensor can be a powerful tool for monitoring the silver ion concentration by visual inspection.

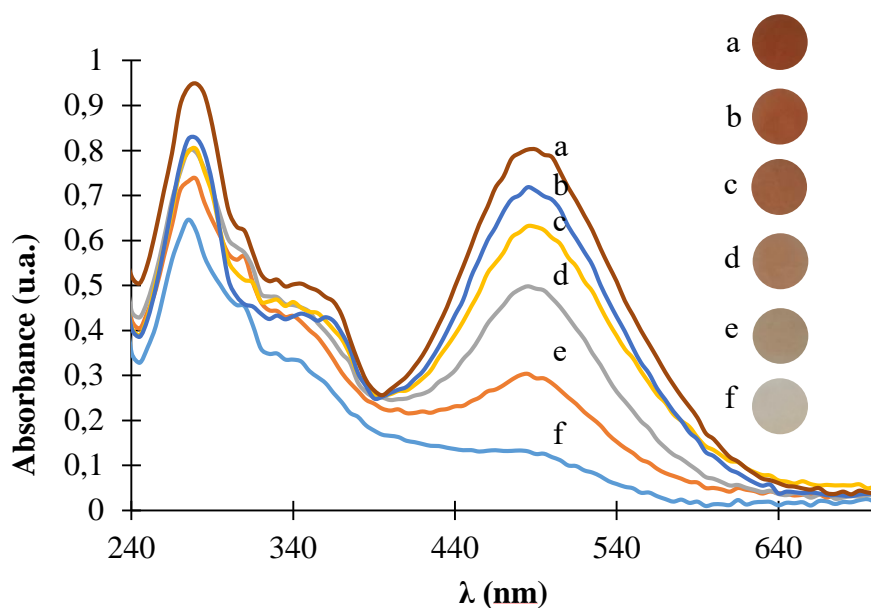


Figure 44. Sensor for the detection of Ag(I). Absorbance spectra obtained by diffuse reflectance for different concentrations of Ag ion (from top to bottom): 0, 1, 2.5, 5, 7.5, 10 μM and change color sensor.

Figure 45A shows the calibration graph to quantify silver ion obtained with diffuse reflectance at 485 nm after 50 min as incubation time and *Figure 45B* gives the yellow and magenta color intensities vs silver ion concentration processed by the GIMP tool from the smartphone photographs. As it has been written in section 4.2.1, it is possible to select different incubation times as function of the needed sensitivity, *Figure 45C* represented the silver ion calibration graphs for several incubation times (10, 20, 30 and 50 minutes).

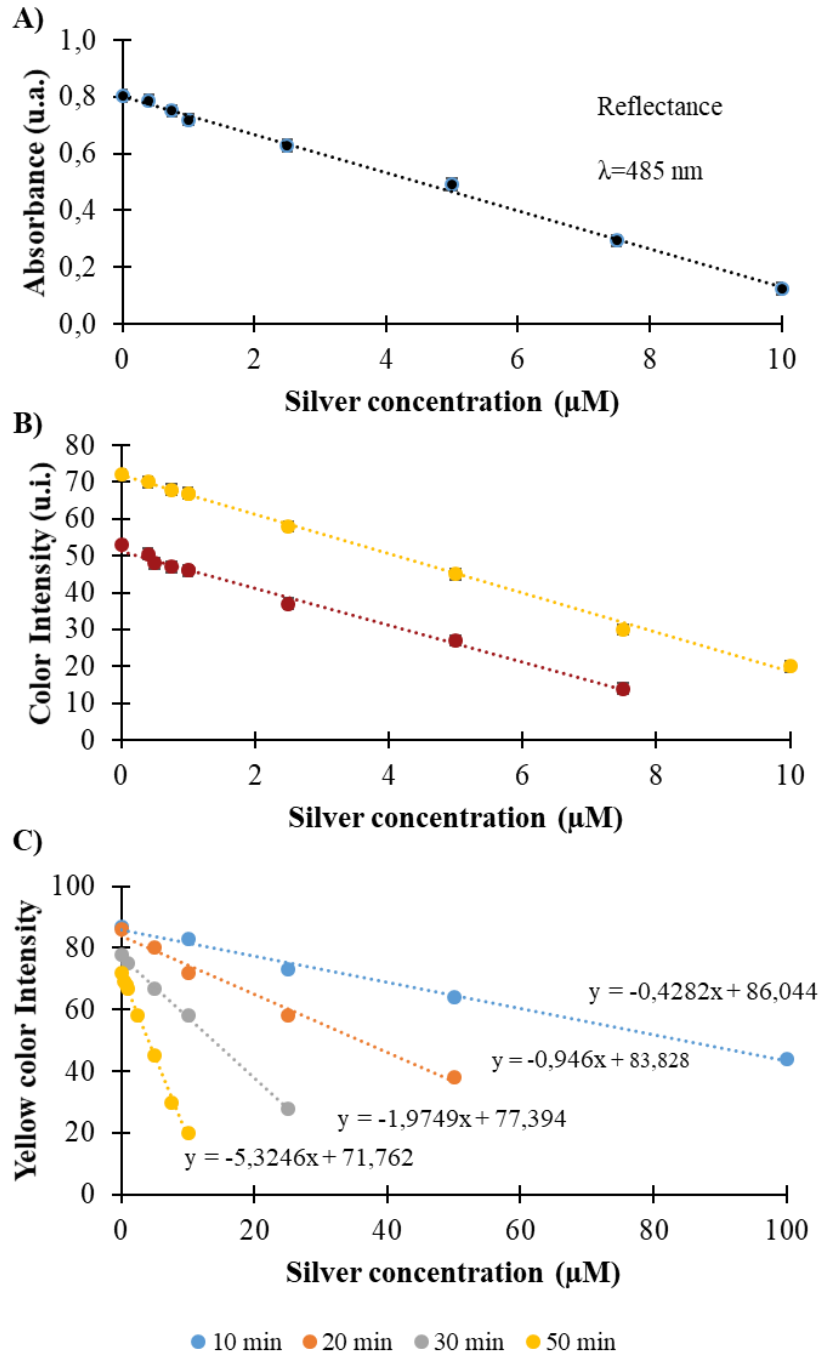


Figure 45. Sensor for the detection of Ag(I). A) Dependence of absorbance at 485 nm on the concentrations of Ag(I). B) Dependence of yellow and magenta color intensities on the concentrations of Ag(I). C) Calibration graphs for several incubation times.

Table 25 shows the analytical performance for the response of silver ion concentration by employing the developed nylon sensor. The results were obtained at several incubation times by using the DR probe and colour sensor processing tool (magenta and yellow). Linear range were varied depending on the incubation time. The precision of the analysis was also evaluated. For the intraday and interday precision, we compared the response of three sensors prepared in three different batches under identical conditions (0.5 μM). Since RSD values < 6 , no significant differences were found. The low RSDs indicated that the proposed sensor is a reproducible device for practical applications. LOD was calculated as $3s_{\text{blank}}/b$ where b is the slope of linear calibration curve and s_{blank} is the standard deviation of the absorbance or color intensity of ten blanks. Similar results in terms of linear range, precision and LOD were reached by using the DR at 50 minutes and by using the GIMP tool (yellow intensity). Therefore, both procedures can be used if quantitative analysis is required. The DR method is more tedious requiring to measure the sensor with a laboratory equipment.

Methods / Incubation time	Linear range (μM)	RSD (%) (n=3)		LOD (μM)
		Intraday	Interday	
Reflectance method / 50 min	0.4 – 10	3	6	0.1
GIMP magenta / 50 min	0.4 - 7.5	1.4	3	0.1
GIMP yellow / 50 min	0.4 – 10	1.4	3	0.1
GIMP yellow / 10 min	10 -100	2	5	3
GIMP yellow / 20 min	5 -50	3	5	1.5
GIMP yellow / 30 min	1 -25	2	4	0.3

Table 25. Figures of merit of the use of the proposed sensor for quantifying silver ion in water.

The developed device is stable for up to four months after sensor storage at room temperature in the dark since their analytical response remained unchanged providing precise responses, with RSD of the signals $\leq 7\%$. Its stability was established by comparing the color sensors response (n=3) for 0.5 μM of silver and incubation time of 50 min. The sensor response was evaluated the same day that they were prepared (day=0) and after four months of its storing at room temperature in the dark. The developed nylon sensor improves the reagents stability due to as it is described in the literature (López-Alarcón and Lissi, 2006) the reagents employed are instable, specifically Phen solutions are stable only for a few days and PGR solutions are usually prepared daily.

4.2.5 Analysis of samples

Silver ion from tap and refrigerate circuits waters were analysed by using the proposed nylon sensor. The incubation time was 30 min or 50 min (see *Table 26*). The sample sensor and blank sensors were photographed together for obtaining silver concentrations by the smartphone images and GIMP software.

The silver ion content in the analysis of tap water analysis was according to the Environmental Protection Agency (EPA) and WHO (Herschly, 2012; "Silver; CASRN 7440-22-4," 1987). A value of 400 nM. Silver ion concentration in waters from refrigeration circuits were up to near 3 μM . This value was according with the manufacturer. In *Table 26* are shown the found concentrations of silver ion in the samples. The accuracy of the method was evaluated by spiking the samples with 0.5 μM of silver ion concentration. The recovery values were between 86% and 119%, thus no matrix effect was

present by using the proposed sensor. Moreover, the analysis silver ion content in two pilot plants (A and B) were carried out to evaluate the release of silver ion from two commercial biocides. Samples were taken at different times, the silver ion content increased with time (see *Table 26*). The samples were fortified with 0.5 μM of silver ion concentration and the recoveries values were close to 100%.

Sample	Leaching/ Incubation time (h)	Found concentration (μM)			Recovery (%)	
		Solution	Colorimetric sensor		Reflectance method	GIMP yellow
			Reflectance method	GIMP yellow		
Water with Biocide A	0.5 / 50 min	0.95 ± 0.12	0.95 ± 0.03	1.095 ± 0.015	87 ± 6	104 ± 8
	1 / 50 min	1.7 ± 0.2	1.62 ± 0.05	2.22 ± 0.03	109 ± 8	102 ± 6
	3 / 50 min	2.2 ± 0.3	2.64 ± 0.08	2.78 ± 0.04	-	-
	5 / 50 min	2.6 ± 0.3	2.70 ± 0.08	2.71 ± 0.04	95 ± 5	102 ± 6
Water with Biocide B	0.5 / 50 min	1.07 ± 0.14	1.17 ± 0.04	1.095 ± 0.015	108 ± 8	104 ± 6
	3 / 50 min	1.7 ± 0.2	1.68 ± 0.05	1.66 ± 0.02	98 ± 6	103 ± 5
	5 / 50 min	1.6 ± 0.2	1.49 ± 0.04	2.22 ± 0.03	99 ± 7	102 ± 6
	7 / 50 min	3.0 ± 0.4	3.14 ± 0.09	3.34 ± 0.05	97 ± 5	102 ± 5
Tap water	- / 50 min	0.32 ± 0.04	0.4 ± 0.1	0.4 ± 0.1	94 ± 6	110 ± 9
Refrigerated System 1	- / 30 min	2.0 ± 0.3	2.1 ± 0.3	2.1 ± 0.3	97 ± 6	106 ± 8
Refrigerated System 2	- / 30 min	2.4 ± 0.3	2.6 ± 0.3	2.7 ± 0.4	96 ± 5	104 ± 6

Biocide A and Biocide B are solid products, which liberate silver ions by leaching and the liberation was simulated in a pilot plant in the lab (see text for more explanation).

Table 26. Results of analysis of water samples.

A confirmatory study was carried out to corroborate the results obtained in solution and by using the sensor with both measurement tools, reflectance and GIMP, were similar. The obtained regressions between the solution method and the colorimetric sensor were $y = (-0.126 \pm 0.185) + (1.10 \pm 0.094)x$; $R^2 = 0.99$ for reflectance method and $y = (0.0933 \pm 0.24) + (1.114 \pm 0.124)x$; $R^2 = 0.99$ for GIMP method (yellow color), where y de analytical signal and x the concentration; the ordinates were consistent with 0 and the slopes included 1. From these results we can conclude that both methodologies provided statistically equal results than those achieved in solution assay, thus the proposed methods can be used to determine silver ion in water samples.

4.2.6 Conclusions

The use of PGR/1,10-phen/Nylon device avoids having two reagent solutions. Furthermore, the device is able to increase the stability of both reagents and reduce the toxicity derived from their handling. The sensor allows an in-situ analysis, thus semiquantitative analysis of waters could be continuously performed through a reference color card. This leads to an economic saving derived from the non-need for conventional equipment and a reduction in qualified personnel. Also, quantitative analysis could be performed by using DR and DI analysis. The results obtained with both measurement methods were similar in terms of accuracy and precision. The proposed optical sensor was successfully applied to determine silver ion in tap water and waters from refrigerate systems. It is noteworthy that the fabrication of the sensor is simpler than many of those reported in the literature. The main advantages of the PGR/1,10-phen/Nylon device are the rapidity, simplicity and portability. Moreover, the developed sensor

minimized risks associated with the manipulation of harmful liquids and it does not need sample preparation and trained personnel.

Finally, this paper shows that it is possible to use non-enzymatic catalysed reactions for developing sensors, which change their color in function of the analyte concentration. We also achieved that the sensor contains together the activator and the dye.

4.3. SILOXANE GROUPS AS SUPPORTING MATERIAL FOR SENSOR DEVELOPING

The use of siloxane groups as support material for covalent binding or encapsulate reagents has been studied in this Thesis. They are suitable supports for developing solid or sol-gel sensors to use in aqueous media.

This section has divided in the follow two subsections:

1. PDMS-based sensor containing HRP for the estimation of hydrogen peroxide.
2. Sensor based on TEOS/MTEOS/luminol sol-gel for controlling dissolved ammonium and organic amino nitrogen.

4.3.1. PDMS-based sensor containing HRP for the estimation of hydrogen peroxide

In this Thesis, PDMS has been proposed as a solid support material for the covalent binding of enzymes. This Si-based material is a suitable support which is able to be activated with hydroxyl groups to subsequently anchor enzymes through their NH_2 groups. The enzyme binding plays a significant role to develop biosensor due to the enzyme has to be chemically attached on the support surface. Moreover, it is important the orientation of the enzyme to allow the substrate entry (Ibarlucea B., Fernández-Sánchez C., Demming S., Büttgenbach S., 2011; Kreider et al., 2013; Sassolas et al., 2012; Sui et al., 2006).

In this section, a reusable biosensor for the determination of H_2O_2 is proposed. The reaction is based on the luminol oxidation reaction carried out

by H_2O_2 and catalysed by HRP, which is covalently immobilized on a PDMS surface placed in a polystyrene tube. As mentioned before, the enzyme binding is a key step to develop the sensor, thus, different procedures described in the literature were studied (Ibarlucea B., Fernández-Sánchez C., Demming S., Büttgenbach S., 2011; Kreider et al., 2013; Sui et al., 2006). Moreover, reagents concentration (luminol, H_2O_2 and HRP) were evaluated in order to achieve a suitable linear range and appropriate sensitivity. In addition, analytical parameters as linear range, sensibility, precision, stability and reusability were estimated and compared with other methods described in the literature (*see Section 1.3.4*). The developed sensor has been used for the in-situ detection of H_2O_2 in a culture medium (DMEM-F12) which was in contact with neuroblast cells and to measure the H_2O_2 release by denture cleaner tablets.

4.3.1.1. Optimization of the HRP/PDMS sensor

Several parameters were studied and optimized in order to carry out the solid sensor fabrication and establish the reaction conditions.

PDMS was chosen as inert support to immobilize the enzyme. This support is biocompatible and it should not interfere with the protein native structure. As it is mentioned before, the anchor of the enzyme is a critical factor to develop the biosensor due to it has to maintain its activity after the covalent binding. Different procedures described in the literature were combined to establish the best immobilization conditions (Ibarlucea B., Fernández-Sánchez C., Demming S., Büttgenbach S., 2011; Kreider et al., 2013; Sui et al., 2006). *Figure 46* shows the schematic description for the biofunctionalization of the PDMS to accomplish the biosensor. First, the

surface of the PDMS was activated with hydroxyl groups (1) by adding an acidic solution containing H₂O, 37% HCl and 30% H₂O₂ in a 5:1:1 (v/v/v) ratio, then, the amino-functionalization of the activated PDMS (2) was carried out by adding a solution which contains APTMS, followed by the addition of glutaraldehyde (3) and finally the covalent immobilization of the HRP (4) (*see Section 3.3.4*). Two different options of carrying out the linking between the HRP to the support were tested to optimize the immobilization process. The first one consisted of linking the GTA to APTMS after HRP and the second one was to obtain the cross-linked enzyme aggregates with GTA and HRP, and the aggregates were linked to APTMS. The obtained results indicated that there were no differences due to the responses were similar in both processes. In conclusion, the amount of immobilized enzyme on the PDMS support was comparable. According to the results, the first option was selected for further experiments as it was the simplest process. It was remarkable that the use of cyanoborohydride reported in the literature (Kreider et al., 2013) to perform the immobilization between glutaraldehyde and HRP was avoided due to this reagent did not favour the immobilization process, moreover it is not an environmental friendly reagent..

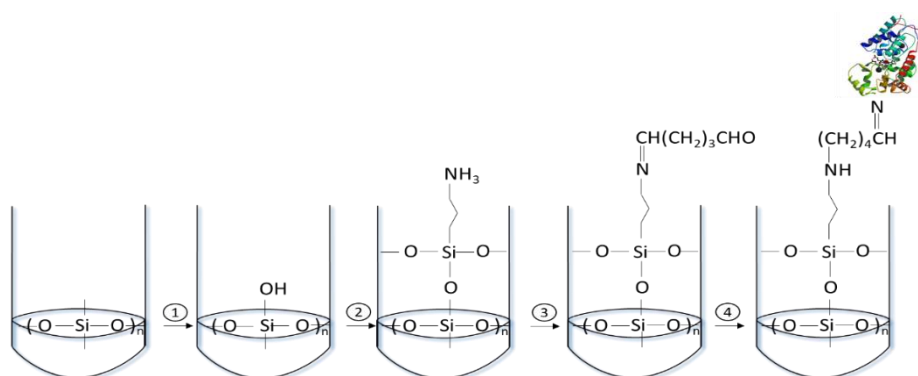


Figure 46. Schematic description of biofunctionalization of PDMS. Activation of PDMS surface (1), silanization using APTMS (2), activation with GTA (3) and linking of link of HRP by GTA (4).

Secondly, it was optimized the linking of the HRP to the activated support. Different concentrations of enzyme (between 0.005 and 5 mg·mL⁻¹) were studied to select the most efficient HRP concentration. The responses of the biosensors were tested by employing 50 μM of H₂O₂ and 17.5 mM of luminol measured after 10 s with a portable luminometer. *Figure 47* shows the results; it is recommended to use enzyme concentrations higher than 0.1 mg mL⁻¹ to achieve the maximum response. Solutions used for HRP immobilization were not discarded, and they were used for other purposes because the remaining enzyme was still active.

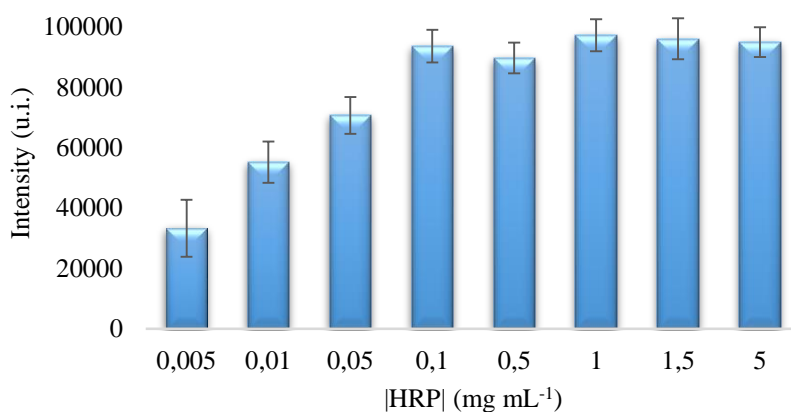


Figure 47. Relative luminescence units recorded with a portable luminometer at 10 seconds by varying the concentration of enzyme dissolution used to immobilize it in the activated PDMS surface.

1) Immobilized enzyme activity measurement

The activity of the immobilized HRP was determined by interpolating the luminescence signal obtained by using the biosensor in two solution calibration curves. Calibration curves were obtained by keeping H₂O₂ and luminol concentration constant (50 or 2.5 μM and 17.5 mM, respectively) and varying the HRP concentration (0.004 – 0.022 mg mL⁻¹). Therefore, the luminescence signal obtained by using the biosensor with 50 or 2.5 μM of

H₂O₂ and 17.5 mM of luminol was interpolated. *Figure 48* shows the two calibration curves obtained after 10 s of the H₂O₂ addition. The results indicated that the theoretical concentration of active HRP immobilized to the PDMS surface was 0.0136 mg mL⁻¹ (0.02 U) obtained by employing 2.5 μM H₂O₂ and 0.0156 mg mL⁻¹ (0.023 U) by employing 50 μM H₂O₂. We concluded that both results are comparable.

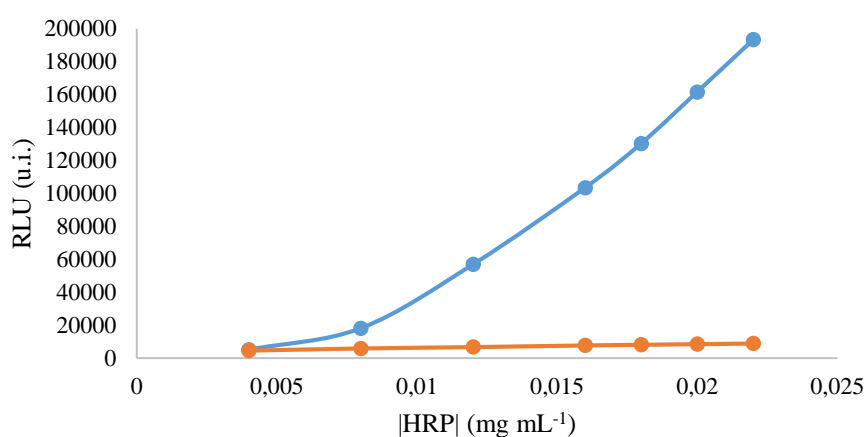


Figure 48. Calibration graphs used for estimating the active amount of HRP in the biosensor •2.50μM H₂O₂ and 17.5mM luminol. •50μM H₂O₂ and 17.5mM luminol.

2) Reaction conditions

First, the reaction was studied in solution to optimize the reagent concentration required by using a conventional spectrofluorometer. *Figure 49A* shows the intensity vs time register by varying the luminol concentration between 0.017 mM and 17 mM; the HRP and H₂O₂ concentration were constants, 1.22 mg L⁻¹ and 0.478 mM, respectively. It can be observed that the luminescence signal from using luminol concentrations higher than 1.7 mM was less dependent on the luminol concentration. Different HRP concentration in a range of 0.36 and 12.2 mg L⁻¹ were assayed maintaining luminol and H₂O₂ concentrations constant at 17 and 0.478 mM, respectively (*Figure 49B*).

Secondly, the reaction was studied by employing the biosensor. The signal was recorded at 10 seconds with a portable luminometer. Different luminol concentrations between 2.5 and 25 mM were assayed for a constant concentration of 50 μM H_2O_2 . Fig. As we can see in *Figure 49C*, the luminescence intensity increases according to the luminol concentration until 17.5 mM where the luminescence intensity was stabilized. The selected luminol concentration was 17.5 mM. Additionally, the biosensor response to H_2O_2 concentrations was evaluated by recording the luminescence intensity during 40 s (*Figure 49D*). It can be observed that the luminescence signal increases rapidly at short times, and then it decreases slowly over time until 40 s. The selected time was 10 s achieving good sensitivity and precision.

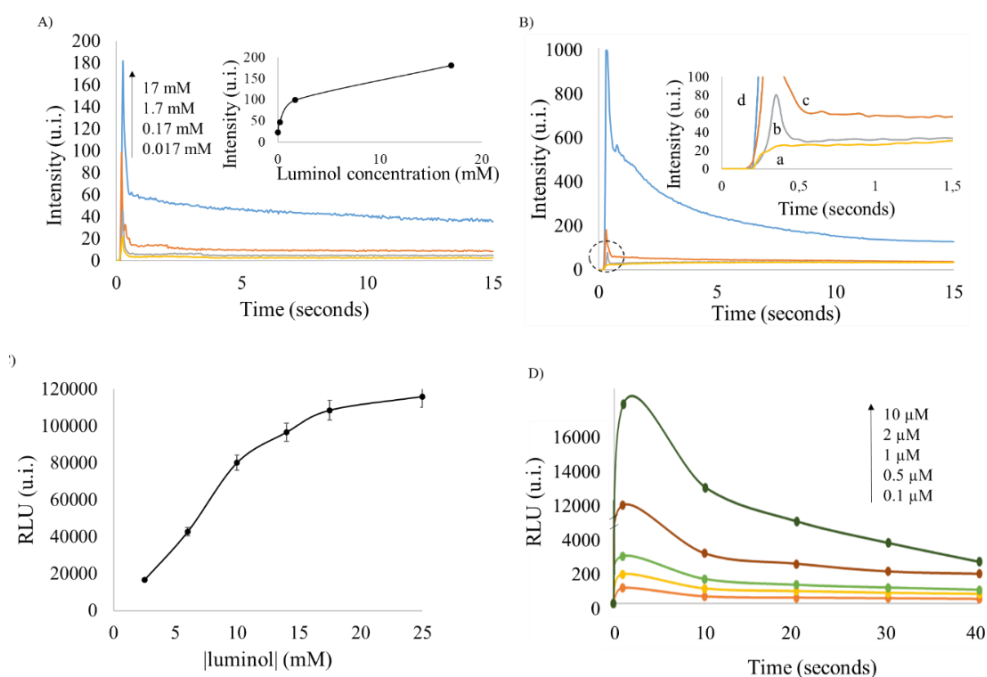


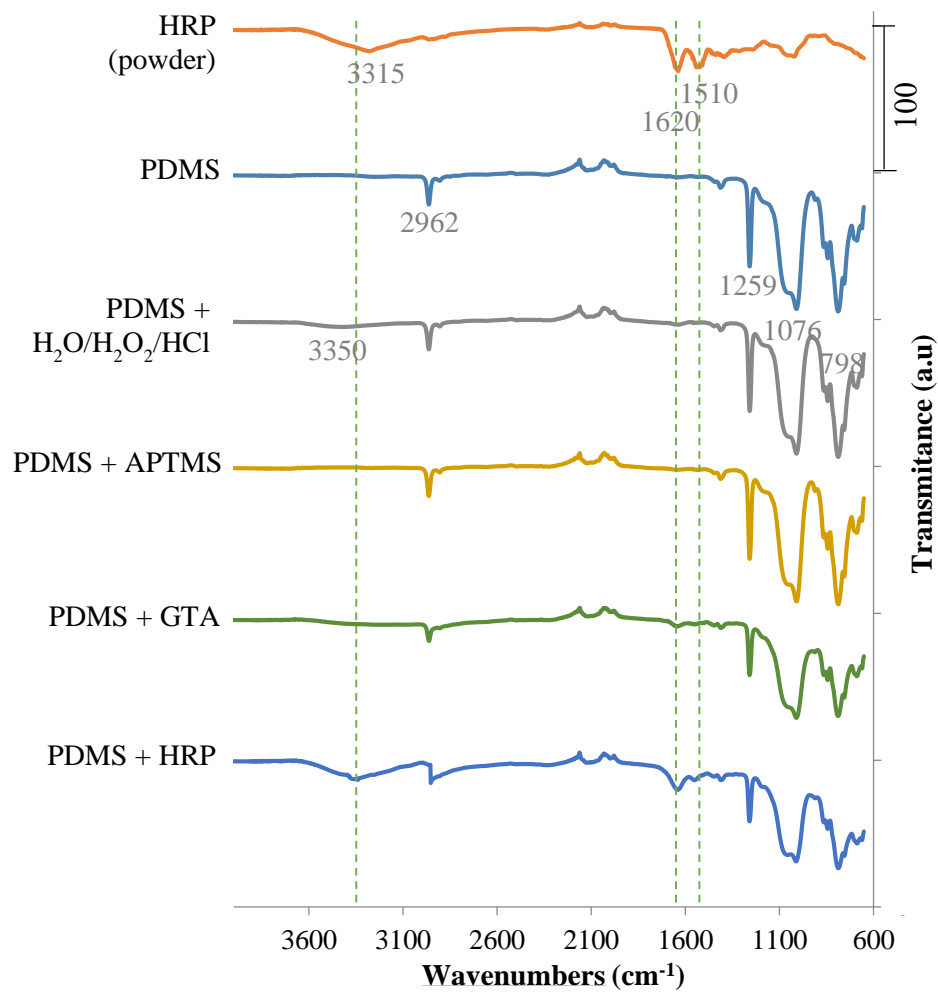
Figure 49. Optimization of the reaction conditions: (A) luminol concentration (0.017, 0.17, 1.7, and 17 mM) and (B) HRP concentration [0.36 (a), 0.6 (b), 1.22 (c), and 12.2 mg L⁻¹ (d)] in solution by using a conventional spectrofluorometer. (C) Luminol concentration (2.5–25 mM at 10 s) and (D) time for different H_2O_2 standard concentrations of 0.1, 0.5, 1, 2, and 10 μM by using the biosensor and a portable luminometer.

4.3.1.2. Characterization of the HRP/PDMS sensor

Attenuated total reflectance–Fourier transform infrared spectra were recorded to check the different steps carried out for obtaining the biofunctionalized sensor (*Figure 50A*). HRP powder has functional groups around 3315 cm^{-1} because of the association of the N–H stretching and at 1510 and 1620 cm^{-1} related to the stretching band of –CONH– (amide I) and (amide II) vibrations in HRP. PDMS has several characteristic infrared bands; at 2962 cm^{-1} (C–H stretching in CH_3), 1259 cm^{-1} (CH_3 symmetric bending in Si– CH_3), 1076 and 1018 cm^{-1} (Si–O–Si), and 798 cm^{-1} (CH_3 rocking in Si– CH_3). Activated PDMS also showed a band at around 3350 cm^{-1} which was assigned to the O–H stretch of surface silanol groups (Jornet-Martínez et al., 2016c). After PDMS surface modification with 3-aminopropyl trimethoxylane (APTMS), the absorption at 3350 cm^{-1} decreases. Subsequently, the surface modification with glutaraldehyde results in a band at 1680 cm^{-1} indicating the C=N vibration. Finally, after HRP immobilized on PDMS, the HRP functional groups emerged at around 3315 cm^{-1} and at 1510 and 1620 cm^{-1} according to HRP powder. These results demonstrated that the HRP was successfully immobilized on PDMS.

The biosensor morphology has been characterized by electronic microscopy. *Figure 50B* shows that the polydimethylsiloxane composite surface is a homogeneous material in accordance with a nonporous material.

A)



B)

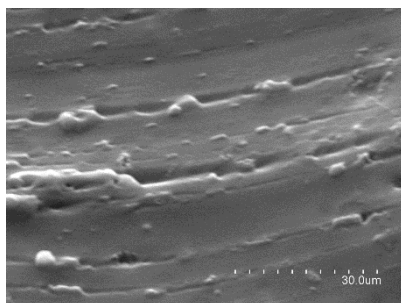


Figure 50. A) ATR-FTIR spectra of pure PDMS and HRP and hybrid PDMS films. B) Scanning electron microscopy image of the sensor.

4.3.1.3. Kinetic Analysis

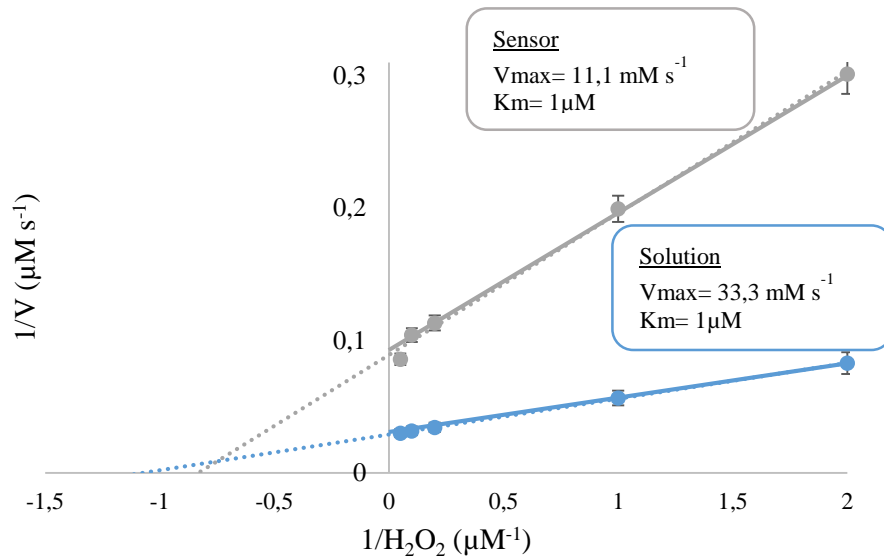
A kinetic study of the reaction between hydrogen peroxide or sodium percarbonate, luminol and HRP was further investigated by including results in solution and with the developed PDMS-HRP sensor. V_{\max} and K_m parameters were estimated through the Lineweaver-Burk linearization (equation 1), where $1/v$ was plotted against $1/[S]$. V_{\max} is the velocity that would be reached when all the enzyme active sites are saturated with the substrate and K_m is defined as the substrate concentration at which a half of the active sites are filled, these parameters characterise the affinity of the enzyme to the substrate.

$$\frac{1}{v} = \frac{1}{V_{\max}} + \frac{K_m}{V_{\max}} \times \frac{1}{[S]} \quad \text{Equation 1}$$

The kinetic study in solution was carried out by adding 10 μL of 0.01 mg mL^{-1} of HRP to the tube containing 200 μL of 35 mM luminol (buffer 0.3M $\text{HCO}_3^-/\text{CO}_3^{2-}$ pH = 10.8) and a variable concentration of H_2O_2 between 0.5 and 20 μM . Moreover, the same procedure was carried out with the biosensor in the tube, which contained the HRP immobilized. The kinetic data were obtained by registering the luminescence signal at 0 and 40 s and the initial rate was calculated by the difference between these two signals. Each experiment was repeated 3 times. *Figure 51* shows the obtained results where the inverse of the velocity was plotted against the inverse of the substrate concentration. The V_{\max} was estimated from the Y-intercept and the K_m from the X-intercept. The ‘apparent’ K_m obtained in solution and with the biosensor for the H_2O_2 and the sodium percarbonate which liberates H_2O_2 was similar. The experimental V_{\max} value was higher in solution than by using the sensor, this result could be explained due to the V_{\max} value depends on the

catalytic capacity of HRP and it could be something less in the sensor due to the immobilization process.

A)



B)

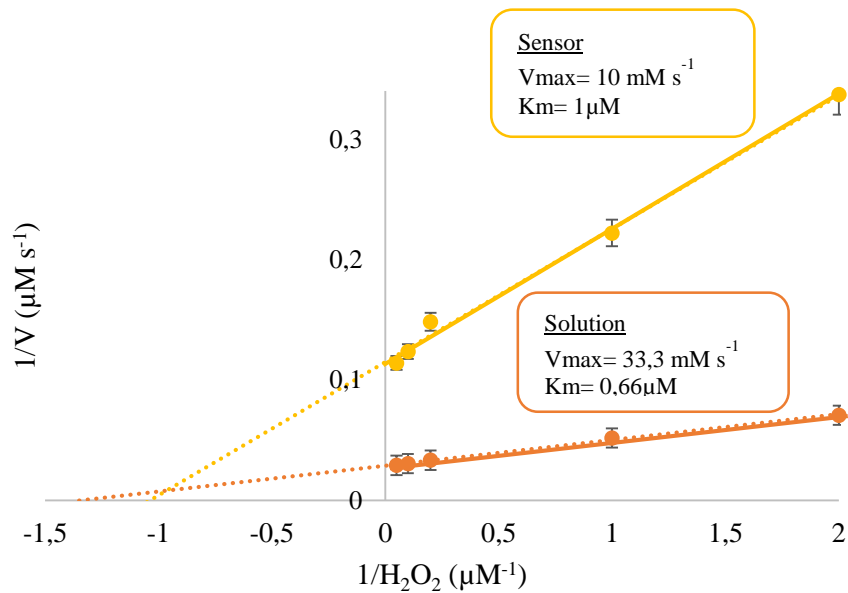


Figure 51. Steady-state kinetic assay for the developed biosensor with hydrogen peroxide and with sodium percarbonate respectively. Conditions: the concentration of luminol was 0.17 mM and H_2O_2 was varied. Insets are the Lineweaver-Burk linearization.

4.3.1.4. Analytical parameters, stability and reusability

The system HRP luminol- H_2O_2 has been used in many CL assay. Peroxidases are usually preferred because luminol can be oxidized in mild conditions and hydrogen peroxide is the most significant oxidizing agent, which increases the luminescent intensity of luminol. Interference may be due to an alteration in the catalytic activity, redox properties, or chemical reactivity with the luminol mixture (Khan et al., 2014).

As shown in *Table 27*, a lineal behaviour was observed between the analytical signals and the standard of H_2O_2 at a range of concentrations, 0.06 μM - 10 μM . The LOD of the developed biosensor was estimated at 0.02 μM and it was calculated as a $3 S_{\text{blank}}/b$ where b is the slope of linear calibration curve and S_{blank} is the standard deviation of the several measurements of blank solutions. For the developed biosensor, the precision was evaluated by obtaining the intra and inter-day RSDs under optimized experimental conditions (200 μL of 10 μM H_2O_2 and 200 μL of 35 mM luminol). The proposed procedure provided satisfactory % RSD values being lower than 10 % in all instances. According to these results, the precision of the method was adequate, and no differences were observed between devices.

Substrate	Calibration graphs equations $y=a+bx$			Precision, %RSD (n=3) ^b	
	Linear range (μM)	Sensibility μM^{-1}	R^2	Intraday/ Interday	LOD (μM)
H_2O_2	0.06-10	1200 ± 9	0.999	5.3/ 5.9	0.02
H_2O_2^a	0.08-10	158 ± 3	0.999	1.7/ 5.9	0.03
$\text{Na}_2\text{CO}_3 \cdot 2\text{H}_2\text{O}_2$	0.06-10	1186 ± 19	0.999	2.1/ 3.1	0.02

Table 27. Comparison of merits obtained with the developed biosensor testing different substrates for the H_2O_2 determination.

The stability of the biosensor over time was examined by comparing the response of three sensors used the same day that they were prepared with the response of three sensor used after several months of its storage at $-20\text{ }^{\circ}\text{C}$. The biosensor retained its activity unchanged for at least three months (see *Figure 52*).

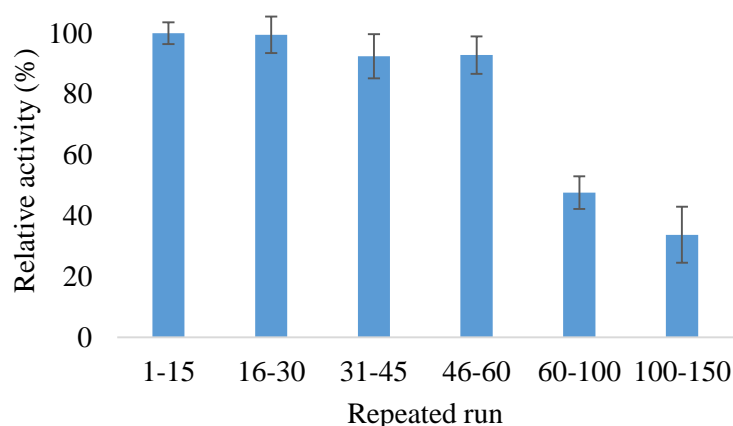


Figure 52. Reusability of the biosensor expressed as relative activity (%).

The biosensor reusability was also studied by using a fixed H_2O_2 concentration ($50\text{ }\mu\text{M}$) freshly prepared. To check this property, the sensor was used and water cleaned before reusing again. The HRP activity remains unchanged after 30 uses (with 99.5 % of activity compared with the first use) and after 60 uses the activity was of 92%. The activity of the biosensor decreased gradually after the 60 uses, obtaining 47% of activity in 75 uses. In the same session ($n=15$), the RSD% of the signals was $<10\%$ (*Figure 52*). The results indicated that this biosensor keep its properties, which are stable over time (at least three months stored in the freezer) and a reusability of at least 60 times.

We compared the reusability of the PDMS biosensor with that achieved by HRP immobilization in polystyrene. From fabrication perspective, namely, easy of prototyping and low cost, PDMS is superior to polystyrene (Halldorsson et al., 2015). The immobilization of HRP on the polystyrene tube by ultrasonication (Sharma et al., 2011) and by using APTMS as a linker (Kaur et al., 2004) was tested. However, after 5 uses, the HRP activity was reduced to 81% with the first method and 20% with the second method. We also tested the same procedure to anchor the enzyme on the PDMS for polystyrene, and the remaining activity after 5 uses was 56%. Therefore, the PDMS matrix was more efficient because it allows reuse of the tube up to 60 times.

4.3.1.5. Analysis of real samples

The release of H_2O_2 were analyzed in two different matrices by using the proposed PDMS-HRP sensor.

1) Culture medium DMEM-F12

It was determined the H_2O_2 concentration produced by neuroblast cells in the culture medium. Preliminary results indicated that there was a matrix effect produce by the culture medium, thus the H_2O_2 had to be calculated by interpolation in the respective calibration curve obtained for standards containing the culture medium instead of water. *Table 28* shows the H_2O_2 found concentration and the recovery value in the samples. The samples were fortified with 2 μ M of H_2O_2 to evaluate the accuracy of the method. The results indicated that the biosensor is appropriated for the extracellular H_2O_2 determination due to the recovery value were between 93 and 109%. Moreover, the RSD value was 7.7%.

Sample	Added (μM)	Found (μM)	Recovery (%)
1	0	0.42	-
	2	2.63	109.3 \pm 1.6
2	0	0.42	-
	2	2.63	109.1 \pm 1.4
3	0	ND	-
	2	1.96	95.1 \pm 0.4
4	0	0.24	-
	2	2.39	106.21 \pm 1.04
5	0	ND	-
	2	1.86	97.2 \pm 0.2
6	0	ND	-
	2	1.94	109.6 \pm 1.4
7	0	ND	-
	2	1.89	99 \pm 2

Table 28. Analysis of Culture medium DMEM-F12 incubated with neuroblast cells.

2) Corega Oxigeno Bio-Activo tablets.

The H_2O_2 released from Corega tablets was quantified for up to 3 min which was the time reported by the manufacturer to perform the denture cleansing process. It was observed a matrix effect that was corrected by the standard addition method. The results are shown in *Figure 53* where it is represented the H_2O_2 concentration found at different times for releasing in presence and absence of the denture. As it was appeared in both cases a state stationary at 180 s, we could confirm that the H_2O_2 is completely released at this time. The H_2O_2 determined at 180 s was 5.3%. The results are according to those indicated by the manufacturer (<10% $\text{Na}_2\text{CO}_3 \cdot 2\text{H}_2\text{O}_2$).

From these results we can conclude that the proposed biosensor is able to determine H_2O_2 in different samples. Moreover, the sensor can quantify H_2O_2 from indirect reaction which generated H_2O_2 .

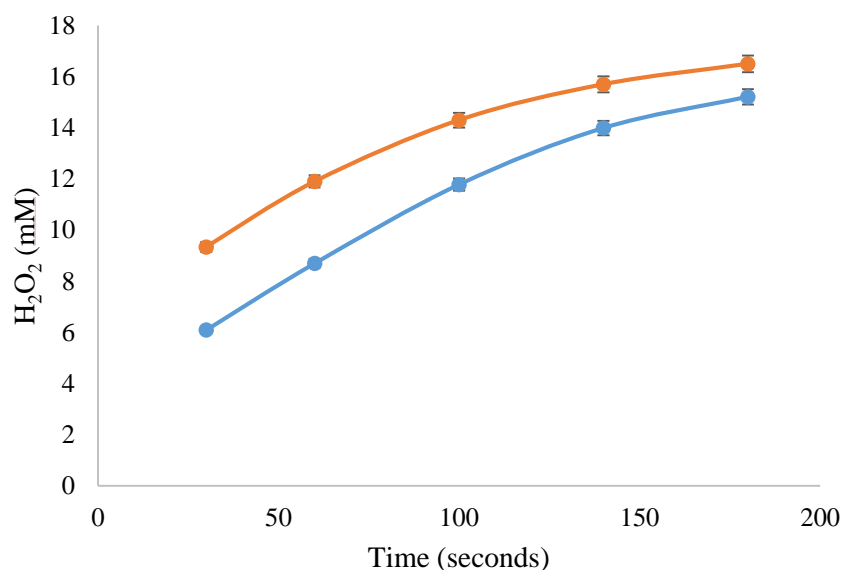


Figure 53. Concentration of sodium percarbonate expressed as H_2O_2 concentration in Corega® Oxígeno Bio-Activo tablets. Orange line was obtained by releasing process in water and blue line was obtained in contact with used denture.

4.3.1.6. Conclusions

In the present study, a novel H_2O_2 biosensor based on an enzymatic reaction has been developed. The sensor has been fabricated using a simple immobilization methodology of HRP enzyme on an activate PDMS surface. The chemiluminescent signal with respect to H_2O_2 concentration was measured by using a portable luminometer for transduction. Optimization of the enzyme immobilization was carried out in order to get maximum signal and better accuracy results. This method has appropriate figures of merit, such

as high sensitivity and provides in situ measurements with high accuracy. Moreover, the measurements can be obtained in a very short time (just 10 s).

The biosensor satisfies the standards in terms of precision, robustness and stability, moreover it should be noticed that the device is reusable allowing use it more than sixty times. The results revealed that the biosensor is a simple and reliable device for the quantitative determination of H₂O₂ by achieving a wide linear range, low detection limit and fast response time. The biosensor has long-term applications due to the implicated in a wide variety of reactions. In this case, H₂O₂ determination was carried out in extracellular fluid and Corega[®] Oxígeno Bio-Activo tablets without any sample preparation.

4.3.2. Sensor based on TEOS/MTEOS/luminol sol-gel for controlling dissolved ammonium and organic amino nitrogen

In this section, we propose a portable sensor, obtained by embedding luminol into TEOS/MTEOS composite, for the quantitative determination of organic amino nitrogen and ammonium in waters with the goal of achieving low levels of concentration. The method is based on the reaction between amino nitrogen compounds and hypochlorite to produce chloramino-derivatives. Then, the remaining hypochlorite reacts with luminol sensor by producing a luminescence signal, which was measured by using a portable luminometer, being inversely proportional to nitrogen concentration. (Kent et al., 2003; Meseguer-Lloret et al., 2006; Pla-Tolós et al., 2015). The liberation of the luminol from sensor is higher than 90 % and the sensor is stable at least a week at room temperature. This portable method was successfully validated and applied to the analysis of several real waters: fountain, river transition, lagoon and seawater with recoveries values between 92 and 112 %, which

indicated that matrix effect was absent. The achieved limit of detection was around $10 \mu\text{gL}^{-1}$ expressed as N. This sensor allows in-situ monitoring owing to its simplicity, rapidity and portability.

4.3.2.1. Optimization of reagent concentration

To establish the optimal conditions for organic amino nitrogen and ammonium determination, the effect of luminol and sodium hypochlorite concentration on the luminescence intensity of the formed compound was previously studied in solution using the portable luminometer. First, the luminol concentration was kept constant (0.4 mM) and the sodium hypochlorite concentrations were varied between 0.025 mM and 0.4 mM. The light intensity was recorded at 10 seconds. As shown in *Figure 54*, it was found that the CL signal increased as sodium hypochlorite concentration increased too. It was interesting to reach the maximum signal of the luminometer without saturation in order to obtain the maximum working range for the analyte due to the presence of the analyte decreases the CL signal. Moreover, it was important that the CL signal was not very dependent on luminol concentration, thus 0.248 mM was selected. Second, the sodium hypochlorite concentration was kept constant (0.248 mM) and the luminol concentration was varied between 0.05 mM and 0.5 mM (*Figure 54*). The light intensity was recorded at 10 seconds. The results showed that the CL signal increased as sodium hypochlorite concentration increase. The selected concentration was 0.4 mM, the first value in the plateau.

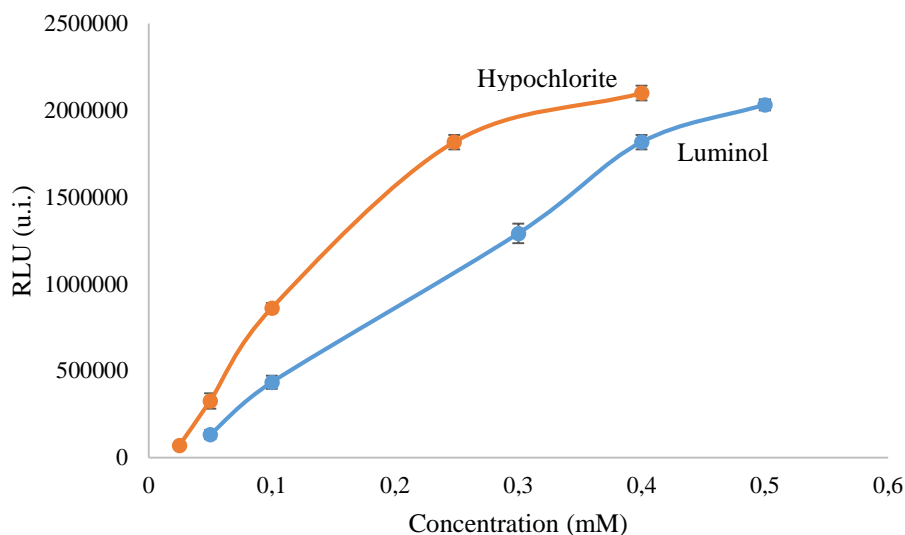


Figure 54. Optimization of concentration of hypochlorite and luminol working in solution to measure organic amino nitrogen and ammonium with a portable luminometer.

4.3.2.2. Optimization of luminol immobilization

To check the greatest support to immobilize and to liberate luminol, different supports were tested. Based on our experience (Argente-García et al., 2017b; Bocanegra-Rodríguez et al., 2018a; Jornet-Martínez et al., 2019; Jornet-Martínez et al., 2018, 2016b, 2016d; Pla-Tolós et al., 2016), several solid supports for luminol entrapment were studied; PDMS, zein and TEOS/MTEOS. Solid support of PDMS (Figure 55A, B) or PDMS-TEOS (Figure 55C, D, E) containing luminol were synthesized. These sensors were added to solutions containing buffer 0.2 M $\text{HCO}_3^-/\text{CO}_3^{2-}$ pH=11.2 to liberate the luminol, then, 50 μL of hypochlorite were added to start the CL reaction. Non-reaction was observed, thus the liberation of luminol was not produced. This behaviour can be attributed to the hydrophobicity of the PDMS support. No differences in behaviour were observed between PDMS or PDMS/TEOS

and different sensor sizes. Furthermore, the covalent binding of luminol on PDMS was tested inside a polystyrene tube, however the immobilization cannot be carried out though the amino group or the immobilization of luminol though NH_2 group impede its oxidation by sodium hypochlorite reagent. Zein was tested as release support too (*Figure 55F*), however it is a protein and its nitrogen groups reacted with the sodium hypochlorite, thus all hypochlorite was consumed and the luminol oxidation was not carried out. Finally, a sol-gel support based on TEOS/MTEOS containing luminol, which provided a hydrosoluble support was assayed. The influence of different compounds in the device composition (*see Section 3.3.5*) was studied in order to select the best sol-gel with suitable sensibility, solidification properties, stability and satisfactory accessibility of the analyte to the reagent. The addition of two plasticizers, PEG and glycerol, in the sol-gel were tested in order to assay their possible benefits in the determination of analytes.

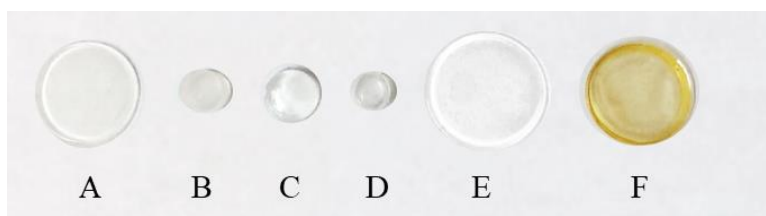


Figure 55. Different support material tested in order to immobilize luminol. A, B) PDMS; C, D, E) PDMS and TEOS; F) zein.

Two parameters were studied in order to select the best components in the sol-gel sensor (*Figure 56A*), first, the loss of activity from the sensor vs the time to heat in the oven, and then, the sensitivity achieved to determinate nitrogen ($7.5 \mu\text{M}$ and $15 \mu\text{M}$ of nitrogen were tested). As it is shown in *Figure 56B*, the time to heat in the oven at $40 \text{ }^\circ\text{C}$ was optimized in order to achieve an optimal functional solid without affecting to the luminol stability. At 4 hours all sensors have been solidified, however, an increase of 2 hours

produces a loss of activity in the sensor, which contained PEG. *Figure 56C* shows the % inhibition achieved by the different sensors, the addition of glycerol makes the sensor less sensible, it can be due to the glycerol change the viscosity of the sensor, which can be related to the luminescence signal obtained.

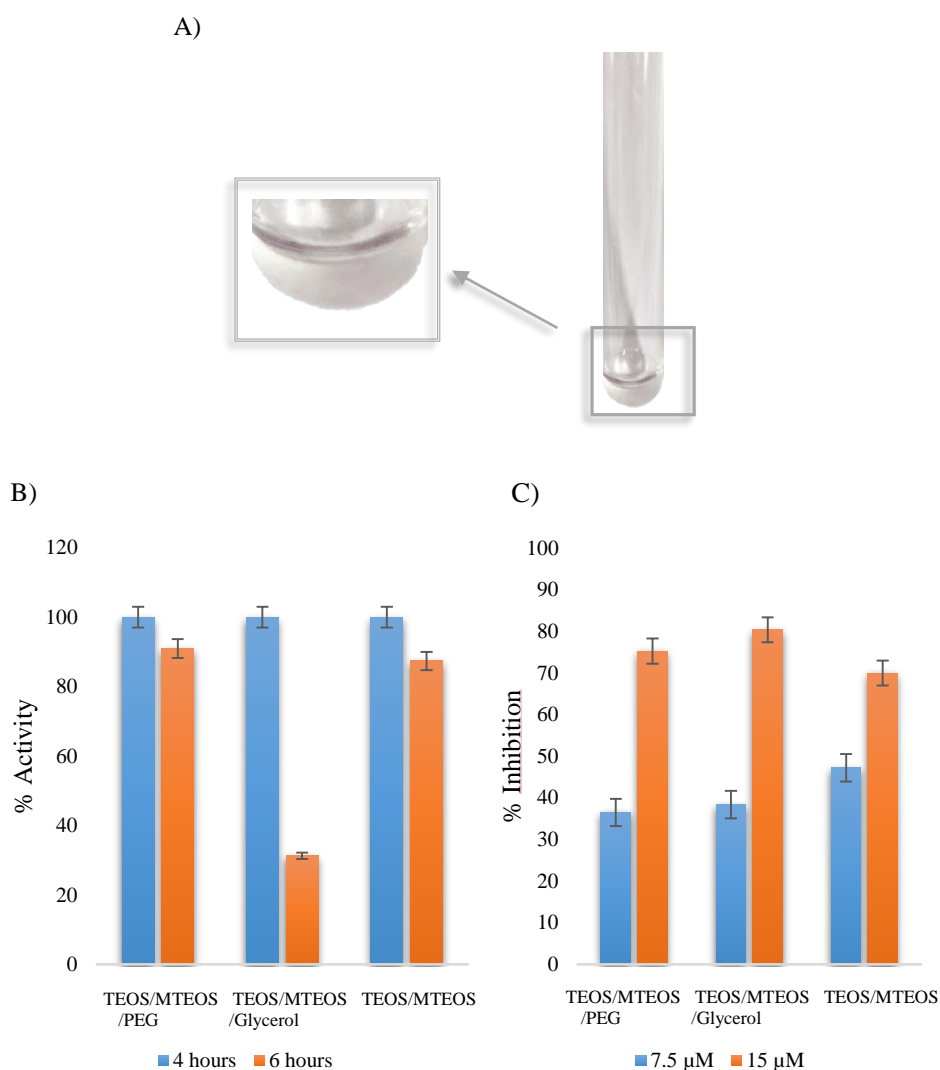


Figure 56. A) Developed TEOS/MTEOS sol-gel sensor in the polystyrene tube. B) % of remaining activity in the developed devices at different time to heat the device in the oven at 40°C. C) % reaction inhibition as function of nitrogen concentration (7.5 μM and 15 μM).

To sum up, it was observed that the addition of PEG did not provide significant advantages, the linear range can be considered similar than that achieved without adding PEG and there was a big different of activity if the sensor was heat during 6 hours for gelling (see *Figure 56B*). The addition of glycerol makes the sensor less sensible. According to the results, the option without PEG or Glycerol was selected for further experiments due to high sensibility and wide linear range obtained.

Once the sensor was developed, the efficacy of luminol releasing was evaluated by comparing the reaction in solution and with the sensor. The y-intercept from the reaction in solution was considered the maximum CL signal to achieve (100%). The stability of the sensor over time was evaluated by using 0.248 μM of sodium hypochlorite. The CL signal was measured after 7 days by storage the sensor at room temperature and in the fridge. The results show a good remaining activity in the sensor at room temperature ($90 \pm 3 \%$), however, in the fridge the sensor is stable only 3 days, it can be due to the sol-gel changed its physic properties.

4.3.2.3. Characterization of the TEOS/MTEOS device

The characterization of the sensor was carried out by microscopy images and infrared spectrum. Microscopy images were obtained of the sol-gel sensor with and without luminol (*Figure 57*). Morphology of the composite containing luminol was more ramified than that corresponding to the composite without luminol.

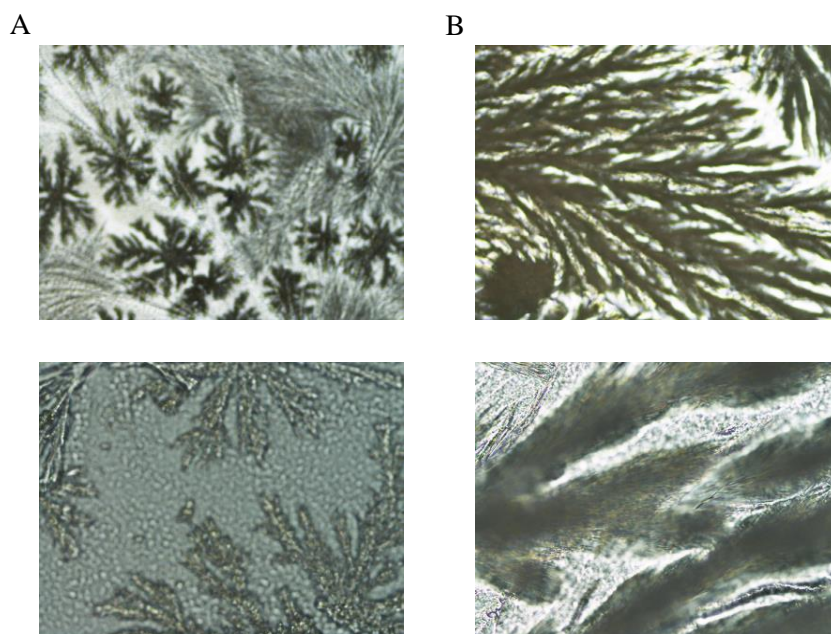


Figure 57. Microscopy images of the developed TEOS/MTEOS sensor. A) Without luminol and B) with luminol (10x and 50x).

Infrared spectrum was measured in order to verify the luminol immobilization. *Figure 58* shows the spectrum of luminol and the sol-gel sensor with and without luminol. At 1750 nm it is observed a characteristic bands corresponding to C=O binding from luminol; the band is higher in the sol-gel spectrum which contains luminol. Moreover, at 1300 nm it can be observed a IR band corresponding to C-N binding.

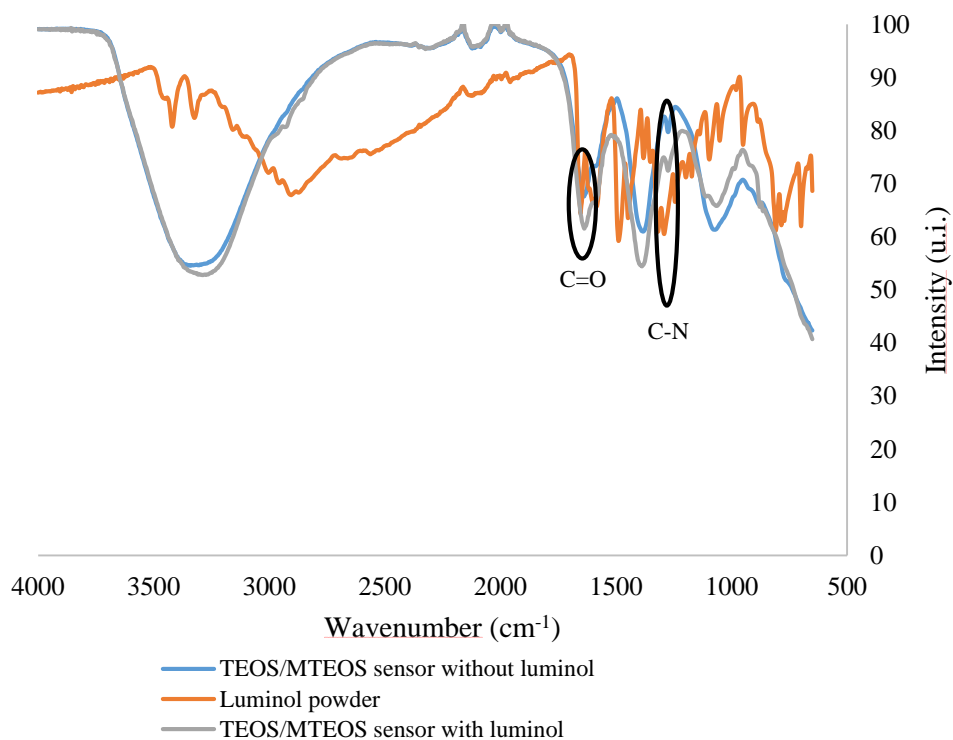


Figure 58. Infrared spectrum of luminol and sol-gel sensor. Orange: luminol; blue: sol-gel without luminol; grey: sol-gel with luminol.

4.3.2.4. Analytical parameters, stability and interferences

The applicability of the sol-gel sensor to determine organic amino nitrogen and ammonium was evaluated by analysing various nitrogen-containing compounds. All concentrations were expressed as nitrogen. The responses of the developed sensor to nitrogen solutions were recorded over 60 seconds. According to the results, 10 seconds were selected as a compromise between the analytical signal and the total analysis time. The slopes of the calibration graphs (μM^{-1} of N) obtained for methylamine as target of primary amines and dimethylamine as target of secondary amines in comparison with that obtained for ammonium were 94 % and 91 %, respectively.

respectively. It has to be noted that tertiary amines (trimethylamine) does not respond to nitrogen concentration. Putrescine and spermine were selected as model compounds of polyamines. The slope values obtained were 108 % and 82 % in comparison with ammonium, respectively. From these results, total nitrogen content of these compounds can be quantify with this procedure., which is in accordance with (Meseguer-Lloret et al., 2006).

Analytical parameters for the determination of dissolved organic nitrogen and ammonium by using a portable luminometer and with a conventional luminometer are given in *Table 29* Although the results obtained with the conventional equipment were measured in solution, the sensitivity achieved by using the portable luminometer with the sensor was higher. This result is due to the portable luminometer capture the luminescence signal at all wavelength. Linear range and LOD are adequate to determine nitrogen in water samples (Meseguer-Lloret et al., 2006) and RSD values verify that the precision of the method can be considered satisfactory (3.4 and 5 % were obtained for intra and inter day by measuring 0.14 ppm nitrogen stock solution). RSD values for the conventional luminometer were obtained by measuring 0.75 ppm nitrogen stock solution. An aim of this paper is to develop a quick procedure that allows evaluating the nitrogen amount in water samples. The species determined have been the organic nitrogen and ammonium. The stability of the sensor over time was evaluated by using 0.248 μM of sodium hypochlorite. The CL signal was measured after 7 days by storage the sensor at room temperature and in the fridge. The results show a good remaining activity in the sensor at room temperature (87%), however, in the fridge the sensor is sable 3 days, it can be due to the sol-gel change its physic properties.

Equipment	Calibration graphs equations $y=a+bx$			Precision, % RSD (n=3)	LOD (mg L ⁻¹)
	Linear range (mg L ⁻¹)	$b\pm sb$ (mg L ⁻¹)	R ²	Intraday	
Portable	0,036-0,350	-4214242,98±203711,7	0.9907	3.4/ 5*	0.012
Convectional ^b	0,24-4,00	-2370±70	0.9938	0.81	0.070

Table 29. Several figures of merit of portable binomial sensor-luminometer and conventional procedure in solution and lab equipment. ^aby using the sensor ^bin solution. *Interday

The influence of salt concentration was studied for sea samples, which have a high salinity (35 mg L⁻¹) through spiked sea water with ammonium (0.07 and 0.105 mg L⁻¹). The recovery was satisfactory (98 and 106 % respectively) (see next section too). The selectivity toward compounds with sulfur atoms and according to Meseguer et al (Meseguer-Lloret et al., 2006), sodium sulfide (S²⁻) and mercaptoethanol (R-SH) decreased the chemiluminescence signal. However, there are not interference at the concentration of biogenic sulfur found in natural waters (~0.25 mg L⁻¹) (Meseguer-Lloret et al., 2006). Moreover, the interference of some metallic ions (Cr(III), Co(II), Cu(II), Fe(III) and Cd(II)) were studied and not signal was observed at the maximum concentration levels established by the European Legislation (Directive 2015/1787), related to the quality of water intended for human consumption.

4.3.2.5. Determination of ammonium and organic ammonium in real water samples

Different water samples with nitrogen compounds were analyzed using the proposed CL device. Samples were fortified and the standard additions method was used to validate the accuracy of the method. *Table 30* shows the

found nitrogen concentration in water samples calculated from the calibration curve of N by external calibration and the recovery percentage of the added nitrogen (0.07 mg L⁻¹ and 0.105 mg L⁻¹). Matrix effects were evaluated by spiking the water samples with nitrogen. The recovery values were between 94 and 112 %, thus no matrix effect was present by using the developed sensor under the optimized experimental conditions. The nitrogen contents can be obtained directly from interpolation in the standard calibration curve. Values of total amino nitrogen found in samples were between 0.073 and 0.268 mg L⁻¹ N.

Sample	Added (mg L ⁻¹ N)	Found (mg L ⁻¹ N)	(%) Recovery
Fountain (S1) ^a	0	0.04 ± 0.01	
	0.07	0.140 ± 0.004	97
	0.105	0.26 ± 0.03	107
River Ulla (S2) ^a	0	0.268 ± 0.009	
	0.07	0.344 ± 0.020	109
Transition (S3) ^a	0	0.073 ± 0.009	
	0.07	0.144 ± 0.011	101
	0.105	0.19 ± 0.02	107
Lagoon Cullera (S4) ^a	0	0.228 ± 0.011	
	0.07	0.306 ± 0.007	112
	0.105	0.327 ± 0.019	94
Sea (S5)	0	0.16 ± 0.03	
	0.07	0.228 ± 0.006	98
	0.105	0.271 ± 0.018	106

^aDiluted as required

Table 30. Nitrogen found and recoveries in different water samples. Processed in situ.

4.3.2.6. Conclusions

The objective of this work was to develop a portable CL sensor for in-situ control of organic amino nitrogen and ammonium where luminol was embedded in a TEOS/MTEOS sol-gel support. The sensor provides a successful release of luminol to the medium. The luminescent signal was measured employing a portable luminometer which allows determine nitrogen in place with high sensitivity. The sensor provides suitable linearity, precision and stability (at least a week at room temperature).

Furthermore, this developed procedure allows a rapid and simple in-situ analysis of nitrogen in samples without trained personnel or complicated sample pre-treatment. The sensor was applied to the measurement of organic amino nitrogen and ammonium in water from different sources (fountain, river, transitional, lagoon and sea). The proposed sensor offers the advantage of simplicity, rapidity, portability and low cost analysis, as well as high sensitivity. This portable solution improved the detection limit achieved and sustainability of a previous paper published by us (Meseguer-Lloret et al., 2006) based on flow injection analysis and chemiluminescence detection. Besides, it conserves the option to be an approximation to Kjeldahl method and it does not require sample treatment, being the measurement time faster (10s).

4.4. NANOCELLULOSE AS SUPPORTING MATERIAL FOR SENSOR DEVELOPING

In this section, an enzymatic H₂O₂ biosensor based on carbon materials with electrically-wired oxidoreductases is proposed. Specifically, HRP was used to develop the biosensor due to be a robust and readily available heme-containing glycoprotein capable of DET bioelectrocatalytic 2e⁻/2H⁺ reduction at carbon electrodes in MWCNTs. Different modifications of MWCNTs electrode were studied to evaluate how the charges and the length of the molecules in the MCNT surface affected to the orientation of the enzyme HRP. Concentration effects on catalytic current as well as voltage output and stability performance were considered for biocathode and biosensor applications. The construction of a new type of HRP bioelectrode incorporating hydrated nanocellulose as an environmentally friendly and sustainable component was subsequently investigated and the resulting sensor and catalytic stability performance evaluated.

4.4.1. Bioelectrocatalysis of HRP/pyrene-modified MWCNT bioelectrodes

The pyrene and functionalised pyrenes employed for non-covalent modification of the MWCNT electrodes, and the subsequent preparation of HRP bioelectrodes for H₂O₂ reduction, are schematically illustrated in *Figure 59*. The MWCNT electrodes were obtained according to our reported strategy that allows the formation of highly stable and reproducible MWCNT coatings on GC electrodes with a film thickness of ca. 6 μm (Gross et al., 2020; Lalaoui et al., 2016). The pyrene-modified MWCNT electrodes were prepared by a simple immersion protocol using a DMF modifier solution with 5 mmol L⁻¹ of the pyrene derivative, followed by rinsing to remove weakly adsorbed species (*see Section 3.3.6*). The effective adsorption of pyrenes including mono/polycyclic and ionisable/ non-ionisable derivatives to CNTs occurs via

physical interactions, particularly pi-pi stacking interactions between CNT sidewalls and the aromatic system of the molecules (Haddad et al., 2010; Sheng et al., 2010). This non-covalent modification strategy is attractive for electrochemical biosensor and biofuel cell applications due to its simplicity, the ability to preserve the aromatic systems and therefore electronic properties of the nanotubes, and the possibility to introduce a wide range of surface functionalities in a straightforward manner (Gross et al., 2017; Haddad et al., 2010).

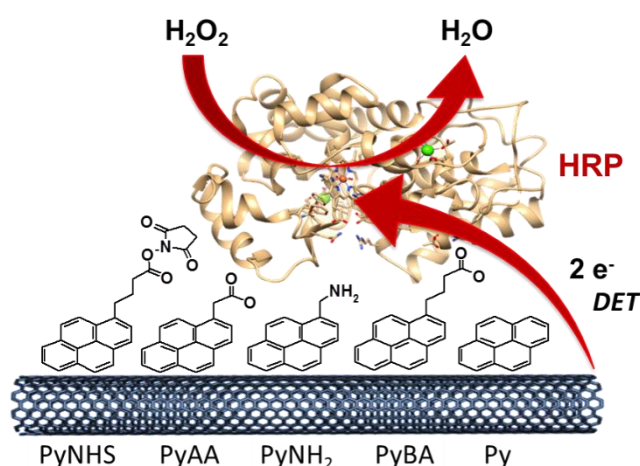


Figure 59. Schematic representation showing the five pyrene compounds used to obtain pyrene-modified MWCNT bioelectrodes with adsorbed HRP for the two-electron bioelectrocatalytic reduction of H_2O_2 to water. Enzyme structure *pdb1H55* of HRP from *Armoracia Rusticana* (Berglund et al., 2002).

To achieve efficient DET bioelectrocatalysis with metalloenzymes it is necessary to optimise enzyme orientation and immobilisation. Little progress has been made regarding the influence of charge and/or other surface functionalities to promote DET bioelectrocatalysis with immobilised HRP. The commercial HRP has a stated isoelectric point (pI) of approximately 3–9

owing to the presence of several isozymes. Nevertheless, important studies by Radola and Delincée on the fractionation of commercially-sourced HRP showed that the predominant isozyme pI is 9.1 (Delincee and Radola, 1978, 1975). At pH 7.0 we therefore expect HRP to be positively charged. As depicted in *Figure 59*, we explored the use of a “classical” pyrene-aliphatic carboxylic acid, pyrene butyric acid (pyBA, pKa 4.8), as well as the shorter chain equivalent, pyrene acetic acid (pyAA, pKa 4.2), a pyrene aliphatic amine (pyNH₂, pKb ~ 10), pyrene, and a pyrene-NHS ester derivative. With all aqueous experiments performed in 0.1 mol L⁻¹ phosphate buffer (pH 7.0), this set of derivatives enabled the comparison of positive (protonated amine), negative (deprotonated carboxylic acid) and neutral (pyrene) charged surface species. Furthermore, the pyNHS derivative comprises the succinimidyl group that may react with amino residues at the surface of the enzyme to form strong covalent bonds, therefore enabling comparison of a “tether” functionality (Karachevtsev et al., 2011).

Catalytic cyclic voltammetry experiments were performed in argon saturated 0.1 mol L⁻¹ phosphate buffer (pH 7.0) for the unmodified and pyrene-modified electrodes after immobilisation of HRP by an immersion protocol then gentle rinsing (*see Section 3.4.7*). *Figure 60* shows the first-scan cyclic voltammograms (CVs) recorded at the MWCNT bioelectrodes from open circuit potential to 0 V vs. Ag/AgCl (sat. KCl) in the presence of “low” 0.5 mmol L⁻¹ and “high” 4 mmol L⁻¹ H₂O₂. CVs recorded in the absence of H₂O₂ showed no reduction processes beyond the background signal of the MWCNT bioelectrode. In the presence of 0.5 mmol L⁻¹ H₂O₂, a large catalytic reduction peak is observed at all electrodes, including the unmodified electrode, consistent with DET bioelectrocatalysis between adsorbed HRP and the MWCNT electrodes (*Figure 60A*). Based on previous

findings, the reaction occurs via the oxyferryl iron-porphyrin pi-cation radical species, $\text{Fe}^{\text{IV}}=\text{O},\text{P}^{+\bullet}$, of the active site of HRP Compound 1 (Jia et al., 2010). Similar catalytic current maximums of -21 to $-24 \mu\text{A}$ are observed for the different pyrene-modified electrodes compared to a slightly lower current of $-20 \mu\text{A}$ for the unmodified MWCNTs electrode, consistent with surface modification leading to a minor enhancement in DET at $0.5 \text{ mmol L}^{-1} \text{ H}_2\text{O}_2$. The pyBA bioelectrode exhibited the highest catalytic current but with unattractively low peak and onset potentials of 0.1 V and 0.49 V , respectively. PyNHS- and pyAA-modified bioelectrodes provided access to the highest onset potentials of 0.61 V and 0.60 V , respectively. The onset potentials are very close to the formal potential of 0.63 V for the redox conversion of HRP compound 1/ferric HRP at $\text{pH } 7.0$ vs. Ag/AgCl (Csöregi et al., 1993). The catalytic improvements observed with pyNHS, pyBA and pyAA indicate that hydrophilic and negatively-charged functionalities, or tether group functionalities, are more favorable compared to positively-charged or entirely hydrophobic modifications at “low” H_2O_2 concentration. Nevertheless, the hydrophobic bioelectrode prepared with pyrene still exhibited enhanced bioelectrocatalysis compared to the unmodified MWCNT electrode. The negatively-charged functionalities that provide catalytic improvements compared to positively-charged functionalities highlight the beneficial electrostatic interactions at $\text{pH } 7$ that favour DET bioelectrocatalysis between positively-charged HRP enzymes and deprotonated aliphatic acids at the electrode. *Figure 60* also shows the variable presence of an apparent redox couple at 0.1 V . Control experiments in *Figure 60C* and *Figure 61* performed at CNT electrodes in the absence and presence of adsorbed HRP, respectively, indicate that these redox peaks originate from the carbon nanotubes. The redox peaks are tentatively attributed to surface quinone functionalities with

a nature similar to those observed at MWCNT and graphite electrodes (Blanchard et al., 2019; Csöregi et al., 1993; Gusmão et al., 2015). At 4 mmol L⁻¹ H₂O₂, markedly different bioelectrocatalytic voltammograms with a more complex wave shape were observed (*Figure 60B*). The H₂O₂ concentration became sufficiently high that notable differences in maximum catalytic currents were observed between the modified electrodes. Generally, with an increase in substrate, higher catalytic currents were observed, particularly at lower potentials of ca. 0–0.1 V. The catalytic wave onset potential observed for pyNHS and pyAA again starts at ca. 0.6 V vs. Ag/AgCl, as observed at the “low” H₂O₂ concentration, which favourably compares to the 0.55 V vs. Ag/AgCl (pH 7.5) (Ruff et al., 2017) and 0.6 V maximum (pH 7) vs. Ag/AgCl (Jia et al., 2010) observed at previous high performing MWCNT DET HRP biocathodes. Such biocathodes clearly offer improved voltage performance compared to cross-linked CNT/HRP on thiol-modified gold (Kafi et al., 2018) with onset potentials starting at -0.05 V vs. Ag/AgCl at pH 7. The second reduction wave is characteristic of a catalytic “boost” linked to an increase in enzymatic activity with driving force. A similar wave shape with a “boost” at low potential was reported by Armstrong and coworkers for fumarate reductase at a graphite electrode in the presence of high substrate concentration (Hudson et al., 2005). It may be that the DET mechanism takes a different route depending on the potential but this was not studied further. The possibility of an mediated electron transfer (MET) or mixed DET/MET mechanism at low potential involving the proposed surface quinone at bare CNTs is not ruled out (Csöregi et al., 1993). A control experiment performed at a MWCNT electrode without HRP in the presence of 4 mmol L⁻¹ H₂O₂ did not show any reductive currents, confirming that the second reduction wave observed in *Figure 60B* is not due to H₂O₂ reduction at unmodified MWCNTs

(Figure 60C). PyNHS and PyAA bioelectrodes exhibited the highest catalytic currents of $-94 \mu\text{A}$ and $-78 \mu\text{A}$ compared to $-24 \mu\text{A}$ observed at the unmodified MWCNT bioelectrode. This represents a 3–4 factor catalytic enhancement and the possibility to achieve up to ca. $1.1\text{--}1.3 \text{ mA cm}^{-2}$ current densities for the tether function and shorter chain acid function. PyBA bioelectrodes produced a mediocre current maximum of $-50 \mu\text{A}$ and globally weaker bioelectrocatalysis compared to the pyNHS and pyAA bioelectrode. The pyrene and pyNH_2 behaved similarly to the pyBA bioelectrodes, thus at “high” 4 mmol L^{-1} concentration, the positive, negative and neutral charges do not play a key role on enhanced DET bioelectrocatalysis. There is no obvious trend due to the use of different aliphatic chain lengths. For reference, voltammograms were not investigated at lower potentials of $\geq -0.15 \text{ V}$ where deactivation of the HRP is observed (Csöregi et al., 1993).

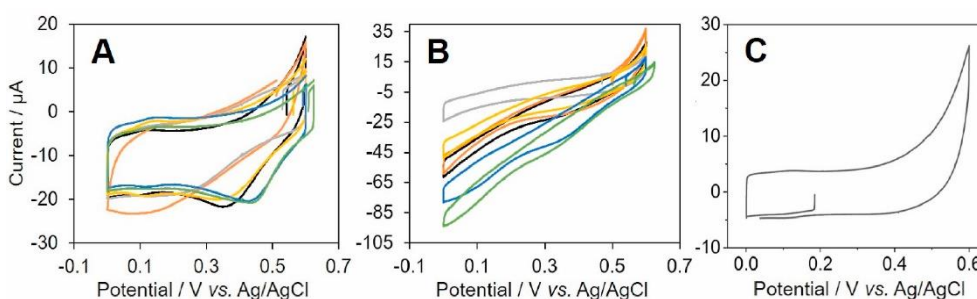


Figure 60. (A, B) CVs recorded at MWCNT-HRP bioelectrodes at 10 mV s^{-1} in 0.1 mol L^{-1} phosphate buffer (pH 7.0) with (A) 0.5 mmol L^{-1} and (B) 4 mmol L^{-1} H_2O_2 : (—) unmodified; (—) py; (—) pyNHS; (—) pyAA; (—) pyBA; (—) pyNH₂. (C) CV recorded from open-circuit potential at unmodified MWCNT without HRP at 10 mV s^{-1} in 0.1 mol L^{-1} phosphate buffer (pH 7.0) with 4 mmol L^{-1} H_2O_2 .

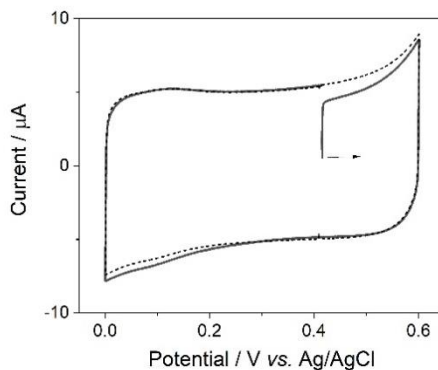


Figure 61. First (solid line) and second (dashed line) CVs recorded at MWCNT-HRP bioelectrode at 10 mV s^{-1} in 0.1 mol L^{-1} phosphate buffer (pH 7.0) without H_2O_2 . The arrow shows the scan direction of the first scan.

In addition to the bioelectrocatalytic H_2O_2 reduction behaviour, an oxidative response was also observed at the pyrene-modified MWCNT electrodes, as shown in *Figure 60*. The oxidative response corresponds to direct electrochemical oxidation of H_2O_2 , as previously reported at carbon electrodes (Jia et al., 2010). The H_2O_2 oxidation occurring at $\geq 0.52 \text{ V}$ therefore competes with the reduction process and diminishes the H_2O_2 reduction current at these bioelectrodes. Considering both 0.5 mmol L^{-1} and 4 mmol L^{-1} concentrations, the most effective bioelectrodes for the parasitic H_2O_2 oxidation are pyBA and pyNH₂ while the least effective was the pyNHS bioelectrode. The insensitivity of the pyNHS bioelectrode towards H_2O_2 is consequently one of the important factors that permits high catalytic H_2O_2 reduction performance, particularly at the “high” peroxide concentration. The steady-state amperometric current responses of the unmodified and pyrene-modified HRP bioelectrodes were subsequently measured at 0 V vs. Ag/AgCl under hydrodynamic conditions from 0.25 mmol L^{-1} to 9 mmol L^{-1} . *Figure 62* shows the current-concentration response curves obtained from the amperometric experiments. The unmodified and modified electrodes show

the same general trend with a linear increase in current to a plateau followed by a drop-off in current. Linear calibration curves ($r^2 \geq 0.98$) from 0.25 mmol L⁻¹ to between 1 mmol L⁻¹ and 4 mmol L⁻¹ were observed, depending on the pyrene derivative used (*Figure 62*). The pyNHS and pyAA bioelectrodes delivered the highest catalytic currents of 98.5 μA (1.4 mA cm⁻²) and 86.5 μA (1.2 mA cm⁻²) at 6 mmol L⁻¹, respectively. Beyond 6 mmol L⁻¹ the catalytic current decreases as a result of enzyme deactivation. Such HRP “suicide inactivation” has previously been observed at low millimolar concentrations of H₂O₂, occurring when the peroxide converts Compound 2 of HRP into a highly reactive peroxy iron (III) porphyrin free radical that subsequently decomposes (Malomo et al., 2011). For a biocathode or biosensor targeting the highest catalytic current or wider dynamic range, the pyNHS is the optimal electrode. If higher catalytic currents or better sensor sensitivity is required at ≤ 1 mmol L⁻¹ concentrations, then the pyBA or pyAA bioelectrode is the better choice. The sensitivities for pyBA and pyNHS bioelectrodes are 5.63 A M⁻¹ cm⁻² (0.40 A M⁻¹) and 2.96 A M⁻¹ cm⁻² (0.21 A M⁻¹) (*Figure 62*). These analytical sensitivities are high performance compared to estimated values of 0.15 A M⁻¹ at activated graphene (López Marzo et al., 2020), 0.298 A M⁻¹ cm⁻² at cross-linked Os redox polymer and modified graphite (Bollella et al., 2018), 0.12 A M⁻¹ cm⁻² at carbon microspheres with integrated chitosan (Chen et al., 2008), ca. 0.0026 A M⁻¹ at a polymer-based CNT electrode (Moyo et al., 2013), or 0.34 A M⁻¹ at a cross-linked CNT on thiol-modified Au electrode (Kafi et al., 2018). The pyBA bioelectrode notably also offers improved analytical sensitivity compared to the high sensitivity of 4.25 A M⁻¹ cm⁻² achieved at an ultramicroelectrode DET biosensor integrating ionic liquid, carbon fibers and SWCNTs (Ren et al., 2017), or a DET biosensor based on commercial

screenprinted carbon electrodes with SWCNTs (Chekin et al., 2015) that yielded $0.0051 \text{ A M}^{-1} \text{ cm}^{-2}$.

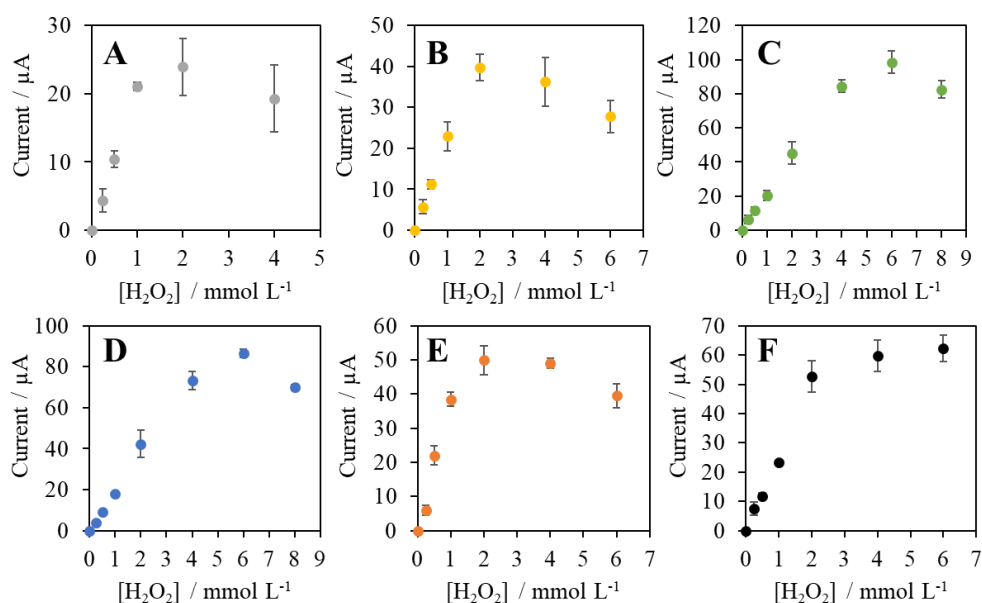


Figure 62. Amperometric current-concentration linear dynamic range curves recorded at MWCNT-HRP electrodes in 0.1 mol L^{-1} phosphate buffer (pH 7.0) before and after increasing additions of H_2O_2 : (A, ●) unmodified; (B, ●) py; (C, ●) pyNHS; (D, ●) pyAA; (E, ●) pyBA; (F, ●) pyNH₂. Current values obtained at 0 V vs. Ag/AgCl from CVs. Error bars correspond to standard deviation from $n = 3$ samples.

4.4.2. Bioelectrocatalysis of pyrroline-NHS modified HRP bioelectrodes with nanocellulose

Towards the development of eco-friendlier biosensor and biofuel cell devices with improvements in properties such as biocompatibility and stability, we explored the development of HRP bioelectrodes integrating bacterial nanocellulose. Bacterial nanocellulose is a natural cellulosic fibrous material that offers advantages such as excellent biocompatibility, biodegradability, hydrophilicity and hydrogel-forming properties at very low solid content via $-\text{OH}$ groups, high specific surface area and porous nanofibrillar network, eco-friendly processing, and low production costs

(Abol-Fotouh et al., 2020; Stanisławska, 2016). Tominaga and coworkers reported the construction of a “one-pot” nanocellulose/CNT laccase biocathode, citing the possibility to improve electrode flexibility and proton conductivity; however, performance was limited compared to other biocathodes and no stability or biocompatibility data was reported (Tominaga et al., 2020). Slaughter and coworkers integrated bacterial nanocellulose sheets with bioelectrodes as a flexible and biocompatible layer to contact with skin (Yuen et al., 2019). The nanocellulose was however not exploited as part of the catalytic matrix to enhance bioelectrocatalysis. Zhang and coworkers developed a second-generation HRP biosensor based on gold nanoparticles with a quinone mediator and bacterial cellulose that offered high performance with a sensitivity of $0.61 \text{ A M}^{-1} \text{ cm}^{-2}$ (Wang et al., 2011). The absence of comparative data makes it difficult to define the enhancement effects specifically related to the nanocellulose.

We developed a nanocellulose bioelectrode design that is illustrated in *Figure 63A*. The pyNHS modified MWCNT electrode was chosen due to the promising results observed for both biocathode and biosensor applications. Two strategies were investigated: (i) “layer-by-layer” with nanocellulose added as an outer layer to the pyNHS HRP bioelectrode, and (ii) a “one-pot” strategy with a mixture of nanocellulose and enzyme first prepared then added as a mixed layer to the pyNHS electrode (*see Section 3.3.6*). *Figure 63B* shows the CVs obtained at the optimised nanocellulose/pyNHS bioelectrode prepared by the one-pot (5 μL) method. The CVs were obtained from 0.6 V to 0 V before after the addition of increasing amounts of H_2O_2 from 0.4 mmol L^{-1} to 8 mmol L^{-1} . At concentrations $\leq 2 \text{ mmol L}^{-1}$, well-defined catalytic reduction peaks are observed that are followed by a slightly lower but constant current, consistent with the current not being diffusion limited,

despite the presence of cellulosic material in the catalytic layer. The CVs recorded at “low” and “high” millimolar H_2O_2 concentrations for the one-pot (5 μL) nanocellulose/pyNHS HRP bioelectrode (Figure 63B) are similar to those observed at the pyNHS HRP bioelectrode without nanocellulose (Figure 60A), except for a few differences at 4 mmol L^{-1} H_2O_2 . First, a higher catalytic current of 110 μA (1.6 mA cm^{-2}) and the highest in this study was observed at the one-pot (5 μL) nanocellulose/pyNHS HRP bioelectrode, representing a 17% increase compared to the pyNHS HRP bioelectrode output at the same H_2O_2 concentration. The other difference is that CVs observed at the one-pot (5 μL) nanocellulose/pyNHS HRP bioelectrode at 4 mmol L^{-1} (and 6 mmol L^{-1}) exhibited two unusual voltages cross-over points at low potential, but their nature is unclear. The crossed CVs may be related to changes in nucleation and/or conductivity of the cellulosic fibers, or result from enzyme activation and deactivation processes that switch abruptly at certain potentials.

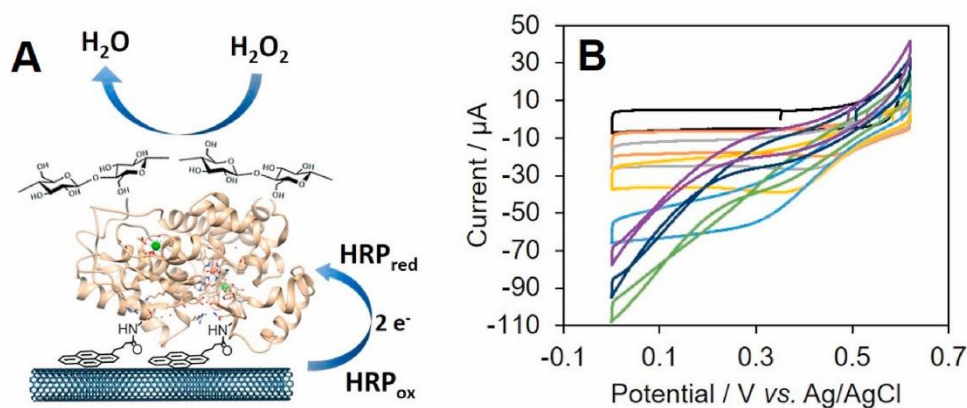


Figure 63. Schematic representation of the MWCNT-HRP electrodes modified with pyNHS and nanocellulose. (B) Representative CVs recorded at 10 mV s^{-1} at the one-pot (5 μL) nanocellulose/pyNHS HRP bioelectrode in 0.1 mol L^{-1} phosphate buffer (pH 7.0) before and after addition of H_2O_2 at (—) 0.4; (—) 0.6; (—) 1; (—) 2; (—) 4; (—) 6; and (—) 8 mmol L^{-1} .

Figure 64 shows the current-concentration response curves for the unmodified and pyrene-NHS modified HRP bioelectrode vs. the one-pot (5 μL) nanocellulose/pyNHS HRP bioelectrodes. Figure 64 reveal either similar or enhanced catalytic current output as well as better sensitivity performance ($3.51 \text{ A M}^{-1} \text{ cm}^{-2}$) across the current range from 0.25 mmol L^{-1} to 8 mmol L^{-1} for the optimised nanocellulose bioelectrode compared to the pyNHS and unmodified bioelectrodes without nanocellulose.

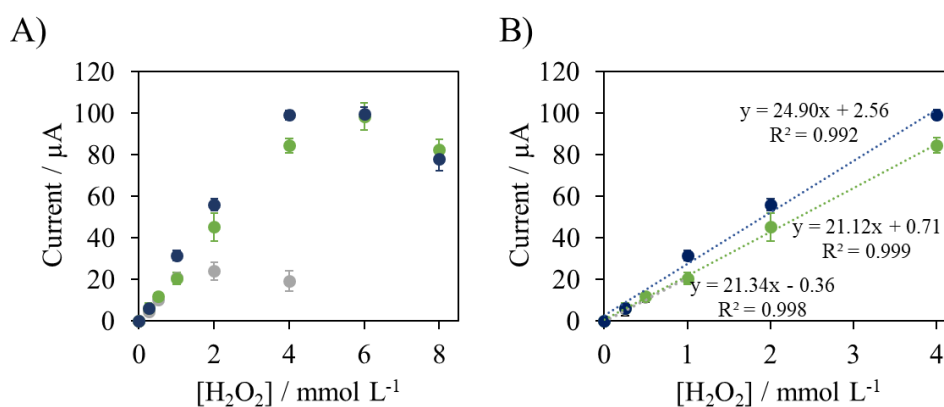


Figure 64. Current-concentration (A) full range and (B) linear dynamic range response curves recorded at MWCNT-HRP electrodes in 0.1 mol L^{-1} phosphate buffer (pH 7.0) before and after increasing additions of H_2O_2 : (•) unmodified; (◐) pyNHS; (◑) one pot (5 μL) nanocellulose/pyNHS. Current values obtained at 0 V vs. Ag/AgCl. Error bars correspond to standard deviation from $n = 3$ samples.

Current-concentration responses for the alternative one-pot (20 μL) and layer-by-layer nanocellulose/pyNHS HRP bioelectrodes are reported in Figure 65. Significantly smaller catalytic currents were observed for these alternative configurations. The most important difference between the alternative nanocellulose preparations and the optimised preparation is that 300% more enzyme and nanocellulose were used for the alternative nanocellulose electrodes. Therefore, it seems likely that the nanocellulose at the alternative electrodes, possibly involving a synergetic effect with enzyme,

hinders effective orientation and electron transport between the HRP and the pyNHS-modified CNTs. The alternative one-pot (20 μL) bioelectrode gave approximately two-fold higher catalytic currents compared to the alternative “layer-by-layer (20 μL)” bioelectrode prepared using the same amounts of enzyme and nanocellulose (*Figure 65*). The incorporation of nanocellulose in the enzyme layer (one-pot) as opposed to on the enzyme layer (layer-by-layer) therefore has a drastic positive effect on the catalytic current. The superior catalytic currents at layer-by-layer compared to one-pot can be explained by two important effects. The first, that the one-pot electrode has increased hydrophilicity and therefore hydration across the bulk nanocellulose-CNT matrix that increases the amount of electrochemically-wired HRP in the porous electrode structure. And second, a steric and/or electrically insulating barrier effect for the layer-by-layer electrode that limits H_2O_2 permeation and enzyme wiring, respectively.

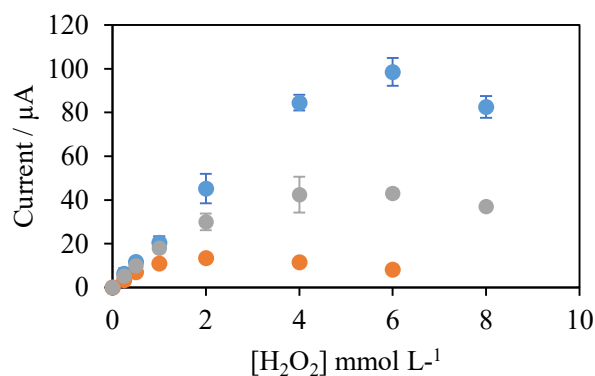


Figure 65. Current-concentration response curves recorded at MWCNT-HRP electrodes in 0.1 mol L^{-1} phosphate buffer (pH 7.0) before and after increasing additions of H_2O_2 : (•) pyNHS; (◐) nanocellulose/pyNHS (one-pot, 20 μL); (◑) nanocellulose/pyNHS (layer-by-layer, 20 μL). Current values obtained at 0 V vs. Ag/AgCl from CVs. Error bars correspond to standard deviation from $n = 3$ samples.

Next our attention focused on evaluating the open-circuit potential (OCP) as an indicator of effective bioelectrocatalysis and as a useful parameter of a

biocathode for estimating the maximum possible operating voltage of a biofuel cell. The OCP is the potential adopted by the electrode at zero current and in this case reflects the highest potential at which the enzyme is capable of DET with the electrode, being typically close to the onset potential for bioelectrocatalytic reduction (Mano and De Pulpiguet, 2018). *Figure 66A* shows the loss in OCP at an increasingly slower rate with increasing additions of H_2O_2 for the one pot (5 μL) nanocellulose bioelectrode. A high and stable OCP and onset potential is highly desirable, particularly for biocathodes with the objective of boosting the voltage output of biofuel cells. Despite the slightly weaker OCP performance by ca. 5% for the nanocellulose bioelectrode, the OCP values of between 0.5 and 0.62 V at $\leq 6 \text{ mmol L}^{-1} \text{H}_2\text{O}_2$ remain in a very practical range for a biocathode.

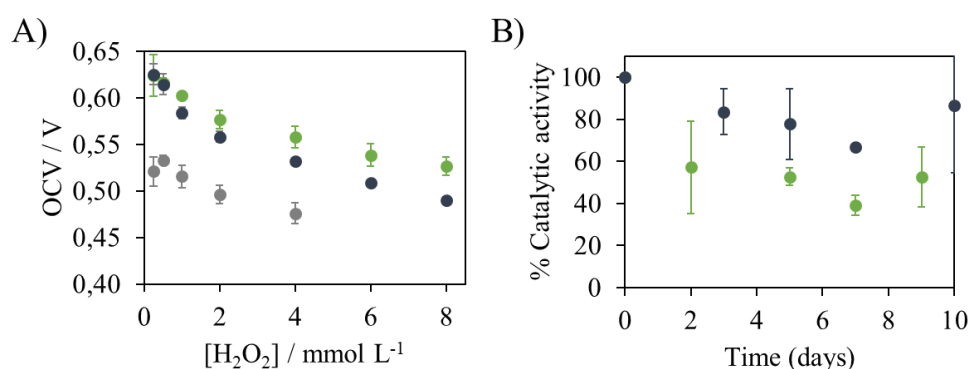


Figure 66. (A) Open circuit voltage-concentration plot recorded at MWCNT-HRP electrodes in 0.1 M phosphate buffer (pH 7.0) before and after increasing additions of H_2O_2 : (•) unmodified; (●) pyNHS; (●) pyNHS-nanocellulose. (B) Bioelectrocatalytic current from CVs recorded at (●) pyNHS and (●) pyNHS-nanocellulose modified MWCNT-HRP electrodes in 0.1 mol L^{-1} phosphate buffer (pH 7.0) in 4 $\text{mmol L}^{-1} \text{H}_2\text{O}_2$. Current values obtained at 0 V vs. Ag/AgCl.

Bioelectrocatalytic stability experiments were performed over a 9-10 day period at the modified electrodes. *Figure 66B* shows a plot of the catalytic currents measured in the presence of 4 $\text{mmol L}^{-1} \text{H}_2\text{O}_2$ at 0 V vs. Ag/AgCl from cyclic voltammograms recorded at 10 mV s^{-1} from 0.6 V to 0 V. The

bioelectrodes were stored in 0.1 M phosphate buffer (pH 7) solution free of H_2O_2 in the fridge at 4 °C. The stability profiles for the pyNHS and nanocellulose/pyNHS bioelectrodes show the same general trend. However, of particular interest, the nanocellulose bioelectrodes exhibit a dramatic enhancement in stability with an average of 67% of the initial activity remaining after 7 days compared to 39% after 7 days for the pyNHS modified bioelectrode without nanocellulose.

4.4.3. Conclusions

The non-covalent modification of multi-walled carbon nanotube electrodes with various pyrene derivatives is a simple and versatile method to promote DET bioelectrocatalysis with immobilised HRP for H_2O_2 . Surface modification with NHS ester and butyric acid groups proved the most effective for both high and low “catalytic boost” potential bioelectrocatalytic H_2O_2 reduction, and the most resistant to parasitic H_2O_2 electro-oxidation. Integration of bacterial nanocellulose by a straightforward one-pot protocol is an extremely promising method that not only enhanced catalytic current output while maintaining a very respectable open circuit potential performance, but also significantly improved the catalytic stability, offering 72% more stability, compared to the equivalent electrode without the nanocellulose. The nanocellulose strategy in principle can be used with any other enzyme at functionalised MWCNT electrodes to improve the activity and stability of a wide range of catalytic bioelectrodes for biosensor and biofuel applications. The nanocellulose biocathode, and future nanocellulose bioelectrodes, may also provide attractive biocompatibility, biodegradability, and mechanical properties for body-integrated applications, but this remains to be explored. Future work integrating HRP and HRP bienzymatic electrodes for biofuel cell applications is envisioned.

CHAPTER 5. GENERAL CONCLUSIONS

The present Thesis is focused on the study on nano and (bio)materials for the development of new strategies for the design of in situ analysis devices. The proposed methodologies have been based on the miniaturization and automatization following the new trends of Green Analytical Chemistry. The final goal has been to develop in situ methodologies by using materials as support material that can be used with a minimum sample treatment and reagents quantity while maintaining high levels of sensitivity and accuracy. The proposed methodologies have been applied to different compounds of interest in the analysis of water, pharmaceutical, clinical and industrial samples.

The main topics considered throughout the Thesis are summarized below.

The importance of choice the material in the development of solid devices as reagents encapsulators and reagents dispensers

The study of diverse materials properties is crucial to select appropriate materials for sensing applications. The selection will be mainly dependent on the analyte and the analytical reaction employed. The reagents will be entrapped or adsorbed in the supports and two different behaviours can be observed, i) the reagents will diffuse into solution ii) the analytes will enter in the solid support.

Zein is a biodegradable material being a protein from corn. Zein is a low cost, biocompatible and sustainable material. Zein can be used to carry out films which can entrapped or adsorbed reagents and enzymes. This film allows the stabilization of different compounds. In this Thesis this support has been used to entrap different chemical species, organic reagents like OMFP, inorganic substances such as hydroxylammonium chloride and

iron(III) chloride hexahydrate, and biomolecules like ALP has been adsorbed. The support acts as reagent delivery device.

Nylon is a synthetic polymer which has the capacity to easy to dye, thus, colorimetric sensors can be developed for semiquantitative analysis by naked-eye. In this thesis, its application in the development of sensors for the determination of silver in biocides has been demonstrated. Pyrogallol red and 1,10-phenanthroline were retained together in this support; the oxidation of PGR was performed also in the support.

PDMS is a hydrophobic material and is a good encapsulant and protector of reagents stability. It is optically transparent and can act as dispenser of reagents to the solution or as solid sensor where the derivatization reaction takes place inside it. In this Thesis it has been demonstrated the covalent immobilization of enzymes (HRP) on the PDMS device which allows the determination of H_2O_2 .

TEOS/MTEOS sol-gel sensor can act as encapsulant material of different compounds. This sol-gel sensor is transparent in the UV and visible spectral range, thus, in this Thesis, it was applied to the development of organic amino nitrogen and ammonium sensor by using optical techniques. Luminol reagent was embedding into the composite and the sensor provided a successful release to the medium.

Bacterial nanocellulose is a biomaterial produced by bacteria. It is hydrophilic and present high capacity of hydration, moreover, its surface contains several hydroxyl groups. In this Thesis, bacterial nanocellulose was used as support material to develop an electrochemical sensor. It was demonstrated that bacterial nanocellulose film increased reagent/enzyme stability.

CNTs have high surface area a large stability. They have a good capacity of interact with several compounds through non-covalent mechanisms, thus CNTs material can be functionalized. In this Thesis, five pyrene derivates adsorbed at CNTs were tested to develop an HRP electrochemical sensor.

The importance of in situ measurements

The detection and control of in situ biomarkers represents a breakthrough in the field of *medicine*. Preventive medicine is focused on the absence of diseases through their control and early detection. Emerging technologies aid in the development of non-invasive personalized and preventive medicine devices by including methods of screening from biomarkers. In situ dispositives appear as a reliable option to achieve some exciting achievements in the medicine field. It has to be selective, sensitive, cheap and portable, thus, no external energy it is needed. Moreover, the possibility of miniaturization makes the analysis more cost-effective due to the reduction of reagents, analysis time and wasted generated. In this Thesis, the sensor developed for the determination of inorganic phosphate in serum and urine allows carry out multi-analysis, which results in a remarkable decrease in the analysis time. Thus a quick result can be obtained which leads to reduce the time of diseases diagnosis.

In the field of *quality control*, by including environmental, pharmaceutical, food and beverage analysis; in situ monitoring technologies appeared as an advance for complementing the classical methods in the laboratory because traditional chemistry analysis sometimes means that a process takes so long that it impedes a quick actuation in the case of not expected outcomes. Moreover, they allow you to decide if you wish collect more samples for laboratory work. In some cases, sensors are used to

complementary analysis in order to provide more information to improve decision making. Throughout the Thesis, five devices have been developed that allow in situ measurement of various analytes.

Two solid devices were developed by the immobilization of hydroxylammonium chloride and iron chloride in zein films for routine quality-control analysis of drugs and pharmaceutical products containing ester groups. The method allows semiquantitative analysis by naked-eye and quantitative analysis by spectrophotometry. The reaction produces a color change from yellow to brown due to the ferric hydroxamic complex formation.

An H₂O₂ device has been fabricated using a simple immobilization methodology of the HRP enzyme on an activate PDMS surface. This method provides in situ measurements with high accuracy and sensitivity. Moreover, the measurements can be obtained in just 10 s. It should be noticed that the device is reusable, allowing its use more than sixty times. The sensor was applied to the determination of in H₂O₂ pharmaceutical tablets.

A portable solid sensor has been developed in nylon for silver ion determination in biocides. The method allows semiquantitative analysis that can be performed by visual inspection of the sensor color and quantitative analysis that can be carried out by DR measurement or by a digital image-processing tool using a smartphone. The sensor helps to easily detect a mismatch in biocide levels that can cause bacteria to grow.

An organic amino nitrogen and ammonium colorimetric sensor has been developed by embedding luminol into TEOS/MTEOS composite. The method produces a luminescence signal which can be measured with a portable luminometer. It should be noted that the method is easy to handle by

nonqualified personnel and allow obtained the results at the place where the sample was taken. The method was applied to the analysis of several real waters.

Future perspectives

In situ devices which allow green analysis have shown great interest in recent years due to they allow the reduction of solvents consumption, waste generation and cost. The development of analytical tools based on color modes are increasing owing to the easy technique for detection and quantification of analytes without trained personnel and expensive equipment. In this sense, the color cards are in high demand in health and industrial areas to prevent unwanted situations from occurring. Long term monitoring provides information allowing to establish patterns that help to achieve control objectives. In addition, the portability and capacity to be calibrated in situ according to the conditions of the place allow act in case of not expected results. On the other hand, (bio)materials are studied as supports for sensors developing. Taking into account the interdisciplinary and knowledge transfer requirement, the research carried out in this Thesis has been applied to solve industrial, environmental and clinical challenges.

The study of (bio)materials as support material to be used in ‘in situ’ analysis has been the key point of the present Thesis as well as one of the main goals of many future research.

REFERENCES

References

- Abba, M., Ibrahim, Z., Chong, C.S., Zawawi, N.A., Kadir, M.R.A., Yusof, A.H.M., Razak, S.I.A., 2019. Transdermal Delivery of Crocin Using Bacterial Nanocellulose Membrane. *Fibers Polym.* 20, 2025–2031. <https://doi.org/10.1007/s12221-019-9076-8>
- Abnous, K., Danesh, N.M., Ramezani, M., Taghdisi, S.M., Emrani, A.S., 2018. A novel colorimetric aptasensor for ultrasensitive detection of cocaine based on the formation of three-way junction pockets on the surfaces of gold nanoparticles. *Anal. Chim. Acta* 1020, 110–115. <https://doi.org/10.1016/j.aca.2018.02.066>
- Abol-Fotouh, D., Hassan, M.A., Shokry, H., Roig, A., Azab, M.S., Kashyout, A.E.H.B., 2020. Bacterial nanocellulose from agro-industrial wastes: low-cost and enhanced production by *Komagataeibacter saccharivorans* MD1. *Sci. Rep.* 10, 1–15. <https://doi.org/10.1038/s41598-020-60315-9>
- Abreu, C., Nedellec, Y., Ondel, O., Buret, F., Cosnier, S., Le Goff, A., Holzinger, M., 2018. Glucose oxidase bioanodes for glucose conversion and H₂O₂ production for horseradish peroxidase biocathodes in a flow through glucose biofuel cell design. *J. Power Sources* 392, 176–180. <https://doi.org/10.1016/j.jpowsour.2018.04.104>
- Adams C. I. and Spaulding G. H., 1955. Determination of organic nitrogen by kjeldahl method without distillation. *Anal. Chem.* 27, 1003–1004. <https://doi.org/10.1021/ac60102a040>
- Addepalli, S., Roy, R., Mehnen, J., 2017. ‘ In - situ ’ inspection technologies : Trends in degradation assessment and associated technologies. *Procedia CIRP* 59, 35–40. <https://doi.org/10.1016/j.procir.2016.10.003>
- Adegoke, O., Pereira-Barros, M.A., Zolotovskaya, S., Abdolvand, A., Daeid, N.N., 2020. Aptamer-based cocaine assay using a nanohybrid composed of ZnS/Ag₂Se quantum dots, graphene oxide and gold nanoparticles as a fluorescent probe. *Microchim. Acta* 187. <https://doi.org/10.1007/s00604-019-4101-6>
- Afiero, O.E., Okorie, O., Okonkwo, T.J.N., 2012. A spectrophotometric method for the determination of ramipril in solid dosage forms. *Trop. J. Pharm. Res.* 11, 275–279. <https://doi.org/10.4314/tjpr.v11i2.15>

References

- Agir, I., Yildirim, R., Nigde, M., Isildak, I., 2020. Internet of Things Implementation of Nitrate and Ammonium Sensors for Online Water Monitoring. *Anal. Sci.* 37,971–976. <https://doi.org/10.2116/analsci.20p396>
- Agnès, C., Reuillard, B., Le Goff, A., Holzinger, M., Cosnier, S., 2013. A double-walled carbon nanotube-based glucose/H₂O₂ biofuel cell operating under physiological conditions. *Electrochem. commun.* 34, 105–108. <https://doi.org/10.1016/j.elecom.2013.05.018>
- Ahamed, A., Ge, L., Zhao, K., Veksha, A., Bobacka, J., Lisak, G., 2021. Environmental footprint of voltammetric sensors based on screen-printed electrodes: An assessment towards “green” sensor manufacturing. *Chemosphere* 278, 130462. <https://doi.org/10.1016/j.chemosphere.2021.130462>
- Akbari, A., Divband, B., Dehghan, P., Moradi, A.H., 2021. Application of nanocomposites based on graphene and metal materials in measurement of nitrate/nitrite in food samples. *Biointerface Res. Appl. Chem.* 11, 12769–12783. <https://doi.org/10.33263/BRIAC115.1276912783>
- Akgöl, S., Ulucan-Karnak, F., kuru, C.İ., Kuşat, K., 2021. The usage of composite nanomaterials in biomedical engineering applications. *Biotechnol. Bioeng.* <https://doi.org/10.1002/bit.27843>
- Alberti, G., Zanoni, C., Magnaghi, L.R., Biesuz, R., 2020. Disposable and low-cost colorimetric sensors for environmental analysis. *Int. J. Environ. Res. Public Health* 17, 1–23. <https://doi.org/10.3390/ijerph17228331>
- Ali, G.W., Ellatif, M.A.A., Abdel-Fattah, W.I., 2021. Extraction of natural cellulose and zein protein from corn silk: Physico-chemical and biological characterization. *Biointerface Res. Appl. Chem.* 11, 10614–10619. <https://doi.org/10.33263/BRIAC113.1061410619>
- Ali Hasim, N.R., Ahaitouf, A., Abdullah, M.Z., 2021. Irreversible bonding techniques for the fabrication of a leakage-free printed circuit board-based lab-on-chip in microfluidic platforms - A review. *Meas. Sci. Technol.* 32. <https://doi.org/10.1088/1361-6501/abeb92>
- Ali, M.M., Wolfe, M., Tram, K., Gu, J., Filipe, C.D.M., Li, Y., Brennan, J.D.,

References

2019. A DNAzyme-Based Colorimetric Paper Sensor for *Helicobacter pylori*. *Angew. Chemie - Int. Ed.* 58, 9907–9911. <https://doi.org/10.1002/anie.201901873>
- Almeida, T., Silvestre, A.J.D., Vilela, C., Freire, C.S.R., 2021. Bacterial nanocellulose toward green cosmetics: Recent progresses and challenges. *Int. J. Mol. Sci.* 22, 1–25. <https://doi.org/10.3390/ijms22062836>
- Alqahtani, M.S., Islam, M.S., Podaralla, S., Kaushik, R.S., Reineke, J., Woyengo, T., Perumal, O., 2017. Food Protein Based Core-Shell Nanocarriers for Oral Drug Delivery: Effect of Shell Composition on in Vitro and in Vivo Functional Performance of Zein Nanocarriers. *Mol. Pharm.* 14, 757–769. <https://doi.org/10.1021/acs.molpharmaceut.6b01017>
- Amin, R., Ramesh, P., Belharouak, I., 2020. Carbon nanotubes: Applications to energy storage devices, in: *Carbon Nanotubes - Redefining the World of Electronics*.
- Anastas, P.T., Warner, J.C., 1998. *Green Chemistry: Theory and Practice*. Green Chem. Theory Pr. Oxford Univ. Press. New York 30.
- Andreu, R., Ferapontova, E.E., Gorton, L., Calvente, J.J., 2007. Direct electron transfer kinetics in horseradish peroxidase electrocatalysis. *J. Phys. Chem. B* 111, 469–477. <https://doi.org/10.1021/jp064277i>
- Antiochia, R., Oyarzun, D., Sánchez, J., Tasca, F., 2019. Comparison of direct and mediated electron transfer for bilirubin oxidase from *myrothecium verrucaria*. Effects of inhibitors and temperature on the oxygen reduction reaction. *Catalysts* 9, 7–9. <https://doi.org/10.3390/catal9121056>
- Argente-García, A., Jornet-Martínez, N., Herráez-Hernández, R., Campíns-Falcó, P., 2017. A passive solid sensor for in-situ colorimetric estimation of the presence of ketamine in illicit drug samples. *Sensors Actuators, B Chem.* 253, 1137–1144. <https://doi.org/10.1016/j.snb.2017.07.183>
- Argente-García, A., Jornet-Martínez, N., Herráez-Hernández, R., Campíns-Falcó, P., 2016a. A solid colorimetric sensor for the analysis of amphetamine-like street samples. *Anal. Chim. Acta* 943, 123–130.

References

<https://doi.org/10.1016/j.aca.2016.09.020>

- Argente-García, A, Moliner-Martínez, Y., López-García, E., Campíns-Falcó, P., Herráez-Hernández, R., 2016. Application of carbon nanotubes modified coatings for the determination of amphetamines by in-tube solid-phase microextraction and capillary liquid chromatography. *Cromatography 3*. <https://doi.org/10.3390/chromatography3010007>
- Argente-García, A., Muñoz-Ortuño, M., Molins-Legua, C., Moliner-Martínez, Y., Campíns-Falcó, P., 2016b. A solid device based on doped hybrid composites for controlling the dosage of the biocide N-(3-aminopropyl)-N-dodecyl-1,3-propanediamine in industrial formulations. *Talanta* 147, 147–154. <https://doi.org/10.1016/j.talanta.2015.09.051>
- Ashraf, M.A., Khan, A.M., Ahmad, M., Sarfraz, M., 2015. Effectiveness of silica based sol-gel microencapsulation method for odorants and flavors leading to sustainable environment. *Front. Chem.* 3, 1–15. <https://doi.org/10.3389/fchem.2015.00042>
- Azeredo, H.M.C., Barud, H., Farinas, C.S., Vasconcellos, V.M., Claro, A.M., 2019. Bacterial Cellulose as a Raw Material for Food and Food Packaging Applications. *Front. Sustain. Food Syst.* 3. <https://doi.org/10.3389/fsufs.2019.00007>
- Aziz, S.B., Brza, M.A., Brevik, I., Hafiz, M.H., Asnawi, A.S.F.M., Yusof, Y.M., Abdulwahid, R.T., Kadir, M.F.Z., 2020. Blending and characteristics of electrochemical double-layer capacitor device assembled from plasticized proton ion conducting chitosan:Dextran:NH₄PF₆ polymer electrolytes. *Polymers (Basel)*. 12. <https://doi.org/10.3390/POLYM12092103>
- Badr, E.S.A., Achterberg, E.P., Tappin, A.D., Hill, S.J., Braungardt, C.B., 2003. Determination of dissolved organic nitrogen in natural waters using high-temperature catalytic oxidation. *TrAC - Trends Anal. Chem.* 22, 819–827. [https://doi.org/10.1016/S0165-9936\(03\)01202-0](https://doi.org/10.1016/S0165-9936(03)01202-0)
- Bagheri, H., Arab, S.M., Khoshshafar, H., Afkhami, A., 2015. A novel sensor for sensitive determination of atropine based on a Co₃O₄-reduced

References

- graphene oxide modified carbon paste electrode. *New J. Chem.* 39, 3875–3881. <https://doi.org/10.1039/c5nj00133a>
- Bai, J., Jiang, X., 2013. A Facile One-Pot Synthesis of Copper Sul fi de-Decorated Reduced Graphene Oxide Composites for Enhanced Detecting of H₂O₂ in Biological Environments. *Anal. Chem.* 85, 8095–8101. <https://doi.org/10.1021/ac400659u>
- Bai, Y., Tong, J., Bian, C., Xia, S., 2013. An electrochemical microsensor based on molybdophosphate complex for fast determination of total phosphorus in water. *The 8th Annual IEEE International Conference on Nano/Micro Engineered and Molecular Systems*, 41–44. <https://doi.org/10.1109/NEMS.2013.6559678>
- Balbinot, S., Srivastav, A.M., Vidic, J., Abdulhalim, I., Manzano, M., 2021. Plasmonic biosensors for food control. *Trends Food Sci. Technol.* 111, 128–140. <https://doi.org/10.1016/j.tifs.2021.02.057>
- Ballester-Caudet, A., Hakobyan, L., Moliner-Martinez, Y., Molins-Legua, C., Campíns-Falcó, P., 2021. Ionic-liquid doped polymeric composite as passive colorimetric sensor for meat freshness as a use case. *Talanta* 223, 121778. <https://doi.org/10.1016/j.talanta.2020.121778>
- Balogun, S.A., Fayemi, O.E., 2021. Electrochemical Sensors for Determination of Bromate in Water and Food Samples — Review Biosensors. 11, 172. <https://doi.org/10.3390/bios11060172>
- Bankey, S., Tapadiya, G.G., Saboo, S.S., Bindaiya, S., Jain, D., Khadbadi, S.S., 2009. Simultaneous determination of Ramipril, hydrochlorothizide and Telmisartan by spectrophotometry. *Int. J. ChemTech Res.* 1, 183–188.
- Beeharry, S., Sihota, S., Kelly, C., 2018. Profiling chlorine residuals using DPD and amperometric field test kits in a chlorinated small drinking water system with ammonia present in source water. *Environ. Heal. Rev.* 61, 39–49. <https://doi.org/10.5864/d2018-011>
- Blanchard, P.Y., Buzzetti, P.H.M., Davies, B., Nedellec, Y., Giroto, E.M., Gross, A.J., Le Goff, A., Nishina, Y., Cosnier, S., Holzinger, M., 2019. Electrosynthesis of Pyrenediones on Carbon Nanotube Electrodes for

References

- Efficient Electron Transfer with FAD-dependent Glucose Dehydrogenase in Biofuel Cell Anodes. *ChemElectroChem* 6, 5242–5247. <https://doi.org/10.1002/celec.201901666>
- Bocanegra-Rodríguez, S., Jornet-Martínez, N., Molins-Legua, C., Campíns-Falcó, P., 2020a. Portable solid sensor supported in nylon for silver ion determination: testing its liberation as biocide. *Anal. Bioanal. Chem.* 412, 4393–4402. <https://doi.org/10.1007/s00216-020-02680-y>
- Bocanegra-Rodríguez, S., Jornet-Martínez, N., Molins-Legua, C., Campíns-Falcó, P., 2020c. New Reusable Solid Biosensor with Covalent Immobilization of the Horseradish Peroxidase Enzyme: In Situ Liberation Studies of Hydrogen Peroxide by Portable Chemiluminescent Determination. *ACS Omega* 5, 2419–2427. <https://doi.org/10.1021/acsomega.9b03958>
- Bocanegra-Rodríguez, S., Jornet-Martínez, N., Molins-Legua, C., Campíns-Falcó, P., 2018. Delivering Inorganic and Organic Reagents and Enzymes from Zein and Developing Optical Sensors. *Anal. Chem.* 90, 8501–8508. <https://doi.org/10.1021/acs.analchem.8b01338>
- Bocanegra-Rodríguez, S., Molins-legua, C., Campíns-falcó, P., Giroud, F., Gross, A.J., Cosnier, S., 2021. Monofunctional pyrenes at carbon nanotube electrodes for direct electron transfer H₂O₂ reduction with HRP and HRP-bacterial nanocellulose. *Biosens. Bioelectron.* 187, 113304. <https://doi.org/10.1016/j.bios.2021.113304>
- Bocanegra-Rodríguez, S., Molins-legua, C., Campíns-falcó, P., 2021. Luminol doped silica-polymer sensor for portable organic amino nitrogen and ammonium determination in water. *Separations*, 8, 149. <https://doi.org/10.3390/separations8090149>
- Bollella, P., Medici, L., Tessema, M., Poloznikov, A.A., Hushpulian, D.M., Tishkov, V.I., Andreu, R., Leech, D., Megersa, N., Marcaccio, M., Gorton, L., Antiochia, R., 2018. Highly sensitive, stable and selective hydrogen peroxide amperometric biosensors based on peroxidases from different sources wired by Os-polymer: A comparative study. *Solid State Ionics* 314, 178–186. <https://doi.org/10.1016/j.ssi.2017.10.015>

References

- Bordbar, M. M., Tashkhourian, J., Hemmateenejad, B., 2019. Structural Elucidation and Ultrasensitive Analyses of Volatile Organic Compounds by Paper-Based Nano-Optoelectronic Noses. *ACS Sens.*, 4 (5), 1442-1451. <https://doi.org/10.1021/acssensors.9b00680>
- Bowler, A.L., Bakalis, S., Watson, N.J., 2020. A review of in-line and on-line measurement techniques to monitor industrial mixing processes. *Chem. Eng. Res. Des.* 153, 463–495. <https://doi.org/10.1016/j.cherd.2019.10.045>
- Bressi, V., Ferlazzo, A., Iannazzo, D., Espro, C., 2021. Graphene quantum dots by eco-friendly green synthesis for electrochemical sensing: Recent advances and future perspectives. *Nanomaterials* 11. <https://doi.org/10.3390/nano11051120>
- Burmistrova, N.A., Meier, R.J., Schreml, S., Duerkop, A., 2014. Chemical Reusable optical sensing microplate for hydrogen peroxide using a fluorescent photoinduced electron transfer probe (HP Green). *Sensors Actuators B. Chem.* 193, 799–805. <https://doi.org/10.1016/j.snb.2013.12.025>
- Cabral, E.S., 2018. Bacterial nano cellulose as non-active pharmaceutical ingredient. Advances and perspectives. *MOJ Drug Des. Dev. Ther.* 2, 230–233. <https://doi.org/10.15406/mojddt.2017.02.00067>
- Camilli, L., Passacantando, M., 2018. Advances on sensors based on carbon nanotubes. *Chemosensors* 6, 1–17. <https://doi.org/10.3390/chemosensors6040062>
- Campins-Falcó, P., Moliner-Martínez, Y., Herráez-Hernández, R., Molins-Legua, C., Verdú-Andrés, J., Jornet-Martínez, N., 2013. Passive device for the detection and or determination in situ of amines in gases. *Pat.* P201300436.
- Cao, J., Su, C., Ji, Y., Yang, G., Shao, Z., 2021. Recent advances and perspectives of fluorite and perovskite-based dual-ion conducting solid oxide fuel cells. *J. Energy Chem.* 57, 406–427. <https://doi.org/10.1016/j.jechem.2020.09.010>
- Cao, S., Zhou, L., Liu, C., Zhang, H., Zhao, Yuxin, Zhao, Yanli, 2021.

References

- Pillararene-based self-assemblies for electrochemical biosensors. *Biosens. Bioelectron.* 181, 113164. <https://doi.org/10.1016/j.bios.2021.113164>
- Cao, X., Wang, N., Jia, S., Shao, Y., 2013. Detection of glucose based on bimetallic PtCu nanochains modified electrodes. *Anal. Chem.* 85, 5040–5046. <https://doi.org/10.1021/ac400292n>
- Capelari, T.B., de Cássia, J., Rianne, L., Carlyne, M., Nunes, P., Pereira, L., Henrique, L., Teixeira, C.R., 2021. Synthesis of novel poly(methacrylic acid)/ β -cyclodextrin dual grafted MWCNT-based nanocomposite and its use as electrochemical sensing platform for highly selective determination of cocaine. *J. Electroanal. Chem.* 880, 114791. <https://doi.org/10.1016/j.jelechem.2020.114791>
- Capella, J. V., Bonastre, A., Campelo, J.C., Ors, R., Peris, M., 2020. A new ammonium smart sensor with interference rejection. *Sensors.* 20, 1–17. <https://doi.org/10.3390/s20247102>
- Capitán-Vallvey, L.F., López-Ruiz, N., Martínez-Olmos, A., Erenas, M.M., Palma, A.J., 2015. Recent developments in computer vision-based analytical chemistry: A tutorial review. *Anal. Chim. Acta* 899, 23–56. <https://doi.org/10.1016/j.aca.2015.10.009>
- Chang, Y., You, H. Efficient Bond of PDMS and Printed Circuit Board with An Application on Continuous-flow Polymerase Chain Reaction. *BioChip J* 14, 349–357 (2020). <https://doi.org/10.1007/s13206-020-4403-0>
- Chekin, F., Gorton, L., Tapsoba, I., 2015. Direct and mediated electrochemistry of peroxidase and its electrocatalysis on a variety of screen-printed carbon electrodes: Amperometric hydrogen peroxide and phenols biosensor. *Anal. Bioanal. Chem.* 407, 439–446. <https://doi.org/10.1007/s00216-014-8282-x>
- Chen, X., Li, C., Liu, Y., Du, Z., Xu, S., Li, L., Zhang, M., Wang, T., 2008. Electrocatalytic activity of horseradish peroxidase/chitosan/carbon microsphere microcomposites to hydrogen peroxide. *Talanta* 77, 37–41. <https://doi.org/10.1016/j.talanta.2008.03.041>
- Chen, Y.J., Liu, C.Y., Tsai, D.Y., Yeh, Y.C., 2018. A portable fluorescence

References

- resonance energy transfer biosensor for rapid detection of silver ions. *Sensors Actuators, B Chem.* 259, 784–788. <https://doi.org/10.1016/j.snb.2017.12.056>
- Chen, Y.T., Lee, Y.C., Lai, Y.H., Lim, J.C., Huang, N.T., Lin, C.T., Huang, J.J., 2020. Review of Integrated Optical Biosensors for Point-Of-Care Applications. *Biosensors* 10, 1–22. <https://doi.org/10.3390/bios10120209>
- Cherian, B., Hassan, A., Balakrishnan, H., Akbari, A., 2013. Advances in natural polymers, *Advanced Structured Materials*. 10. <https://doi.org/10.1007/978-3-642-20940-6>
- Chin, C.D., Linder, V., Sia, S.K., 2007. Lab-on-a-chip devices for global health: Past studies and future opportunities. *Lab Chip* 7, 41–57. <https://doi.org/10.1039/b611455e>
- Choi, H.K., Lee, M.-J., Lee, S.N., Kim, T.-H., Oh, B.-K., 2021. Noble Metal Nanomaterial-Based Biosensors for Electrochemical and Optical Detection of Viruses Causing Respiratory Illnesses. *Front. Chem.* 9, 1–9. <https://doi.org/10.3389/fchem.2021.672739>
- Cinti, S., Talarico, D., Palleschi, G., Moscone, D., Arduini, F., 2016. Novel reagentless paper-based screen-printed electrochemical sensor to detect phosphate. *Anal. Chim. Acta* 919, 78–84. <https://doi.org/10.1016/j.aca.2016.03.011>
- Ciriminna, R., Fidalgo, A., Pandarus, V., Béland, F., Ilharco, L.M., Pagliaro, M., 2013. The sol-gel route to advanced silica-based materials and recent applications. *Chem. Rev.* 113, 6592–6620. <https://doi.org/10.1021/cr300399c>
- Coffey, C.C., Pearce, T.A., 2010. Direct-reading methods for workplace air monitoring. *J. Chem. Heal. Saf.* 17, 10–21. <https://doi.org/10.1016/j.jchas.2009.08.003>
- Csöregi, E., Jönsson-Pettersson, G., Gorton, L., 1993. Mediatorless electrocatalytic reduction of hydrogen peroxide at graphite electrodes chemically modified with peroxidases. *J. Biotechnol.* 30, 315–337. [https://doi.org/10.1016/0168-1656\(93\)90147-F](https://doi.org/10.1016/0168-1656(93)90147-F)

References

- Curulli, A., 2021. Electrochemical Biosensors in Food Safety: Challenges and Perspectives. *Molecules* 26, 2940. <https://doi.org/10.3390/molecules26102940>
- Czaczyk, K., Myszka, K., 2007. Biosynthesis of extracellular polymeric substances (EPS) and its role in microbial biofilm formation. *Pol. J. Environ. Stud.* 16, 799–806.
- Dadkhah, A., Rofouei, M.K., Mashhadizadeh, M.H., 2014. Sensors and Actuators B : Chemical Synthesis and characterization of N , N -bis (benzophenone imine) formamidine as ionophores for silver-selective electrodes. *Sensors Actuators B. Chem.* 202, 410–416. <https://doi.org/10.1016/j.snb.2014.05.090>
- Dai, G., Hu, J., Zhao, X., Wang, P., 2017. A colorimetric paper sensor for lactate assay using a cellulose-Binding recombinant enzyme. *Sensors Actuators, B Chem.* 238, 138–144. <https://doi.org/10.1016/j.snb.2016.07.008>
- Dai, H., Lü, W., Zuo, X., Zhu, Q., Pan, C., Niu, X., Liu, J., Chen, H.L., Chen, X., 2017. A novel biosensor based on boronic acid functionalized metal-organic frameworks for the determination of hydrogen peroxide released from living cells. *Biosens. Bioelectron.* 95, 131–137. <https://doi.org/10.1016/j.bios.2017.04.021>
- Dai, Z., Ottesen, V., Deng, J., Helberg, R.M.L., Deng, L., 2019. A brief review of nanocellulose based hybrid membranes for CO₂ separation. *Fibers* 7, 1–18. <https://doi.org/10.3390/FIB7050040>
- Dart, A.J., Dart, C.M., 2011. Suture material: Conventional and stimuli responsive, *Comprehensive Biomaterials.* Elsevier Ltd. <https://doi.org/10.1016/b978-0-08-055294-1.00245-2>
- De Rycke, E., Foubert, A., Dubruel, P., Bol'hakov, O.I., De Saeger, S., Beloglazova, N., 2021. Recent advances in electrochemical monitoring of zearalenone in diverse matrices. *Food Chem.* 353, 129342. <https://doi.org/10.1016/j.foodchem.2021.129342>
- Dean, R.L., 2002. Kinetic studies with alkaline phosphatase in the presence and absence of inhibitors and divalent cations. *Biochem. Mol. Biol.*

References

- Educ. 30, 401–407. <https://doi.org/10.1002/bmb.2002.494030060138>
- Deep, N., Mishra, P., 2018. Evaluation of mechanical properties of functionalized carbon nanotube reinforced PMMA polymer nanocomposite. *Karbala Int. J. Mod. Sci.* 4, 207–215. <https://doi.org/10.1016/j.kijoms.2018.02.001>
- Delincee, H., Radola, B.J., 1978. Determination of isoelectric points in thin-layer isoelectric focusing: The importance of attaining the steady state and the role of CO₂ interference. *Anal. Biochem.* 90, 609–623. [https://doi.org/10.1016/0003-2697\(78\)90154-9](https://doi.org/10.1016/0003-2697(78)90154-9)
- Delincee, H., Radola, B.J., 1975. Fractionation of Horseradish Peroxidase by Preparative Isoelectric Focusing, Gel Chromatography and Ion-Exchange Chromatography. *Eur. J. Biochem.* 52, 321–330. <https://doi.org/10.1111/j.1432-1033.1975.tb04000.x>
- Demirkol, D.O., Dornbusch, K., Feller, K.H., Timur, S., 2011. Microfluidic devices and true-color sensor as platform for glucose oxidase and laccase assays. *Eng. Life Sci.* 11, 182–188. <https://doi.org/10.1002/elsc.201000068>
- Di Nonno, S., Ulber, R., 2021. Smartphone-based optical analysis systems. *Analyst* 146, 2749–2768. <https://doi.org/10.1039/d1an00025j>
- DiRienzo, M., 2006. New Applications for Silver. *LBMA Precious Met. Conf.* 85–90.
- Donnell, G., Denver, A., 1999. Antiseptics and Disinfectants: Activity, Action, and Resistance. *Clin. Microbiol. Rev.* 12, 147–179.
- Du, J., Shi, J., Obadi, M., Han, J., Li, Y., Sun, J., Chen, Z., Xu, B., 2020. Decolorization of commercial zein via protein precipitation involving organic solvents at low temperatures. *Colloids Surfaces A Physicochem. Eng. Asp.* 596, 124738. <https://doi.org/10.1016/j.colsurfa.2020.124738>
- Duffy, G., Maguire, I., Heery, B., Nwankire, C., Ducrée, J., Regan, F., 2017. PhosphaSense: A fully integrated, portable lab-on-a-disc device for phosphate determination in water. *Sensors Actuators, B Chem.* 246, 1085–1091. <https://doi.org/10.1016/j.snb.2016.12.040>

References

- Duffy, G., Regan, F., 2017. Recent developments in sensing methods for eutrophying nutrients with a focus on automation for environmental applications. *Analyst* 142, 4355–4372. <https://doi.org/10.1039/c7an00840f>
- Duong, H.D., Rhee, J. Il, 2019. Development of Ratiometric Fluorescence Sensors Based on CdSe / ZnS Quantum Dots for the Detection. *Sensors*. 19, 4977. <https://doi.org/10.3390/s19224977>
- Eatemadi, A., Daraee, H., Karimkhanloo, H., Kouhi, M., Zarghami, N., Akbarzadeh, A., Abasi, M., Hanifehpour, Y., Joo, S.W., 2014. Carbon nanotubes: Properties, synthesis, purification, and medical applications. *Nanoscale Res. Lett.* 9, 1–13. <https://doi.org/10.1186/1556-276X-9-393>
- Ekrami, E., Pouresmaieli, M., Shariati, P., Mahmoudifard, M., 2021. A review on designing biosensors for the detection of trace metals. *Appl. Geochemistry* 127, 104902. <https://doi.org/10.1016/j.apgeochem.2021.104902>
- Elouarzaki, K., Bourourou, M., Holzinger, M., Le Goff, A., Marks, R.S., Cosnier, S., 2015. Freestanding HRP-GOx redox buckypaper as an oxygen-reducing biocathode for biofuel cell applications. *Energy Environ. Sci.* 8, 2069–2074. <https://doi.org/10.1039/c5ee01189b>
- Eman Yossri Frag, Mohamed, M.E., Elhassan, M.O., 2020. Validated Potentiometric Sensors for Determination of Ramipril in Pharmaceuticals and Biological Fluids using in situ Screen Printed and Carbon Paste Electrodes. *J. Anal. Chem.* 75, 384–395. <https://doi.org/10.1134/S1061934820030041>
- Ensafi, A.A., Abarghoui, M.M., Rezaei, B., 2014. Chemical Electrochemical determination of hydrogen peroxide using copper / porous silicon based non-enzymatic sensor. *Sensors Actuators B. Chem.* 196, 398–405. <https://doi.org/10.1016/j.snb.2014.02.028>
- Ensafi, Ali A, Rezaloo, F., Rezaei, B., 2016. Chemical Electrochemical sensor based on porous silicon / silver nanocomposite for the determination of hydrogen peroxide. *Sensors Actuators B. Chem.* 231, 239–244. <https://doi.org/10.1016/j.snb.2016.03.018>

References

- Ensafi, Ali A., Zandi-Atashbar, N., Rezaei, B., Ghiaci, M., Chermahini, M.E., Moshiri, P., 2016. Non-enzymatic glucose electrochemical sensor based on silver nanoparticle decorated organic functionalized multiwall carbon nanotubes. *RSC Adv.* 6, 60926–60932. <https://doi.org/10.1039/c6ra10698f>
- EU Commission, 2015. Commission Directive (EU) 2015/1787 of 6 October 2015 amending Annexes II and III to Council Directive 98/83/EC on the quality of water intended for human consumption. *Off. J. Eur. Union.* <http://data.europa.eu/eli/dir/2015/1787/oj> L260, 6–17.
- Fadhel, A.A., Johnson, M., Trieu, K., Koculi, E., Campiglia, A.D., 2017. Selective nano-sensing approach for the determination of inorganic phosphate in human urine samples. *Talanta* 164, 209–215. <https://doi.org/10.1016/j.talanta.2016.11.017>
- Fan, J., Meng, Z., Dong, X., Xue, M., Qiu, L., Liu, X., Zhong, F., He, X., 2020. Colorimetric screening of nitramine explosives by molecularly imprinted photonic crystal array. *Microchem. J.* 158, 105143. <https://doi.org/10.1016/j.microc.2020.105143>
- Farag, M.A., Tanios, M., AlKarimy, S., Ibrahim, H., Guirguis, H.A., 2021. Biosensing approaches to detect potential milk contaminants: a comprehensive review. *Food Addit. Contam. Part A* 38, 1169–1192. <https://doi.org/10.1080/19440049.2021.1914864>
- Farahmand, E., Ibrahim, F., Hosseini, S., Rothan, H.A., Yusof, R., Koole, L.H., Djordjevic, I., 2015. A novel approach for application of nylon membranes in the biosensing domain. *Appl. Surf. Sci.* 353, 1310–1319. <https://doi.org/10.1016/j.apsusc.2015.07.004>
- Farhadi, K., Matin, A.A., Amanzadeh, H., Biparva, P., Tajik, H., Farshid, A.A., Pirkharrati, H., 2014. A novel dispersive micro solid phase extraction using zein nanoparticles as the sorbent combined with headspace solid phase micro-extraction to determine chlorophenols in water and honey samples by GC-ECD. *Talanta* 128, 493–499. <https://doi.org/10.1016/j.talanta.2014.06.002>
- Fatemi, S.M., Foroutan, M., 2016. Recent developments concerning the

References

- dispersion of carbon nanotubes in surfactant/polymer systems by MD simulation. *J. Nanostructure Chem.* 6, 29–40. <https://doi.org/10.1007/s40097-015-0175-9>
- Fazilati, M., 2012. A biosensor by using modified glassy carbon electrode with HRP enzyme and ZnO nanoparticles for detect of H₂O₂. *Annals of Biological Research.* 3, 5350–5357.
- Feldman, J.A., Robb, B.J., 1970. Colorimetric determination of atropine, homatropine, scopolamine, and their derivatives by the ferric hydroxamate method. *J. Pharm. Sci.* 59, 1646–1647. <https://doi.org/10.1002/jps.2600591121>
- Felgueiras, C., Azoia, N.G., Gonçalves, C., Gama, M., Dourado, F., 2021. Trends on the Cellulose-Based Textiles: Raw Materials and Technologies. *Front. Bioeng. Biotechnol.* 9, 1–20. <https://doi.org/10.3389/fbioe.2021.608826>
- Ferapontova, E., Puganova, E., 2002. Effect of pH on direct electron transfer between graphite and horseradish peroxidase. *J. Electroanal. Chem.* 518, 20–26. [https://doi.org/10.1016/S0022-0728\(01\)00692-1](https://doi.org/10.1016/S0022-0728(01)00692-1)
- Firooz, A.R., Ensafi, A.A., Kazemifard, N., Sharghi, H., 2012. Talanta A highly sensitive and selective bulk optode based on benzimidazol derivative as an ionophore and ETH5294 for the determination of ultra trace amount of silver ions. *Talanta* 101, 171–176. <https://doi.org/10.1016/j.talanta.2012.09.018>
- Fu, J., Lai, H., Zhang, Z., Li, G., 2021. UiO-66 metal-organic frameworks/gold nanoparticles based substrates for SERS analysis of food samples. *Anal. Chim. Acta* 1161, 338464. <https://doi.org/10.1016/j.aca.2021.338464>
- Gale, B.K., Eddings, M.A., Sundberg, S.O., Hatch, A., Kim, J., Ho, T., Karazi, S.M., 2016. Low-Cost MEMS Technologies, Reference Module in Materials Science and Materials Engineering. <https://doi.org/10.1016/b978-0-12-803581-8.00530-0>
- Gałaszka, A., Migaszewski, Z., Namieśnik, J., 2013. The 12 principles of green analytical chemistry and the SIGNIFICANCE mnemonic of green

References

- analytical practices. *TrAC - Trends Anal. Chem.* 50, 78–84.
<https://doi.org/10.1016/j.trac.2013.04.010>
- Ganesh, E.N., 2013. Single Walled and Multi Walled Carbon Nanotube Structure. *Synth. Appl.* 2, 311–320.
- Gao, L., Xiang, W., Deng, Z., Shi, K., Wang, H., Shi, H., 2020. Cocaine detection using aptamer and molybdenum disulfide-gold nanoparticle-based sensors. *Nanomedicine* 15, 325–335.
<https://doi.org/10.2217/nnm-2019-0046>
- Garkani Nejad, F., Tajik, S., Beitollahi, H., Sheikhshoaie, I., 2021. Magnetic nanomaterials based electrochemical (bio)sensors for food analysis. *Talanta* 228, 122075. <https://doi.org/10.1016/j.talanta.2020.122075>
- Gezer, P.G., Liu, G.L., Kokini, J.L., 2016. Detection of acrylamide using a biodegradable zein-based sensor with surface enhanced Raman spectroscopy. *Food Control* 68, 7–13.
<https://doi.org/10.1016/j.foodcont.2016.03.002>
- Ghica, M.E., Brett, C.M.A., 2014. Poly(brilliant green) and poly(thionine) modified carbon nanotube coated carbon film electrodes for glucose and uric acid biosensors. *Talanta* 130, 198–206.
<https://doi.org/10.1016/j.talanta.2014.06.068>
- Gilbert, L., Jenkins, A.T.A., Browning, S., Hart, J.P., 2011. Development of an amperometric, screen-printed, single-enzyme phosphate ion biosensor and its application to the analysis of biomedical and environmental samples. *Sensors Actuators, B Chem.* 160, 1322–1327.
<https://doi.org/10.1016/j.snb.2011.09.069>
- Glassmaker, N., Rahimi, R., 2019. Development of a nickel oxide/oxyhydroxide-modified printed carbon electrode as an all solid-state sensor for potentiometric phosphate detection. *New Journal of Chemistry.* 43, 18619–18628. <https://doi.org/10.1039/c9nj04502c>
- Golmohammadi, H., Morales-Narváez, E., Naghdi, T., Merkoçi, A., 2017. Nanocellulose in Sensing and Biosensing. *Chem. Mater.* 29, 5426–5446.
<https://doi.org/10.1021/acs.chemmater.7b01170>

References

- Gong, P., Li, X., Zhou, X., Zhang, Y., Chen, N., Wang, S., Zhang, S., Zhao, Y., 2021. Optical fiber sensors for glucose concentration measurement: A review. *Opt. Laser Technol.* 139, 106981. <https://doi.org/10.1016/j.optlastec.2021.106981>
- González-Fuenzalida, R.A., Moliner-Martínez, Y., González-Béjar, M., Molins-Legua, C., Verdú-Andres, J., Pérez-Prieto, J., Campins-Falcó, P., 2013. In situ colorimetric quantification of silver cations in the presence of silver nanoparticles. *Anal. Chem.* 85, 10013–10016. <https://doi.org/10.1021/ac402822d>
- Goud, K.Y., Reddy, K.K., Khorshed, A., Kumar, V.S., Mishra, R.K., Oraby, M., Ibrahim, A.H., Kim, H., Gobi, K.V., 2021. Electrochemical diagnostics of infectious viral diseases: Trends and challenges. *Biosens. Bioelectron.* 180, 113112. <https://doi.org/10.1016/j.bios.2021.113112>
- Gross, A.J., Chen, X., Giroud, F., Abreu, C., Le Goff, A., Holzinger, M., Cosnier, S., 2017. A High Power Buckypaper Biofuel Cell: Exploiting 1,10-Phenanthroline-5,6-dione with FAD-Dependent Dehydrogenase for Catalytically-Powerful Glucose Oxidation. *ACS Catal.* 7, 4408–4416. <https://doi.org/10.1021/acscatal.7b00738>
- Gross, A.J., Tanaka, S., Colomies, C., Giroud, F., Nishina, Y., Cosnier, S., Tsujimura, S., Holzinger, M., 2020. Diazonium Electrografting vs. Physical Adsorption of Azure A at Carbon Nanotubes for Mediated Glucose Oxidation with FAD-GDH. *Chem. Electro. Chem.* 7, 4543–4549. <https://doi.org/10.1002/celec.202000953>
- Guler, E., Yilmaz Sengel, T., Gumus, Z.P., Arslan, M., Coskunol, H., Timur, S., Yagci, Y., 2017. Mobile Phone Sensing of Cocaine in a Lateral Flow Assay Combined with a Biomimetic Material. *Anal. Chem.* 89, 9629–9632. <https://doi.org/10.1021/acs.analchem.7b03017>
- Gusmão, R., Melle-Franco, M., Geraldo, D., Bento, F., Paiva, M.C., Proença, F., 2015. Probing the surface of oxidized carbon nanotubes by selective interaction with target molecules. *Electrochem. commun.* 57, 22–26. <https://doi.org/10.1016/j.elecom.2015.04.016>
- Habibi, B., Jahanbakhshi, M., 2015. Sensitive determination of hydrogen

References

- peroxide based on a novel nonenzymatic electrochemical sensor : silver nanoparticles decorated on nanodiamonds. *J. Iran. Chem. Soc.* 8, 1431–1438. <https://doi.org/10.1007/s13738-015-0611-2>
- Haddad, R., Holzinger, M., Maaref, A., Cosnier, S., 2010. Pyrene functionalized single-walled carbon nanotubes as precursors for high performance biosensors. *Electrochim. Acta* 55, 7800–7803. <https://doi.org/10.1016/j.electacta.2010.03.021>
- Haghnazari, N., Alizadeh, A., Karami, C., Hamidi, Z., 2013. Simple optical determination of silver ion in aqueous solutions using benzo crown-ether modified gold nanoparticles. *Microchim. Acta* 180, 287–294. <https://doi.org/10.1007/s00604-012-0928-9>
- Halldorsson, S., Lucumi, E., Gómez-Sjöberg, R., Fleming, R.M.T., 2015. Advantages and challenges of microfluidic cell culture in polydimethylsiloxane devices. *Biosens. Bioelectron.* 63, 218–231. <https://doi.org/10.1016/j.bios.2014.07.029>
- Hartati, Y.W., Topkaya, S.N., Gaffar, S., Bahti, H.H., Cetin, A.E., 2021. Synthesis and characterization of nanoceria for electrochemical sensing applications. *RSC Adv.* 11, 16216–16235. <https://doi.org/10.1039/d1ra00637a>
- Hassouna, M.E.M., Elsuccary, S.A.A., Graham, J.P., 2010. N , N-Bis (3-methyl-1-phenyl-4-benzylidene-5-pyrazolone) propylenediamine Schiff base as a neutral carrier for silver (I) ion-selective electrodes. *Sensors Actuators B. Chem.* 146, 79–90. <https://doi.org/10.1016/j.snb.2010.02.012>
- Hersch, R.W., 2012. Water quality for drinking: WHO guidelines. *Encycl. Earth Sci. Ser.* 876–883. https://doi.org/10.1007/978-1-4020-4410-6_184
- Heurich, M., Kadir, M.K.A., Tothill, I.E., 2011. An electrochemical sensor based on carboxymethylated dextran modified gold surface for ochratoxin A analysis. *Sensors Actuators, B Chem.* 156, 162–168. <https://doi.org/10.1016/j.snb.2011.04.007>
- Hosu, O., Lettieri, M., Papara, N., Ravalli, A., Sandulescu, R., Cristea, C.,

References

- Marrazza, G., 2019. Colorimetric multienzymatic smart sensors for hydrogen peroxide, glucose and catechol screening analysis. *Talanta* 204, 525–532. <https://doi.org/10.1016/j.talanta.2019.06.041>
- Hosu, O., Ravalli, A., Lo Piccolo, G.M., Cristea, C., Sandulescu, R., Marrazza, G., 2017. Smartphone-based immunosensor for CA125 detection. *Talanta* 166, 234–240. <https://doi.org/10.1016/j.talanta.2017.01.073>
- Hu, J., Zhang, Z., 2020. Application of electrochemical sensors based on carbon nanomaterials for detection of flavonoids. *Nanomaterials* 10, 1–14. <https://doi.org/10.3390/nano10102020>
- Hudson, J.M., Heffron, K., Kotlyar, V., Sher, Y., Maklashina, E., Cecchini, G., Armstrong, F.A., 2005. Electron transfer and catalytic control by the iron-sulfur clusters in a respiratory enzyme, *E. coli* fumarate reductase. *J. Am. Chem. Soc.* 127, 6977–6989. <https://doi.org/10.1021/ja043404q>
- Hušek, P., Švagera, Z., Hanzlíková, D., Šimek, P., 2012. Survey of several methods deproteinizing human plasma before and within the chloroformate-mediated treatment of amino/carboxylic acids quantitated by gas chromatography. *J. Pharm. Biomed. Anal.* 67–68, 159–162. <https://doi.org/10.1016/j.jpba.2012.04.027>
- Ibarlucea B., Fernández-Sánchez C., Demming S., Büttgenbach S., L.A., 2011. Selective functionalisation of PDMS-based photonic lab on a chip for biosensing. *Analyst.* 136, 3496–3502. <https://doi.org/10.1039/c0an00941e>
- Iijima, S., 1991. Helical microtubules of graphitic carbon. *Nature* 354, 56–58. <https://doi.org/10.1038/354056a0>
- Iijima, S., 1991. Helical microtubules of graphitic carbon. *Nature* 354, 56–58.
- Jaikang, P., Paengnakorn, P., Grudpan, K., 2020. Simple colorimetric ammonium assay employing well microplate with gas pervaporation and diffusion for natural indicator immobilized paper sensor via smartphone detection. *Microchem. J.* 152, 104283. <https://doi.org/10.1016/j.microc.2019.104283>

References

- Jali, M.H., Rahim, H.R.A., Md Johari, M.A., Yusof, H.H.M., Ahmad, A., Thokchom, S., Dimiyati, K., Harun, S.W., 2021. Humidity sensing using microfiber-ZnO nanorods coated glass structure. *Optik (Stuttg)*. 238, 166715. <https://doi.org/10.1016/j.ijleo.2021.166715>
- Jangju, A., Farhadi, K., Hatami, M., Amani, S., Esmali, F., Moshkabadi, A., Hajilari, F., 2017. Application of zein-modified magnetite nanoparticles in dispersive magnetic micro-solid-phase extraction of synthetic food dyes in foodstuffs. *J. Sep. Sci.* 40, 1343–1352. <https://doi.org/10.1002/jssc.201600856>
- Jeong, H., Park, J., Kim, H., 2013. Determination of NH₄⁺ in environmental water with interfering substances using the modified nessler method. *J. Chem.* 2013. <https://doi.org/10.1155/2013/359217>
- Jia, D., Yang, C., Zhang, W., Ding, Y., 2021. Dyes inspired sensor arrays for discrimination of glycosaminoglycans. *Dye. Pigment.* 190, 109266. <https://doi.org/10.1016/j.dyepig.2021.109266>
- Jia, W., Schwamborn, S., Jin, C., Xia, W., Muhler, M., Schuhmann, W., Stoica, L., 2010. Towards a high potential biocathode based on direct bioelectrochemistry between horseradish peroxidase and hierarchically structured carbon nanotubes. *Phys. Chem. Chem. Phys.* 12, 10088–10092. <https://doi.org/10.1039/c0cp00349b>
- Jiang, T., Sun, X., Wei, L., Li, M., 2020. Determination of hydrogen peroxide released from cancer cells by a Fe-Organic framework/horseradish peroxidase-modified electrode. *Anal. Chim. Acta* 1135, 132–141. <https://doi.org/10.1016/j.aca.2020.09.040>
- Jørgensen, N.O.G., 2009. Organic nitrogen. *Earth Syst. Environ. Sci.* 832–851. <https://doi.org/10.1016/B978-012370626-3.00119-8>
- Jornet-Martínez, N., Bocanegra-Rodríguez, S., González-Fuenzalida, R.A., Molins-Legua, C., Campíns-Falcó, P., 2019. In situ analysis devices for estimating the environmental footprint in beverages industry. *Processing and Sustainability of Beverages*, Elsevier Inc. Vol.2, 275–317. <https://doi.org/10.1016/B978-0-12-815259-1.00009-4>
- Jornet-Martínez, N., Campíns-Falcó, P., Hall, E.A.H., 2016. Zein as

References

- biodegradable material for effective delivery of alkaline phosphatase and substrates in biokits and biosensors. *Biosens. Bioelectron.* 86, 14–19. <https://doi.org/10.1016/j.bios.2016.06.016>
- Jornet-Martínez, N., Gómez-Ojea, R., Tomás-Huercio, O., Herráez-Hernández, R., Campíns-Falcó, P., 2018. Colorimetric determination of alcohols in spirit drinks using a reversible solid sensor. *Food Control* 94, 7–16. <https://doi.org/10.1016/j.foodcont.2018.06.020>
- Jornet-Martínez, Neus, Hakobyan, L., Argente-García, A.I., Molins-Legua, C., Campíns-Falcó, P., 2019. Nylon-supported plasmonic assay based on the aggregation of silver nanoparticles: in situ determination of hydrogen sulfide-like compounds in breath samples as a proof of concept. *ACS Sensors* 4, 2164–2172. <https://doi.org/10.1021/acssensors.9b01019>
- Jornet-Martínez, N., Herráez-Hernández, R., Campíns-Falcó, P., 2021. Scopolamine analysis in beverages: Bicolorimetric device vs portable nano liquid chromatography. *Talanta* 232, 122406. <https://doi.org/10.1016/j.talanta.2021.122406>
- Jornet-Martínez, N., Herráez-Hernández, R., Campíns-Falcó, P., 2019a. Stabilization of formaldehyde into polydimethylsiloxane composite: application to the in situ determination of illicit drugs. *Anal. Bioanal. Chem.* 411, 2141–2148. <https://doi.org/10.1007/s00216-019-01644-1>
- Jornet-Martínez, N., Moliner-Martínez, Y., Herráez-Hernández, R., Molins-Legua, C., Verdú-Andrés, J., Campíns-Falcó, P., 2016b. Designing solid optical sensors for in situ passive discrimination of volatile amines based on a new one-step hydrophilic PDMS preparation. *Sensors Actuators, B Chem.* 223, 333–342. <https://doi.org/10.1016/j.snb.2015.09.097>
- Jornet-Martínez, N., Moliner-Martínez, Y., Molins-Legua, C., Campíns-Falcó, P., 2017. Trends for the development of in situ analysis devices. *Encyclopedia of Analytical Chemistry*. <https://doi.org/10.1002/9780470027318.a9593>
- Jornet-Martínez, N., Samper-Avilés, M., Herráez-Hernández, R., Campíns-Falcó, P., 2019b. Modifying the reactivity of copper (II) by its

References

- encapsulation into polydimethylsiloxane: A selective sensor for ephedrine-like compounds. *Talanta* 196, 300–308. <https://doi.org/10.1016/j.talanta.2018.12.054>
- Jouber, R., Strub, J.M., Zugmeyer, S., Kobi, D., Carte, N., Van Dorsselaer, A., Boucherie, H., Jaquet-Gutfreund, L., 2001. Quantification of individual zein isoforms resolved by two-dimensional electrophoresis: Genetic variability in 45 maize inbred lines. *Electrophoresis*. 22, 2983-2989. [https://doi.org/10.1002/1522-2683\(200108\)22:14<2983::AID-ELPS2983>3.0.CO;2-#](https://doi.org/10.1002/1522-2683(200108)22:14<2983::AID-ELPS2983>3.0.CO;2-#)
- Jouyban, A., Rahimpour, E., 2021. Optical sensors for determination of water in the organic solvents: a review. *J. Iran. Chem. Soc.* <https://doi.org/10.1007/s13738-021-02290-0>
- Jozala, A.F., de Lencastre-Novaes, L.C., Lopes, A.M., de Carvalho Santos-Ebinuma, V., Mazzola, P.G., Pessoa-Jr, A., Grotto, D., Gerenutti, M., Chaud, M.V., 2016. Bacterial nanocellulose production and application: a 10-year overview. *Appl. Microbiol. Biotechnol.* 100, 2063–2072. <https://doi.org/10.1007/s00253-015-7243-4>
- Junqueira, A.M., Mao, F., Mendes, T.S.G., Simões, S.J.C., Balestieri, J.A.P., Hannah, D.M., 2021. Estimation of river flow using CubeSats remote sensing. *Sci. Total Environ.* 788, 147762. <https://doi.org/10.1016/j.scitotenv.2021.147762>
- Juska, V.B., Pemble, M.E., 2020. A critical review of electrochemical glucose sensing: Evolution of biosensor platforms based on advanced nanosystems. *Sensors (Switzerland)* 20, 1–28. <https://doi.org/10.3390/s20216013>
- Kafi, A.K.M., Naqshabandi, M., Yusoff, M.M., Crossley, M.J., 2018. Improved peroxide biosensor based on Horseradish Peroxidase/Carbon Nanotube on a thiol-modified gold electrode. *Enzyme Microb. Technol.* 113, 67–74. <https://doi.org/10.1016/j.enzmictec.2017.11.006>
- Kahveci, Z., Martínez-Tomé, M.J., Mallavia, R., Mateo, C.R., 2017. Fluorescent biosensor for phosphate determination based on immobilized polyfluorene-liposomal nanoparticles coupled with

References

- alkaline phosphatase. *ACS Appl. Mater. Interfaces* 9, 136–144. <https://doi.org/10.1021/acsami.6b12434>
- Kangas, M.J., Burks, R.M., Atwater, J., Lukowicz, R.M., Williams, P., Holmes, A.E., 2017. Colorimetric Sensor Arrays for the Detection and Identification of Chemical Weapons and Explosives. *Crit. Rev. Anal. Chem.* 47, 138–153. <https://doi.org/10.1080/10408347.2016.1233805>
- Karachevtsev, V.A., Stepanian, S.G., Glamazda, A.Y., Karachevtsev, M. V., Eremenko, V. V., Lytvyn, O.S., Adamowicz, L., 2011. Noncovalent interaction of single-walled carbon nanotubes with 1-pyrenebutanoic acid succinimide ester and glucoseoxidase. *J. Phys. Chem. C* 115, 21072–21082. <https://doi.org/10.1021/jp207916d>
- Karimi-Maleh, H., Orooji, Y., Karimi, F., Alizadeh, M., Baghayeri, M., Rouhi, J., Tajik, S., Beitollahi, H., Agarwal, S., Gupta, V.K., Rajendran, S., Ayati, A., Fu, L., Sanati, A.L., Tanhaei, B., Sen, F., Shabani-Nooshabadi, M., Asrami, P.N., Al-Othman, A., 2021. A critical review on the use of potentiometric based biosensors for biomarkers detection. *Biosens. Bioelectron.* 184, 113252. <https://doi.org/10.1016/j.bios.2021.113252>
- Karimi, M.A., Mohammadi, S.Z., Mohadesi, A., Hatefi-mehrjardi, A., 2011. Sharif University of technology determination of silver (I) by flame atomic absorption spectrometry after separation / preconcentration using modified magnetite nanoparticles. *Sci. Iran.* 18, 790–796. <https://doi.org/10.1016/j.scient.2011.06.008>
- Karrat, A., Amine, A., 2020. Recent advances in chitosan-based electrochemical sensors and biosensors. *Arab. J. Chem. Environ. Res.* 07, 66–93.
- Karydis, M., 2009. Eutrophication assessment of coastal waters based on indicators : a literature review. *Global Nest Journal.* 11, 373–390.
- Kaur, J., Singh, K. V., Raje, M., Varshney, G.C., Suri, C.R., 2004. Strategies for direct attachment of hapten to a polystyrene support for applications in enzyme-linked immunosorbent assay (ELISA). *Anal. Chim. Acta* 506, 133–135. <https://doi.org/10.1016/j.aca.2003.11.009>

References

- Kędziora, A., Speruda, M., Krzyżewska, E., Rybka, J., Łukowiak, A., Bugla-Płoskońska, G., 2018. Similarities and differences between silver ions and silver in nanoforms as antibacterial agents. *Int. J. Mol. Sci.* 19, 444. <https://doi.org/10.3390/ijms19020444>
- Kenji Onodera, Jean d'Offay, U.M., 2002. Nylon Membrane-Immobilized PCR for Detection of Bovine Viruses. *Biotechniques* 32, 74–80. <https://doi.org/10.2144/02321st03>
- Kent, E.J.M., Elliot, D.A., Miskelly, G.M., 2003. Inhibition of Bleach-Induced Luminol. *J Forensic Sci.* 48, 9–12.
- Kerr, C.J., Osborn, K.S., Rickard, A.H., Robson, G.D., Handley, P.S., 2003. Biofilms in water distribution systems, *Handbook of Water and Wastewater Microbiology*. Elsevier. <https://doi.org/10.1016/B978-0-12-470100-7.50042-X>
- Khan, P., Idrees, D., Moxley, M.A., Corbett, J.A., Ahmad, F., Von Figura, G., Sly, W.S., Waheed, A., Hassan, M.I., 2014. Luminol-based chemiluminescent signals: Clinical and non-clinical application and future uses. *Appl. Biochem. Biotechnol.* 173, 333-355. <https://doi.org/10.1007/s12010-014-0850-1>
- Kim, C., Hong, C., Lee, K., 2021. Structures and strategies for enhanced sensitivity of polydiacetylene(PDA) based biosensor platforms. *Biosens. Bioelectron.* 181, 113120. <https://doi.org/10.1016/j.bios.2021.113120>
- Kim, D.M., Park, J.S., Jung, S.W., Yeom, J., Yoo, S.M., 2021. Biosensing Applications Using Nanostructure-Based Localized Surface Plasmon Resonance Sensors. *Sensors* 21, 1–27. <https://doi.org/10.3390/s21093191>
- Kim, H.J., Kim, Y., Park, S.J., Kwon, C., Noh, H., 2018. Development of Colorimetric Paper Sensor for Pesticide Detection Using Competitive-inhibiting Reaction. *Biochip J.* 12, 326–331. <https://doi.org/10.1007/s13206-018-2404-z>
- Kobayashi, N., Izumi, H., Morimoto, Y., 2017. Review of toxicity studies of carbon nanotubes. *J. Occup. Health* 59, 394–407. <https://doi.org/10.1539/joh.17-0089-RA>

References

- Kobetičová, K., Černý, R., 2019. Terrestrial eutrophication of building materials and buildings: An emerging topic in environmental studies. *Sci. Total Environ.* 689, 1316–1328. <https://doi.org/10.1016/j.scitotenv.2019.06.423>
- Kong, D., Zhang, K., Tian, J., Yin, L., Sheng, X., 2021. Biocompatible and Biodegradable Light-Emitting Materials and Devices. *Adv. Mater. Technol.* 2100006, 2100006. <https://doi.org/10.1002/admt.202100006>
- Kratz, A., Ferraro, M., Sluss, P.M., Lewandrowski, K.B., 2004. Laboratory reference values. *N. Engl. J. Med.* 351, 1548–1563. <https://doi.org/10.1056/NEJMcp049016>
- Kreider, A., Richter, K., Sell, S., Fenske, M., Tornow, C., Stenzel, V., Grunwald, I., 2013. Applied Surface Science Functionalization of PDMS modified and plasma activated two-component polyurethane coatings by surface attachment of enzymes. *Appl. Surf. Sci.* 273, 562–569. <https://doi.org/10.1016/j.apsusc.2013.02.080>
- Kriss, R., Pieper, K.J., Parks, J., Edwards, M.A., 2021. Challenges of Detecting Lead in Drinking Water Using at-Home Test Kits. *Environ. Sci. Technol.* 55, 1964–1972. <https://doi.org/10.1021/acs.est.0c07614>
- Kuah, H.X., Loh, X.J., 2016. Silicones: The future for beauty and everyday care. *RSC Polym. Chem. Ser.* 2016-Janua, 135–153. <https://doi.org/10.1039/9781782623984-00135>
- Kulkarni, S., Tembe, S., Karve, M., 2015. Development of acid phosphate inhibition-based amperometric biosensor for determination of inorganic phosphate. *ISPTS 2015 - 2nd Int. Symp. Phys. Technol. Sensors Dive Deep Into Sensors, Proc.* 63–66. <https://doi.org/10.1109/ISPTS.2015.7220083>
- Kunst, S.R., Longhi, M., Rossa Beltrami, L.V., Zini, L.P., Boniatti, R., Piaggio Cardoso, H.R., Ortega Vega, M.R., De Fraga Malfatti, C., 2017. Effect of concentrations of plasticizers on the sol-gel properties developed from alkoxides precursors. *Polimeros* 27, 346–352. <https://doi.org/10.1590/0104-1428.12916>
- Kurup, C.P., Tlili, C., Zakaria, S.N.A., Ahmed, M.U., 2021. Recent trends in

References

- design and development of nanomaterial-based aptasensors. *Biointerface Res. Appl. Chem.* 11, 14057–14077. <https://doi.org/10.33263/BRIAC116.1405714077>
- Lalaoui, N., Holzinger, M., Le Goff, A., Cosnier, S., 2016. Diazonium Functionalisation of Carbon Nanotubes for Specific Orientation of Multicopper Oxidases: Controlling Electron Entry Points and Oxygen Diffusion to the Enzyme. *Chem. - A Eur. J.* 22, 10494–10500. <https://doi.org/10.1002/chem.201601377>
- Lawton, J.W., 2002. Zein: A history of processing and use. *Cereal Chem.* 79, 1-18. <https://doi.org/10.1094/CCHEM.2002.79.1.1>
- Le Goff, A., Holzinger, M., Cosnier, S., 2015. Recent progress in oxygen-reducing laccase biocathodes for enzymatic biofuel cells. *Cell. Mol. Life Sci.* 72, 941–952. <https://doi.org/10.1007/s00018-014-1828-4>
- Lee, I., Probst, D., Klonoff, D., Sode, K., 2021. Continuous glucose monitoring systems - Current status and future perspectives of the flagship technologies in biosensor research. *Biosens. Bioelectron.* 181, 113054. <https://doi.org/10.1016/j.bios.2021.113054>
- Lee, J.N., Park, C., Whitesides, G.M., 2003. Solvent Compatibility of Poly(dimethylsiloxane)-Based Microfluidic Devices. *Anal. Chem.* 75, 6544–6554. <https://doi.org/10.1021/ac0346712>
- Lee, S., Jang, K., Park, C., You, J., Kim, T., Im, C., Kang, J., Shin, H., Choi, C.H., Park, J., Na, S., 2015. Ultra-sensitive in situ detection of silver ions using a quartz crystal microbalance. *New J. Chem.* 39, 8028–8034. <https://doi.org/10.1039/c5nj00668f>
- Lee, W., Westerhoff, P., 2005. Dissolved organic nitrogen measurement using dialysis pretreatment. *Environ. Sci. Technol.* 39, 879–884. <https://doi.org/10.1021/es048818y>
- Leonardi, A.A., Lo Faro, M.J., Irrera, A., 2021. Biosensing platforms based on silicon nanostructures: A critical review. *Anal. Chim. Acta* 1160, 338393. <https://doi.org/10.1016/j.aca.2021.338393>
- Li, B., Wang, Yanxin, Huang, L., Qu, H., Han, Z., Wang, Yao, Kipper, M.J.,

References

- Belfiore, L.A., Tang, J., 2021. Review of performance improvement strategies for doped graphene quantum dots for fluorescence-based sensing. *Synth. Met.* 276, 116758. <https://doi.org/10.1016/j.synthmet.2021.116758>
- Li, F., Ma, W., Liu, J., Wu, X., Wang, Y., He, J., 2018. Luminol, horseradish peroxidase, and glucose oxidase ternary functionalized graphene oxide for ultrasensitive glucose sensing. *Anal. Bioanal. Chem.* 543–552.
- Li, J., Dasgupta, P.K., 1999. Chemiluminescence detection with a liquid core waveguide: Determination of ammonium with electrogenerated hypochlorite based on the luminol-hypochlorite reaction. *Anal. Chim. Acta* 398, 33–39. [https://doi.org/10.1016/S0003-2670\(99\)00378-5](https://doi.org/10.1016/S0003-2670(99)00378-5)
- Li, Q., Wu, J.-T., Liu, Y., Qi, X.-M., Jin, H.-G., Yang, C., Liu, J., Li, G.-L., He, Q.-G., 2021. Recent advances in black phosphorus-based electrochemical sensors: A review. *Anal. Chim. Acta* 1170, 338480. <https://doi.org/10.1016/j.aca.2021.338480>
- Li, Z., Zhou, J., Dong, T., Xu, Y., Shang, Y., 2021. Application of electrochemical methods for the detection of abiotic stress biomarkers in plants. *Biosens. Bioelectron.* 182, 113105. <https://doi.org/10.1016/j.bios.2021.113105>
- Li Z, Paul R, Tis T B, Saville A C, Hansel J C, Yu T, Ristaino J B, Wei Q S. 2019. Non-invasive plant disease diagnostics enabled by smartphone-based fingerprinting of leaf volatiles. *Nat. Plants*, 5(8): 856–866
- Liang, J., Yan, H., Wang, X., Zhou, Y., Gao, X., Puligundla, P., Wan, X., 2017. Encapsulation of epigallocatechin gallate in zein/chitosan nanoparticles for controlled applications in food systems. *Food Chem.* 231, 19–24. <https://doi.org/10.1016/j.foodchem.2017.02.106>
- Lim, J.W., Kim, T.Y., Woo, M.A., 2021. Trends in sensor development toward next-generation point-of-care testing for mercury. *Biosens. Bioelectron.* 183, 113228. <https://doi.org/10.1016/j.bios.2021.113228>
- Lin, B., Li, T., Zhao, Y., Huang, F., Guo, L., Feng, Y., 2008. Preparation of a TiO₂ nanoparticle-deposited capillary column by liquid phase deposition and its application in phosphopeptide analysis. *J.*

References

- Chromatogr. A. 1192, 95–102.
<https://doi.org/10.1016/j.chroma.2008.03.043>
- Liu, H.J., Yang, D.W., Liu, H.H., 2012. A hydrogen peroxide sensor based on the nanocomposites of poly(brilliant cresyl blue) and single walled-carbon nanotubes. *Anal. Methods* 4, 1421–1426.
<https://doi.org/10.1039/c2ay05881b>
- Liu, J., Lu, L., Li, A., Tang, J., Wang, S., Xu, S., Wang, L., 2015. Simultaneous detection of hydrogen peroxide and glucose in human serum with upconversion luminescence. *Biosens. Bioelectron. J.* 68, 204–209. <https://doi.org/10.1016/j.bios.2014.12.053>
- Liu, Y., Liu, X., Guo, Z., Hu, Z., Xue, Z., Lu, X., 2017. Horseradish peroxidase supported on porous graphene as a novel sensing platform for detection of hydrogen peroxide in living cells sensitively. *Biosens. Bioelectron.* 87, 101–107. <https://doi.org/10.1016/j.bios.2016.08.015>
- Long, H.P., Lai, C.C., Chung, C.K., 2017. Polyethylene glycol coating for hydrophilicity enhancement of polydimethylsiloxane self-driven microfluidic chip. *Surf. Coatings Technol.* 320, 315–319.
<https://doi.org/10.1016/j.surfcoat.2016.12.059>
- Long, J., Xu, J., Xia, S., 2011. Volatile organic compound colorimetric array based on zinc porphyrin and metalloporphyrin derivatives. *Energy Procedia* 12, 625–631. <https://doi.org/10.1016/j.egypro.2011.10.085>
- López-Alarcón, C., Lissi, E., 2006. A novel and simple ORAC methodology based on the interaction of Pyrogallol Red with peroxy radicals. *Free Radic. Res.* 40, 979–985. <https://doi.org/10.1080/10715760500481233>
- López Marzo, A.M., Mayorga-Martinez, C.C., Pumera, M., 2020. 3D-printed graphene direct electron transfer enzyme biosensors. *Biosens. Bioelectron.* 151, 111980. <https://doi.org/10.1016/j.bios.2019.111980>
- Louchis, K., Driscoll, S.O., 2011. Fundamental sensing limit of electrochemical glucose sensors. *Annu Int Conf Eng Med Biol Soc.* 7670–7673. <https://doi.org/10.1109/IEMBS.2011.6091890>
- Lourenço, N.D., Lopes, J.A., Almeida, C.F., Sarraguça, M.C., Pinheiro,

References

- H.M., 2012. Bioreactor monitoring with spectroscopy and chemometrics: A review. *Anal. Bioanal. Chem.* 404, 1211–1237. <https://doi.org/10.1007/s00216-012-6073-9>
- Lu, H., Wang, Q., Li, G., Qiu, Y., Wei, Q., 2017. Electrospun water-stable zein/ethyl cellulose composite nanofiber and its drug release properties. *Mater. Sci. Eng. C* 74, 86–93. <https://doi.org/10.1016/j.msec.2017.02.004>
- Lu, S., Shao, J., Ma, K., Chen, D., Wang, X., Zhang, L., Meng, Q., Ma, J., 2018. Flexible, mechanically resilient carbon nanotube composite films for high-efficiency electromagnetic interference shielding. *Carbon N. Y.* 136, 387–394. <https://doi.org/10.1016/j.carbon.2018.04.086>
- Lukin, R.Y., Kuchkaev, A.M., Sukhov, A. V., Bekmukhamedov, G.E., Yakhvarov, D.G., 2020. Platinum-catalyzed hydrosilylation in polymer chemistry. *Polymers (Basel)*. 12, 1–22. <https://doi.org/10.3390/POLYM12102174>
- Luo, H., Kaneti, Y.V., Ai, Y., Wu, Y., Wei, F., Fu, J., Cheng, J., Jing, C., Yuliarto, B., Eguchi, M., Na, J., Yamauchi, Y., Liu, S., 2021. Nanoarchitected Porous Conducting Polymers: From Controlled Synthesis to Advanced Applications. *Adv. Mater.* 33, 29, 2007318. <https://doi.org/10.1002/adma.202007318>
- Luo, M., Wang, W., Zhao, Q., Li, M., Chen, Y., Lu, Z., Liu, K., Wang, D., 2017. Chemiluminescence biosensor for hydrogen peroxide determination by immobilizing horseradish peroxidase onto PVA-co-PE nanofiber membrane. *Eur. Polym. J.* 91, 307–314. <https://doi.org/10.1016/j.eurpolymj.2017.04.018>
- Luo, Y., Wang, Q., 2014. Zein-based micro- and nano-particles for drug and nutrient delivery: A review. *J. Appl. Polym. Sci.* 131, 16. <https://doi.org/10.1002/app.40696>
- Mahmood, A.K., 2012. Development of two different spectrophotometric methods for the determination of atropine drug in pure form and pharmaceutical preparations. *J. Pure Appl. Sci.* 25, 226–241.
- Majdinasab, M., Daneshi, M., Louis Marty, J., 2021. Recent developments in

References

- non-enzymatic (bio)sensors for detection of pesticide residues: Focusing on antibody, aptamer and molecularly imprinted polymer. *Talanta* 232, 122397. <https://doi.org/10.1016/j.talanta.2021.122397>
- Malhotra, B.D., Srivastava, S., Augustine, S., 2015. Biosensors for food toxin detection: Carbon nanotubes and graphene. *MRS Online Proceedings Library..* 1725, 24–34. <https://doi.org/10.1557/opl.2015.165>
- Mano, N., De Poulpiquet, A., 2018. O₂ Reduction in Enzymatic Biofuel Cells. *Chem. Rev.* 118, 2392–2468. <https://doi.org/10.1021/acs.chemrev.7b00220>
- Manoj, D., Shanmugasundaram, S., Anandharamakrishnan, C., 2021. Nanosensing and nanobiosensing: Concepts, methods, and applications for quality evaluation of liquid foods. *Food Control* 126, 108017. <https://doi.org/10.1016/j.foodcont.2021.108017>
- Mao, K., Ma, J., Li, X., Yang, Z., 2019. Rapid duplexed detection of illicit drugs in wastewater using gold nanoparticle conjugated aptamer sensors. *Sci. Total Environ.* 688, 771–779. <https://doi.org/10.1016/j.scitotenv.2019.06.325>
- Mark, D., Haeberle, S., Roth, G., Stetten, F. Von, Zengerle, R., 2010. Microfluidic lab-on-a-chip platforms: Requirements, characteristics and applications. *Chem. Soc. Rev.* 39, 1153–1182. <https://doi.org/10.1039/b820557b>
- Marques, M.R.C., Loebenberg, R., Almukainzi, M., 2011. Simulated biologic fluids with possible application in dissolution testing. *Dissolution Technol.* 15–28. <https://doi.org/10.1002/jps.23029>
- Martínez-Aviño, A., Hakobyan, L., Ballester-caude, A., Moliner-Martínez, Y., Molins-Legua, C., Campins-Falcó, P., 2021a. NQS-Doped PDMS solid sensor : from water matrix to urine enzymatic application. *Biosens.* 11, 186. <https://doi.org/10.3390/bios11060186>
- Martínez-Aviño, A., Molins-Legua, C., Campins-Falcó, P., 2021b. Scaling the analytical information given by several types of colorimetric and spectroscopic instruments including smartphones: rules for their use and establishing figures of merit of solid chemosensors. *Anal. Chem.* 93,

References

- 6043–6052. <https://doi.org/10.1021/acs.analchem.0c03994>
- Martínez-Soroa, I., de Frutos-Lezaun, M., Ostra, M., Egía, A., Irastorza, M.B., Bachiller, M.P., 2016. Determination of phosphate concentration in glaucoma eye drops commercially available in Spain. *Arch. la Soc. Española Oftalmol.* (English Ed.) 91, 363–371. <https://doi.org/10.1016/j.oftale.2016.04.028>
- Masson, J.F., 2017. Surface Plasmon Resonance Clinical Biosensors for Medical Diagnostics. *ACS Sensors* 2, 16–30. <https://doi.org/10.1021/acssensors.6b00763>
- Mata, A., Fleischman, A.J., Roy, S., 2005. Characterization of Polydimethylsiloxane (PDMS) Properties for Biomedical Micro/Nanosystems. *Biomed. Microdevices* 7, 281–293. <https://doi.org/10.1007/s10544-005-6070-2>
- McDonagh, C., Bowe, P., Mongey, K., MacCraith, B.D., 2002. Characterisation of porosity and sensor response times of sol-gel-derived thin films for oxygen sensor applications. *J. Non. Cryst. Solids* 306, 138–148. [https://doi.org/10.1016/S0022-3093\(02\)01154-7](https://doi.org/10.1016/S0022-3093(02)01154-7)
- Meenakshi, S., Rama, R., Pandian, K., Gopinath, S.C.B., 2021. Modified electrodes for electrochemical determination of metronidazole in drug formulations and biological samples: An overview. *Microchem. J.* 165, 106151. <https://doi.org/10.1016/j.microc.2021.106151>
- Meseguer-Lloret, S., Molins-Legua, C., Campins-Falco, P., 2002. Ammonium determination in water samples by using OPA-NAC reagent: A comparative study with nessler and ammonium selective electrode methods. *Int. J. Environ. Anal. Chem.* 82, 475–489. <https://doi.org/10.1080/0306731021000018107>
- Meseguer-Lloret, S., Molins-Legua, C., Verdú-Andrés, J., Campíns-Falcó, P., 2006. Chemiluminescent method for detection of eutrophication sources by estimation of organic amino nitrogen and ammonium in water. *Anal. Chem.* 78, 7504–7510. <https://doi.org/10.1021/ac0604437>
- Mesquita, R.B.R., Ferreira, M.T.S.O.B., Tóth, I. V., Bordalo, A.A., McKelvie, I.D., Rangel, A.O.S.S., 2011. Development of a flow method

References

- for the determination of phosphate in estuarine and freshwaters- Comparison of flow cells in spectrophotometric sequential injection analysis. *Anal. Chim. Acta* 701, 15–22. <https://doi.org/10.1016/j.aca.2011.06.002>
- Moe, S.M., 2008. Disorders involving calcium, phosphorus, and magnesium. *Prim Care* 35, 215. <https://doi.org/10.1016/j.pop.2008.01.007>
- Mohamed, G.G., Yossri, F., Mohamed, M., 2019. Modified screen-printed and carbon paste as ion-selective electrodes for the determination of ramipril drug in pharmaceutical and biological samples. *Anal. Chem. Lett.* 9, 311–328. <https://doi.org/10.1016/j.jpha.2013.03.008>
- Mojsiewicz-Pieńkowska, K., 2012. Size exclusion chromatography with evaporative light scattering detection as a method for speciation analysis of polydimethylsiloxanes. III. Identification and determination of dimeticone and simeticone in pharmaceutical formulations. *J. Pharm. Biomed. Anal.* 58, 200–207. <https://doi.org/10.1016/j.jpba.2011.09.003>
- Moliner-martínez, Y., Garcia, H.P., Ribera, A., Coronado, E., Campíns-falcó, P., 2012. Magnetic in-tube solid phase microextraction. *Anal. Chem.* 84, 7233–7240. <https://doi.org/10.1021/ac301660k>
- Moliner-Martínez, Y., Herráez-Hernández, R., Campíns-Falcó, P., 2005. Improved detection limit for ammonium/ammonia achieved by Berthelot's reaction by use of solid-phase extraction coupled to diffuse reflectance spectroscopy. *Anal. Chim. Acta* 534, 327–334. <https://doi.org/10.1016/j.aca.2004.11.044>
- Molins-legua, C., 2018. Delivering inorganic and organic reagents and enzymes from zein and developing optical sensors. *Anal. Chem.* 90, 8501–8508. <https://doi.org/10.1021/acs.analchem.8b01338>
- Molins-Legua, C., Meseguer-Lloret, S., Moliner-Martinez, Y., Campíns-Falcó, P., 2006. A guide for selecting the most appropriate method for ammonium determination in water analysis. *TrAC - Trends Anal. Chem.* 25, 282–290. <https://doi.org/10.1016/j.trac.2005.12.002>
- Momany, F.A., Sessa, D.J., Lawton, J.W., Selling, G.W., Hamaker, S.A.H., Willett, J.L., 2006. Structural characterization of α -zein. *J. Agric. Food*

References

- Chem. 54, 543-547. <https://doi.org/10.1021/jf058135h>
- Morin, M.A., Zhang, W., Mallik, D., Organ, M.G., 2021. Sampling and Analysis in Flow: The Keys to Smarter, More Controllable, and Sustainable Fine-Chemical Manufacturing. *Angew. Chemie - Int. Ed.* 2–23. <https://doi.org/10.1002/anie.202102009>
- Moyo, M., Okonkwo, J.O., Agyei, N.M., 2013. A novel hydrogen peroxide biosensor based on adsorption of horseradish peroxidase onto a nanobiomaterial composite modified glassy carbon electrode. *Electroanalysis* 25, 1946–1954. <https://doi.org/10.1002/elan.201300165>
- Mukhopadhyay, S.K., 2009. Manufacturing, properties and tensile failure of nylon fibres. *Handb. Tensile Prop. Text. Tech. Fibres* 197–222. <https://doi.org/10.1533/9781845696801.2.197>
- Murawski, C., Gather, M.C., 2021. Emerging Biomedical Applications of Organic Light-Emitting Diodes. *Adv. Opt. Mater.* <https://doi.org/10.1002/adom.202100269>
- Murphy, M., Theyagarajan, K., Thenmozhi, K., Senthilkumar, S., 2020. Quaternary Ammonium Based Carboxyl Functionalized Ionic Liquid for Covalent Immobilization of Horseradish Peroxidase and Development of Electrochemical Hydrogen Peroxide Biosensor. *Electroanalysis* 32, 2422–2430. <https://doi.org/10.1002/elan.202060240>
- Musa, A.M., Kiely, J., Luxton, R., Honeychurch, K.C., 2021. Recent progress in screen-printed electrochemical sensors and biosensors for the detection of estrogens. *TrAC - Trends Anal. Chem.* 139, 116254. <https://doi.org/10.1016/j.trac.2021.116254>
- Nantaphol, S., Chailapakul, O., Siangproh, W., 2015. Sensitive and selective electrochemical sensor using silver nanoparticles modified glassy carbon electrode for determination of cholesterol in bovine serum. *Sensors Actuators, B Chem.* 207, 193–198. <https://doi.org/10.1016/j.snb.2014.10.041>
- Nash, D.G., Leith, D., 2010. Use of passive diffusion tubes to monitor air pollutants. *J. Air Waste Manag. Assoc.* 60, 204–209. <https://doi.org/10.3155/1047-3289.60.2.204>

References

- Nasirizadeh, N., Shekari, Z., Nazari, A., 2015. Fabrication of a novel electrochemical sensor for determination of hydrogen peroxide in different fruit juice samples. *J. Food Drug Anal.* 24, 72–82. <https://doi.org/10.1016/j.jfda.2015.06.006>
- Navas A., Ramos M. C., Torrijas M.C., 1998. Sol-gel horseradish peroxidase biosensor for hydrogen peroxide detection by chemiluminescence. *Anal. Chim. Acta* 363, 221–227.
- Nazri, N.A.A., Azeman, N.H., Luo, Y., A Bakar, A.A., 2021. Carbon quantum dots for optical sensor applications: A review. *Opt. Laser Technol.* 139, 106928. <https://doi.org/10.1016/j.optlastec.2021.106928>
- Nguyen, H.Q., Ta, B.Q., Hoivik, N., Halvorsen, E., Aasmundtveit, K.E., 2013. Carbon nanotube based gas sensor for expiration detection of perishable food. *Proc. IEEE Conf. Nanotechnol.* 675–678. <https://doi.org/10.1109/NANO.2013.6721008>
- Nunes, P., Magalhães, A.M., 2016. Preparation and characterization of an eco-friendly polymer electrolyte membrane (PEM) Based in a Blend of Sulphonated Poly(Vinyl Alcohol)/Chitosan Mechanically Stabilised by Nylon 6,6. *Mater. Res.* 19, 954–962. <https://doi.org/10.1590/1980-5373-MR-2016-0387>
- Omar, M.H., Razak, K.A., Ab Wahab, M.N., Hamzah, H.H., 2021. Recent progress of conductive 3D-printed electrodes based upon polymers/carbon nanomaterials using a fused deposition modelling (FDM) method as emerging electrochemical sensing devices. *RSC Adv.* 11, 16557–16571. <https://doi.org/10.1039/d1ra01987b>
- Omran, O.A., Elgendy, F.A., Nafady, A., 2016. Fabrication and applications of potentiometric sensors based on p-tert-butylthiacalix[4]arene comprising two triazole rings ionophore for silver ion detection. *Int. J. Electrochem. Sci.* 11, 4729–4742. <https://doi.org/10.20964/2016.06.35>
- Oncescu, V., O'Dell, D., Erickson, D., 2013. Smartphone based health accessory for colorimetric detection of biomarkers in sweat and saliva. *Lab Chip* 13, 3232–3238. <https://doi.org/10.1039/c3lc50431j>
- Ong, J.J., Pollard, T.D., Goyanes, A., Gaisford, S., Elbadawi, M., Basit, A.W.,

References

2021. Optical biosensors - Illuminating the path to personalized drug dosing. *Biosens. Bioelectron.* 188, 113331. <https://doi.org/10.1016/j.bios.2021.113331>
- Owens, G.J., Singh, R.K., Foroutan, F., Alqaysi, M., Han, C.M., Mahapatra, C., Kim, H.W., Knowles, J.C., 2016. Sol-gel based materials for biomedical applications. *Prog. Mater. Sci.* 77, 1–79. <https://doi.org/10.1016/j.pmatsci.2015.12.001>
- Paerl, H.W., Piehler, M.F., 2008. Nitrogen and Marine Eutrophication, Nitrogen in the Marine Environment. <https://doi.org/10.1016/B978-0-12-372522-6.00011-6>
- Paliwal, R., Palakurthi, S., 2014. Zein in controlled drug delivery and tissue engineering. *J. Control. Release* 189, 108–122. <https://doi.org/10.1016/j.jconrel.2014.06.036>
- Pan, M., Yin, Z., Liu, K., Du, X., Liu, H., Wang, S., 2019. Carbon-based nanomaterials in sensors for food safety. *Nanomaterials* 9, 1–23. <https://doi.org/10.3390/nano9091330>
- Pandey, S.P., Shukla, T., Dhote, V.K., Mishra, D.K., Maheshwari, R., Tekade, R.K., 2018. Use of polymers in controlled release of active agents, *Basic Fundamentals of Drug Delivery*. Elsevier Inc. <https://doi.org/10.1016/B978-0-12-817909-3.00004-2>
- Pang, F., Han, X., Chu, F., Geng, J., Cai, H., Qu, R., Fang, Z., 2007. Sensitivity to alcohols of a planar waveguide ring resonator fabricated by a sol-gel method. *Sensors Actuators, B Chem.* 120, 610–614. <https://doi.org/10.1016/j.snb.2006.03.031>
- Pauliukaite, R., Ghica, M.E., Barsan, M.M., Brett, C.M.A., 2010. Phenazines and polyphenazines in electrochemical sensors and biosensors. *Anal. Lett.* 43, 1588–1608. <https://doi.org/10.1080/00032711003653791>
- Pena-Pereira, F., Bendicho, C., Pavlović, D.M., Martín-Esteban, A., Díaz-Álvarez, M., Pan, Y., Cooper, J., Yang, Z., Safarik, I., Pospiskova, K., Segundo, M.A., Psillakis, E., 2021. Miniaturized analytical methods for determination of environmental contaminants of emerging concern – A review. *Anal. Chim. Acta* 1158.

References

<https://doi.org/10.1016/j.aca.2020.11.040>

- Phanthong, P., Reubroycharoen, P., Hao, X., Xu, G., Abudula, A., Guan, G., 2018. Nanocellulose: Extraction and application. *Carbon Resour. Convers.* 1, 32–43. <https://doi.org/10.1016/j.crcon.2018.05.004>
- Pla-Tolós, J., Moliner-Martinez, Y., Molins-Legua, C., Campins-Falcó, P., 2016. Colorimetric biosensing dispositive based on reagentless hybrid biocomposite: Application to hydrogen peroxide determination. *Sensors Actuators, B Chem.* 231, 837–846. <https://doi.org/10.1016/j.snb.2016.03.094>
- Pla-Tolós, J., Moliner-Martínez, Y., Molins-Legua, C., Campíns-Falcó, P., 2018. Solid glucose biosensor integrated in a multi-well microplate coupled to a camera-based detector: Application to the multiple analysis of human serum samples. *Sensors Actuators, B Chem.* 258, 331–341. <https://doi.org/10.1016/j.snb.2017.11.069>
- Pla-Tolós, J., Moliner-Martínez, Y., Molins-Legua, C., Herráez-Hernández, R., Verdú-Andrés, J., Campíns-Falcó, P., 2015. Selective and sensitive method based on capillary liquid chromatography with in-tube solid phase microextraction for determination of monochloramine in water. *J. Chromatogr. A* 1388, 17–23. <https://doi.org/10.1016/j.chroma.2015.02.024>
- Popa, CV., Vasilescu, A., Litescu, SC., Albu, C., Danet, AF., 2020. Metal Nano-Oxide based Colorimetric Sensor Array for the Determination of Plant Polyphenols with Antioxidant Properties. *Anal. Lett.*, 53 (4), 627–645. <https://doi.org/10.1080/00032719.2019.1662430>
- Postu, P.A., Ion, L., Drochioiu, G., Petre, B.A., Glocker, M.O., 2019. Mass spectrometric characterization of the zein protein composition in maize flour extracts upon protein separation by SDS-PAGE and 2D gel electrophoresis. *Electrophoresis* 40, 2747–2758. <https://doi.org/10.1002/elps.201900108>
- Pourbeyram, S., Soltanpour, M., Fathalipour, S., 2019. Determination of phosphate in human serum with zirconium/ reduced graphene oxide modified electrode. *Anal. Sci.* 35, 739–743.

References

<https://doi.org/10.2116/analsci.18P548>

- Pramanik, C., Gissinger, J.R., Kumar, S., Heinz, H., 2017. Carbon Nanotube Dispersion in Solvents and Polymer Solutions: Mechanisms, Assembly, and Preferences. *ACS Nano* 11, 12805–12816. <https://doi.org/10.1021/acsnano.7b07684>
- Prieto-Blanco, M.C., Ballester-Caudet, A., Souto-Varela, F.J., López-Mahía, P., Campíns-Falcó, P., 2020. Rapid evaluation of ammonium in different rain events minimizing needed volume by a cost-effective and sustainable PDMS supported solid sensor. *Environ. Pollut.* 265. <https://doi.org/10.1016/j.envpol.2020.114911>
- Prieto-Blanco, M.C., Jornet-Martínez, N., Moliner-Martínez, Y., Molins-Legua, C., Herráez-Hernández, R., Verdú Andrés, J., Campíns-Falcó, P., 2015. Development of a polydimethylsiloxane-thymol/nitroprusside composite based sensor involving thymol derivatization for ammonium monitoring in water samples. *Sci. Total Environ.* 503–504, 105–112. <https://doi.org/10.1016/j.scitotenv.2014.07.077>
- Prieto-Blanco, M.C., Jornet-Martinez, N., Verdú-Andrés, J., Molíns-Legua, C., Campíns-Falcó, P., 2019. Quantifying both ammonium and proline in wines and beer by using a PDMS composite for sensing. *Talanta* 198, 371–376. <https://doi.org/10.1016/j.talanta.2019.02.001>
- Qian, P., Qin, Y., Lyu, Y., Li, Y., Wang, L., Wang, S., Liu, Y., 2019. A hierarchical cobalt/carbon nanotube hybrid nanocomplex-based ratiometric fluorescent nanosensor for ultrasensitive detection of hydrogen peroxide and glucose in human serum. *Anal. Bioanal. Chem.* 411, 1517–1524. <https://doi.org/10.1007/s00216-019-01573-z>
- Qin, W., Zhang, Z., Li, B., Peng, Y., 1999. Chemiluminescence flow system for the determination of ammonium ion. *Talanta* 48, 225–229. [https://doi.org/10.1016/S0039-9140\(98\)00246-X](https://doi.org/10.1016/S0039-9140(98)00246-X)
- Quality, D., 1996. Silver in Drinking-water Background document for development of 2.
- Raghavan, V.S., O’Driscoll, B., Bloor, J.M., Li, B., Katare, P., Sethi, J., Gorthi, S.S., Jenkins, D., 2021. Emerging graphene-based sensors for

References

- the detection of food adulterants and toxicants – A review. *Food Chem.* 355. <https://doi.org/10.1016/j.foodchem.2021.129547>
- Ramu, B.K., Raghubabu, K., Syambabu, M., 2011. Development of a Spectrophotometric Method Based on Ferric Hydroxamate Reaction for Determination of Ramipril in Formulations 1, 152–159.
- Rao, A. V., Kalesh, R.R., Pajonk, G.M., 2003. Hydrophobicity and physical properties of TEOS based silica aerogels using phenyltriethoxysilane as a synthesis component. *J. Mater. Sci.* 38, 4407–4413. <https://doi.org/10.1023/A:1026311905523>
- Rayappa, M.K., Viswanathan, P.A., Rattu, G., Krishna, P.M., 2021. Nanomaterials Enabled and Bio/Chemical Analytical Sensors for Acrylamide Detection in Thermally Processed Foods: Advances and Outlook. *J. Agric. Food Chem.* <https://doi.org/10.1021/acs.jafc.0c07956>
- Reda, A., El-Safty, S.A., Selim, M.M., Shenashen, M.A., 2021. Optical glucose biosensor built-in disposable strips and wearable electronic devices. *Biosens. Bioelectron.* 185, 113237. <https://doi.org/10.1016/j.bios.2021.113237>
- Ren, Q.Q., Wu, J., Zhang, W.C., Wang, C., Qin, X., Liu, G.C., Li, Z.X., Yu, Y., 2017. Real-time in vitro detection of cellular H₂O₂ under camptothecin stress using horseradish peroxidase, ionic liquid, and carbon nanotube-modified carbon fiber ultramicroelectrode. *Sensors Actuators, B Chem.* 245, 615–621. <https://doi.org/10.1016/j.snb.2017.02.001>
- Reshmy, R., Eapen, P., Aravind, M., Raveendran, S., Arivalagan, P., Parameswaran, B., Ranjna, S., Mukesh Kumar, A., Ayon, T., Ashok, P., 2021. Advanced biomaterials for sustainable applications in the food industry: Updates and challenges. *Environ. Pollut.* 283, 117071. <https://doi.org/10.1016/j.envpol.2021.117071>
- Review, A., 2021. Application of Electrospun Nanofibers for Fabrication of Versatile and Highly Efficient Electrochemical Devices :
- Rocha, R.G., Ribeiro, J.S., Santana, M.H.P., Richter, E.M., Muñoz, R.A.A., 2021. 3D-printing for forensic chemistry: Voltammetric determination

References

- of cocaine on additively manufactured graphene-poly(lactic acid) electrodes. *Anal. Methods* 13, 1788–1794. <https://doi.org/10.1039/d1ay00181g>
- Roda, A., Michelini, E., Zangheri, M., Di Fusco, M., Calabria, D., Simoni, P., 2016. Smartphone-based biosensors: A critical review and perspectives. *TrAC - Trends Anal. Chem.* 79, 317–325. <https://doi.org/10.1016/j.trac.2015.10.019>
- Rodrigues, C., Souza, V.G.L., Coelho, I., Fernando, A.L., 2021. Bio-based sensors for smart food packaging—current applications and future trends. *Sensors* 21, 1–24. <https://doi.org/10.3390/s21062148>
- Roger, T., Bhakoo, M., Zhang, Z., 2008. Bacterial adhesion and biofilms on surfaces 18, 1049–1056. <https://doi.org/10.1016/j.pnsc.2008.04.001>
- Romanholo, P.V.V., Razzino, C.A., Raymundo-Pereira, P.A., Prado, T.M., Machado, S.A.S., Sgobbi, L.F., 2021. Biomimetic electrochemical sensors: New horizons and challenges in biosensing applications. *Biosens. Bioelectron.* 185, 113242. <https://doi.org/10.1016/j.bios.2021.113242>
- Rouf, T.B., Díaz-Amaya, S., Stanciu, L., Kokini, J., 2020. Application of corn zein as an anchoring molecule in a carbon nanotube enhanced electrochemical sensor for the detection of gliadin. *Food Control* 117, 107350. <https://doi.org/10.1016/j.foodcont.2020.107350>
- Ruff, A., Pinyou, P., Nolten, M., Conzuelo, F., Schuhmann, W., 2017. A Self-Powered Ethanol Biosensor. *ChemElectroChem* 4, 890–897. <https://doi.org/10.1002/celec.201600864>
- Ruff, A., Szczesny, J., Marković, N., Conzuelo, F., Zacarias, S., Pereira, I.A.C., Lubitz, W., Schuhmann, W., 2018. A fully protected hydrogenase/polymer-based bioanode for high-performance hydrogen/glucose biofuel cells. *Nat. Commun.* 9. <https://doi.org/10.1038/s41467-018-06106-3>
- Ryu, H., Li, B., De Guise, S., McCutcheon, J., Lei, Y., 2021. Recent progress in the detection of emerging contaminants PFASs. *J. Hazard. Mater.* 408, 124437. <https://doi.org/10.1016/j.jhazmat.2020.124437>

References

- S, Barizuddin, S, Bok, 2016. Plasmonic Sensors for Disease Detection - A Review. *J. Nanomed. Nanotechnol.* 7. <https://doi.org/10.4172/2157-7439.1000373>
- Sadighbayan, D., Ghafar-Zadeh, E., 2021. Portable Sensing Devices for Detection of COVID-19: A Review. *IEEE Sens. J.* 21, 10219–10230. <https://doi.org/10.1109/JSEN.2021.3059970>
- Safavi, A., Ahmadi, R., Mohammadpour, Z., 2017. Colorimetric sensing of silver ion based on anti aggregation of gold nanoparticles. *Sensors Actuators, B Chem.* 242, 609–615. <https://doi.org/10.1016/j.snb.2016.11.043>
- Sánchez-Pomales, G., Mudalige, T.K., Lim, J.H., Linder, S.W., 2013. Rapid determination of silver in nanobased liquid dietary supplements using a portable X-ray fluorescence analyzer. *J. Agric. Food Chem.* 61, 7250–7257. <https://doi.org/10.1021/jf402018t>
- Sardaremelli, S., Hasanzadeh, M., Razmi, H., 2021. Chemical binding of horseradish peroxidase enzyme with poly beta-cyclodextrin and its application as molecularly imprinted polymer for the monitoring of H₂O₂ in human plasma samples. *J. Mol. Recognit.* <https://doi.org/10.1002/jmr.2884>
- Sassolas, A., Blum, L.J., Leca-Bouvier, B.D., 2012. Immobilization strategies to develop enzymatic biosensors. *Biotechnol. Adv.* 30, 489–511. <https://doi.org/10.1016/j.biotechadv.2011.09.003>
- Saxena, S., Srivastava, A.K., 2020. Carbon nanotube-based sensors and their application, *Nano-Optics*. Elsevier Inc. <https://doi.org/10.1016/b978-0-12-818392-2.00010-x>
- Schindler, D.W., Dillon, P.J., Schreier, H., 2006. A review of anthropogenic sources of nitrogen and their effects on Canadian aquatic ecosystems 25–44. <https://doi.org/10.1007/s10533-006-9001-2>
- Schwenke, K.U., Spiehl, D., Krauß, M., Riedler, L., Ruppenthal, A., Villforth, K., Meckel, T., Biesalski, M., Rupprecht, D., Schwall, G., 2019. Analysis of free chlorine in aqueous solution at very low concentration with lateral flow tests. *Sci. Rep.* 9, 1–11.

References

<https://doi.org/10.1038/s41598-019-53687-0>

- Sekhar, P.K., Brosha, E.L., Mukundan, R., Garzon, F.H., 2010. Chemical sensors for environmental monitoring and homeland security. *Electrochem. Soc. Interface* 19, 35–40. <https://doi.org/10.1149/2.F04104if>
- Serra-Mora, P., Jornet-Martinez, N., Moliner-Martinez, Y., Campíns-Falcó, P., 2017. In tube-solid phase microextraction-nano liquid chromatography: Application to the determination of intact and degraded polar triazines in waters and recovered struvite. *J. Chromatogr. A* 1513, 51–58. <https://doi.org/10.1016/j.chroma.2017.07.053>
- Serra-Mora, P., Rodríguez-Palma, C., Verdú-Andrés, J., Herráez-Hernández, R., Campíns-Falcó, P., 2018a. Improving the On-Line Extraction of Polar Compounds by IT-SPME with Silica Nanoparticles Modified Phases. *Separations* 5, 10. <https://doi.org/10.3390/separations5010010>
- Serra-Mora, P., Rodríguez-Palma, C.E., Verdú-Andrés, J., Herráez-Hernández, R., Campíns-Falcó, P., 2018b. Improving the on-line extraction of polar compounds by IT-SPME with silica nanoparticles modified phases. *Separations* 5. <https://doi.org/10.3390/separations5010010>
- Shahamirifard, S.A., Ghaedi, M., Hajati, S., 2018. A new silver (I) ions optical sensor based on nanoporous thin films of sol-gel by rose bengal dye. *Sensors Actuators, B Chem.* 259, 20–29. <https://doi.org/10.1016/j.snb.2017.12.030>
- Sharma, P., Kannoujia, D.K., Basir, S.F., Nahar, P., 2011. Rapid immobilization of enzymes onto solid supports by ultrasound waves. *Artif. Cells, Blood Substitutes, Biotechnol.* 39, 289–292. <https://doi.org/10.3109/10731199.2011.563361>
- Sheikhzadeh, E., Beni, V., Zourob, M., 2021. Nanomaterial application in bio/sensors for the detection of infectious diseases. *Talanta* 230, 122026. <https://doi.org/10.1016/j.talanta.2020.122026>
- Sheng, G.D., Shao, D.D., Ren, X.M., Wang, X.Q., Li, J.X., Chen, Y.X., Wang, X.K., 2010. Kinetics and thermodynamics of adsorption of

References

- ionizable aromatic compounds from aqueous solutions by as-prepared and oxidized multiwalled carbon nanotubes. *J. Hazard. Mater.* 178, 505–516. <https://doi.org/10.1016/j.jhazmat.2010.01.110>
- Shin, J.H., Lee, M.J., Choi, J.H., Song, J. ae, Kim, T.H., Oh, B.K., 2020. Electrochemical H₂O₂ biosensor based on horseradish peroxidase encapsulated protein nanoparticles with reduced graphene oxide-modified gold electrode. *Nano Converg.* 7. <https://doi.org/10.1186/s40580-020-00249-0>
- Shooshtari, M., Salehi, A., Vollebregt, S., 2021. Effect of Humidity on Gas Sensing Performance of Carbon Nanotube Gas Sensors Operated at Room Temperature. *IEEE Sens. J.* 21, 5763–5770. <https://doi.org/10.1109/JSEN.2020.3038647>
- Shu, T., Gao, B., Yang, H., Su, L., Zhang, X., 2016. Horseradish Peroxidase-modified Single-walled Carbon Nanotubes as Biocathode for Assembling a Membrane-less Glucose-H₂O₂ Biofuel Cell. *Curr. Nanosci.* 12, 405–410. <https://doi.org/10.2174/1573413712666151120220428>
- Shufang, J., Ying, C., Min, L., 2013. Nanocellulose applications in environmental protection. *Adv. Mater. Res.* 662, 198–201. <https://doi.org/10.4028/www.scientific.net/AMR.662.198>
- Shukla, R., Cheryan, M., 2001. Zein: The industrial protein from corn. *Ind. Crops Prod.* [https://doi.org/10.1016/S0926-6690\(00\)00064-9](https://doi.org/10.1016/S0926-6690(00)00064-9)
- Silveira, G. de O., Belitsky, Í.T., Loddi, S., Rodrigues de Oliveira, C.D., Zucoloto, A.D., Fruchtengarten, L.V.G., Yonamine, M., 2016. Development of a method for the determination of cocaine, cocaethylene and norcocaine in human breast milk using liquid phase microextraction and gas chromatography-mass spectrometry. *Forensic Sci. Int.* 265, 22–28. <https://doi.org/10.1016/j.forsciint.2016.01.007>
- Silver ; CASRN 7440-22-4, 1987. 1–13.
- Silwana, B., Horst, C. Van Der, Iwuoha, E., 2017. Evaluation of a reduced graphene oxide antimony nanocomposite horseradish peroxidase biosensor matrix for hydrogen peroxide. *Procedia Technol.* 27, 172–176.

References

<https://doi.org/10.1016/j.protcy.2017.04.075>

- Simsek, M., Wongkaew, N., 2021. Carbon nanomaterial hybrids via laser writing for high-performance non-enzymatic electrochemical sensors: a critical review. *Anal. Bioanal. Chem.* <https://doi.org/10.1007/s00216-021-03382-9>
- Singh, D., Dahiya, M., Kumar, R., Nanda, C., 2021. Sensors and systems for air quality assessment monitoring and management: A review. *J. Environ. Manage.* 289, 112510. <https://doi.org/10.1016/j.jenvman.2021.112510>
- Singh, P., Hirsch, A., Kumar, S., 2021. Perylene diimide-based chemosensors emerging in recent years: From design to sensing. *TrAC - Trends Anal. Chem.* 138, 116237. <https://doi.org/10.1016/j.trac.2021.116237>
- Skočaj, M., 2019. Bacterial nanocellulose in papermaking. *Cellulose* 26, 6477–6488. <https://doi.org/10.1007/s10570-019-02566-y>
- Skorjanc, T., Shetty, D., Valant, M., 2021. Covalent Organic Polymers and Frameworks for Fluorescence-Based Sensors. *ACS Sensors.* <https://doi.org/10.1021/acssensors.1c00183>
- Song, Y., Bian, C., Tong, J., Li, Y., Xia, S., 2015. Selective electrochemical sensor for phosphate determination toward a silicate interference free method in freshwater. 2015 IEEE SENSORS - Proc. 2–5. <https://doi.org/10.1109/ICSENS.2015.7370477>
- Sorribes-Soriano, A., Herrero-Martínez, J.M., Esteve-Turrillas, F.A., Armenta, S., 2020. Molecularly imprinted polymer-based device for field collection of oral fluid samples for cocaine identification. *J. Chromatogr. A* 1633, 461629. <https://doi.org/10.1016/j.chroma.2020.461629>
- Šraj, L.O.C., Almeida, M.I.G.S., Swearer, S.E., Kolev, S.D., McKelvie, I.D., 2014. Analytical challenges and advantages of using flow-based methodologies for ammonia determination in estuarine and marine waters. *TrAC - Trends Anal. Chem.* 59, 83–92. <https://doi.org/10.1016/j.trac.2014.03.012>

References

- Stanisławska, A., 2016. Bacterial nanocellulose as a microbiological derived nanomaterial. *Adv. Mater. Sci.* 16, 45–57. <https://doi.org/10.1515/adms>
- Study of the Silver-catalysed Pyrogallol Red - Peroxodisulphate Reaction with 1,10-Phenanthroline as Activator, 1986. 111, 1417–1422.
- Subramanian, S., Sampath, S., 2007. Adsorption of zein on surfaces with controlled wettability and thermal stability of adsorbed zein films. *Biomacromolecules* 8, 2120–2128. <https://doi.org/10.1021/bm0701999>
- Suganya, P., Vaseeharan, B., Vijayakumar, S., Balan, B., Govindarajan, M., Alharbi, N.S., Kadaikunnan, S., Khaled, J.M., Benelli, G., 2017. Biopolymer zein-coated gold nanoparticles: Synthesis, antibacterial potential, toxicity and histopathological effects against the Zika virus vector *Aedes aegypti*. *J. Photochem. Photobiol. B Biol.* 173, 404–411. <https://doi.org/10.1016/j.jphotobiol.2017.06.004>
- Sui, G., Wang, J., Lee, C., Lu, W., Lee, S.P., Leyton, J. V, Wu, A.M., Tseng, H., 2006. Solution-Phase Surface Modification in Intact Poly (dimethylsiloxane) Microfluidic Channels. *Anal. Chem.* 78, 5543–5551. <https://doi.org/10.1021/ac060605z>
- Sun, G., Liu, S., Hua, K., Lv, X., Huang, L., Wang, Y., 2007. Electrochemical chlorine sensor with multi-walled carbon nanotubes as electrocatalysts. *Electrochem. commun.* 9, 2436–2440. <https://doi.org/10.1016/j.elecom.2007.07.015>
- Syakinah, N., Halim, A., Dzul, M., Wirzal, H., Bilad, M.R., Abdul, N., Nordin, H., Putra, Z.A., Sambudi, N.S., 2019. Improving performance of electrospun Nylon 6,6 nanofiber membrane for produced water filtration via solvent vapor treatment. *Polymers (Basel)*. 11.
- Tachibana, K., Urano, Y., Numata, K., 2013. Biodegradability of nylon 4 film in a marine environment. *Polym. Degrad. Stab.* 98, 1847–1851. <https://doi.org/10.1016/j.polymdegradstab.2013.05.007>
- Talarico, D., Arduini, F., Amine, A., Moscone, D., Palleschi, G., 2015. Screen-printed electrode modified with carbon black nanoparticles for phosphate detection by measuring the electroactive phosphomolybdate complex. *Talanta*. <https://doi.org/10.1016/j.talanta.2015.04.006>

References

- Tapia, M.A., Gusmão, R., Serrano, N., Sofer, Z., Ariño, C., Díaz-Cruz, J.M., Esteban, M., 2021. Phosphorene and other layered pnictogens as a new source of 2D materials for electrochemical sensors. *TrAC - Trends Anal. Chem.* 139. <https://doi.org/10.1016/j.trac.2021.116249>
- Thongsai, N., Supchoksoonthorn, P., Dwyer, J.H., Wei, W., Sun, J., Gopalan, P., Paoprasert, P., 2020. High-capacity adsorbent/sensor from nylon 6 derived carbon dots on SiO₂ substrate via one-step surface grafting. *Mater. Sci. Eng. B Solid-State Mater. Adv. Technol.* 262, 114692. <https://doi.org/10.1016/j.mseb.2020.114692>
- Tian, J., Xu, J., Zhu, F., Lu, T., Su, C., Ouyang, G., 2013. Application of nanomaterials in sample preparation. *J. Chromatogr. A* 1300, 2–16. <https://doi.org/10.1016/j.chroma.2013.04.010>
- Tominaga, M., Kuwahara, K., Tsushida, M., Shida, K., 2020. Cellulose nanofiber-based electrode as a component of an enzyme-catalyzed biofuel cell. *RSC Adv.* 10, 22120–22125. <https://doi.org/10.1039/d0ra03476b>
- Tong, Y., Jiao, X., Yang, H., Wen, Y., Su, L., Zhang, X., 2016. Reverse-bumpy-ball-type-nanoreactor-loaded nylon membranes as peroxidase-mimic membrane reactors for a colorimetric assay for H₂O₂. *Sensors (Switzerland)* 16. <https://doi.org/10.3390/s16040465>
- Torres-Giner, S., Gimenez, E., Lagaron, J.M., 2008. Characterization of the morphology and thermal properties of Zein Prolamine nanostructures obtained by electrospinning. *Food Hydrocoll.* 22, 601–614. <https://doi.org/10.1016/j.foodhyd.2007.02.005>
- Torres-rivero, K., Florido, A., Bastos-arrieta, J., 2021. Recent trends in the improvement of the electrochemical response of screen-printed electrodes by their modification with shaped metal nanoparticles. *Sensors* 21. <https://doi.org/10.3390/s21082596>
- Trantidou, T., Elani, Y., Parsons, E., Ces, O., 2017. Hydrophilic surface modification of pdms for droplet microfluidics using a simple, quick, and robust method via pva deposition. *Microsystems Nanoeng.* 3. <https://doi.org/10.1038/micronano.2016.91>

References

- Tseng, S.Y., Li, S.Y., Yi, S.Y., Sun, A.Y., Gao, D.Y., Wan, D., 2017. Food Quality Monitor: Paper-Based Plasmonic Sensors Prepared Through Reversal Nanoimprinting for Rapid Detection of Biogenic Amine Odorants. *ACS Appl. Mater. Interfaces* 9, 17306–17316. <https://doi.org/10.1021/acsami.7b00115>
- Udvardi, M., Brodie, E.L., Kaeppler, S., 2015. Impacts of agricultural nitrogen on the environment and strategies to reduce these impacts. *Procedia Environ. Sci.* 29, 303. <https://doi.org/10.1016/j.proenv.2015.07.275>
- Upadhyay, L.S.B., Verma, N., 2015. Alkaline phosphatase inhibition based conductometric biosensor for phosphate estimation in biological fluids. *Biosens. Bioelectron.* 68, 611–616. <https://doi.org/10.1016/j.bios.2015.01.064>
- Uzunçar, S., Meng, L., Turner, A.P.F., Mak, W.C., 2021. Processable and nanofibrous polyaniline:polystyrene-sulphonate (nano-PANI:PSS) for the fabrication of catalyst-free ammonium sensors and enzyme-coupled urea biosensors. *Biosens. Bioelectron.* 171, 112725. <https://doi.org/10.1016/j.bios.2020.112725>
- Valero, E., Hancock, J., Killard, A.J., 2013. Electrochemical detection of extracellular hydrogen peroxide in *Arabidopsis thaliana*: a real-time marker of oxidative stress. *Plant, Cell Environ.* 36, 869–878. <https://doi.org/10.1111/pce.12023>
- Valles, M., Kamaruddin, A.F., Wong, L.S., Blanford, C.F., 2020. Inhibition in multicopper oxidases: A critical review. *Catal. Sci. Technol.* 10, 5386–5410. <https://doi.org/10.1039/d0cy00724b>
- Vanova, V., Mitrevska, K., Milosavljevic, V., Hynek, D., Richtera, L., Adam, V., 2021. Peptide-based electrochemical biosensors utilized for protein detection. *Biosens. Bioelectron.* 180, 113087. <https://doi.org/10.1016/j.bios.2021.113087>
- Vashist, S.K., van Oordt, T., Schneider, E.M., Zengerle, R., von Stetten, F., Luong, J.H.T., 2015. A smartphone-based colorimetric reader for bioanalytical applications using the screen-based bottom illumination

References

- provided by gadgets. *Biosens. Bioelectron.* 67, 248–255. <https://doi.org/10.1016/j.bios.2014.08.027>
- Vianello, F., Zennaro, L., Rigo, A., 2007. A coulometric biosensor to determine hydrogen peroxide using a monomolecular layer of horseradish peroxidase immobilized on a glass surface. *Biosens. Bioelectron.* 22, 2694–2699. <https://doi.org/10.1016/j.bios.2006.11.007>
- Victor, A., Ribeiro, J., F. Araújo, F., 2019. Study of PDMS characterization and its applications in biomedicine: A review. *J. Mech. Eng. Biomech.* 4, 1–9. <https://doi.org/10.24243/jmeb/4.1.163>
- Villemin, E., Raccurt, O., 2021. Optical lithium sensors. *Coord. Chem. Rev.* 435, 213801. <https://doi.org/10.1016/j.ccr.2021.213801>
- Vinothkumar, T.S., Kandaswamy, D., Arathi, G., Dinesh, K., 2011. Influence of different organic solvents on degree of swelling of poly (dimethyl siloxane)-based sealer. *J. Conserv. Dent.* 14, 156–159. <https://doi.org/10.4103/0972-0707.82621>
- Voisin, H., Bergström, L., Liu, P., Mathew, A.P., 2017. Nanocellulose-based materials for water purification. *Nanomaterials* 7. <https://doi.org/10.3390/nano7030057>
- Vráblová, M., Koutník, I., Smutná, K., Marková, D., Veverková, N., 2021. Combined spri sensor for simultaneous detection of nitrate and ammonium in wastewater. *Sensors (Switzerland)* 21, 1–12. <https://doi.org/10.3390/s21030725>
- Wagner, B.A., Witmer, J.R., Erve, T.J. Van, Buettner, G.R., 2013. Redox Biology An assay for the rate of removal of extracellular hydrogen peroxide by cells. *Redox Biol.* 1, 210–217. <https://doi.org/10.1016/j.redox.2013.01.011>
- Wang, D., Bierwagen, G.P., 2009. Sol-gel coatings on metals for corrosion protection. *Prog. Org. Coatings* 64, 327–338. <https://doi.org/10.1016/j.porgcoat.2008.08.010>
- Wang, T., Xu, Z., Huang, Y., Dai, Z., Wang, X., Lee, M., Bagtzoglou, C., Brückner, C., Lei, Y., Li, B., 2020. Real-time in situ auto-correction of

References

- K⁺ interference for continuous and long-term NH₄⁺ monitoring in wastewater using solid-state ion selective membrane (S-ISM) sensor assembly. *Environ. Res.* 189, 109891. <https://doi.org/10.1016/j.envres.2020.109891>
- Wang, W., Zhang, T.J., Zhang, D.W., Li, H.Y., Ma, Y.R., Qi, L.M., Zhou, Y.L., Zhang, X.X., 2011. Amperometric hydrogen peroxide biosensor based on the immobilization of heme proteins on gold nanoparticles-bacteria cellulose nanofibers nanocomposite. *Talanta* 84, 71–77. <https://doi.org/10.1016/j.talanta.2010.12.015>
- Wang, Y., Chen, G., Zhang, H., Zhao, C., Sun, L., Zhao, Y., 2021. Emerging Functional Biomaterials as Medical Patches. *ACS Nano* 15, 5977–6007. <https://doi.org/10.1021/acsnano.0c10724>
- Wang, Y., Yang, L., Liu, B., Yu, S., Jiang, C., 2018. A colorimetric paper sensor for visual detection of mercury ions constructed with dual-emission carbon dots. *New J. Chem.* 42, 15671–15677. <https://doi.org/10.1039/C8NJ03683G>
- Wang, Y., Li, Y.Y., Liu, Y., Han, J., Xia, J., Bao, X., Ni, L., Tang, X., 2016. A mobile laboratory for rapid on-site analysis of catechols from water samples with real-time results production. *RSC Adv.* 6(84), 80885–80895. <https://doi.org/10.1039/C6RA12052K>
- Wei, H., Hossein Abtahi, S.M., Vikesland, P.J., 2015. Plasmonic colorimetric and SERS sensors for environmental analysis. *Environ. Sci. Nano* 2, 120–135. <https://doi.org/10.1039/c4en00211c>
- Wei, K., Xiao, X., Xu, W., Han, Z., Wu, Y., 2021. Large programmable coefficient of thermal expansion in additively manufactured bi-material mechanical metamaterial. *Virtual Phys. Prototyp.* 0, 1–13. <https://doi.org/10.1080/17452759.2021.1917295>
- Whelan, É., Steuber, F.W., Gunnlaugsson, T., Schmitt, W., 2021. Tuning photoactive metal–organic frameworks for luminescence and photocatalytic applications. *Coord. Chem. Rev.* 437. <https://doi.org/10.1016/j.ccr.2020.213757>
- Wirojsaengthong, S., Aryuwananon, D., Aeungmaitrepirom, W., Pulpoka, B.,

References

- Tuntulani, T., 2021. A colorimetric paper-based optode sensor for highly sensitive and selective determination of thiocyanate in urine sample using cobalt porphyrin derivative. *Talanta* 231, 122371. <https://doi.org/10.1016/j.talanta.2021.122371>
- Woo, K.J., Hye, C.K., Ki, W.K., Shin, S., So, H.K., Yong, H.P., 2008. Antibacterial activity and mechanism of action of the silver ion in *Staphylococcus aureus* and *Escherichia coli*. *Appl. Environ. Microbiol.* 74, 2171–2178. <https://doi.org/10.1128/AEM.02001-07>
- Wu, J., Dong, M., Zhang, C., Wang, Y., Xie, M., Chen, Y., 2017. Magnetic lateral flow strip for the detection of cocaine in urine by naked eyes and smart phone camera. *Sensors (Switzerland)* 17. <https://doi.org/10.3390/s17061286>
- Wu, X., Ma, P., Sun, Y., Du, F., Song, D., Xu, G., 2021. Application of MXene in Electrochemical Sensors: A Review. *Electroanalysis* 1–26. <https://doi.org/10.1002/elan.202100192>
- Xia, Y., Larock, R.C., 2010. Vegetable oil-based polymeric materials: Synthesis, properties, and applications. *Green Chem.* 12, 1893–1909. <https://doi.org/10.1039/c0gc00264j>
- Xie, C., Lu, R., Huang, Y., Wang, Q., Xu, X., 2010. Effects of ions and phosphates on alkaline phosphatase activity in aerobic activated sludge system. *Bioresour. Technol.* 101, 3394–3399. <https://doi.org/10.1016/j.biortech.2009.12.047>
- Xu, B., Li, D., Li, W., Xia, S., Lin, Y., Hu, C., 2010. Measurements of dissolved organic nitrogen (DON) in water samples with nanofiltration pretreatment. *Water Res.* 44, 5376–5384. <https://doi.org/10.1016/j.watres.2010.06.034>
- Xu, S., Qin, X., Zhang, X., Zhang, C., 2015. A third-generation biosensor for hydrogen peroxide based on the immobilization of horseradish peroxidase on a disposable carbon nanotubes modified screen-printed electrode. *Microchim. Acta* 182, 1241–1246. <https://doi.org/10.1007/s00604-014-1444-x>
- Yamamoto, K., Shi, G., Zhou, T., Xu, F., Xu, J., Kato, T., Jin, J.Y., Jin, L.,

References

2003. Study of carbon nanotubes-HRP modified electrode and its application for novel on-line biosensors. *Analyst* 128, 249–254. <https://doi.org/10.1039/b209698f>
- Yang, F., Ma, K., Cao, Y., Ni, C., 2021. Improved liquid-liquid extraction by modified magnetic nanoparticles for the detection of eight drugs in human blood by HPLC-MS. *RSC Adv.* 11, 19874–19884. <https://doi.org/10.1039/d1ra01530c>
- Yang, X., Wu, X., Hao, H., He, Z., 2008. Mechanisms and assessment of water eutrophication * 9, 197–209. <https://doi.org/10.1631/jzus.B0710626>
- Yang, Y., Zhang, Y., Xie, S., Tang, Y., Zeng, Z., Tang, B.Z., 2021. Hydrogel-derived luminescent scaffolds for biomedical applications. *Mater. Chem. Front.* 5, 3524–3548. <https://doi.org/10.1039/d0qm01140a>
- Yu, H., Guo, W., Lu, X., Xu, H., Yang, Q., Tan, J., Zhang, W., 2021. Reduced graphene oxide nanocomposite based electrochemical biosensors for monitoring foodborne pathogenic bacteria: A review. *Food Control* 127, 108117. <https://doi.org/10.1016/j.foodcont.2021.108117>
- Yuan, L., Zhang, M., Zhao, T., Li, T., Zhang, H., Chen, L., Zhang, J., 2020. Flexible and breathable strain sensor with high performance based on MXene/nylon fabric network. *Sensors Actuators, A Phys.* 315, 112192. <https://doi.org/10.1016/j.sna.2020.112192>
- Yuen, J.D., Baingane, A., Hasan, Q., Shriver-Lake, L.C., Walper, S.A., Zabetakis, D., Breger, J.C., Stenger, D.A., Slaughter, G., 2019. A Fully-Flexible Solution-Processed Autonomous Glucose Indicator. *Sci. Rep.* 9, 1–9. <https://doi.org/10.1038/s41598-019-43425-x>
- Zamarayeva, A.M., Yamamoto, N.A.D., Toor, A., Payne, M.E., Woods, C., Pister, V.I., Khan, Y., Evans, J.W., Arias, A.C., 2020. Optimization of printed sensors to monitor sodium, ammonium, and lactate in sweat. *APL Mater.* 8. <https://doi.org/10.1063/5.0014836>
- Zepli, H., Cisneros, J.L.H. De, Naranjo-rodriguez, I., Temsamani, K.R., 2007. Stripping voltammetry of silver ions at polythiophene-modified platinum electrodes 71, 1594–1598.

References

<https://doi.org/10.1016/j.talanta.2006.07.052>

- Zhai, X., Li, Y., Li, J., Yue, C., Lei, X., 2017. Electrochemical sensor for detection of hydrogen peroxide modified with prussian blue electrodeposition on nitrogen, phosphorus and sulfur co-doped porous carbons-chitosan. *Mater. Sci. Eng. C* 77, 1242–1246. <https://doi.org/10.1016/j.msec.2016.11.106>
- Zhang, A., Miao, C., Shi, H., Xiang, H., Huang, C., Jia, N., 2016. A novel solid-state electrochemiluminescence sensor for atropine determination based on Ru(bpy)₃²⁺/carbon nanospheres/Nafion composite film. *Sensors Actuators, B Chem.* 222, 433–439. <https://doi.org/10.1016/j.snb.2015.08.075>
- Zhang, C., Gao, J., Hankett, J., Varanasi, P., Kerobo, C.O., Zhao, S., Chen, Z., 2021. Interfacial Structure and Interfacial Tension in Model Carbon Fiber-Reinforced Polymers. <https://doi.org/10.1021/acs.langmuir.1c00403>
- Zhang, C., Suslick, K.S., 2007. Colorimetric sensor array for soft drink analysis. *J. Agric. Food Chem.* 55, 237–242. <https://doi.org/10.1021/jf0624695>
- Zhang, Y., Lei, Y., Lu, H., Shi, L., Wang, P., Ali, Z., Li, J., 2021. Electrochemical detection of bisphenols in food: A review. *Food Chem.* 346, 128895. <https://doi.org/10.1016/j.foodchem.2020.128895>
- Zhang, Y., Li, Y., Wu, W., Jiang, Y., Hu, B., 2014. Chitosan coated on the layers' glucose oxidase immobilized on cysteamine/Au electrode for use as glucose biosensor. *Biosens. Bioelectron.* 60, 271–276. <https://doi.org/10.1016/j.bios.2014.04.035>
- Zhang, Z., Yang, B., 2017. Effect of deposition temperature on bimetallic PtCu membrane electrode catalytic activity toward hydrogen evolution reaction. *Compos. Part B Eng.* 121, 145–151. <https://doi.org/10.1016/j.compositesb.2017.03.035>
- Zhao, M., Yu, H., He, Y., 2019. A dynamic multichannel colorimetric sensor array for highly effective discrimination of ten explosives. *Sensors Actuators, B Chem.* 283, 329–333.

References

<https://doi.org/10.1016/j.snb.2018.12.061>

- Zhou, H., Song, Y., Yang, Z., 2019. A Reversible Spectrophotometric Method Based on a Coupled Microfluidic Chip for Highly Selective Ammonium Detection. *J. Chem.* 2019. <https://doi.org/10.1155/2019/3720308>
- Zhou, Q., Fang, J., Gao, H., Loo, L.S., 2013. Substrate effects on the surface properties of nylon 6. *Appl. Surf. Sci.* 282, 115–120. <https://doi.org/10.1016/j.apsusc.2013.05.075>
- Zhu, A., Chen, B., Zhang, L., 2015a. Improved Analysis of Dissolved Organic Nitrogen in Water via Electrodialysis Pretreatment. <https://doi.org/10.1021/ac504224r>
- Zhu, A., Chen, B., Zhang, L., Westerhoff, P., 2015b. Improved analysis of dissolved organic nitrogen in water via electrodialysis pretreatment. *Anal. Chem.* 87, 2353–2359. <https://doi.org/10.1021/ac504224r>
- Zhu, G., Lin, N., 2019. Nanocellulose: From Fundamentals to Advanced Materials, in: Wiley-VCH. pp. 115–153.
- Zhu, Y., Chen, L., Zhang, C., Guan, Z., 2018. Preparation of hydrophobic antireflective SiO₂ coating with deposition of PDMS from water-based SiO₂-PEG sol. *Appl. Surf. Sci.* 457, 522–528. <https://doi.org/10.1016/j.apsusc.2018.06.177>
- Zia, S., Afzali, D., Ali, M., Mohammad, Y., 2009. Talanta Ligandless dispersive liquid – liquid microextraction for the separation of trace amounts of silver ions in water samples and flame atomic absorption spectrometry determination 80, 875–879. <https://doi.org/10.1016/j.talanta.2009.08.009>
- Zong, C., Wang, M., Li, B., Liu, X., Zhao, W., Zhang, Q., 2017. Sensing of hydrogen peroxide and glucose in human serum via quenching fluorescence of biomolecule-stabilized Au nanoclusters assisted by the Fenton reaction. *RSC Adv.* 7, 26559–26565. <https://doi.org/10.1039/C7RA01498H>
- Zou, Y., Zhong, J., Pan, R., Wan, Z., Guo, J., Wang, J., Yin, S., Yang, X.,

References

2017. Zein/tannic acid complex nanoparticles-stabilised emulsion as a novel delivery system for controlled release of curcumin. *Int. J. Food Sci. Technol.* 52, 1221–1228. <https://doi.org/10.1111/ijfs.13380>

ANNEX

A.1. Abbreviations

Annex

1,10-phen	1,10-phenantroline
ACN	Acetonitrile
ALP	Alkaline phosphatase
APTMS	Amino propyl trimethoxy silane
ATR-FTIR	Attenuated total reflectance–Fourier transform infrared
BCN	Bacterial nanocellulose
Box	Bilirubin oxidase
CE	Counter electrode
CL	Chemiluminescence
CMYK	Cyan-magenta-yellow-black
CNS	Central nervous system
CNTs	Carbon nanotubes
DET	Direct electron transfer
DDGS	Distiller's dried grains with solubles
DI	Digital image
DIN	Dissolved inorganic nitrogen
DMEM-F12	Dulbecco's modified eagle medium F12
DMAc	Dimethylacetamide
DMF	Dimethylformamide
DMSO	Dimethyl sulfoxide
DON	Dissolved organic nitrogen
DR	Diffuse reflectance
EPA	Environmental Protection Agency
GC	Glassy carbon
GDH	Glucose deshydrogenase

Annex

GIMP	Digital image-processing tool
GOx	Glucose oxidase
GTA	Glutaraldehyde
H ₂ O ₂	Hydrogen peroxide
HRP	Horseradish peroxidase
HVS	Hue-saturation-value
IR	Infrared
IT-SPME	In-tube-solid-phase microextraction
LC	Liquid chromatography
LOD	Detection limit
LOQ	Quantification limit
MET	Mediated electron transfer
MTEOS	Methyltriethoxysilane
MWCNTs	Multi-walled carbon nanotubes
NMP	N-methyl pyrrolidinone
OMF	3-O-methylfluorescein
OMFP	3-O-methylfluorescein 6-phosphate
OCP	Open-circuit potential
PAN	Polyacrylonitrile
PEG	Polyethylene glycol
PGR	Pyrogallol red
PDMS	Polydimethylsiloxane
pyAA	Pyrene acetic acid
PyBA	Pyrene butyric acid
pyNHS ester	Pyrene N-hydroxysuccinimide ester

Annex

PMMA	Polymethylmethacrylate
RE	Reference electrode
RD	Reflectance diffuse
RSD	Relative standard deviation
RGB	Red-green-blue
PVA	Polyvinyl alcohol
SWCNTs	Single-walled carbon nanotubes
TDN	Total dissolved nitrogen
TEOS	Tetraethylortosilicate
TKN	Total Kjeldahl nitrogen
WE	Working electrode
WHO	World Health Organization

A.2. Figure list

Figure 1. Schematic representation of online, in-line and off-line analytical methods.	5
Figure 2. Number of citations on Web of Science for matching the following search term ‘in-situ analysis’ AND ‘sensor’ in the 2000-2021 period (September 2021).	9
Figure 3. Schematic of a colorimetric device.	14
Figure 4. Schematic of an electrochemical biosensor.	22
Figure 5. Number of citations on Web of Science for matching the following search term ‘zein’ in the 2010-2021 period (September 2021).	28
Figure 6. Number of record account on Web of Science for matching the following search term ‘Zein’ in the 2010-2021 period (September 2021). .	29
Figure 7. Number of record count on Web of Science for matching the following search term ‘Nylon’ in the 2010-2021 period (September 2021).	32
Figure 8. Number of record count on Web of Science for matching the following search term ‘PDMS’ in the 2010-2021 period (September 2021).	35
Figure 9. Number of record count on Web of Science for matching the following search term ‘TEOS’ or ‘MTEOS’ in the 2010-2021 period (September 2021).	39
Figure 10. Number of record count on Web of Science for matching the following search term ‘Bacterial nanocellulose’ in the 2010-2021 period (September 2021).	43
Figure 11. Number of record count on Web of Science for matching the following search term ‘CNT’ in the 2010-2021 period (September 2021)..	46
Figure 12. Structure of atropine, cocaine and ramipril.	54
Figure 13. Security pictograms which classify the different substances and chemical mixtures.	81
Figure 14. A) Cary 60 Fiber Optic UV-VIS spectrophotometer. B) Portable spectrophotometer Maya2000 Pro. C) Optical fiber accessory.	85
Figure 15. Remote fiber optic DR accessory.	86
Figure 16. Cary 630 FTIR-ATR spectrophotometer.	87
Figure 17. Spectrofluorometer Jasco FP 750.	87
Figure 18. Portable tube luminometer from Berthold Technologies.	88
Figure 19. A) Cary Eclipse Fluorescence Spectrophotometer. B) Microplate reader accessory.	88

Figure 20. Nikon microscope Eclipse E200LED MV Series.....	90
Figure 21. Different configurations tested: (Entrapped 1) ALP entrapped at the bottom, (Entrapped 2) ALP entrapped at the top, (Adsorbed 1) ALP adsorbed on the OMFP sensor, (Adsorbed 2) ALP adsorbed on the glycerol layer.....	91
Figure 22. Procedure of (A) iron/zein and (B) hydroxylammonium/zein sensors fabrication.....	93
Figure 23. Procedure of iron/PDMS sensors fabrication.	94
Figure 24. Preparation of the solid sensor containing both reagents, pyrogallol red and 1,10-phenantroline.	95
Figure 25. Procedure of TEOS/MTEOS/luminol sensors fabrication.	96
Figure 26. Scheme of the fluorimetric assay based on the inhibition of ALP in the presence of OMFP.....	103
Figure 27. Ester compounds reaction with hydroxylamine.....	105
Figure 28. Silver catalytic oxidation of PGR by persulphate ($S_2O_8^{2-}$) in the presence of 1,10-phenanthroline (Phen) as activator.	106
Figure 29. Procedure to obtain the colorimetric response of nylon sensor.	108
Figure 30. Oxidation of luminol by hydrogen peroxyde.....	109
Figure 31. Luminol oxidation reaction carried out by hypochlorite.	110
Figure 32. Processing in situ samples by the sensor.	115
Figure 33. Different configurations tested: (E1) ALP entrapped at the bottom, (E2) ALP entrapped at the top, (A1) ALP adsorbed on the OMFP sensor, and (A2) ALP adsorbed on the glycerol layer.	121
Figure 34. Optimization of the multi-well biosensor. Study of the release (in red) and inhibition by phosphate at 0.5 and 2.5 mg/L (in black and grey respectively) for different configuration of the sensor.....	122
Figure 35. Study of operational stability for the developed sensor by measuring the initial activity over time.....	127
Figure 36. Photography of the sensors after being cured for 1 day. A) iron-PDMS sensor, B) iron-zein sensor and C) hydroxyammonium-zein sensor.	131
Figure 37. (A) Spectra obtained for (1) 0.1Mpropyl acetate, (2) 0.1 M cocaine, (3) 0.3 M ramipril, and (4) 0.1 M atropine. (B) Photographs of the colors of the solution after the assay for the calibration curve: (1) propylacetate from 0 to 3.74 mM, (2) cocaine from 0 to 1.81 mM (3), ramipril	

from 0 to 11.19 mM, (4) and atropine from 0 to 3.67 mM. The heating temperature was 100 °C.	133
Figure 38. Ferric hydroxamate assay using paper for propyl acetate determination from 0 to 80 mM.	134
Figure 39. Influence of pH on the catalyzed reaction in solution. Conditions: PGR 5.4×10^{-5} M, Ag(I) 2×10^{-6} M, $K_2S_2O_8$ 17×10^{-3} M, Phen 6.8×10^{-3} M	138
Figure 40. A) Reagents (PGR and Phen) retained in a solid support a) PDMS, b) zein, c) nylon. B) Reagent supports in solution in presence of Ag^+ and persulfate in acid medium. C) Membrane after PGR oxidation reaction a) PDMS, b) zein, c) nylon.....	139
Figure 41. A) Optimization of the sensor development for 1,10-Phen concentration (0.095, 0.12, 0.15, 0.17 M) at 50 min. B) $K_2S_2O_8$ concentration (16.4, 19.7, 22.7 mM) at 50 min.	141
Figure 42. Optimization the reaction time (different Ag^+ standard concentrations 0.5, 1, and 5 μ M).....	142
Figure 43. A) Optical microscopic images $\times 10$ of nylon, nylon with the reagents (PGR, 1,10-Phen), and in presence of different Ag(I) concentrations. B) IR spectra	143
Figure 44. Sensor for the detection of Ag(I). Absorbance spectra obtained by diffuse reflectance for different concentrations of Ag ion (from top to bottom): 0, 1, 2.5, 5, 7.5, 10 μ M and change color sensor.	145
Figure 45. Sensor for the detection of Ag(I). A) Dependence of absorbance at 485 nm on the concentrations of Ag(I). B) Dependence of yellow and magenta color intensities on the concentrations of Ag(I). C) Calibration graphs for several incubation times.....	146
Figure 46. Schematic description of biofunctionalization of PDMS. Activation of PDMS surface (1), silanization using APTMS (2), activation with GTA (3) and linking of link of HRP by GTA (4).	155
Figure 47. Relative luminescence units recorded with a portable luminometer at 10 seconds by varying the concentration of enzyme dissolution used to immobilize it in the activated PDMS surface.	156
Figure 48. Calibration graphs used for estimating the active amount of HRP in the biosensor •2.50 μ M H_2O_2 and 17.5mM luminol. •50 μ M H_2O_2 and 17.5mM luminol.....	157

Figure 49. Optimization of the reaction conditions: (A) luminol concentration (0.017, 0.17, 1.7, and 17 mM) and (B) HRP concentration [0.36 (a), 0.6 (b), 1.22 (c), and 12.2 mg L ⁻¹ (d)] in solution by using a conventional spectrofluorometer. (C) Luminol concentration (2.5–25 mM at 10 s) and (D) time for different H ₂ O ₂ standard concentrations of 0.1, 0.5, 1, 2, and 10 μM and (D) by using the biosensor and a portable luminometer.	158
Figure 50. A) ATR–FTIR spectra of pure PDMS and HPR and hybrid PDMS films. B) Scanning electron microscopy image of the sensor.	160
Figure 51. Steady-state kinetic assay for the developed biosensor with hydrogen peroxide and with sodium percarbonate respectively. Conditions: the concentration of luminol was 0.17mM and H ₂ O ₂ was varied. Insets are the Lineweaver-Burk linearization.....	162
Figure 52. Reusability of the biosensor expressed as relative activity (%).	164
Figure 53. Concentration of sodium percarbonate expressed as H ₂ O ₂ concentration in Corega® Oxígeno Bio-Activo tablets. Orange line was obtained by releasing process in water and blue line was obtained in contact with used denture.	167
Figure 54. Optimization of concentration of hypochlorite and luminol working in solution to measure organic amino nitrogen and ammonium with a portable luminometer.	170
Figure 55. Different support material tested in order to immobilize luminol. A, B) PDMS; C, D, E) PDMS and TEOS; F) zein.....	171
Figure 56. A) Developed TEOS/MTEOS sol-gel sensor in the polystyrene tube. B) % of remaining activity in the developed devices at different time to heat the device in the oven at 40°C. C) % reaction inhibition as function of nitrogen concentration (7.5 μM and 15μM).	172
Figure 57. Microscopy images of the developed TEOS/MTEOS sensor. A) Without luminol and B) with luminol (10x and 50x).	174
Figure 58. Infrared sprectrum of luminol and sol-gel sensor. Orange: luminol; blue: sol-gel without luminol; grey: sol-gel with luminol.	175
Figure 59. Schematic representation showing the five pyrene compounds used to obtain pyrene-modified MWCNT bioelectrodes with adsorbed HRP for the two-electron bioelectrocatalytic reduction of H ₂ O ₂ to water. Enzyme structure pdb1H55 of HRP from <i>Armoracia Rusticana</i> (Berglund et al., 2002).	181

- Figure 60.** (A, B) CVs recorded at MWCNT-HRP bioelectrodes at 10 mV s^{-1} in 0.1 mol L^{-1} phosphate buffer (pH 7.0) with (A) 0.5 mmol L^{-1} and (B) 4 mmol L^{-1} H_2O_2 : (—) unmodified; (—) py; (—) pyNHS; (—) pyAA; (—) pyBA; (—) pyNH₂. (C) CV recorded from open-circuit potential at unmodified MWCNT without HRP at 10 mV s^{-1} in 0.1 mol L^{-1} phosphate buffer (pH 7.0) with 4 mmol L^{-1} H_2O_2 185
- Figure 61.** First (solid line) and second (dashed line) CVs recorded at MWCNT-HRP bioelectrode at 10 mV s^{-1} in 0.1 mol L^{-1} phosphate buffer (pH 7.0) without H_2O_2 . The arrow shows the scan direction of the first scan. 186
- Figure 62.** Amperometric current-concentration linear dynamic range curves recorded at MWCNT-HRP electrodes in 0.1 mol L^{-1} phosphate buffer (pH 7.0) before and after increasing additions of H_2O_2 : (A, •) unmodified; (B, •) py; (C, •) pyNHS; (D, •) pyAA; (E, •) pyBA; (F, •) pyNH₂. Current values obtained at 0 V vs. Ag/AgCl from CVs. Error bars correspond to standard deviation from $n = 3$ samples..... 188
- Figure 63.** Schematic representation of the MWCNT-HRP electrodes modified with pyNHS and nanocellulose. (B) Representative CVs recorded at 10 mV s^{-1} at the one-pot ($5 \mu\text{L}$) nanocellulose/pyNHS HRP bioelectrode in 0.1 mol L^{-1} phosphate buffer (pH 7.0) (—) before and after addition of H_2O_2 at (—) 0.4 ; (—) 0.6 ; (—) 1 ; (—) 2 ; (—) 4 ; (—) 6 ; and (—) 8 mmol L^{-1} 190
- Figure 64.** Current-concentration (A) full range and (B) linear dynamic range response curves recorded at MWCNT-HRP electrodes in 0.1 mol L^{-1} phosphate buffer (pH 7.0) before and after increasing additions of H_2O_2 : (•) unmodified; (•) pyNHS; (•) one pot ($5 \mu\text{L}$) nanocellulose/pyNHS. Current values obtained at 0 V vs. Ag/AgCl. Error bars correspond to standard deviation from $n = 3$ samples..... 191
- Figure 65.** Current-concentration response curves recorded at MWCNT-HRP electrodes in 0.1 mol L^{-1} phosphate buffer (pH 7.0) before and after increasing additions of H_2O_2 : (•) pyNHS; (•) nanocellulose/pyNHS (one-pot, $20 \mu\text{L}$); (•) nanocellulose/pyNHS (layer-by-layer, $20 \mu\text{L}$). Current values obtained at 0 V vs. Ag/AgCl from CVs. Error bars correspond to standard deviation from $n = 3$ samples..... 192
- Figure 66.** (A) Open circuit voltage-concentration plot recorded at MWCNT-HRP electrodes in 0.1 M phosphate buffer (pH 7.0) before and after increasing additions of H_2O_2 : (•) unmodified; (•) pyNHS; (•) pyNHS-

nanocellulose. (B) Bioelectrocatalytic current from CVs recorded at (•) pyNHS and (●) pyNHS-nanocellulose modified MWCNT-HRP electrodes in 0.1 mol L⁻¹ phosphate buffer (pH 7.0) in 4 mmol⁻¹ H₂O₂ . Current values obtained at 0 V vs. Ag/AgCl. 193

A.3. Table list








Table 1. Classification and some properties of the in situ devices.....	6
Table 2. Covered topics of the optical sensor in the 34 review articles. Database web of science (access September 2021).	12
Table 3. Covered topics of the electrochemical sensor in the 33 review articles. Database web of science (access September 2021).....	20
Table 4. Features of different solid supports. See test for more explanation.	27
Table 5. Zein.....	31
Table 6. Nylon properties	34
Table 7. PDMS	38
Table 8. TEOS and MTEOS.....	41
Table 9. Bacterial nanocellulose properties.....	45
Table 10. CNTs	49
Table 11. Determination of inorganic phosphate on solid supports through different methods	53
Table 12. In situ methods for atropine and ramipril quantification in the pharmaceutical industry and for cocaine quantification in drug abuse area	56
Table 13. Some analytical parameters for selected assays and sensors developed for silver ion estimation.	59
Table 14. Comparison of HRP immobilization methods on solid supports for H ₂ O ₂ sensing.	64
Table 15. Comparison of different sensors to determine ammonium, ammonia and organic amino nitrogen. Surface plasmon resonance imaging	70
Table 16. Reagents list uses in this Thesis with their commercial suppliers and respective security pictogram where  = flammable;  = oxidizing;  = corrosive;  =toxic;  = harmful;  = health hazard;  = environmental hazard.	84
Table 17. Different mixtures tested in order to develop a luminol sensor. For all mixtures 4.4 µL of nanopure water was used.	97
Table 18. Experimental conditions used in several works of this Thesis based on polymeric sensor	101
Table 19. Samples per analytes studied.....	112
Table 20. Study of layer configurations for the development of a multiwell biosensor for phosphate determination.	123

Table 21. Comparison of the figures of merits obtained for phosphate determination in solution and from the A2 biodevice.....	126
Table 22. Confirmatory study of the multiwell plate A2 biosensor vs the ammonium-molibdate method: estimated concentrations of phosphorus in serum samples.	129
Table 23. Comparison of the figures of merit obtained the determination of an ester compound (propyl acetate) by the zein and paper-based sensor and by the reagents in solution and analytical parameters using the zein-based sensor for propyl acetate, atropine, cocaine and ramipril.	132
Table 24. Inter- and intraday relative-standard-deviation values of the zein sensors. Responses to a blank and a propyl acetate standard obtained in two experiments with the same batch or with different batches.	134
Table 25. Figures of merit of the use of the proposed sensor for quantifying silver ion in water.....	147
Table 26. Results of analysis of water samples.	150
Table 27. Comparison of merits obtained with the developed biosensor testing different substrates for the H ₂ O ₂ determination.	163
Table 28. Analysis of Culture medium DMEM-F12 incubated with neuroblast cells.....	166
Table 29. Several figures of merit of portable binomial sensor-luminometer and conventional procedure in solution and lab equipment. ^a by using the sensor ^b in solution. * Interday.....	177
Table 30. Nitrogen found and recoveries in different water samples. Processed in situ.....	178

A.4. PhD contributions to publications

1. **S. Bocanegra-Rodríguez**, N. Jornet-Martínez, C. Molins-Legua, P. Campíns-Falcó. Delivering Inorganic and Organic Reagents and Enzymes from Zein and Developing Optical Sensors, *Anal. Chem.* 90 (2018) 8501–8508. Contribution 100%.
2. N. Jornet-Martínez, **S. Bocanegra-Rodríguez**, R.A. González-Fuenzalida, C. Molins-Legua, P. Campíns-Falcó. In Situ Analysis Devices for estimating the environmental footprint in beverages industry. In *Processing and Sustainability of Beverages*, Grumezescu, A.M., Holban, A.M., Eds.; Elsevier: Amsterdam, The Netherlands, 2019; Volume 2, Chapter 9; pp. 275–317. Contribution 60%.
3. **S. Bocanegra-Rodríguez**, N. Jornet-Martínez, C. Molins-Legua, P. Campíns-Falcó. New reusable solid biosensor with covalent immobilization of the Horseradish Peroxidase enzyme: in situ liberation studies of hydrogen peroxide by portable chemiluminescent determination. *ACS Omega* 5 (2020) 2419-2427. Contribution 100%.
4. **S. Bocanegra-Rodríguez**, N. Jornet-Martínez, C. Molins-Legua, P. Campíns-Falcó. Portable solid sensor supported in nylon for silver ion determination: testing its liberation as biocide. *Anal Bioanal Chem* 412 (2020) 4393-4402. Contribution 100%.
5. **S. Bocanegra-Rodríguez**, C. Molins-Legua, P. Campíns-Falcó. Luminol doped silica-polymer sensor for portable organic amino nitrogen and ammonium determination in water. *Sep.* 2021 (Separations). Contribution 100%.

6. **S. Bocanegra-Rodríguez**, C. Molins-Legua, P. Campíns-Falcó, F. Giroud, A. J. Gross. Monofunctional pyrenes at carbon nanotube electrodes for direct electron transfer H₂O₂ reduction with HRP and HRP-bacterial nanocellulose. *Biosens. Bioelectron.* 187 (2021) 113304. Contribution 80%.